



Durham E-Theses

Improved tribology and materials for a new generation of hip prostheses

Blamey, J.M.

How to cite:

Blamey, J.M. (1993) *Improved tribology and materials for a new generation of hip prostheses*, Durham theses, Durham University. Available at Durham E-Theses Online: <http://etheses.dur.ac.uk/5629/>

Use policy

The full-text may be used and/or reproduced, and given to third parties in any format or medium, without prior permission or charge, for personal research or study, educational, or not-for-profit purposes provided that:

- a full bibliographic reference is made to the original source
- a [link](#) is made to the metadata record in Durham E-Theses
- the full-text is not changed in any way

The full-text must not be sold in any format or medium without the formal permission of the copyright holders.

Please consult the [full Durham E-Theses policy](#) for further details.

The copyright of this thesis rests with the author.
No quotation from it should be published without
his prior written consent and information derived
from it should be acknowledged.

Improved Tribology and Materials for a New Generation of Hip Prostheses

J.M.Blamey B.Sc. M.Sc.

**A Thesis submitted for the Degree of Doctor of Philosophy at the
University of Durham.**

**The School of Engineering and Computer Science (S.E.C.S),
Science Laboratories,
The University of Durham,
South Road, Durham, DH 1 3 LE.**



- 9 JUL 1993

Note on the Layout of this Thesis

Much of this project has concentrated on development of the soft layer prosthesis. Because of this, a diverse range of materials, tribological parameters and measurement techniques were involved. The nature of the corresponding literature meant that to avoid confusion and constant referring back to the beginning of the report, two sections were used to review the general literature for the MATERIALS and TRIBOLOGY Sections. The more specialist literature is reviewed as it becomes necessary to the reader. I hope this forms the basis of an interesting and readable thesis.

Acknowledgements

Thanks must be extended to a number of university members involved in this work.

Professor Tony Unsworth for his help and access to his extensive collection of literature, as well as his comments on interim reports to my funding organisations and this Thesis.

Dr. Mark Percy and Dr. Jimmy Cunningham assisted in steering the research in the right direction and took time to discuss apparatus and test results as well as being involved in the preparation of papers.

Sanjoy Rajan, Debbie Walker and Paul Mullan, performed work on the degradation and the bonding work during the course of their studies and their involvement in the project provided a number of new ideas and directions for research.

Mr. George Turnbull managed to turn ideas into reality with startling results through his technical assistance in the Engineering Workshop.

Thanks must also go to Mrs. Susan Carter as well as the postgraduate and undergraduate students at Durham University who have been a constant source of encouragement.

Finally, I would like to extend my warmest thanks to Action Research and The Wolfson Foundation for their financial support during the course of my research.

Summary

Soft layers, when incorporated into an experimental hip prosthesis, have proved effective in reducing friction by improving the lubrication mechanisms. However, further development was required prior to clinical trials. The two aspects that needed consideration were the optimisation of the material and the tribological properties.

A number of bio-compatible polyurethanes were investigated during the course of the study. All of the polymers showed reduced hardness and elastic moduli during *in-vitro* studies due to the uptake of small quantities of fluid (1.5-2.0%), but little degradation was noticed for Tecoflex or Pellethane polyurethanes under long term soaking in Mammalian Ringer's solution at 37°C. Hardness testing of elastomers was investigated extensively, and correlations were found between the elastic modulus of the material and the hardness for lubricated and bonded samples of a range of thicknesses.

Tecoflex EG 93°A and Pellethane 2363-80°A have both shown good fatigue properties, with tensile samples having completed 9 million cycles from zero to 15% extension with little change in elastic modulus (0 - 5.2MPa Stress) and little change in ultimate strength and extension when compared with control samples.

The design of the composite acetabular component was investigated in detail. Successful bonding of the polyurethane to an UHMWPE backing through primarily mechanical interlock has provided a bio-compatible composite component which has been tested through peel and blister tests.

A number of new experimental techniques for measuring the contact area in the loaded hip prosthesis were investigated, and following tests on UHMWPE joints these were applied to soft layers where the equivalent ball-on-plate model is inaccurate. Theoretical studies of contact area and lubrication mechanisms in currently available prostheses and in soft layer joints indicated differences in lubrication performance, which were confirmed through experimental work in a new hip function simulator, which allowed the lubrication mechanisms to be isolated. Squeeze Film Action and the Dynamic Loading Cycle were dominant factors, with Micro-Elastohydrodynamic (Micro-EHL) providing a small effect.

Modification of the surface of the layer was accomplished by laser ablation. This was done to provide a reservoir of fluid which could be utilised during periods of high loading and low surface velocity. However, results indicated that increases in roughness of the surface caused by laser damage around the holes was detrimental to tribological performance under most conditions. This technique of surface modification required further work, and suggestions were made.

List of Symbols

- a Contact Radius (mm)
- b Blister Radius (mm)
- c Clearance of the Hip Joint Arrangement (mm)
- c_b Initial Crack Length for Blister Test (mm)
- d Diameter of the Loaded Indentor (mm)
- e Penetration (mm)
- e_r Reduced Penetration (mm)
- E_1, E_2 Elastic Modulus of the Femoral / Acetabular Components (MPa)
- E' Equivalent Elastic Modulus of the Prosthesis (MPa)
- $$E' = 2 \left[\left(\frac{1 - \nu_1^2}{E_1} \right) + \left(\frac{1 - \nu_2^2}{E_2} \right) \right]^{-1}$$
- F Load applied during Hardness Test (N)
- F_D Desired Load Applied by the Simulator (N)
- h_{\min} Minimum Film Thickness (μm)
- h_s Film Thickness after T, Squeeze Film Time (μm)
- h_o Starting Film Thickness for Squeeze Film (μm)
- K Ellipticity Factor for Lubrication Contacts (Dimensionless)
- p Pressure in the Contact Area (MPa)
- p_a Maximum Amplitude of the Pressure Distribution in Micro-EHL (MPa)
- P Critical Pressure applied during the Blister Test (MPa)
- R_1, R_2 Radius of the Femoral / Acetabular Components (mm)
- R_x Equivalent radius of the Ball-on Plate Model (mm) $R_x = \left[\frac{1}{R_1} - \frac{1}{R_2} \right]^{-1}$
- t Thickness of the Polyurethane Layer (mm)
- T Squeeze Film Time (s)

u_1, u_2	Surface Velocity of Articulating Surfaces (mm/s)
W	Load Applied in the Prosthesis (N)
x	Distance along Contact from Pole (mm)
x_a	Distance from the peak of an individual asperity (μm)
α	Angle of Laser Pores from Base of Cup ($^\circ$)
β	Peel Test Angle ($^\circ$)
δ	Deformation of Asperities (μm)
Δ_1	Height of Surface Asperities on Femoral Component (μm)
Δ_2	Height of Surface Asperities on Acetabular Component (μm)
ε_1	Initial Eccentricity of the Hemispherical Seat (dimensionless)
ε_2	Final Eccentricity of the Hemispherical Seat (dimensionless)
ϕ	Permeability ($\text{m}^4/\text{N s}$)
η	Viscosity of Lubricants (Pa s)
λ	Wavelength of Asperities (μm)
Λ	Dimensionless Film Thickness Parameter (dimensionless)
μ	Friction Factor (dimensionless - see below)
ν_1	Poisson's Ratio of the Femoral Component (dimensionless)
ν_2	Poisson's Ratio of the Acetabular Component (dimensionless)
θ	Adhesive Fracture Energy (J/m^2)
τ_{max}	Maximum Shear Stress at the Layer interface (MPa)
ψ	Permeability Parameter (dimensionless)

Definitions

$$\text{Friction Factor} = \frac{\text{Frictional Torque}}{\text{Normal Load} \times \text{Joint Radius}} \quad (\text{Unsworth, 1978})$$

$$\text{Engineering Stress} = \frac{\text{Load Applied}}{\text{Original Cross Sectional Area of the Sample}}$$

$$\text{True Stress} = \frac{\text{Load Applied}}{\text{Actual Cross Sectional Area of the Sample}}$$

List of Figures

Chapter 2

- 2.1 Stainless Steel Backed Acetabular Cups
- 2.2a Moulds used for the preparation of Experimental Polyurethane/polyethylene Bonded Samples
- 2.2b Mould and Platen Temperatures for the preparation of a Bonded Acetabular Cup
- 2.3 A Plot of Load / Penetration for the DIN 53456 Hardness Test
- 2.4 Indentor Penetration and its relation to the DIN 53456 Hardness Value
- 2.5 Calibration of the DIN 53456 Hardness Test
- 2.6 The Effect of Sample Thickness on Hardness Values (DIN 53456) for two Grades of Castomer Polymers
- 2.7 The Effect of Sample Thickness on Hardness Values (DIN 53456) for Five Bio-compatible Polyurethanes
- 2.8 The Visco-Elasticity of thin Samples of Bio-compatible Polyurethanes undergoing Hardness Testing
- 2.9 The Change in Hardness with Penetration of the Indentor as a percentage of the sample thickness for Castomer Materials
- 2.10 The Change in Hardness with Penetration of the Indentor as a percentage of the sample thickness for the Bio-compatible Polyurethanes
- 2.11 The effect of the bond with the backing material on the Indentor Penetration for the Hardness Test.
- 2.12a A Schematic Diagram of Engineering Stress / Strain for Polyurethane
- 2.12b A Schematic Diagram of True Stress / Strain for Polyurethane
- 2.13a Elastic Modulus against results from the DIN 53456 Hardness Test, showing Hertzian Theory

- 2.13b Elastic Modulus against results from the DIN 53456 Hardness Test, showing Hertzian Theory
- 2.14 "Waters" Theoretical Results and Comparisons with Experimental Data for Bio-compatible Polymers

Chapter 3

- 3.1a The Increase in Mass of Bio-compatible Polyurethanes from Dry to Mammalian Ringers' Solution at 37°C for 24 hours
- 3.1b The Increase in Mass of Bio-compatible Polyurethanes from Dry to Laboratory Conditions after 7 days
- 3.2a The Change in Elastic Modulus of Hydrated Polyurethanes
- 3.2b The Change of Hardness (DIN 53456) of Hydrated Polyurethanes
- 3.3a The Change in Elastic Modulus of Polyurethanes at 37°C in Mammalian Ringers Solution
- 3.3b The Change in Hardness of Polyurethanes at 37°C in Mammalian Ringers Solution
- 3.3c A Schematic Diagram of the Change in Mechanical Properties of Polyurethanes with Temperature
- 3.4a The Change in Elastic Modulus of Samples placed in Mammalian Ringers Solution at 37°C
- 3.4b The Change in Elastic Modulus of Samples placed in Mammalian Ringers Solution at 37°C
- 3.4c The Change in Elastic Modulus of Samples placed in Mammalian Ringers Solution at 37°C
- 3.4d The Change in Elastic Modulus of Samples placed in Mammalian Ringers Solution at 37°C
- 3.5a The Change in Hardness of Samples placed in Mammalian Ringers at 37°C

- 3.5b The Change in Hardness of Samples placed in Mammalian Ringers at 37°C
- 3.5c The Change in Hardness of Samples placed in Mammalian Ringers at 37°C
- 3.5d The Change in Hardness of Samples placed in Mammalian Ringers at 37°C
- 3.6a The Change in Mass of Samples placed in Mammalian Ringers at 37°C
- 3.6b The Change in Mass of Samples placed in Mammalian Ringers at 37°C
- 3.6c The Change in Mass of Samples placed in Mammalian Ringers at 37°C
- 3.6d The Change in Mass of Samples placed in Mammalian Ringers at 37°C
- 3.7a The Change in Hardness of Estane cup samples placed in Mammalian Ringers Solution at 37°C
- 3.7b The Change in Hardness of Pellethane, Tecoflex and Estane '57' cup samples placed in Mammalian Ringers Solution at 37°C
- 3.7c The appearance of Polyurethanes following *In-vitro* degradation
- 3.8 The Friction Factor of Polyurethane Cups tested in the Hip Simulator with 0.010Pa s Lubricant
- 3.9 The Friction Factor of Polyurethane Cups tested in the Hip Simulator with 0.010Pa s Lubricant
- 3.10 The Tensile Fatigue Rig
- 3.11a The Elastic Modulus of Samples of Tecoflex 93°A undergoing fatigue in Mammalian Ringers Solution at 37°C
- 3.11b The Mass of Fluid contained in samples of Tecoflex 93°A undergoing fatigue in Mammalian Ringers Solution at 37°C
- 3.12a The Elastic Modulus of Samples of Pellethane 80°A undergoing fatigue in Mammalian Ringers Solution at 37°C
- 3.12b The Mass of Fluid contained in samples of Pellethane 80°A undergoing fatigue in Mammalian Ringers Solution at 37°C
- 3.13a Tensile Loading of an Adhesive Bond
- 3.13b Cleavage in Tension of an Adhesive Bond

- 3.13c Shear Loading of a Lap Joint
- 3.13d Peel of an Adhesive Joint
- 3.14 Stainless Steel backed Acetabular Cups
- 3.15 A Castomer Cup showing signs of Degradation
- 3.16 The Blister Test Arrangement
- 3.17 Typical Bonded Samples
- 3.18 The Polyurethane/Polyethylene Bond Line
- 3.19 The Floating Roller Peel Test Arrangement
- 3.20 The Change in the Adhesive Fracture Energy as t/b is altered
- 3.21 Compression Fatigue Rig for DARTEC used in testing Acetabular Cup Samples
- 3.22 Typical Fatigue Curves for Metals and Polymers

Chapter 4

- 4.1 A Stribeck Plot of Lubrication Mechanisms
- 4.2a The Squeeze Film Lubrication Mechanism
- 4.2b The Hydrodynamic Lubrication Mechanism
- 4.2c The Effect of Asperities on Lubrication : Micro-EHL
- 4.3 The Human Hip Joint
- 4.4a The Loading Applied to the Hip (Paul, 1967)
- 4.4b The Loading Applied to the Hip (English & Kilvington, 1979)

Chapter 5

- 5.1 The Existing Hip Function Simulator
- 5.2 The Motion of the Hip Joint
- 5.3 The Loading Applied to the Hip
- 5.4 The Large Dead-Band in Early Proportional Valves
- 5.5 Comparative Response for Servo and Proportional Valves

- 5.6 A Schematic Diagram of the Hydraulic System
- 5.7 Response of the Proportional Valve following changes in the PID Module
- 5.8 The General Control Circuit
- 5.9 The Die Set Arrangement
- 5.10 The Hydrostatic Bearings mounted on the Strain Gauged Beams
- 5.11 The New Simulator
- 5.12 The Simply Supported Beams
- 5.13 The Strain Gauge Arrangement and Wheatstone Bridge Circuit
- 5.14 Primary Calibration of the Strain Gauge Load Cells of Old and New Simulators
- 5.15 The Encoder Position on the Input Shaft to the Machine
- 5.16 The Scotch Yoke and Rack Arrangement
- 5.17 The Upper (Oscillating) Cradle
- 5.18 The Friction Carriage showing the Transducer and Bearing Arrangement
- 5.19 The Calibration Data File
- 5.20 The Real Data File Produced by the PC Following a Typical Run
- 5.21 A Typical File used to Construct a Stribeck Plot
- 5.22 The Effect of the Proportional Valve on the Response of the Strain Gauge
- 5.23 The Load Patterns used for Fine Tuning of the PID Module
- 5.24a The Calibration of the Loading Applied by the Simulator
- 5.24b Calibration of the Kistler Friction Transducer
- 5.24c Calibration of the Potentiometer
- 5.25a Loading Cycle I applied by the Simulator to represent walking
- 5.25b Loading Cycle II applied by the Simulator
- 5.25c Loading Cycle III applied by the Simulator
- 5.26a Vertical Component of Loading Cycle Applied to the Hip (Paul, 1967)
- 5.26b Resultant of Loading Cycle Applied to the Hip (Paul, 1967)
- 5.26c Angle of Resultant Force applied to the Hip (Paul, 1967)

- 5.27a A plot of Shear Rate against Viscosity for CMC and Diseased Synovial Fluids
- 5.27b A plot of Shear Rate against Viscosity for CMC and Healthy Synovial Fluids

Chapter 6

- 6.1 The Pathway for Prosthetic Loosening due to wear debris
- 6.2 The Typical Pressure Distribution for an Acetabular/Femoral contact from Hertzian Theory
- 6.3 The Ball-in-Cup to Ball-on-Plate Transformation
- 6.4 The Effect of Clearance on Contact Radius and the Maximum Pressure Generated
- 6.5 Rotary Talysurf Trace for a Polyethylene Cup produced on the CNC Lathe
- 6.6 The Effect of Clearance on Contact Radius for UHMWPE Joints including experimental results from Dye Transfer and Silicone Mouldings
- 6.7 Typical Dyed Regions from Loaded Prosthetic Devices
- 6.8 Typical Silicone Rubber Mouldings from Loaded Prosthetic Devices
- 6.9a A Typical Load/Penetration Plot for a 2mm thick layer of Tecoflex 85^oA bonded to a steel cup.
- 6.9b The Contact Radius and Pressures for Soft Layers from Penetration Studies, with the results of Dye Transfer and Silicone Mouldings included
- 6.10 Stribeck Plots for UHMWPE Joints (Material I) of different Clearances
- 6.11 Stribeck Plots for UHMWPE Joints (Material II) of different Clearances
- 6.12 The angular relationship of the components of the Charnley Arthroplasty in the body and the simulator
- 6.13 Stribeck Plot of Explanted and Unused Charnley Prostheses
- 6.14 A Typical Stribeck Plot for a Soft Layer Joint of Hardness $< 9.00\text{N/mm}^2$, a Soft Layer Joint of Hardness $> 9.00\text{N/mm}^2$ and a Charnley Joint
- 6.15 The Friction Factor for Soft Layer Joints with 0.010Pa s Lubricant

- 6.16 Proximity of the Contact Region of Soft Layer Prostheses to the edge of the Acetabular Cup
- 6.17a The Film Thickness variation for a Soft Layer Prosthesis under Normal Walking Loads - Squeeze Analysis of Deformed Layer
- 6.17b The Film Thickness variation for a Tecoflex 100^oA Prosthesis under Normal Walking Loads - Squeeze Analysis of Deformed Layer
- 6.18 The Film Thickness variation for a Soft Layer Prosthesis under Paul's Loading Cycle during Walking - Squeeze Analysis of Deformed Layer
- 6.19 The Film Thickness variation for an UHMWPE/Metal Prosthesis under Walking with 0.010Pa.s Lubricant - Squeeze Analysis of Deformed Layer
- 6.20 The Film Thickness variation for an UHMWPE/Metal Prosthesis under Walking with 0.050Pa.s Lubricant - Squeeze Analysis of Deformed Layer
- 6.21 The Film Thickness variation for an UHMWPE/Metal Prosthesis under Walking with 0.100Pa.s Lubricant - Squeeze Analysis of Deformed Layer
- 6.22 The Film Thickness variation for an UHMWPE/Metal Prosthesis under Walking with 0.200Pa.s Lubricant - Squeeze Analysis of Deformed Layer
- 6.23 The Femoral Head and Electrical Circuit used for Film Thickness Analysis
- 6.24 Resistance Measurements for Soft Layer and UHMWPE Hip Prostheses

Chapter 7

- 7.1 The Configuration of the Optical System for the Laser
- 7.2 The Jig used to hold samples undergoing Laser modification
- 7.3 The positioning of the Laser produced Pores
- 7.4 A Typical Surface Micrograph of a Laser Ablated Pore under Favourable Conditions
- 7.5 A Typical Surface Micrograph of a Laser Ablated Pore under Unfavourable Conditions

- 7.6a Pore Ablation at 9mJ in Tecoflex 93°A
- 7.6b Pore Ablation at 4mJ in Tecoflex 93°A, showing poor hole formation
- 7.7a A Stribeck Plot for a Tecoflex 85°A Cup before and after Laser modification, tested with the Loading Cycle I
- 7.7b A Stribeck Plot for a Tecoflex 85°A Cup before and after Laser modification, tested with the Loading Cycle II
- 7.8a A Stribeck Plot for a Tecoflex 85°A Cup before and after Laser modification, tested with the Loading Cycle I
- 7.8b A Stribeck Plot for a Tecoflex 85°A Cup before and after Laser modification, tested with the Loading Cycle II
- 7.8c A Stribeck Plot for a Tecoflex 85°A Cup before and after Laser modification, tested with the Loading Cycle III
- 7.9 A Stribeck Plot for the Pellethane samples before and after Laser ablation, tested with the Loading Cycle I
- 7.10 A Stribeck Plot for the Pellethane samples before and after Laser ablation, tested with the Loading Cycle II
- 7.11 A Stribeck Plot for the Pellethane samples before and after Laser ablation, tested with the Loading Cycle III
- 7.12 The surface of polyurethane at the base of the laser ablated pore
- 7.13 The surface of polyurethane at the side of the laser ablated pore

Contents

Notes on the Layout of this Thesis	i
Acknowledgements	ii
Summary	iii
List of Symbols	v
List of Figures	vii
Contents	xv
1 Introduction	1
1.1 General Introduction	1
1.2 Project Introduction	5
1.2.1 Materials and Design	5
1.2.2 Tribology	6
Part I Materials	
2 Materials and Methods of Soft Layer and Hard Layer Joints	7
2.1 Criteria for Materials <i>in-vivo</i>	7
2.2 Surgical Polymers	8
2.3 Polyurethanes	8
2.3.1 Pellethane 2363	9
2.3.2 Tecoflex	11
2.3.3 Estane 5714F1	12
2.3.4 Estane 58271	13
2.4 Mechanical Requirements for the Material and Design of the Prosthesis	13
2.5 Preparation of Specimens	16
2.5.1 Vacuum Moulding	16
2.5.2 Compression Moulding	17
2.5.3 Injection Moulding	21
2.6 Hardness and Elastic Modulus Experiments	21
2.6.1 Introduction to Hardness	21
2.6.2 Theory behind Hardness Testing and the DIN Standard Hardness Test	22
2.6.3 The Effects of Sample Thickness on Hardness Values	26

	2.6.3.1	Materials and Methods	26
	2.6.3.2	Results	27
	2.6.3.3	Discussion	30
2.7		Introduction to Elastic Modulus and Measurement for Polymers	32
	2.7.1	The Theory of Hardness and Elastic Modulus Interactions	34
	2.7.2	Results	35
	2.7.3	Discussion	36
2.8		Conclusions	39
3		Degradation, Hydration and Fatigue Response of	
		Bio-compatible Polyurethanes	40
3.1		Mechanical Changes to Polyurethanes under <i>In-vitro</i> Conditions	40
	3.1.1	Introduction	40
	3.1.2	Hydration Changes of Materials	40
		3.1.2.1 Introduction	40
		3.1.2.2 Materials and Methods	40
		3.1.2.3 Results	41
	3.1.3	Testing at 37°C	47
		3.1.3.1 Materials and Methods	47
		3.1.3.2 Results	47
3.2		Discussion	49
3.3		Degradation of Polyurethanes	52
	3.3.1	Introduction	52
	3.3.2	Materials and Methods	52
		3.3.2.1 Hardness Testing	52
		3.3.2.2 Elastic Modulus	52
		3.3.2.3 Hip Function Simulator	53
		3.3.2.4 Materials	53
		3.3.2.5 Methods of Testing	54
		3.3.2.6 Frictional Testing	54
	3.3.3	Results of the Strip Samples	54
		3.3.3.1 Elastic Modulus	54b
		3.3.3.2 Hardness	54b
		3.3.3.3 Mass Increase	63
	3.3.4	Results of the Cup Samples	63

	3.3.4.1 Hardness	63
	3.3.4.2 Frictional Measurements	71
3.4	Discussion	74
3.5	Fatigue of Polyurethane Strip Samples	76
	3.5.1 Introduction	76
	3.5.2 Methods of Measurement of Fatigue Response	77
	3.5.3 Results	79
	3.5.4 Discussion	85
3.6	Bonding of Polyurethanes to a Rigid Backing Material	87
	3.6.1 Introduction	87
	3.6.2 Theory of Joint Design	88
	3.6.2.1 Tensile/Compressive Loading	88
	3.6.2.2 Shear Loading	88
	3.6.2.3 Peel Loading	90
	3.6.3 Materials	90
	3.6.4 Adhesive Theory	92
	3.6.4.1 Hot-Melt Adhesives	92
	3.6.4.2 Polyurethane Adhesives	93
	3.6.4.3 Solvent Cast Systems	93
	3.6.4.4 Alternative Systems	94
	3.6.4.5 Contributing Considerations	94
	3.6.5 Bond Analysis	95
	3.6.6 Methods of Sample Preparation	98
	3.6.7 Methods of Peel Testing	100
	3.6.8 Results of Peel Testing	102
	3.6.9 Methods of Blister Testing	103
	3.6.10 Results from Blister Tests	104
	3.6.11 Discussion	104
3.7	Fatigue of PE/PU Cups	106
	3.7.1 Introduction	106
	3.7.2 Methods of Measurement of Fatigue Response	107
	3.7.3 Results	107
	3.7.4 Discussion	109

Part II Tribology

4	Introduction and Literature Review for Section 2	111
4.1	Basic Lubrication Theory	111
4.1.1	Lubrication Regimes	111
4.1.1.1	Fluid Film Lubrication	111
4.1.1.2	Boundary Lubrication	112
4.1.1.3	Mixed Lubrication	113
4.1.1.4	Analysis of the Lubrication Regime	113
4.2	Lubrication Mechanisms	115
4.2.1	Squeeze Film	116
4.2.2	Hydrodynamic Lubrication	120
4.2.3	Elasto-hydrodynamic	120
4.2.4	Micro-EHL	121
4.2.5	Weeping or Boosted Lubrication	122
4.2.6	Methods of Measuring the Thickness of Lubricating Films	123
4.3	Human Joints	124
4.3.1	Cartilage	124
4.3.2	Synovial Fluid	127
4.3.3	Loading and Motion Cycles	127
4.4	Soft Layer Joints	129
4.4.1	Weeping and Boosted	130
4.4.2	Elasto-hydrodynamic	130
4.4.3	Squeeze Film	131
4.4.4	Boundary Lubricants	131
4.5	Current Prostheses	132
5	Design and Commissioning of the Simulator	133
5.1	Simulation of the Hip Joint	133
5.2	Currently used Simulation Devices	136
5.3	Design of the New Simulator	140
5.3.1	Application of the Load	140
5.3.2	Measurement of the Loading Applied to the Prosthesis	152
5.3.3	Oscillatory Motion of the Simulator	154
5.3.4	Measurement of Frictional Torque Developed in the Joint	159
5.3.5	Prosthetic Mounting	159

5.3.6	Data Acquisition and Analysis	161
5.3.6.1	Calibration Routines	162
5.4	Commissioning of the Simulator	165
5.4.1	Hydrostatic Bearings	165
5.4.2	Proportional Valve	166
5.4.3	Data Analysis Software and Hardware	168
5.4.4	Calibration	168
5.5	Loading Cycles	170
5.5.1	Dynamic Loading	170
5.5.2	Constant Loading	175
5.5.3	The Minimum Load	175
5.5.4	The True Walking Cycle Loading	175
5.6	Lubricants	178
6	Tribological Studies and Contact Area Assessment of Hip Prostheses	182
6.1	Introduction to the Importance of Tribological Properties	182
6.2	Contact Analysis of Currently Available Systems	182
6.2.1	Introduction	182
6.2.2	Materials and Methods	189
6.2.3	Assessment of Cup Sizes	191
6.2.4	Experimental Contact Area Studies	193
6.2.4.1	Direct Contact Measurement	193
6.2.4.2	Mouldings and Castings	193
6.2.5	Results	195
6.2.6	Discussion	197
6.3	Contact Analysis of Soft Layer Prostheses	199
6.3.1	Introduction	199
6.3.2	Materials and Methods	199
6.3.3	Results	200
6.3.4	Discussion	203
6.4	Tribological Studies of Polyethylene on Stainless Steel Joints	204
6.4.1	The Effect of Clearance and Material on Friction Factor	204
6.4.1.1	Materials and Methods	204
6.4.1.2	Results	204
6.4.1.3	Discussion	207

6.4.2	Investigation of New and Explanted Charnley Prostheses	208
6.4.2.1	Introduction	208
6.4.2.2	Materials and Methods	208
6.4.2.3	Results	211
6.4.3	Conclusions	214
6.5	Tribological Studies of Soft Layer Prostheses	215
6.5.1	Introduction	215
6.5.2	Materials and Methods	215
6.5.3	Results	216
6.5.4	Discussion	218
6.5.5	Conclusions	221
6.6	Theoretical Calculations of Lubrication Film Thickness	222
6.6.1	Introduction	222
6.6.2	Results	224
6.6.3	Discussion with Experimental Results	228
6.7	Experimental Determinations of Lubricant Films	233
6.7.1	Materials and Methods	233
6.7.2	Results	234
6.7.3	Discussion	234
6.8	Extended Testing of Polyurethane Prostheses	237
6.9	Inducing Effects of Three Body Wear	237
6.10	Conclusions	238
7	Surface Modifications	240
7.1	Tribological Theory of Surface Modifications	240
7.2	Methods of Producing Discrete Surface Pores	241
7.3	Laser Theory	242
7.4	Apparatus for Laser Modification	244
7.5	Materials and Methods	245
7.5.1	Stage I	247
7.5.2	Stage II	250
7.6	Scanning Electron Microscopy of the pores	251
7.6.1	Stage I	251
7.6.2	Stage II	255
7.7	Tribological Results	258
7.7.1	Stage I	258

7.7.2	Stage II	258
7.8	Discussion	264
7.9	Conclusions	270
8	Conclusions	273
8.1	Mechanical Properties of Bio-compatible Polyurethanes	273
8.2	Degradation and Fatigue Testing of Polyurethanes	273
8.3	Fabrication of the Prosthesis	274
8.4	Contact Area Measurements and Influence on Performance	274
8.5	Lubrication of Polyurethane and Polyethylene Joints	275
8.6	Recommendations for Future Research	276
	References	277
	Bibliography	289
	Engineering Standards	291
	Appendix I	292
	Appendix II	293
	Appendix III	299
	Appendix IV	300
	Published Papers	301

Chapter 1 : Introduction

1.1 General Introduction

The application of engineering principles to medicine has been expanded over the past 50 years to include most of the currently available implantable devices. This has led to considerable advances in many fields, including the improved design of artificial joints. Because of the perceived success of currently available prostheses compared with earlier designs, there has been a tendency to curtail development in such areas as hip prostheses. However, there are still problems and premature failure of these joints does occur. The average time to failure is still only about 10 years (Smeathers and Wright, 1990).

Osteo- and Rheumatoid-arthritis are the two most common disabling conditions which affect the human hip joint often resulting in the need for replacement. In general terms, changes in the joint structure and the lubricant can cause wear and therefore a degenerative process operates, reducing mobility and causing pain. The only successful treatment today requires a new joint surface to be constructed.

Initially, designs of prostheses copied the architecture of the natural joint and were constructed of such materials as ivory, perspex (Judet and Judet, 1950) and Bakelite (Smith Peterson, 1948). These were largely unsuitable for the applied loading or the hostile biological environment. However, current prostheses use biologically compatible materials capable of withstanding the applied loads.

This is largely as a result of the pioneering work of Charnley (Charnley, 1979). Charnley changed the hip prosthesis in 1958 with the introduction of an acetabular cup made of a polymer, PTFE (polytetrafluoro ethylene). This articulated on a stainless

steel ball of 22mm diameter. The reduction in size from the human synovial joint (45-49mm diameter) (Gore *et al*, 1981, Dowson *et al*, 1991) reduced the frictional torque developed by the joint in use. Charnley had indicated that the frictional torque was a major cause of failure at the cement-bone interface. Although a low friction material PTFE exhibited poor wear properties and after 3 years (and 300 operations) a number of cups had worn through, exposing the acetabulum to the stainless steel head. Improvements were made with the introduction of polyethylene for the acetabular cup (1961) which proved successful and forms the basis of the acetabular cup in the majority of hip prostheses implanted today.

In modern joints the bearing surfaces consist of a sphere, normally stainless steel, cobalt chrome-molybdenum alloy, titanium or ceramic, which articulates in a hemispherical cup. The cup is normally machined from a solid block of ultra high molecular weight polyethylene (UHMWPE). The femoral component consists of a stem, which provides the attachment to the femur, with an integral ball forged as one item or separately in a modular system.

Wear particles from the joints can cause body reaction, with the formation of giant cells around the particle sites and bone loss which gives rise to instances of loosening at the prosthesis/cement/bone interfaces (Mathieson *et al*, 1987; Villacin and Bullough, 1978). Loosening of both components is an important long-term problem of hip arthroplasty. Revision surgery is much more complicated than the initial implantation and earlier reports of the operation have indicated infection rates of 25% (Gruebel-Lee, 1983). Generally, incidences of infection only account for 1-2% of cases (Buchholz *et al*, 1981).

Reduction of wear debris has been investigated and the use of UHMWPE has improved wear compared with the high density form, which was initially investigated by Charnley. The use of alumina ceramic femoral heads in some joints (Muller, Protek & Allopro prostheses) is claimed to reduce the quantity of wear debris (Semlitsch *et al*, 1977). However, the use of ceramics introduces a number of other problems associated with the low fracture toughness of the material, requiring modifications to the prosthetic system to reduce stress concentrations or regions of high tensile stress.

In order to improve fixation, both the prosthesis and the cement have undergone scrutiny. Cements, made from polymerised methyl methacrylate, have been subjected to a number of developments since the early experiments of Charnley (1970). Strengthening media based on soft particles or carbon fibres have improved the toughness and strength of the bulk material (Taylor *et al*, 1988). However, little influence on the strength of the cement interfaces has been noticed as they act as fillers with little adhesive strength. Low viscosity pressurised systems seem to show an improvement in adhesion due to an improved mechanical interlock (Bannister & Miles, 1988).

The prosthesis stem has been under constant development, with changes of shape, size, material and surface topography. The use of cementless systems with hydroxyapatite coatings is currently showing promise. The coating provides a surface into which the bone can grow, eliminating the need for cement (Oonishi *et al*, 1989). Porous in growth media have also been used both with and without cement fixation. These are either plasma sprayed or sintered cobalt chrome or titanium applied over the proximal stem of the femoral component and the pelvic interface of the acetabular component. Favourable performance has been evident with this system (Engh *et al*, 1990). Analysis of the stresses at the interfaces using finite element techniques has led

to the development of "isoelectric" stems by a number of groups. The idea of this is to reduce the stress shielding effect of the prosthesis and so reduce bone resorption. Mathys and Burri (1983) have produced stems from reinforced polyacetyl resins which have shown a similar success rate in the short/medium term to conventional stems. In addition commercial hollow prostheses are available.

The difficulty faced by the developments described above is that in many cases they are addressing the effects and not the cause of the problem. The concept behind the use of soft elastic surface layers is to eliminate many of the fundamental problems of current prosthetic design by producing a system as close to the natural system as possible. A joint where the surfaces are completely separated by a film of synovial fluid should give minimal wear since the articulating surfaces are not in contact. Lubrication theory predicts that as articulating systems move from mixed lubrication, such as exists in currently available prostheses (Unsworth *et al*, 1975; Unsworth, 1978), to fluid film lubrication, the frictional torque decreases. The reduction in frictional torque may reduce the incidence of loosening as well as prolonging the life of the joint surface since wear would be much reduced. The human joint can give excellent performance for 70 years, much greater than the typical 10-20 year life of current prostheses (Smeathers & Wright, 1990). Improving the life of the prosthesis will certainly improve the availability of the operative procedure to younger people suffering from rheumatic conditions.

Current orthopaedic procedures (e.g. Charnley and Hardinge techniques) retain a large portion of the synovial membrane. Consequently, the source of synovial fluid is maintained and a prosthesis which can work well in the presence of such a lubricant, such as the soft layer joint, has the opportunity to do so *in-vivo*.

The first soft layered acetabular components were tested by Unsworth *et al* (1981). Later work by Unsworth *et al* (1987, 1988) showed that very low frictional torques were encountered using a realistic walking cycle, with friction factors of 0.005 being measured over a range of viscosities of synthetic lubricants. This compared with values of 0.030 measured for Muller prostheses using identical tribological conditions. However, this work involved the use of polyurethanes which were not compatible with the biological environment.

1.2 Project Introduction

The objective of the work on soft layers was to turn a laboratory model into a commercially viable product. This involved a number of aspects, each of which had to be considered carefully. This meant that the research was split into two main sections.

1.2.1 Materials and Design

The hydrophilicity of the currently available bio-compatible materials had to be assessed to improve the tribological properties since the lubricant (synovial fluid) is a water based fluid. The effects of degradation in a hydrolysing media needed to be assessed using a range of bio-compatible polymers by measurement of the elastic modulus and hardness of tensile test specimens and experimental cup samples. The effect of these *in vitro* tests on tribological properties was also considered to be important. When subjected to an aqueous environment at body temperature, 37°C, the mechanical properties of many polymers change. This is important to consider, especially when such a small range of hardness values had proved to be suitable in promoting fluid film lubrication (Unsworth *et al*, 1988). The response of the polymers to fatigue was considered and measured in a suitable environment.

A manufacturing process which would result in a reproducible, smooth, defect-free surface had to be found and a reliable and effective bonding mechanism between

the elastomer and the rigid backing material had to be produced. A prosthesis design which could be incorporated into current commercially available systems would also be advantageous. This would speed up the introduction of clinical studies and allow a simplified revision operation if any problems occurred.

1.2.2 Tribology

The very low friction factors which had been measured previously had to be a consistent property of the layers. Theoretical lubrication studies and favourable comparisons with currently available artificial joints were also deemed to be important to gain acceptance by orthopaedic surgeons. The tribological properties had to be consistent over the lifetime of the joint. In addition, methods of maintaining the film of fluid under conditions of low velocity and extended periods under load (e.g. standing) would be advantageous in reducing wear under 'dry' conditions. The contribution that the individual lubrication mechanisms made on the overall effect, both theoretically and experimentally, have been investigated. Through this, the layers have been optimised. A new hip simulator, with increased loading potential and the ability to input a wide range of steady and dynamic loading cycles, was required in order to study this.

With such a wide range of objectives and research directions strict time limitations had to be set. The two distinct parts of the work were both important in producing a clinical device. Previous work had concentrated on non-compatible, *in-situ* moulded polymers, but for a clinical device expected to withstand 20-50 years in the body, bio-compatibility was important. Materials already accepted as bio-compatible were preferred and the ability to process these materials, bond them to a backing material and obtain good tribological results were paramount.

Chapter 2 : Materials and Methods of Soft Layer and Hard Layer

Joints

2.1 Criteria for Materials *In-Vivo*

In-vivo use requires a material to show good bio-compatibility, with little adverse tissue reaction, as well as minimal degradation in a hostile environment. The extra-cellular fluid, which is an isotonic saline solution, is very hostile to metal components. However high polymers of synthetic origin and high molecular mass should show little degradation. This is a generalisation and some polymers, in particular those constructed from hetero-chains, are not totally resistant to bio-degradation (Williams, 1982). The degradation can be divided into hydration and enzymic or chemical attack from the host organism. Hydration depends on the base material and is mainly applicable to polymers only. It normally results in reductions in molecular mass by a depolymerisation process or the breakdown of cross links, both of which modify the mechanical properties of the material. The relative effects of immersion and 100% humidity have been examined without a clear consensus (Schollenberger and Steward, 1971). Chemical attack tends to affect the groups forming the chains and can result in a complete change in properties.

Some research has shown that the bio-compatibility of currently used orthopaedic bio-materials is in question (Albertsson, 1992). Certainly the reaction of the body to particles of UHMWPE (Villacin and Bullough, 1978) and metallosis (Black *et al*, 1990), the products of wear in artificial joints, has been substantial. This form of body reaction seems to be the main cause of prosthetic failure and subsequent revision (Chapter 1)

2.2 Surgical Polymers

The last thirty to forty years has seen the use of polymeric bio-materials in medical and surgical applications grow and diversify. Many of the applications involve intimate contact with living tissue. Studies of degradation cannot be fully represented by *in-vitro* work in simple saline as the physiological environment consists of a fluid containing anions, cations and organic species. To effect a full study of a polymer both *in-vivo* and *in-vitro* tests should be performed. This introduces the discrepancies between bio-degradation and degradation. Degradation is action brought about by the aqueous extra-cellular fluid, such as hydrolysis, which does not involve a vital function of the host. However, bio-degradation may be referred to if the attack is due to enzymes or other chemicals produced by the host organism.

2.3 Polyurethanes

The polyurethanes used were block co-polymers. The chains are composed of alternating segments of hard and soft material. The hard segment is urethane based with a molecular weight of 300 - 3000 and the soft segment polyester or -ether based (M_w 500-5000). These combine to form the measured mechanical properties of the polymer. The chemical incompatibility of the hard and soft segments leads to segregation of material into domains, with the hard segments, semi-crystalline or glassy, acting as sites of cross linkage between the chains. The -ester or -ether groups also provide some degree of linking through hydrogen bonding.

Polyester based urethanes tend to be unstable in an aqueous medium, with resulting hydrolysis of the ester linkage and shortening of the chain lengths. This can be so severe that considerable changes can occur within six months *in-vivo* (Redler, 1962) involving severe molecular changes and disintegration. Polyether urethanes in

general tend to be more stable in a hydrolytic environment although limitations of the suitability of both types of material exist.

2.3.1 Pellethane 2363

This is a segmented polyurethane elastomer which can be fabricated by injection moulding, compression moulding or solvent casting. It is based on polytetramethylene Glycol (PTMEG or PTMO), methylene di-phenyl di-isocyanate (MDI) and 1,4 Butanediol and produced as an aromatic polyether urethane. The MDI linking component (shown below) is responsible for the aromatic notation of the material.



Manufacture relies on processing aids which indicate potential biocompatibility problems, in particular when used in long term implants. However, Pellethane has been successfully used in the lead tubing for heart pacemakers, blood bags and other devices although its blood compatibility is regarded to be inferior to some other polyurethanes (Nyilas *et al*, 1972). Its application in pacemaker leads has caused problems with surface fissuring and some sample groups have shown a failure rate of 10%. A number of groups have looked at the biostability of this material and compared it with Tecoflex urethanes (Stokes *et al*, 1984). Results have indicated that stability of both materials has a high dependence on the grade of material and the method of fabrication.

Several mechanisms have been proposed to explain surface fissuring, including protein and lipid absorption (Parins *et al*, 1985), processing related residual stresses, oxidation of the ether chain and stress induced cracking (Stokes *et al*, 1984). In addition, this can be a symptom of acute hydrolytic degradation. Molecular weight of

the chains decreases to a critical level below which the elasticity of the chains is too low to avoid breakage (Hepburn, 1982). Dr. Ratner, in a round table discussion during the "Polyurethane in Medical Technics" conference (1983) suggested that fissuring was an inherent problem of Pellethane due to leeching out of the processing aids. This was expanded by Dr. Pundy who showed that problem was not apparent with harder grades which did not use processing aids (Polyurethanes in Biomedical Engineering, 1984). However, recent information from Dow Corning, the manufacturers of the Pellethane range of polyurethanes, regarding *in-vivo* problems have resulted in the bio-compatible notation being temporarily removed.

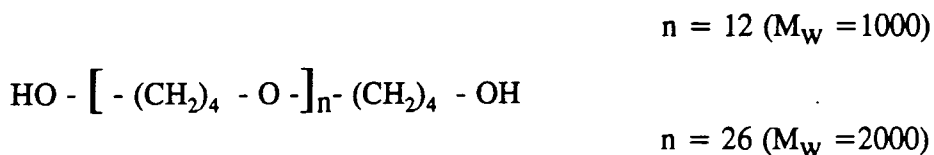
In-vivo experimentation by Lemm (1984) revealed that after 9 months subcutaneous implantation in rats, average molecular weights had reduced by 25% with surface fissuring also in evidence. Similar studies over a five month period of implantation in calves also indicated surface cracking of this material (Hennig, 1984). However, fixed strain tests by Lelah and Cooper (1986) suggested that the resistance of Pellethane to surface crack propagation is similar to Tecoflex samples of comparable hardness. Both are described as being vastly superior to the Biomer range of polymers.

The flex life of this material has also been investigated (Lemm & Buckerl, 1984) with a view to usage in artificial heart components. This application requires a material to withstand 40-50 million cycles per year. It was found that by using Pellethane with high average molecular weights, flex lives of over 240 million cycles could be obtained. Sterilisation by irradiation has also proved to have minimal effect on the mechanical properties of Pellethane (Ulrich and Bonk, 1984), an important consideration for an implant material.

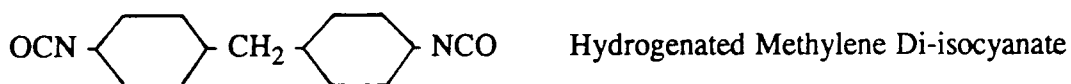
Pellethane 2363 - 80°A grade was used throughout the research work at Durham. This followed previous work with Castomer (a non-biocompatible resin) which suggested that a material hardness of about 80°A Shore provided good tribological properties.

2.3.2 Tecoflex

A second segmented polyurethane elastomer was supplied by Thermedics. It was available in extrusion and solvent castable grades and a range of Shore hardness values from 80°A to 72°D. This is a polyether urethane based on hydrogenated MDI (HMDI), PTMO and 1,4 Butanediol. Material grades up to 85°A (Shore Hardness) make use of PTMO 2000 (average molecular weight of 2000) as the polyether-diol and the harder grades use PTMO 1000. Variations in the ratios of hard to soft segments alter the hardness of the product to give the range specified.



The weights of the polyol components are responsible for the variation in processing temperatures exhibited by this material, which is from 150-160°C (75-85°A Shore) and 140-150°C (93 and 100°A Shore) (Dawber and Healey, 1991). HMDI (below) is considered to produce an aliphatic product due to saturation of the cyclohexane rings.



The aliphatic chain tends to promote surface hydrophilicity (Williams, 1982). *In-vivo* tests of up to two years have been carried out and results concluded that Tecoflex exhibits minimal tissue reaction and remains bio-compatible throughout (Dasse *et al*, 1988). It is utilised in artificial hearts (Dasse, 1984). In fact aromatic and aliphatic polyurethanes show similar properties in such areas as bio-compatibility, mechanical strength and elongation, the range of hardnesses available and hydrolytic stability. However, the differences between the chemical structure are potentially very important. Thermedics literature states that aliphatic urethanes can be extruded at temperatures 55°C below those required for aromatic urethanes, reducing the thermal history of the product and the chance of impaired mechanical properties. In addition improper processing of aromatic polyurethanes can lead to the production of carcinogens (Brown, 1988).

Tecoflex has proved to respond well to fatigue environments, with 50 million flex cycles exceeded without failure in experimental heart valves (Szycher *et al*, 1977). However, research on this material has not been as extensive as on Pellethane.

Initially three grades of Tecoflex were obtained, all of extrusion grade and of designated Shore hardness values of 80°A, 85°A and 93°A. However, following processing and the response of the polymer to a warm hydrating atmosphere, a harder grade was also considered at Shore 100°A.

2.3.3 Estane 5714F1

Estane "57" is a polyether urethane which can be fabricated by solvent casting, injection moulding or compression moulding. Its use as a biomedical polymer has been limited despite its excellent resistance to hydrolysis and fungus attack (Estane literature) and showing little softening in the body environment. Boretos and Detmer (1970)

demonstrated its promise in biomedical applications and its use in Left Ventricular Assist Devices (LVAD's) has also been well received (Bernstein *et al*, 1974)

Bio-compatibility seems good with minimal response following six weeks implantation in rats (Calnan, 1963). Lemm (1984) noted that Estane "57" showed no reduction in average molecular weight following six months sub-cutaneous implantation in rats, unlike Pellethane which showed a reduction of 25%.

Cross-linking of this elastomer is possible which can result in increases in hardness and improvements in fatigue life. The grade used in this study had a specified Shore hardness of 77^oA.

2.3.4 Estane 58271

This material from the family of Estane polymers is a polyester urethane and as such should be susceptible to the actions of hydrolysis. It was included in the study to provide a control for the *in-vitro* studies. Boretos *et al* (1971) examined a similar grade of this material as sub-cutaneous implants in mongrel dogs and after 18 months the samples had fragmented so badly that less than 20% of the original implant was visible. The grade of material used had a Shore hardness of 83^oA and showed very similar mechanical properties to the Estane "57" material.

2.4 Mechanical Requirements for the Material and Design of the Prosthesis

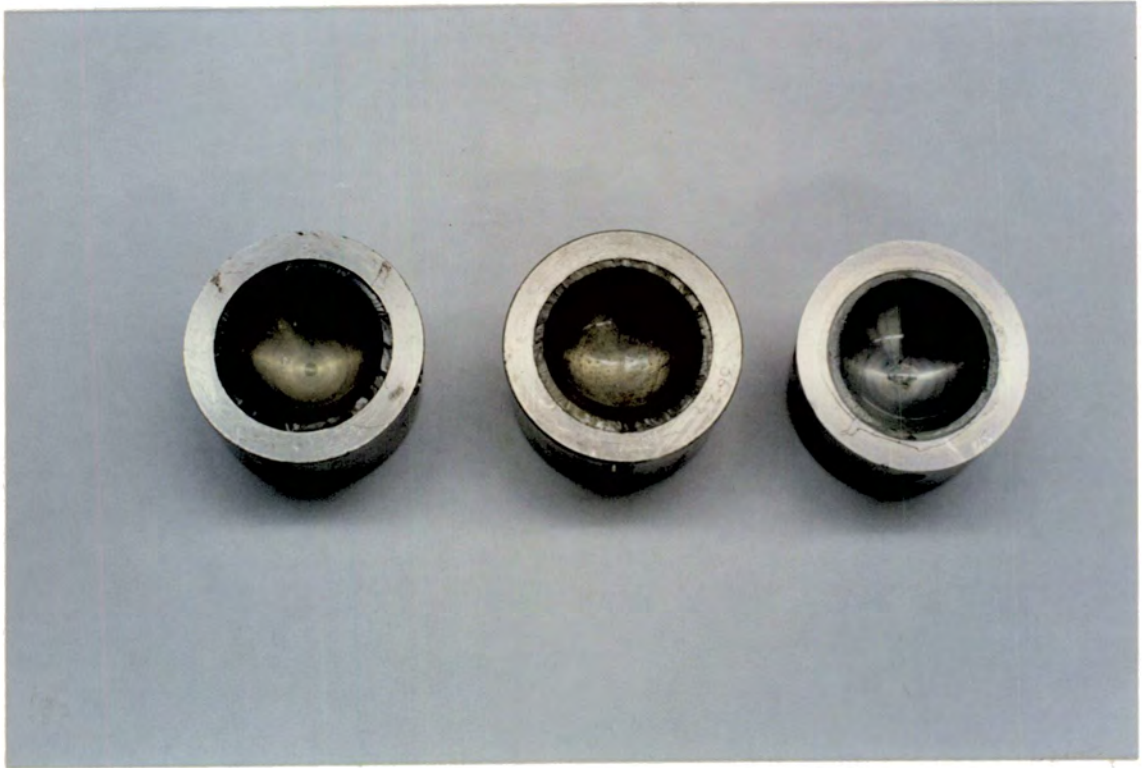
Polyurethanes are currently used in the body only in lightly loaded situations. Even in a heart valve the stresses are small, even though large deflections are often present. Although resistance to fungal growth is important in these applications, surface roughening, possibly brought about by surface fissuring or stress induced cracking is not critical unless acting as an initiator for failure. Thus, to consider these

materials for use in an artificial joint requires a great deal of material testing in representative conditions. At the outset of the project only Castomer, a material toxic to the body had been successfully used as an elastomeric layer. This was chosen for initial studies due to the simple processing and the range of hardnesses which could be made.

The material would have to withstand peak compressive stresses of 10MPa (for example when jumping) and be able to operate under extended cyclic loading to 3.5MPa (Section 6.3). In addition shear stresses at the bond between the layer and the backing material would also be high. At these stress levels, deformations of 0.250-0.400mm were expected and with a layer thickness of 2.0-2.5mm the strain could reach 20%. In addition the resistance of the polyurethane to abrasion and erosion would be an important advantage in this application as there can be particles of bone and cement (PMMA) in the joint cavity following the operation. Polyurethanes have been shown to be highly resistant to this form of wear and in some industrial applications have replaced steel and ceramics (Li and Hutchings, 1990).

Stainless steel backed cups were initially used. These were produced both with and without lugs at the periphery by a vacuum moulding technique (figure 2.1). The chemical bond between the two materials was found to be weak and this has been confirmed by other groups (Laberge *et al*, 1992). Thus, lugs were used on all later samples. The stainless steel (316L) was formed into a tapered cylinder which located in the friction carriage of the simulator (Section 5.3.6). The cups were produced on a CNC lathe with good accuracy and a spherical inner radius of 18.13 ($+0.00/-0.05$) mm.

Figure 2.1 : Stainless Steel Backed Acetabular Cups



2.5 Preparation of Specimens

A number of methods were used to form the test pieces for mechanical and tribological assessment of the polymers. All of the techniques involved the softening of the polyurethanes through heating, followed by moulding. Through these methods, a flaw free sample could be obtained. However, the heat history of the sample was kept to a minimum to reduce the possibility of thermal degradation. The use of solvent casting techniques was largely dismissed due the possibilities of the residual solvent affecting bio-compatibility and the fact that a production process (Section 3.6) was more likely to rely on a hot melt processing technique. Solvent casting is more applicable to thin films (<0.5mm) cast on a flat surface than a 2-3mm layer bonded to a curved acetabular cup. However, the use of Tecoflex dissolved in Tetra-hydro Furan (THF) as an adhesive is discussed in Section 3.6.

2.5.1 Vacuum Moulding

This method of preparation made use of the vacuum oven to overcome bubble and pore formation in the elastomer during processing. The method was largely successful in producing metal backed cups for tribological analysis. Pellets of polyurethane were used in the preparation of cup samples after they had been dried in open trays at 37°C. The pellets were then placed in a stainless steel cup in a pre-heated oven under vacuum (30-50mbar) for 20-25 minutes. The temperature used was dependent on the polymer, with Tecoflex 93 & 100°A processing at 170°C, and 180-185°C used for Tecoflex 80 & 85°A, Pellethane 80°A and the two Estane polyurethanes. The cups were then removed from the oven and pressure applied to a 16.38mm diameter sphere which was indented into the polymer to produce the cup. The assembly was then force cooled in water. Shrinkage of the elastomers produced final cup dimensions with an internal radius of 16.13mm (0.250mm radial clearance

when used with a 15.88mm radius femoral head). All the polymers could be manufactured without bubbles, but Pellethane was the easiest to process.

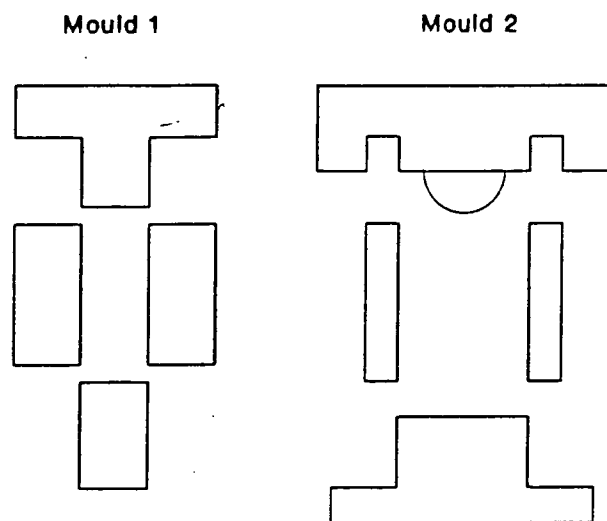
2.5.2 Compression Moulding

Thin tensile and plate specimens (of the order of 1-2mm thickness) were prepared by compression moulding between heated platens. Typically 20-30 tonnes was applied over a 10cm square sample, by means of a hydraulic ram. Platen temperatures of 150-160°C were typical. Specimens were produced from both pellets (which was the form in which all of the biological polyurethanes were received) and injection moulded sheets of 4mm thickness from UMIST with good reproducibility and few voids. Overheating resulted in highly porous samples.

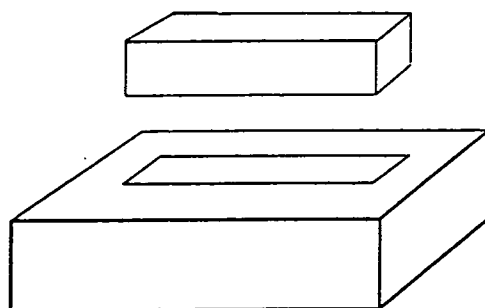
Compression moulding formed the basis of bonding of the layers to rigid UHMWPE backing materials (Section 3.6). The melting temperatures of polyurethanes (155-170°C) and the polyethylene (130°C) were sufficiently close to allow this. In addition, the high molecular weight of the grades of polyethylene used increased their melting temperature closer to that of the urethanes. Temperature control allowed the platens to be adjusted independently and loads of up to 45 tonnes could be applied. Blister tests samples, peel samples and cup samples were produced in three moulds, shown schematically in figure 2.2a.

Mould 1 enabled disc specimens of 31mm diameter and up to 8mm thickness to be produced. These could easily be prepared without bubbles because of the simplicity of the mould. Blister test specimens were constructed by incorporating a disc of PTFE (to stop bonding) over the central portion of the PE/PU interface. The discs were also sliced to yield peel test specimens, although these had a relatively short bond length which could lead to inaccuracies (BS 5350 C9-14).

Figure 2.2a: The Moulds used in the preparation of Experimental Polyurethane/Polyethylene Bonded Samples



Mould 3



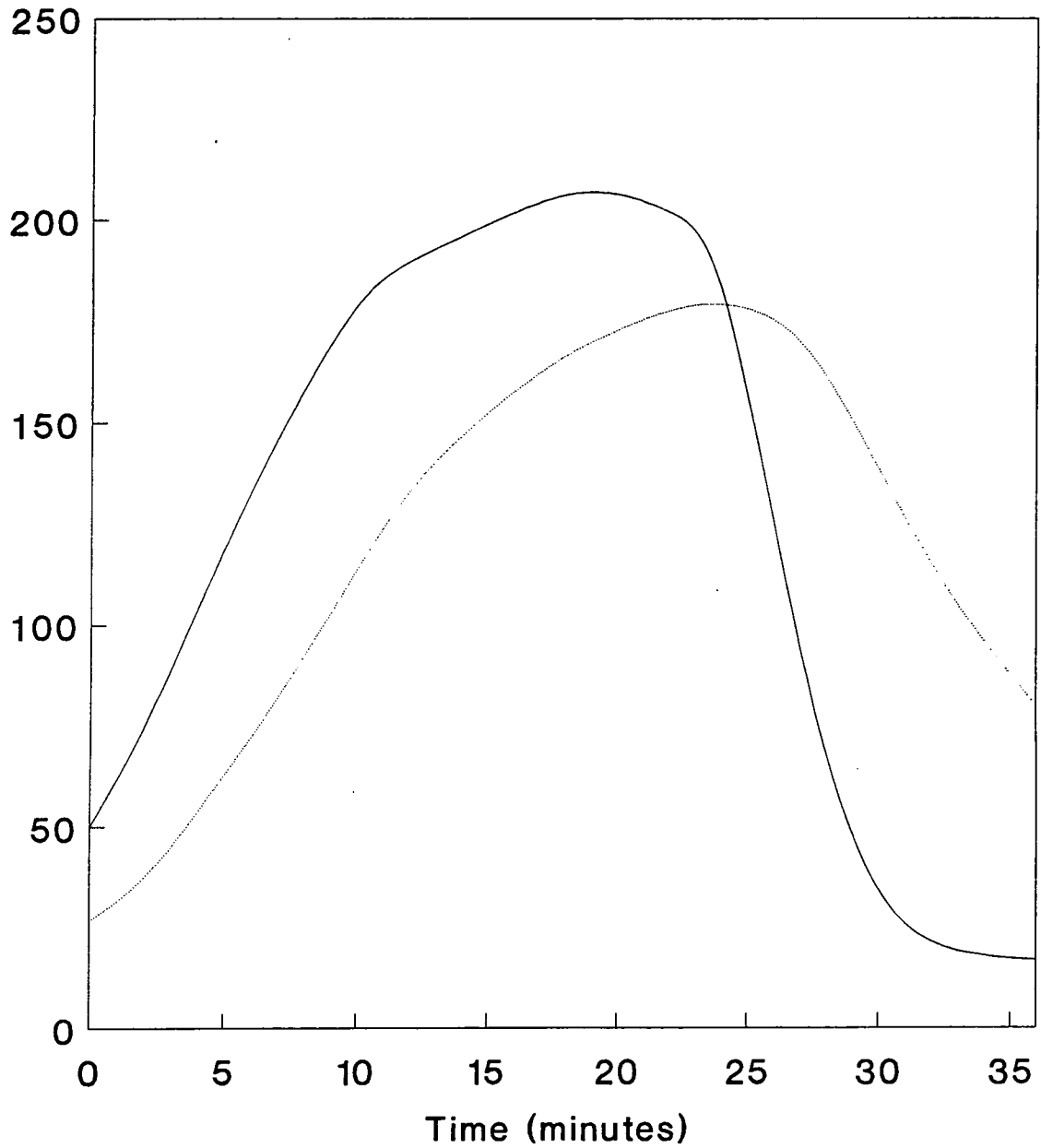
Mould 2 allowed prototype acetabular cups to be constructed. These required a layer thickness of at least 2mm to give the required cup hardness for acceptable tribological properties. To facilitate this, a number of acetabular moulding balls were made which allowed accurate construction of the cup when coupled with monitored quantities of polymers.

Mould 3 addressed the problem of Mould 1 and produced specimens of 70mm in length and 20mm in width. PTFE was used initially in the moulding process to yield an unbonded region but it was found that slicing along the bond line was adequate to start the "crack" so the use of PTFE was abandoned.

Extensive experimentation concluded that the best components were formed when the component was made in one heat cycle. Powdered UHMWPE was compacted under a load of 10-30 tonnes, depending on the mould (a surface pressure of 120MPa). Polyurethane granules (circa. 3mm in diameter) were then added and compressed into the polyethylene surface under a pressure of 60MPa and heat was added. Thermal degradation can be a problem with polyurethanes so it is advantageous for the sample to spend as little time as possible at the higher temperatures. A higher pressure tended to allow better conduction between the mould and the sample but on occasion, was seen to hinder the removal of trapped air from the sample. The acetabular cup specimens proved to be the most difficult samples to produce without bubbles. A compromise pressure was found by experimentation to be 15-30MPa, and this was used at the higher temperatures during the moulding process. A graph of platen and mould temperatures for a bubble free Polyethylene/Polyurethane acetabular cup is shown in figure 2.2b. The temperature in the centre of the mould can be seen to lag behind the platen temperatures due to the length and large thermal mass of the die.

Figure 2.2b : Mould and Platen Temperatures for the Preparation of a Bonded Acetabular Cup

Temperature ($^{\circ}\text{C}$)



— Platen Temp. ($^{\circ}\text{C}$) - - - Die Temp. ($^{\circ}\text{C}$)

2.5.3 Injection Moulding

Plates 100mm square and of 4mm thickness together with 4mm thick tensile specimens were produced on a Negri-Bossi injection moulding machine at the Materials Science Centre, UMIST. For a commercial prosthesis, ideally the cup would be made by this process as pores within the samples were extremely rare. Barrel temperatures of 170-190°C were used with a shot size of 150mm. The platens were maintained at 20°C to act as a heat sink. During flushing of the machine it was noticed that polyurethane and polyethylene (low density) will mix to form a polymer blend and this may form the basis for injection moulding of a bonded sample.

2.6 Hardness and Elastic Modulus Measurements

The importance of the hardness and elastic modulus of the polyurethanes to be used was seen as critical to the production of a successful joint and test protocols were produced and revised in order to allow accurate testing of the materials.

2.6.1 Introduction to Hardness

The tribological properties of elastomeric layers are highly dependent on their mechanical properties. Unsworth *et al* (1987, 1988) concluded that an acetabular cup of hardness 3.5-9.0N/mm² (H20/30 DIN53456) provided the best tribological performance.

Hardness is a measurement of the ability of an indenter to penetrate a surface (DIN 53456, Brinell or Vickers) or the loss of energy of a ball dropped onto the surface (Shore). It can be used to estimate the elastic modulus of a material (Taylor and Kragh, 1970; Waters, 1965). However, hardness is dependent on the thickness of the layer as well as its surface properties. In addition, the interface between indenter

and layer and the layer and the rigid substrate are important (Jaffar, 1989). Changing the applied load can lead to changes in the measured hardness values. As such it is only possible to use hardness measurement as a comparison with other materials tested under identical conditions. In addition visco-elastic materials tend to show different hardness values as many of the tests require the load to be maintained for a number of seconds.

The aim of this part of the study was therefore to assess the effect of changing layer parameters on the hardness values obtained from tests based on DIN 53456 with a holding load of 5N and a maximum load of 25N. A comparison was also made between hardness and the elastic modulus measurements in order to make comparisons between the experimental and theoretical results. This enabled a calibration to be made from the performance of the strip samples which could be applied to metal or UHMWPE backed cups.

2.6.2 Theory behind Hardness Testing and the DIN Standard Hardness Test

The hardness test detailed in DIN 53456 seemed the most appropriate to use for an elastic material since the penetration is monitored during the test. This is unlike the Brinell test, which relies on measurements of the size of the indentation left in the surface following removal of the load (the plastic deformation).

The DIN 53456 hardness test relies on a loaded steel ball (Vickers Hardness > 800) penetrating the surface of a layer and defines

$$\text{Ball indentation hardness} = \frac{\text{Major Load}}{\text{Area of Indentation}}$$

which can be written as:

$$H (20/30) = \left[\frac{0.21}{0.21 - e_r + e} \right] \left[\frac{F}{\pi d e_r} \right] \quad 8.1$$

A minor load is applied to the specimen to allow accurate determination of the starting penetration. The minor load was held for 5 seconds and then quickly ramped to the major load. The major load could be chosen to give a penetration between 0.150 and 0.350mm after thirty seconds at that value, as detailed in DIN 53456. A computer controlled Hounsfield testing machine was used for the measurements at room temperature and a Lloyd 6000R testing machine with a temperature cabinet was used for the measurements at 37°C (Section 3.3).

A plot of load against penetration for Estane '57', one of the bio-compatible polyurethanes is shown in figure 2.3. It can be seen that at low loads (below 3-4N) the initial contact is still being formed and results would be inaccurate if a load below this were used as the minor load. The minimum load was altered and the change in final hardness values recorded.

Table 2.1

Minor Load (N)	Major Load (N)	Hardness (N/mm ²)
2.5	22.5	2.99
5.0	25.0	3.28
10.0	25.0	3.32

A load change (Major Load - Minor Load) of 20N was chosen to give a range of Hardness values of 3.4-9.5N/mm², corresponding to the acceptable range of penetrations (figure 2.4).

Figure 2.3 : A Plot of Load/Penetration for the DIN 53456
Hardness Test

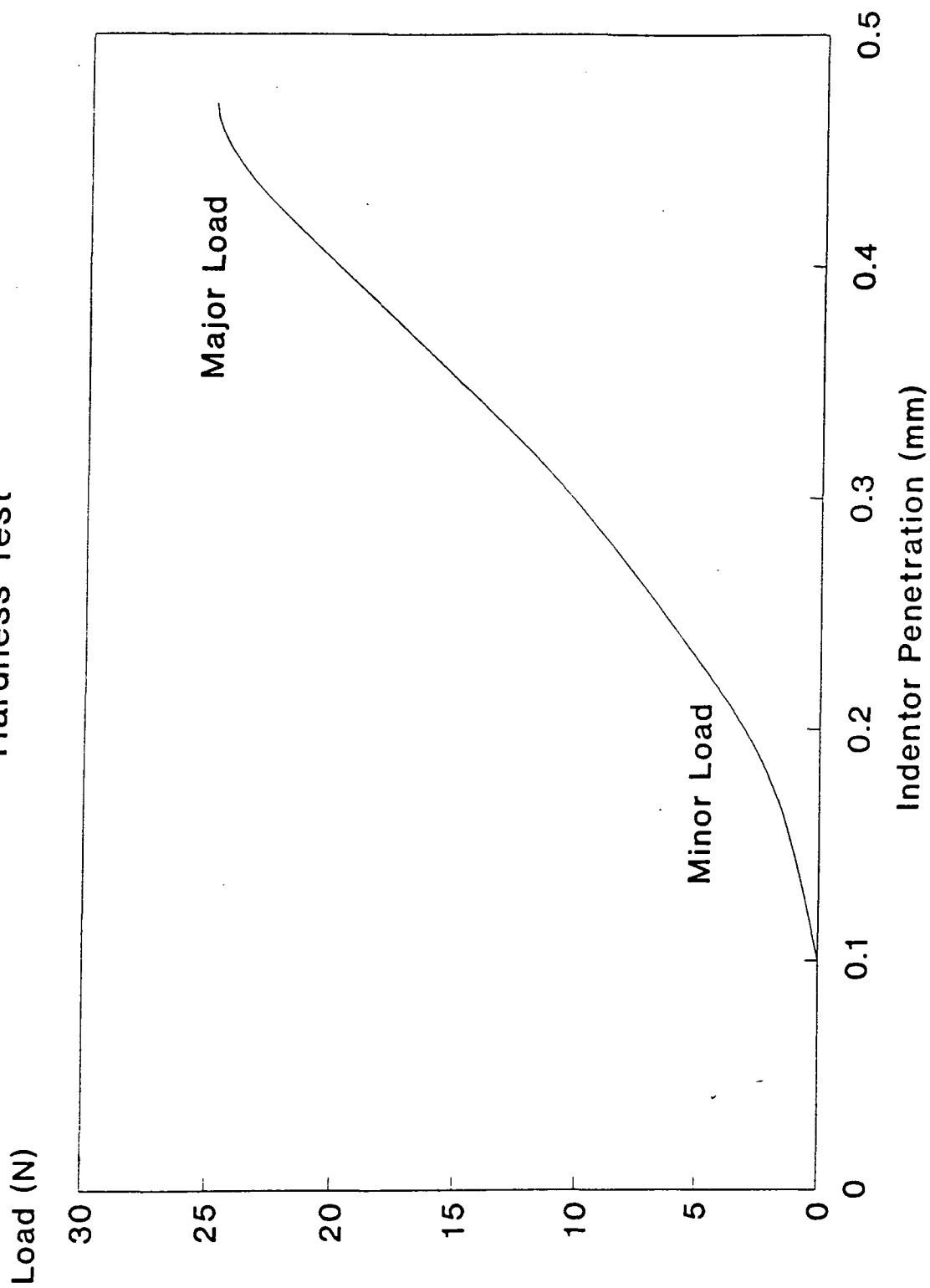


Figure 2.4 : Indentor Penetration and its relation to the DIN 53456 Hardness Value

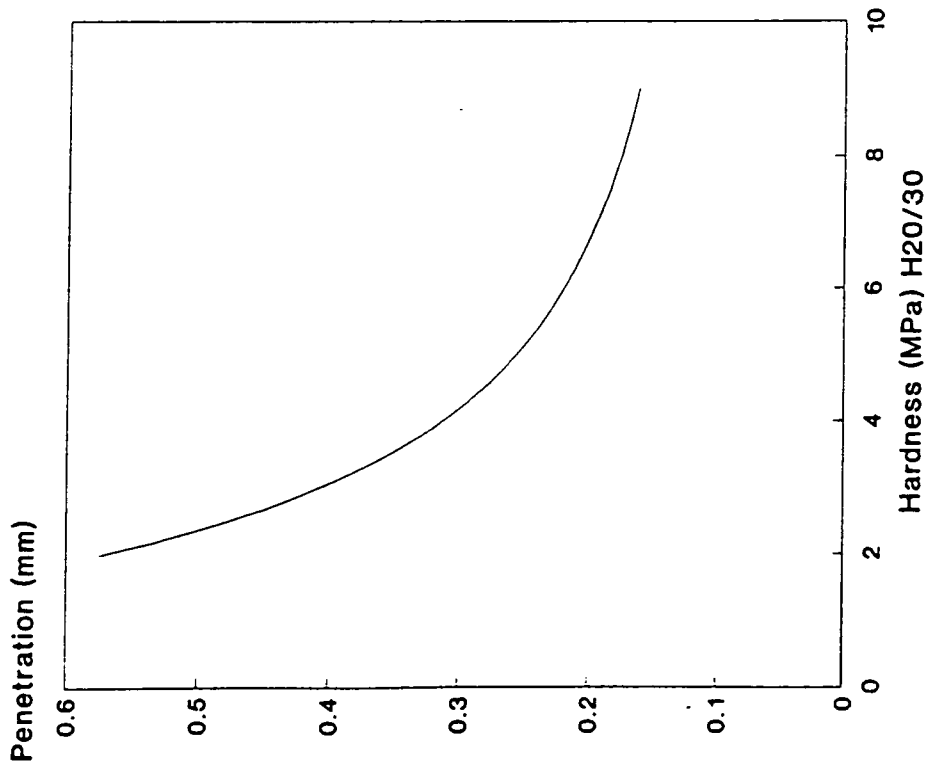
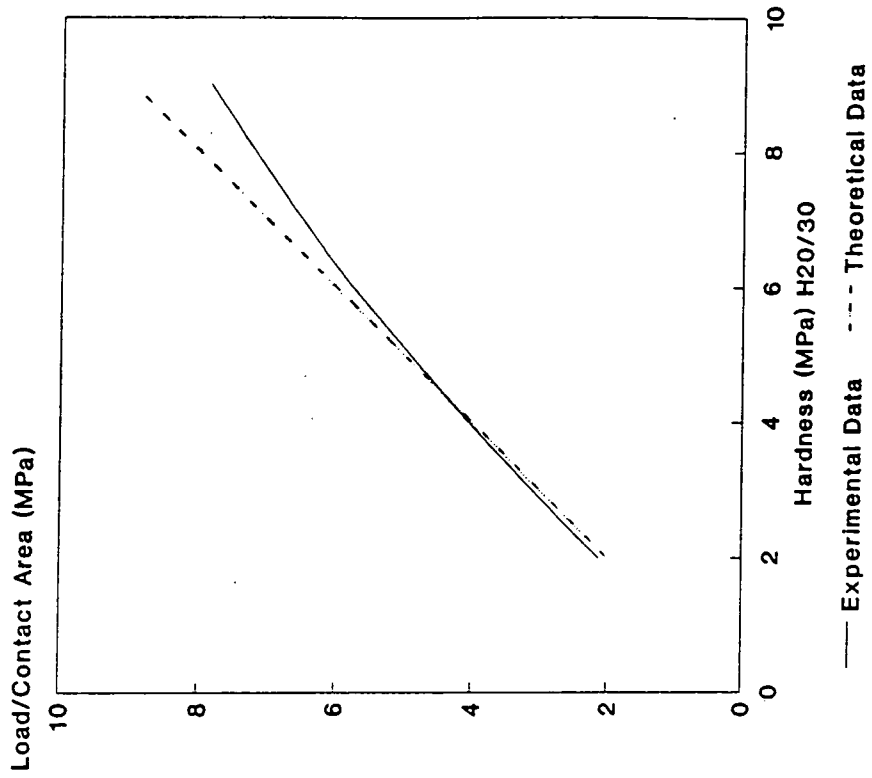


Figure 2.5 : Calibration of the DIN 53456 Hardness Test



At low penetrations or with harder samples the results from equation 2.1 tended to drift away from the load/indentation area plot (figure 2.5), indicating the problem of using too small an indentation. At low values of hardness the curves are very similar, thus it is likely that penetrations greater than 0.350mm are acceptable (providing the samples are thick enough). This increased the range of hardness values that could be accurately measured to 9.5-2.0N/mm².

The DIN test specified a minimum material thickness of 4mm to eliminate the effects of the backing material. Unsworth *et al* (1987, 1988) concluded that layer thicknesses of 2mm gave good tribological results and by using a thin layer the shear stresses at the interface between this layer and its backing material can be reduced (Armstrong, 1986). Thus, for the cup samples it was likely that the backing material and the bond of the urethane to it would have an effect on the measured values of hardness.

2.6.3 The Effects of Sample Thickness on Hardness Values

2.6.3.1 Materials and Methods

The effect of layer thickness and the percentage penetration of the indenter on hardness values was investigated. A number of commercially available elastomers were used covering a range of specified hardness values, measured on the Shore scale.

The Castomer polyurethane was produced in three grades; 75, 80 and 85^oA, and cast onto flat plates to form the samples. The upper surface was not constrained by a plate as a better surface finish could be obtained by leaving it to cure in air. The bio-compatible polyurethanes were formed using two methods. The thicker samples (4mm) were produced by injection moulding while the thinner samples were made by compression moulding between flat plates. In this way, thickness could be controlled

by shims placed between the plates. Tecoflex 80, 85, 93 & 100^oA grades were all investigated as was Pellethane 2363-80^oA and Estane 5714F1(77^oA) and 58271(83^oA). A large range of Tecoflex polyurethanes (in particular those of harder Shore Grades) were investigated, as the Hardness values obtained using the DIN 53456 test were lower than expected from the Shore values. For comparison Tecoflex grades 85, 93 and 100^oA gave hardness values (DIN 53456) of 1.95, 2.4 and 3.55N/mm² respectively, which compared with 3.10N/mm² for Estane 5714F1 (77^oA) and 3.40N/mm² for Pellethane (80^oA). Although the DIN 53456 standard does not quantify the flatness and parallelism of samples, these were measured. Surface roughness was measured on a number of samples as 0.6 μ m R_a, which is sufficiently low to cause few problems. The samples were tested on a lubricated flat steel plate.

2.6.3.2 Results

As expected, the hardness values for all of the elastomers increased as the sample thickness was reduced. Figure 2.6 shows the results for the customer samples and figure 2.7 shows a similar plot for the bio-compatible polyurethanes. The general shape of the curves is the same with a lower limit of hardness at thicknesses greater than about 4.0mm. This represents the stage at which the stressed region under the ball is not affected by the lower surface of the material. At very low thickness values it would be expected that the curves for all of the materials would coincide as the effect of the steel support becomes dominant. This is suggested by the shape of the curves in figures 2.6 and 2.7. During the period at maximum loading it was noted that the Tecoflex elastomers, in particular the 93 and 100^oA grades, showed extensive 'creep' with the penetration increasing by as much as 0.15mm. This is much greater than the other bio-compatible elastomers where increases were only about 0.03mm. This was investigated further and the results are displayed in figure 2.8. Hardness measurements were made at 0 and 30 seconds application of the maximum load. It can be seen that

Figure 2.6 : The Effect of Sample Thickness on Hardness Values (DIN 53456) for two Grades of Castomer Polymers

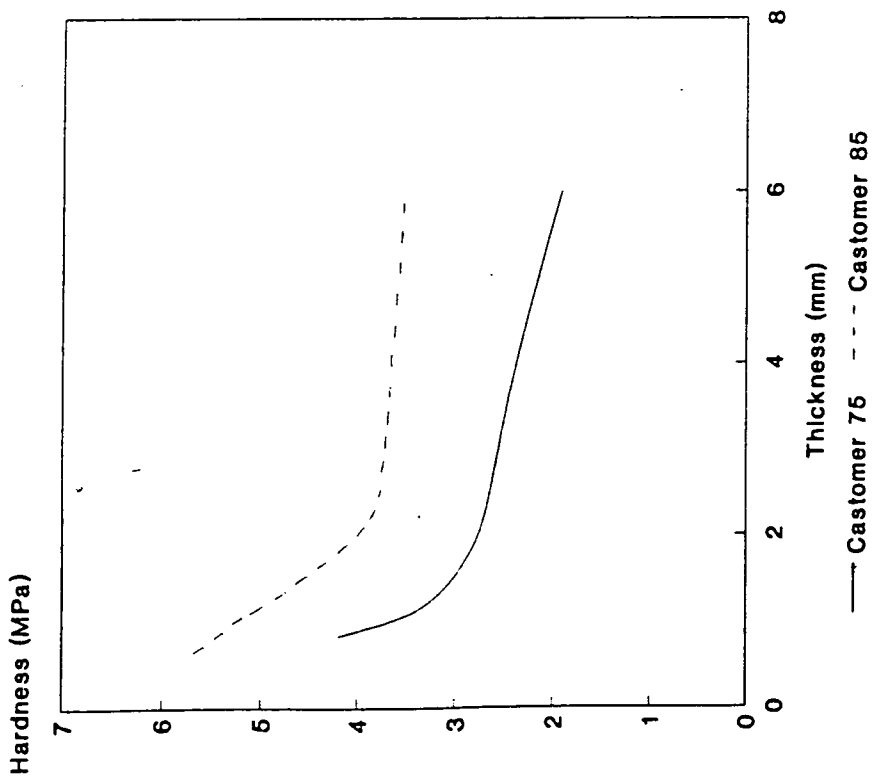


Figure 2.7 : The Effect of Sample Thickness on Hardness Values (DIN 53456) for Five Biocompatible Polyurethanes

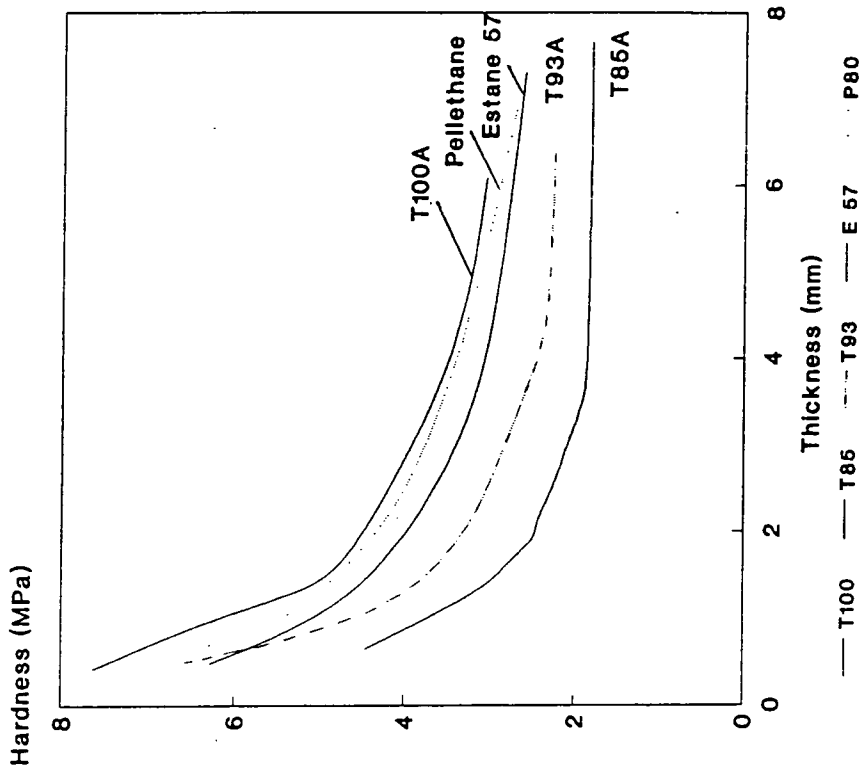
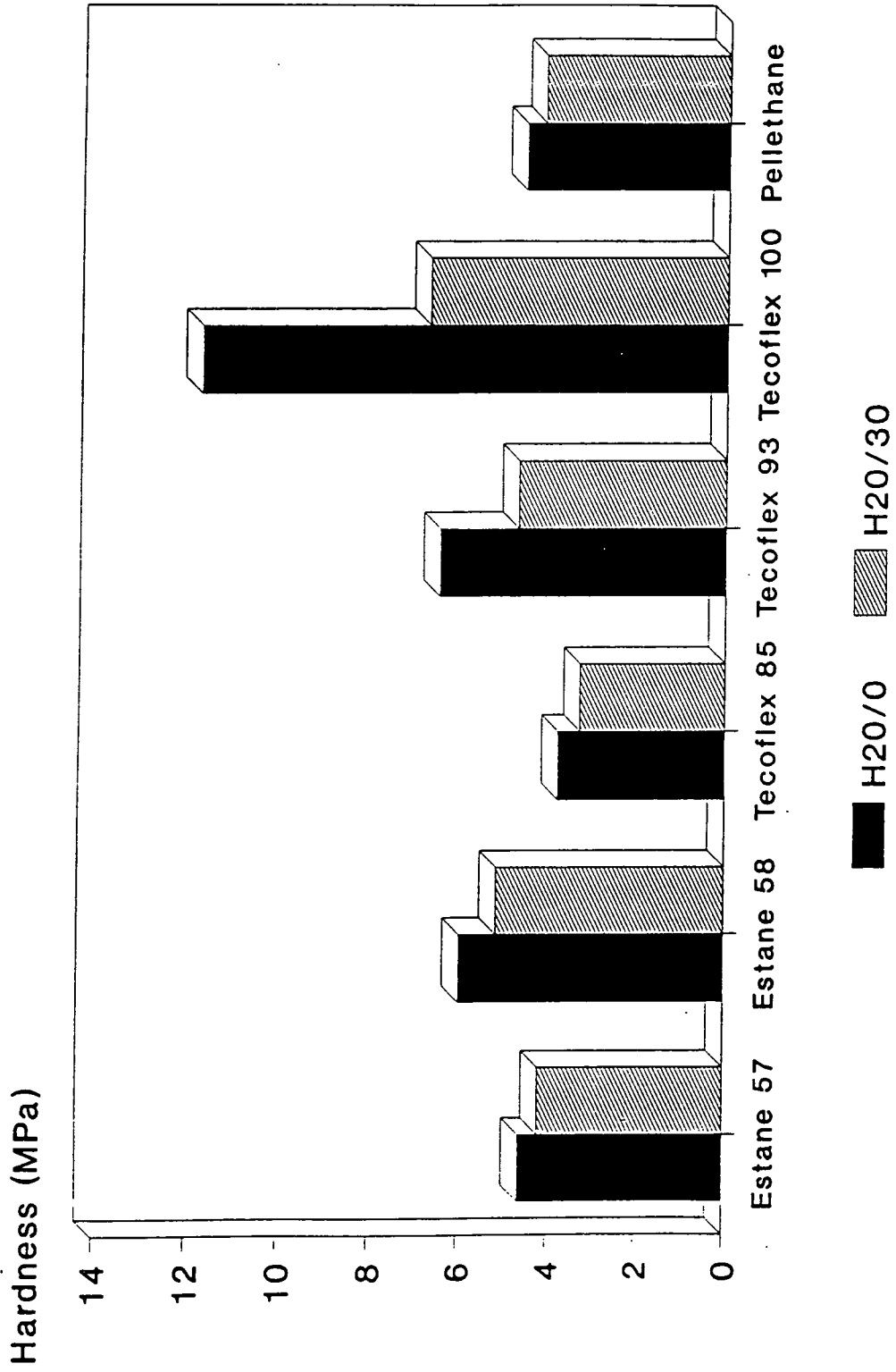


Figure 2.8 : The Visco-Elasticity of thin Samples of Biocompatible Polyurethanes undergoing Hardness Testing



this causes a large decrease in the hardness of Tecoflex 100^oA (up to 43%) and Tecoflex 93^oA (27.3%), with differences of 9-14% for the other polyurethanes.

2.6.3.3 Discussion

The DIN 53456 hardness test specifies that "the maximum penetration of the ball into the samples should not exceed 10% of the sample thickness". To investigate the changes that occur at large relative penetrations, the data from figures 2.6 and 2.7 were modified to produce figures 2.9 and 2.10 where hardness is plotted against the percentage penetration of the indenter. This showed that hardness was approximately constant up to 20% of the sample thickness. Therefore if this test is being performed on samples where the material properties are important then penetration values must be kept below this proportion of the sample thickness.

However, with samples destined for tribological testing, a bond between the polyurethane and the backing material was required. The effect of this bond on the hardness value was also assessed. A 13.3% reduction in hardness was obtained when the bond to the metal backing was destroyed. This was with a 2mm layer, which is the optimum thickness for the cup, and indicates the effect of the backing material even though the penetration of the indenter was less than 20%. It is thought that this is due to the reduction in the flow of the elastomer with a 100% bond (figure 2.11).

Figure 2.11 : The effect of the bond with the backing material on the indenter penetration for the Hardness Test

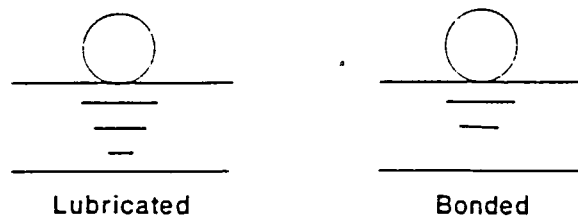


Figure 2.9 : The Change in Hardness with Penetration of the Indentor as a percentage of the sample thickness for Customer Materials

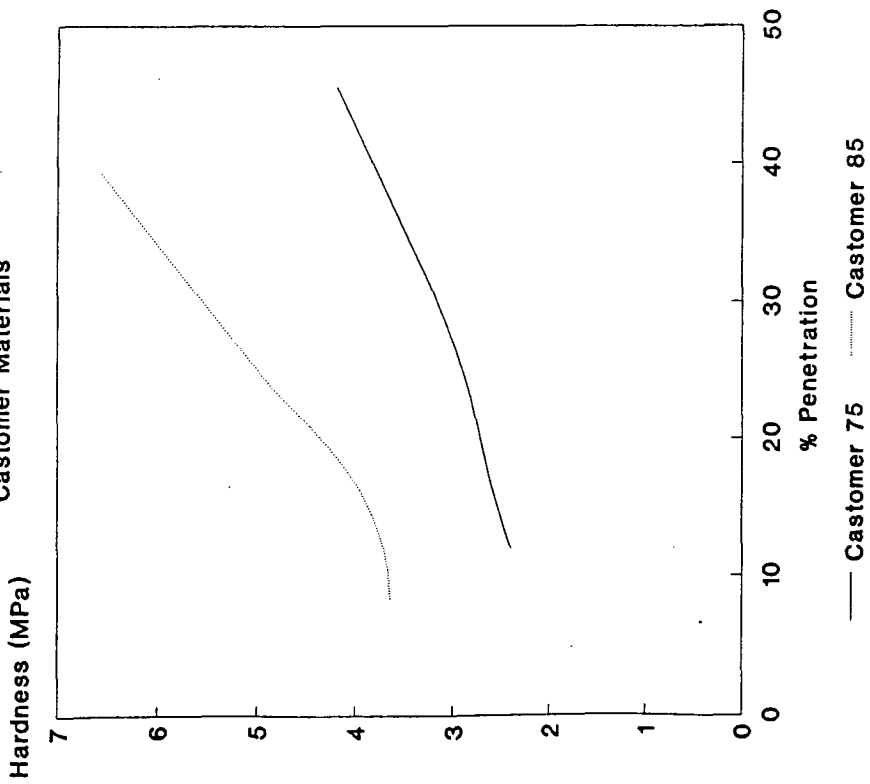


Figure 2.10: The Change in Hardness with Penetration of the Indentor as a percentage of the sample thickness for the Biocompatible Polyurethanes

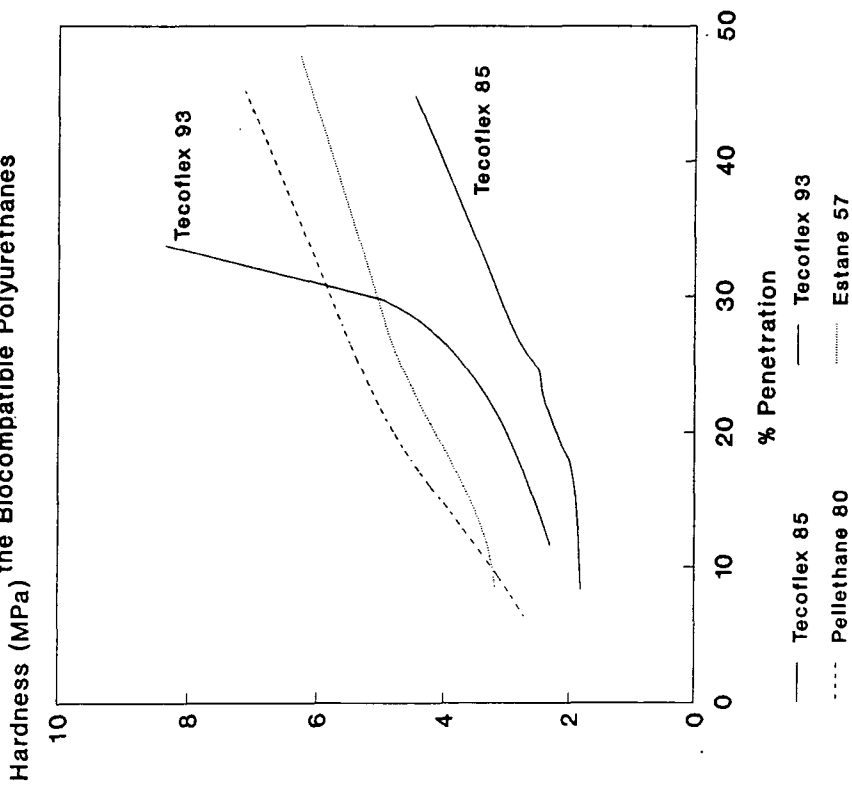


Figure 2.7 indicates that a successful bond with the backing material seems to reduce the effective layer thickness by about 15%. Therefore, this must be taken into account when estimating the hardness of the bonded layers.

The visco-elastic behaviour of the harder grades of Tecoflex appears to be a characteristic of these polyurethanes. The harder grades differ from the 85°A and 80°A grades by using PTMEG (1000) instead of the higher molecular weight PTMEG (2000) in the production of the material, as well as smaller amounts of 1,4 Butane-diol, and these seem likely to cause the changes.

2.7 Introduction to Elastic Modulus and its Measurement for Polymers

Load/extension curves for polymers show many different stages which represent activities within the matrix. Polyurethanes consist of many chains containing both hard and soft segments, and variations in the quantity of each alters the mechanical properties of the polymers.

A typical Engineering Stress/Strain curve is shown in figure 2.12a. At low loads the curve is quite steep, representing a stiff sample. This corresponds to untangling of the coils of the chains which make up the polymer and a re-orientation of these chains. This part of the curve can be explained theoretically with a good degree of accuracy. The second part of the curve, which shows a constant gradient, involves stretching of the coils of polymer to produce straight chains of material. The increase in the gradient of the curve at high strains represents the behaviour of the chains which have been stretched near to their maximum lengths, with the corresponding exponential increase in the atomic forces. The gradient and extent of the final region can indicate crystallisation induced by molecular orientation. As the load is reduced the recovery curve follows a similar profile. Hysteresis effects are in evidence and often the sample

Figure 2.12a: A Schematic Diagram of Engineering Stress / Strain for Polyurethane

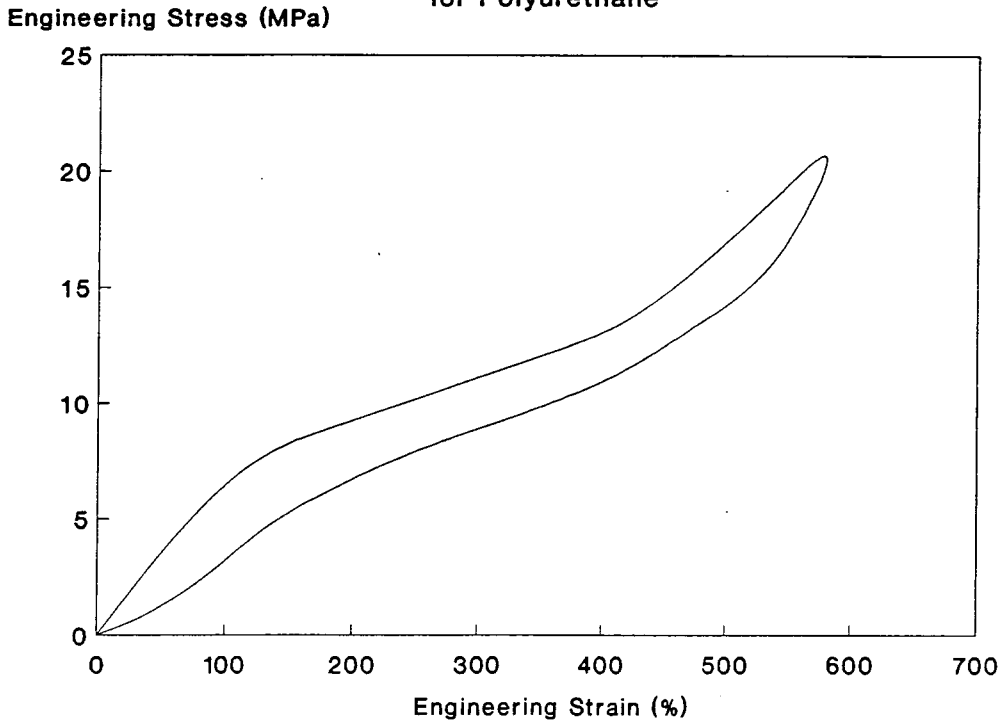
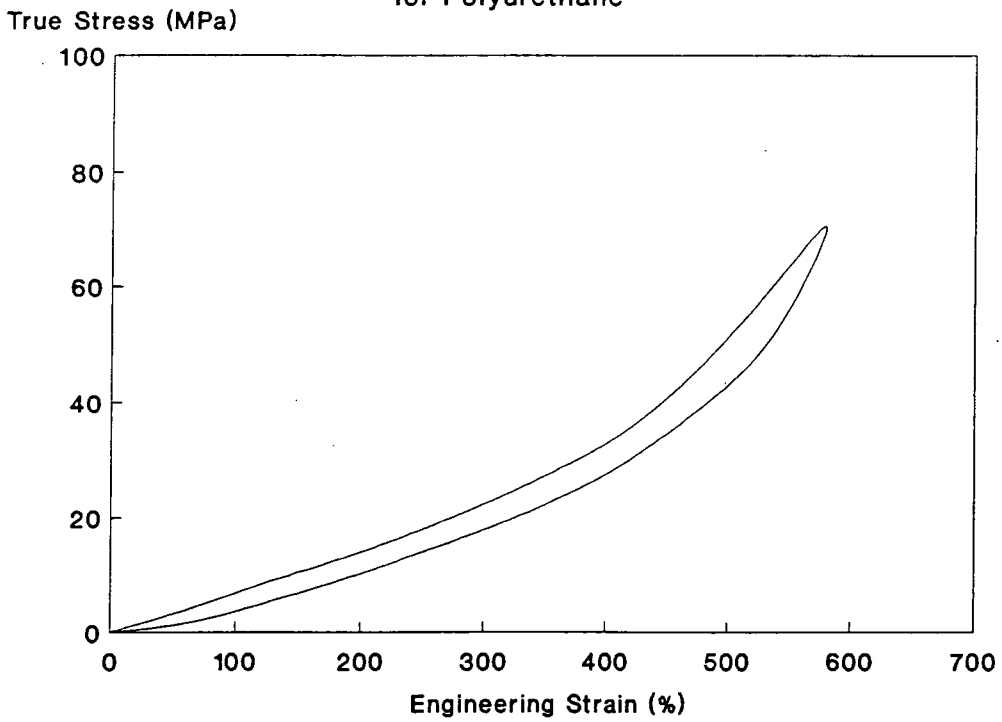


Figure 2.12b: A Schematic Diagram of True Stress / Strain for Polyurethane



is deformed from its original length on removal of the load. Much of this deformation is time dependent and recovery takes a few hours. If True Stress is plotted against Strain (figure 2.12b), the reduction in the cross section of the material upon deformation means that the elastic modulus increases very quickly as the strain increases and the three regions are not as distinct.

The value of elastic modulus is highly dependent on the part of the curve used. In use as a compliant layer in an artificial prosthesis it has previously been calculated that the maximum value of compressive stress caused by walking is in the region of 3.5MPa (Section 6.3). This value of stress corresponds to a point on the first region of the load/extension curve, even under *in-vitro* conditions, so the modulus during this region is most important. For this reason measurements made on samples being investigated for degradation and hydrated samples at 37°C (Section 3.3-3.5) concentrated on this part of the curve.

2.7.1 The Theory of Hardness and Elastic Modulus Interactions

Hertzian theory predicts that elastic modulus may be calculated directly from parameters obtained from indentation of a ball into the surface of the solid. This is the same arrangement as the hardness test used in this study.

$$E = \left[\frac{9}{16} \right] \left[\frac{F d}{2 a^3} \right] \quad 8.2$$

The contact radius, a , is calculated from the penetration of the ball between the minimum load of 5N and the maximum load of 25N used for the hardness test.

$$a = (d e - e^2)^{1/2} \quad 8.3$$

This analysis does not take into account the effects of sample thickness and as such relies on an infinite solid. From the previous hardness tests (figure 2.7) it can be

seen that for thickness values greater than 4mm the effect of further changes in thickness is minimal. Therefore, this analysis should be limited to thickness at or above 4mm.

Waters (1965) used results obtained by Timoshenko and Goodier (1951; 1970) to obtain expressions for elastic modulus from indentations on thin sheets, where interaction with the backing material was apparent. He used a number of ball sizes from 3-10mm in diameter pressed into thin rubber sheets which were 1.5-18.5mm thick. They were supported on a rigid metal block. His experimental results allowed the following equation to be obtained:

$$E = \left[\frac{9}{16} \right] \left[\frac{2 F}{d} \right] \left[\frac{\{1 - (\exp)^{-A/a}\}}{e} \right]^{3/2} \quad 8.4$$

$A = 0.67$ for a lubricated lower boundary, 0.41 for a non-lubricated lower boundary.

In all of the tests performed on polyurethane sheets a PTFE spray was used to ensure lubricated conditions. Thus, a value of 0.67 was used for A in the theoretical analysis.

2.7.2 Results

Results were collated on three graphs. Figures 2.13a and 2.13b show the accuracy of the basic Hertzian theory for sheets of 4mm thickness. It can be seen that the slope of the experimental data, which comprises a number of different polyurethanes, fits well with the theoretical line. Tecoflex 93^oA showed a lower hardness than expected from Hertzian theory. This can be explained by the strain rate dependent properties of the material and the creep it exhibits under load (figure 2.8). This led to increases in the penetration of the indenter of about 0.100mm under application of the major load (25N) for 30 seconds. This represents a reduction in

Hardness of about 30% due to the this time under load, which is not a factor in the elastic modulus measurements.

Differences in the magnitude of the hardness values from experiment and theory for measured elastic moduli are also small. Figures 2.6 and 2.7 showed that the variation of hardness with thickness was similar for all of the elastomers and so only the bio-compatible polyurethanes were used to investigate Waters' theoretical results. The results of his work were displayed as lines of constant elastic modulus in figure 2.14. It can be seen that there is good agreement between the theoretical curve and the measured data.

2.7.3 Discussion

Measurement of the elastic modulus of a material is not easy to accomplish. It relies on testing samples which can rarely be produced from the finished component. Tensile samples have to be produced, leading to possible inaccuracies if processing has been accomplished differently. The tensile specimens have to be cut and checked for stress concentrations and then accurately measured dimensionally. The testing machine must have grips which provide good transference of stress with minimal slippage and the forces developed can be quite high necessitating a stiff loading frame on the testing machine.

Figures 2.13a, 2.13b and 2.14 have shown that the elastic modulus can be determined easily and simply from hardness tests on any thickness of sample. Allowance can even be made for the backing material, such as in the case of cup samples used for tribological assessment. The test is both simple and quick to perform and the spread of results from samples of the same material is normally small. The use

Figure 2.13a : Elastic Modulus against results from the
DIN 53456 Hardness Test, showing Hertzian Theory

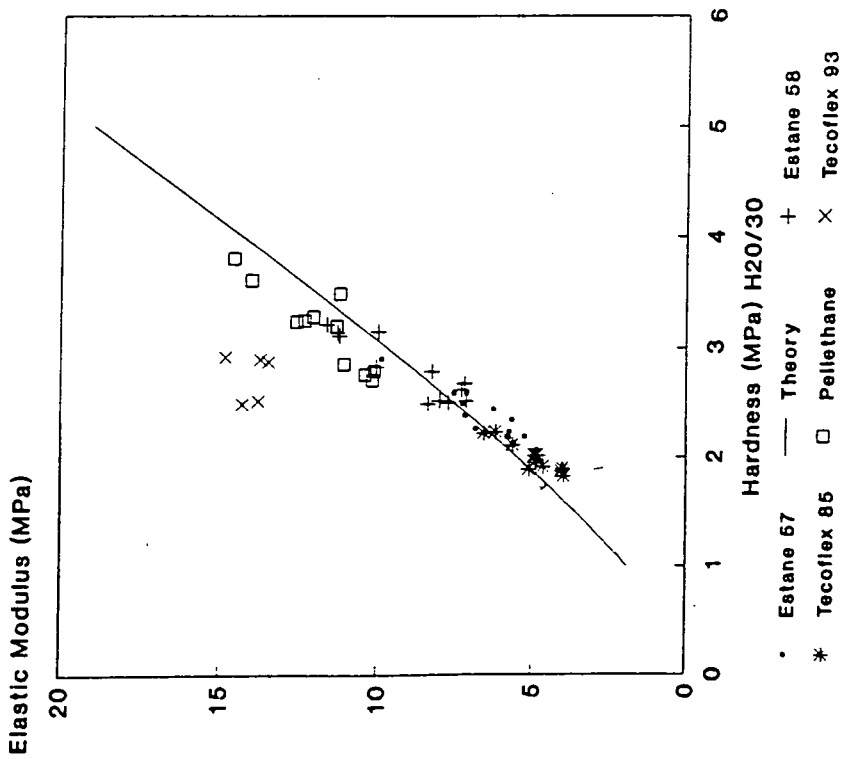


Figure 2.13b : Elastic Modulus against results from the
DIN 53456 Hardness Test, including Hertzian Theory

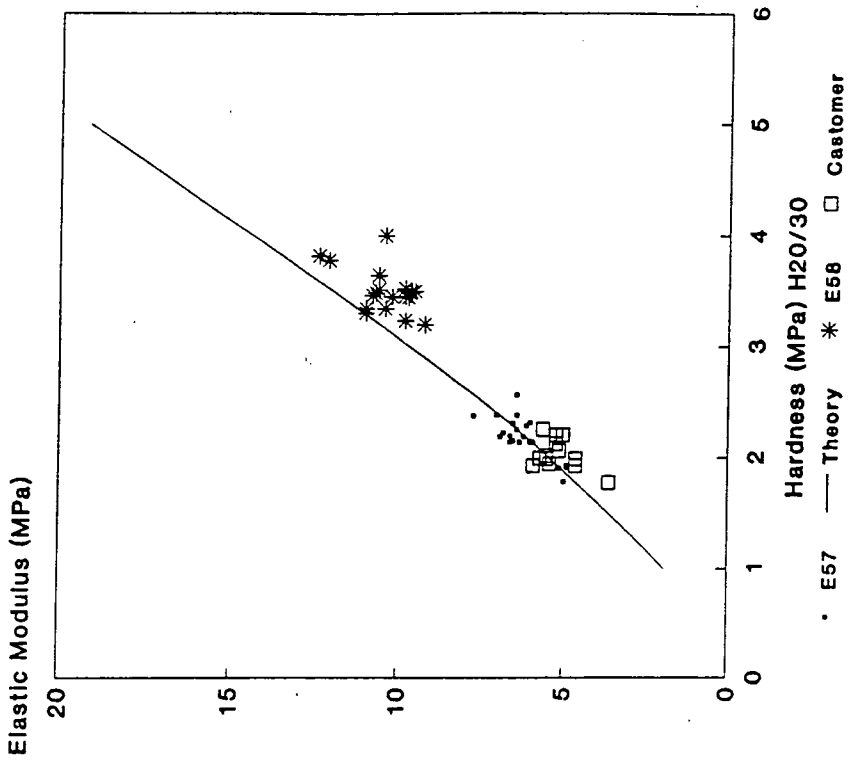
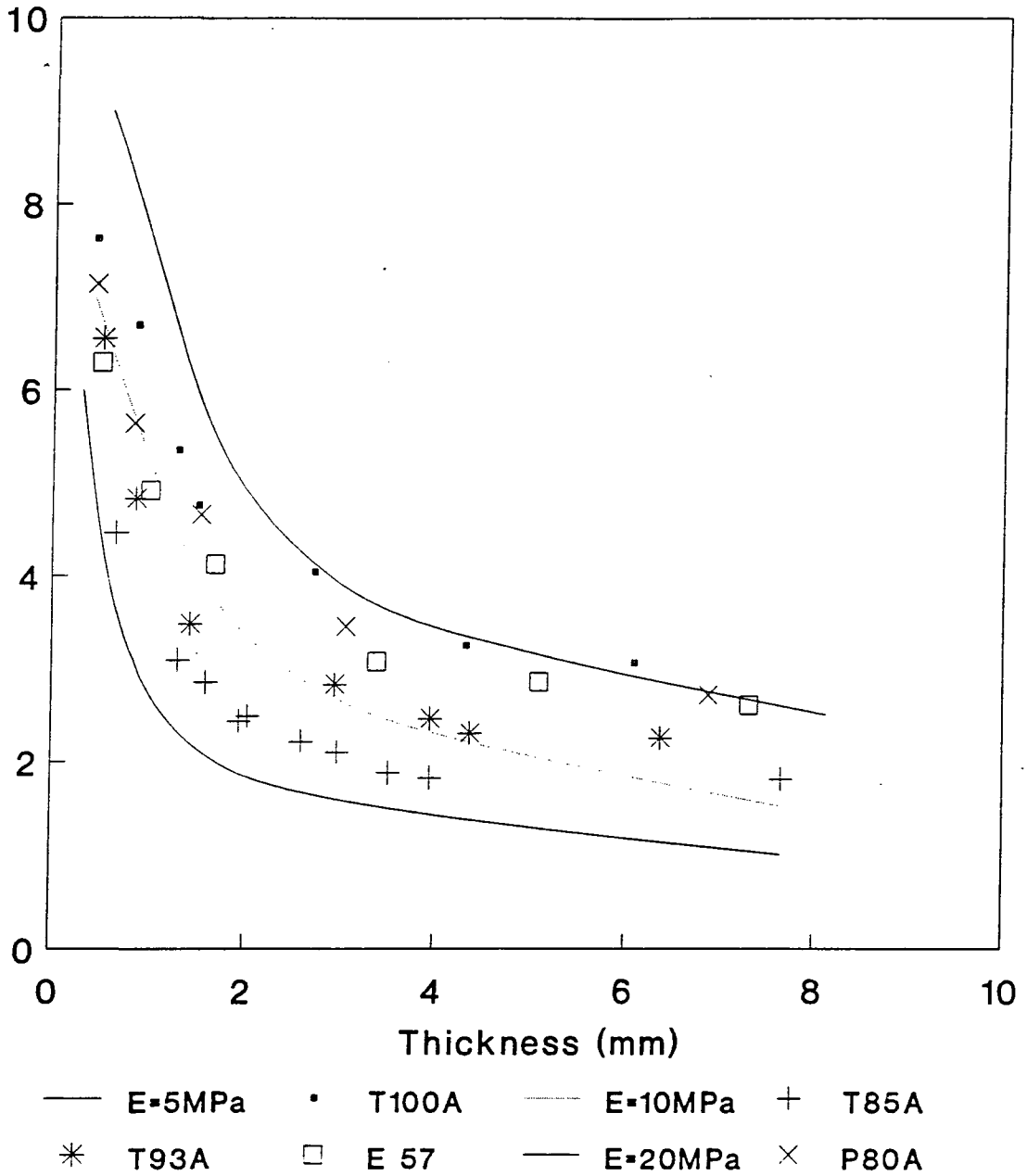


Figure 2.14 : "Waters" Theoretical Results & Comparisons with Experimental Data for Biocompatible Polymers

Hardness (MPa)



of this method will certainly speed up research in this area and will help *in-vivo* testing as smaller samples could be used.

2.8 Conclusions

The modified DIN 53456 standard, using maximum/minimum loads of 5/25N applied through a 5mm indenter, has given consistent results for the elastomers. The hard base plate resulted in minimal increases in hardness for penetrations up to 20% of the sample thickness. The hardness of lubricated and bonded samples of polyurethane has been examined. A good bond to the backing material reduced the effective thickness of the soft material by about 15%, even when penetrations only extended to 20% of the original thickness. The test gave variations in hardness for materials which exhibited visco-elastic properties, such as Tecoflex 100^oA. This was much softer than anticipated, but in the high loading rates applied during walking (ramping to 2000N in 0.1s) the material will respond as if harder than the hardness test indicated. High loading rate tensile tests confirmed this. This means that for some materials more representative results would be obtained by reducing the time at the maximum load prior to measurement.

Chapter 3 : Degradation, Hydration and Fatigue Response of Biocompatible Polyurethanes

3.1 Mechanical Properties to Polyurethanes under *In-Vitro* Conditions

3.1.1 Introduction

The elastic modulus and hardness of soft layers have been introduced as being very important in determining tribological performance. However these properties must be within the required limits *in-vivo*. The effect of a raised temperature and a hydrating medium have not been well documented in the past. This is because many of the biomedical applications of polyurethanes are not dependent on elastic modulus. Hardness values of between 3.5 and 9N/mm² have provided good tribological performance as detailed in Chapter 6. Although this is dependent on the layer thickness and the backing material as well as the elastic modulus of the polyurethane, changes in the values of modulus *in-vivo* will lead to changes in the layer hardness.

3.1.2 Hydration Changes to Materials

3.1.2.1 Introduction

Polyurethanes can take up water/fluid when in a hydrating environment. This is carried in the lattice by the hydrogen bonding and a reduction in the elastic modulus is often noted. Even in a laboratory environment these materials pick up moisture, which leads to a change in properties when compared with dry samples. During fatigue studies it was important to ensure that identical conditions were maintained for both stressed and control samples.

3.1.2.2 Materials & Methods

The uptake of moisture was monitored for four bio-compatible polyurethanes. These consisted of Tecoflex (85, 93 and 100^oA grades), Pellethane 2363-80^oA, Estane

'57' and Estane '58'. The samples were dried for 7 days at 37°C and then transferred to Mammalian Ringer's solution (Appendix I) and maintained at 37°C. Five samples of each polyurethane were used, prepared from compression moulded sheets of material of 1.50mm nominal thickness and cut into standard tensile samples. Seven millimeter holes were punched in the ends of the samples to facilitate mounting in the tensile testing machine. The elastic moduli of the materials were measured at varying water contents to monitor the effects of the fluid. A Lloyd 6000R tensile testing machine was used with samples cycled for five cycles to a maximum stress of 5.2MPa and measurements were made on the fifth cycle. The range of stresses applied to the material in the body is expected to be circa 3MPa (Armstrong, 1986). In order to approach the rates of loading applied to the acetabular cup in the body, a rate of 5.00mm/s was applied. Bolt together grips were used to eliminate slippage, which was initially observed with these samples when wedge, capstan wedge and cam grips were used.

Hardness measurements were made (H20/30 DIN 53456) over the centre section of each sample. Measurements of indenter penetration were also made upon reaching the major load, as it had been noticed that some of the polymers were exhibiting visco-elastic properties under load which had to be quantified. This allowed the calculation of Hardness (H20/0). A rigid base material was used as the backing, with a PTFE coating to ensure minimal friction (Section 2.6). A loading rate of 0.025mm/s was used.

3.1.2.3 Results

Figures 3.1a and 3.1b show the mass of fluid absorbed by the samples, expressed as a percentage of their dry mass. This corresponds to the amount of water taken up by the lattice. Full hydration occurred after about 20 hours for all of the

Figure 3.1a: The Increase in Mass of Biocompatible Polyurethanes from Dry to Mammalian Ringers' at 37°C for 24 hrs

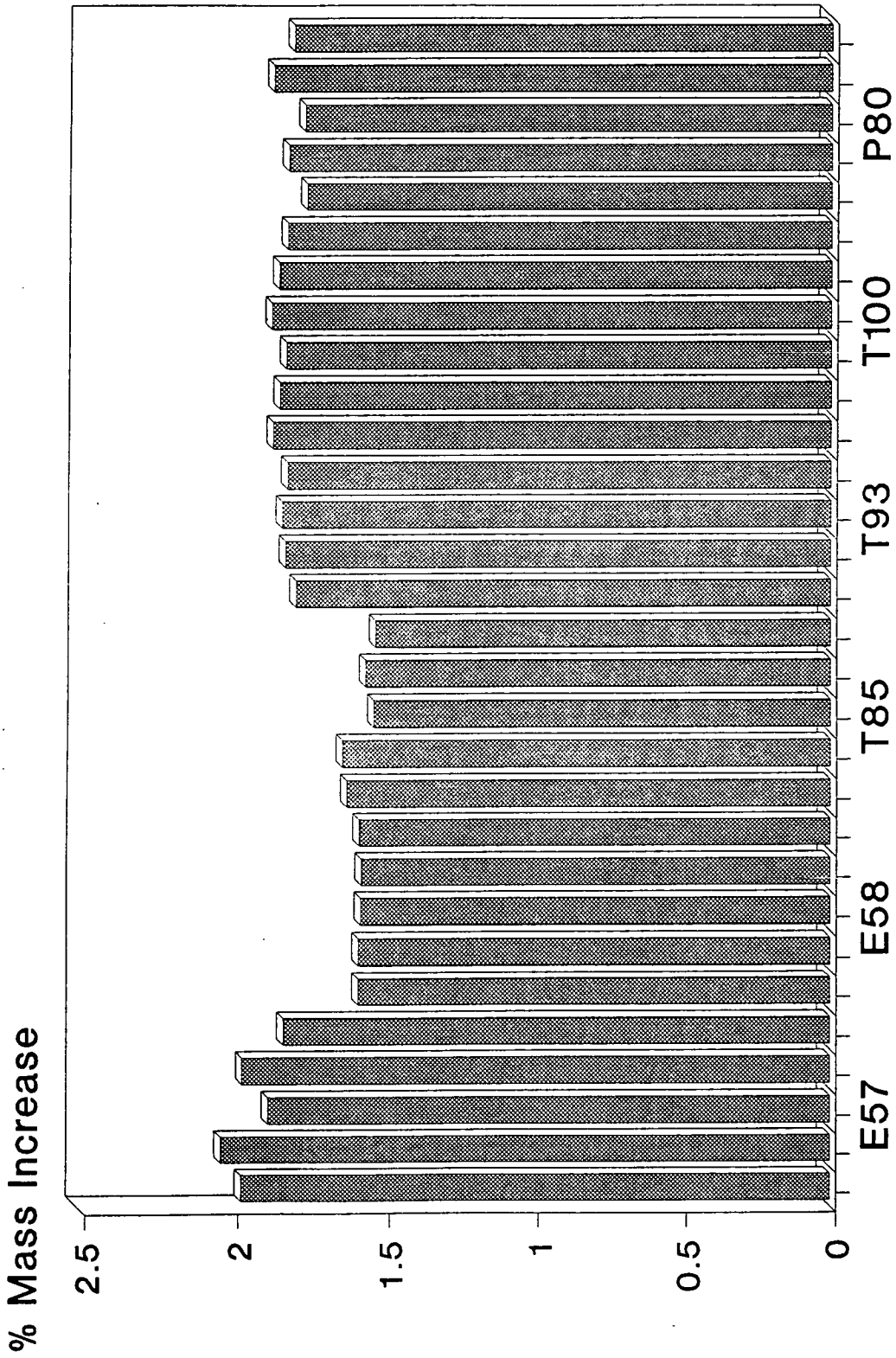
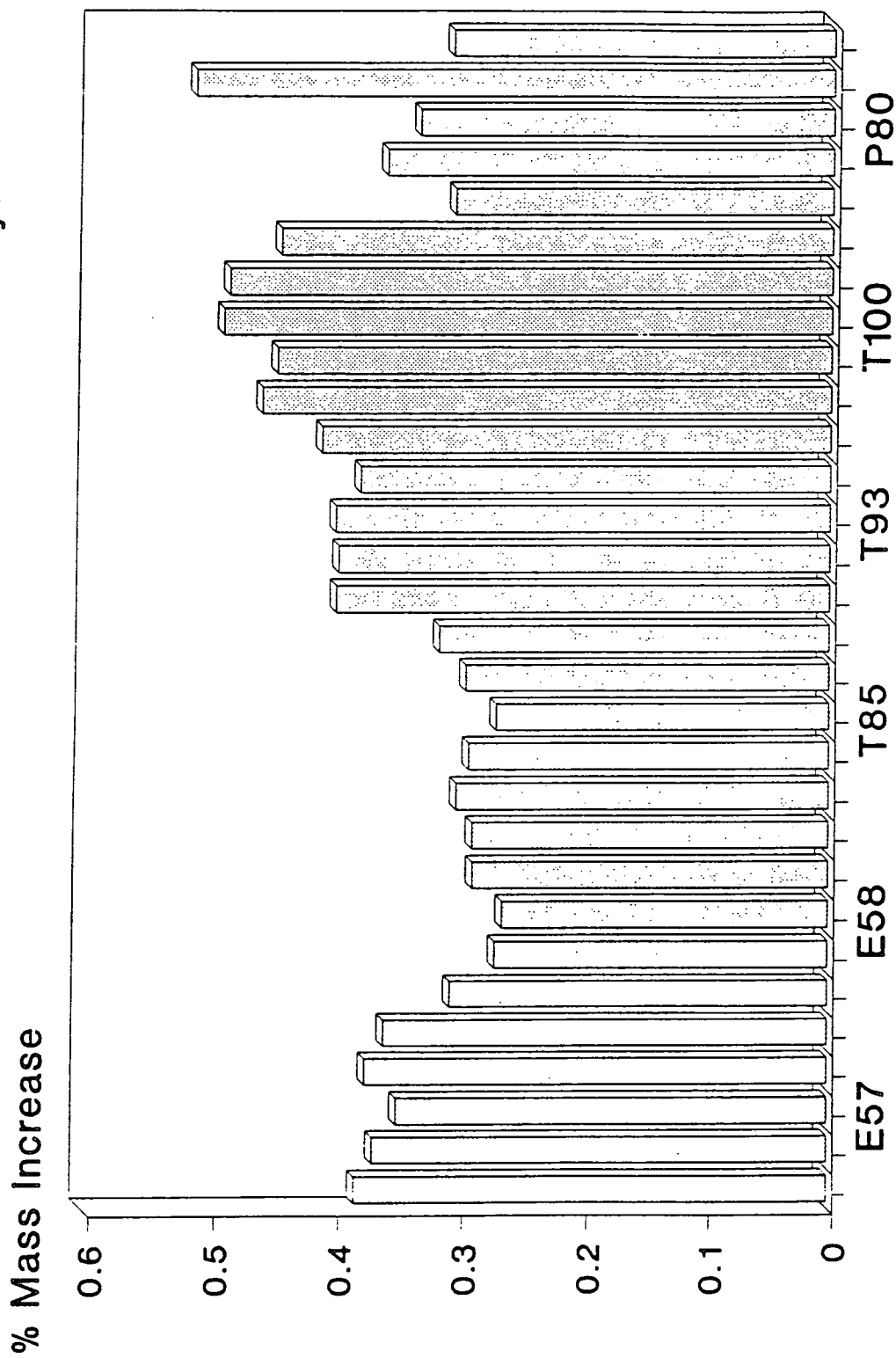


Figure 3.1b: The Increase in Mass of Biocompatible Polyurethanes from Dry to Laboratory Conditions after 7 days



polymers. However, after 4.5 hours the polyurethanes had taken up 1.05-1.20% of fluid which represents about 70% of the maximum amount of fluid which could be absorbed. All of the samples took up an appreciable quantity of water from the laboratory environment (0.3-0.5% by mass), which resulted in a reduction in elastic modulus, in particular for the harder grades of Tecoflex. The elastic modulus decreased with water uptake for all of the polymers and under conditions of full hydration, substantial reductions were measured (figure 3.2a). As expected from the company literature the reduction for both Estane '57' and '58' was less, with reductions of 10% from the laboratory tests and 28% from tests made on dry samples. Tecoflex 85°A showed similar reductions, with Pellethane and Tecoflex 93°A showing similar reductions in elastic modulus of 26% from laboratory maintained and 39% from dry samples. Tecoflex 100°A showed the largest reduction in modulus, with a decrease of 60% from the dry to hydrated samples.

The hardness (figure 3.2b) showed very little change for Tecoflex 85°A and Pellethane (<3%), but larger decreases for Tecoflex 93°A (5%), Estane '57' (12%), Estane '58' (20%) and Tecoflex 100°A (22%). However, it can be seen that the visco-elastic properties of Tecoflex 93°A and 100°A are substantially reduced as fluid is absorbed, indicated by the reduction in the gap between hardness results from H20/30 (**CREEP**) and H20/0 (**No Creep**).

After only 4.5 hours in Mammalian Ringer's Solution the elastic moduli of Pellethane, Tecoflex 93°A and Estane '57' had reduced to close to the fully hydrated level. This length of time in Mammalian Ringers' corresponded to mass increases of 1.11, 1.05 and 1.20% respectively. This shows how important it is to measure Elastic Modulus under identical conditions and to monitor the mass of samples, during degradation or fatigue studies. It also stresses the need for control samples to be kept

Figure 3.2a: The Change in Elastic Modulus of Hydrated Polyurethanes

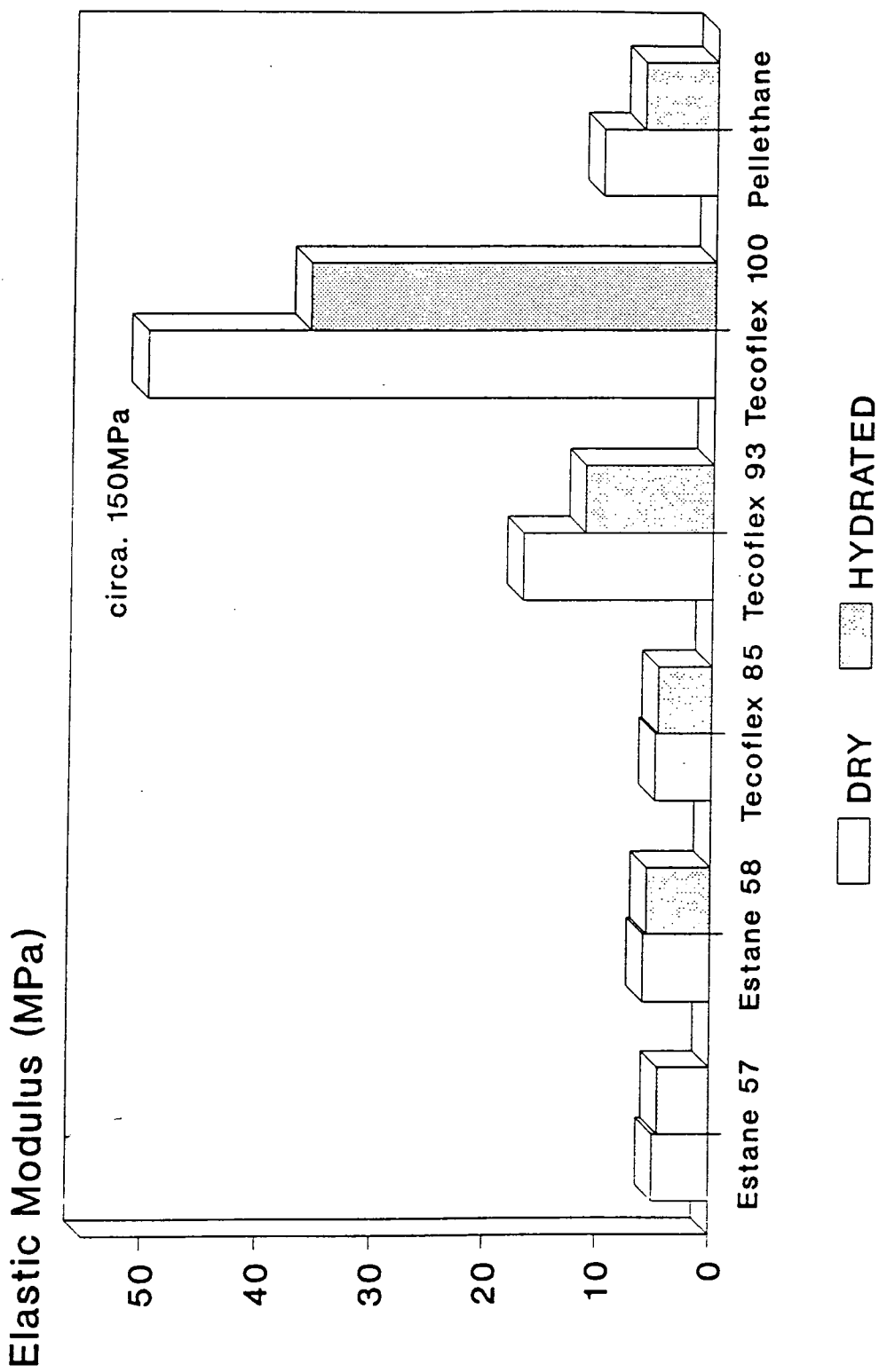
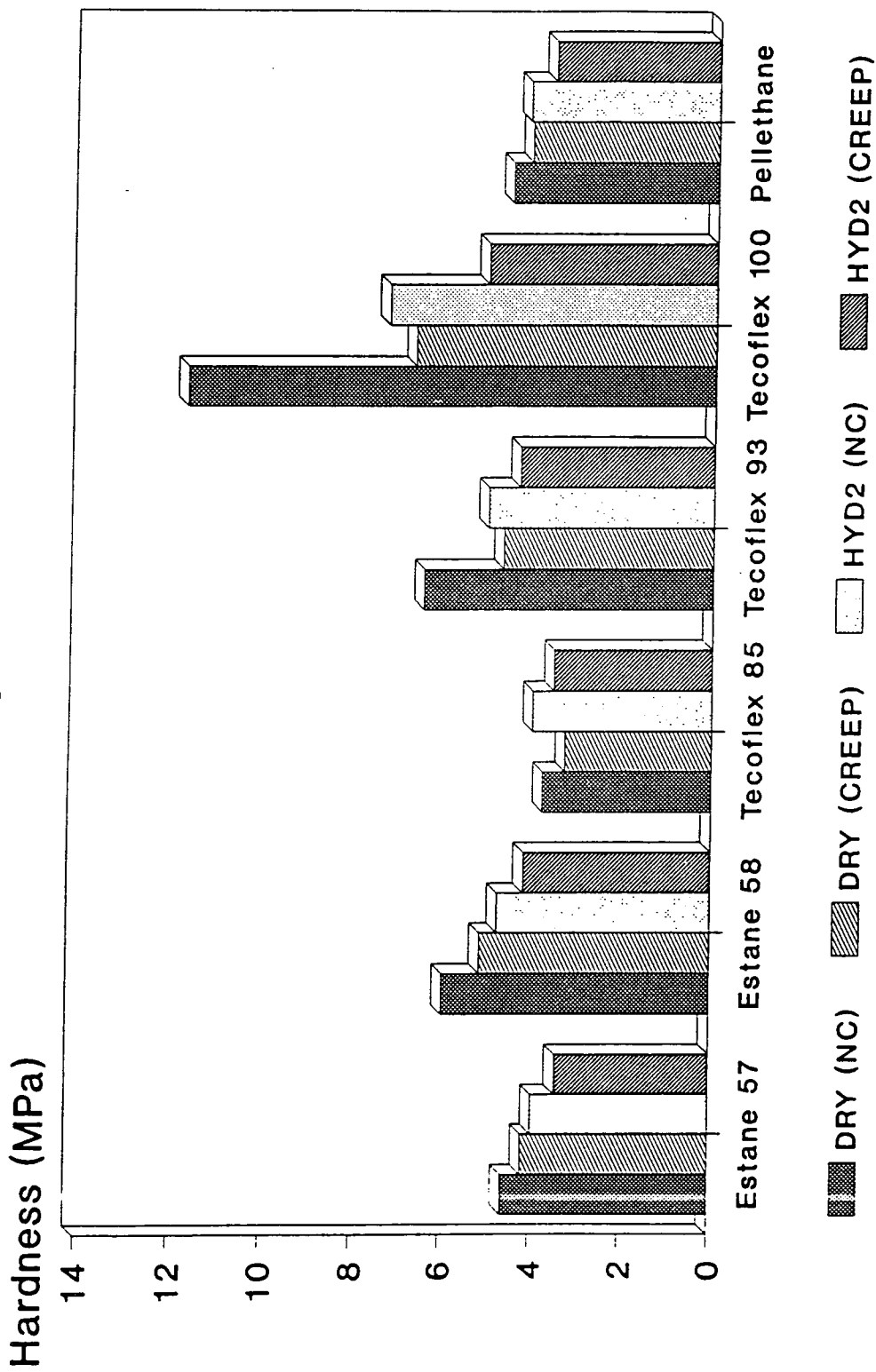


Figure 3.2b: The Change in Hardness (DIN 53456) of Hydrated Polyurethanes



under identical environmental conditions to those undergoing fatigue studies (Section 3.5).

3.1.3 Testing at 37°C

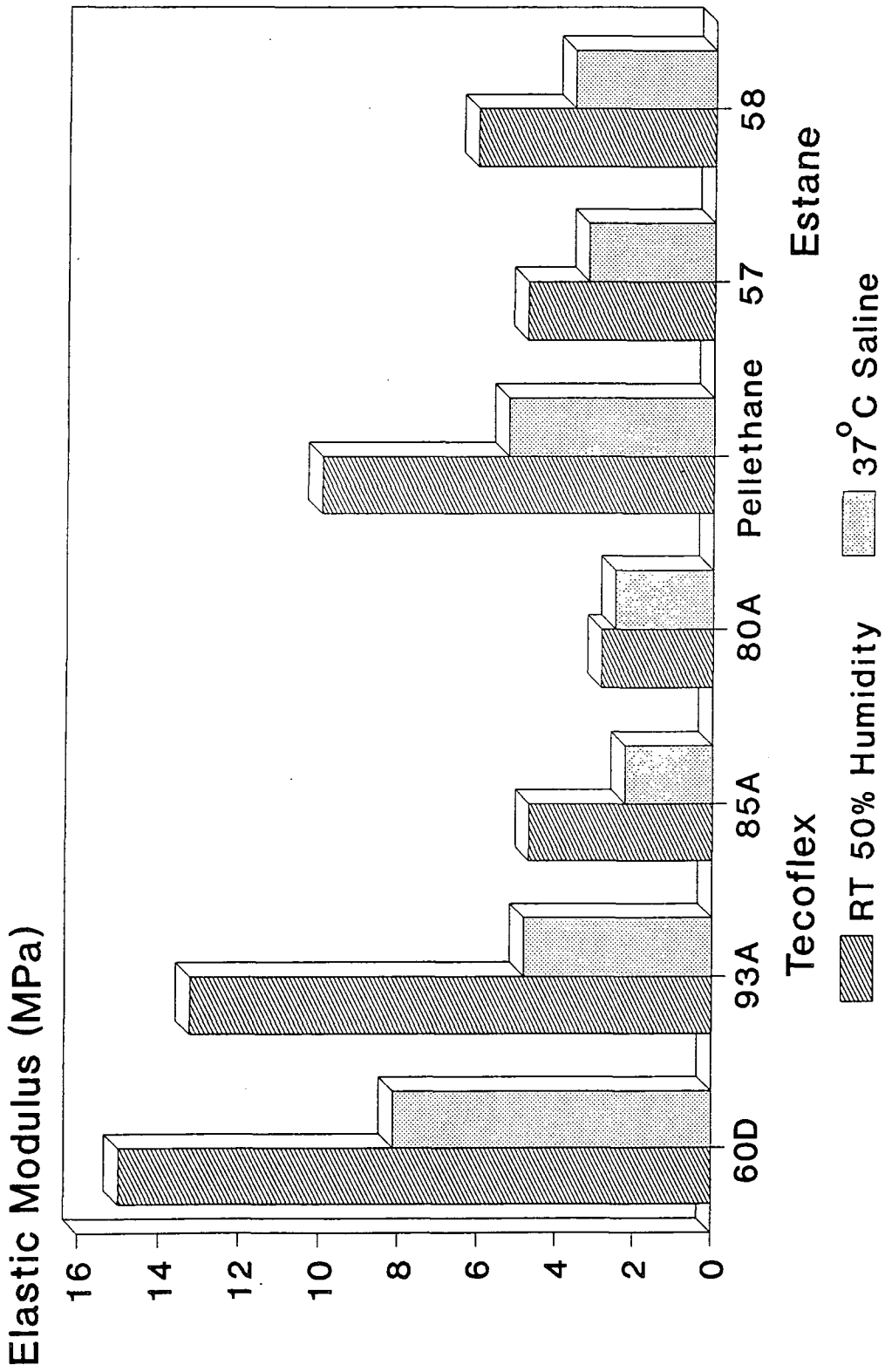
3.1.3.1 Materials and Methods

The second part of this study was conducted at 37°C. Identical samples were used for this part of the study as in the previous experiments. The samples were tested for elastic modulus after being dried at room temperature and in a bath of Mammalian Ringer's Solution at 37°C in the thermal cabinet which was used with the Lloyd machine. Prior to testing in Mammalian Ringer's the samples were allowed to reach fully hydrated conditions in saline. Loading rates were doubled when samples were moved from dry to hydrated states, with values of 5.0 and 10.0mm/s used for the two sets of conditions. This was to ensure that similar strain rates would be maintained throughout.

3.1.3.2 Results

The results are displayed in figure 3.3a. The Tecoflex polyurethanes showed the largest decreases in elastic modulus when at 37°C in Mammalian Ringer's solution with a reduction of 64% for the 93°A grade. The softer grade of material, Tecoflex 85°A also showed a large reduction, with a percentage change of 51%. However, this was from an original value of only 4.3MPa. Values from the Thermedics Laboratory for the 80°A and 60°D (105°A) were obtained and displayed in figure 3.3a. Pellethane showed a reduction of 47%, and at 37°C when hydrated had a higher elastic modulus than Tecoflex 93°A. The two Estane polyurethanes showed smaller reductions of 32.5% for the '57' material (the polyether urethane) and 41% for the '58' grade (the polyester urethane). Analysis of the stress-strain curves revealed little change in shape for the Tecoflex or Pellethane samples. However, the Estanes showed a curve with a

Figure 3.3a : The Change in Elastic Modulus of Polyurethanes at 37° C in Mammalian Ringers'



steep initial region for the dry samples, with a value of elastic modulus of 15MPa, up to a stress value of 2.5MPa. This region was almost absent with the hydrated samples, which may partly explain the reduction in elastic modulus of the Estane samples. However, their properties seemed to be the least affected by hydration.

3.2 Discussion

The uptake of water for the biomedical polymers reached a limit of between 1.5 and 2.0% by mass. This is much lower than values for human articular cartilage, which means that lubricant carried in the urethane lattice is unlikely to provide a large lubrication effect. Water is taken up by the polymer lattice, with slight swelling occurring. This was measured by a slight increase in sample dimensions, which would necessitate adequate clearances in an artificial joint to prevent grabbing under *in-vitro* conditions. Hydrogen bonding seems to be the most likely mechanism for holding the water molecule. This bond was easily broken when the hydrating medium was removed as evidenced by the reduction in mass and recovery in elastic modulus.

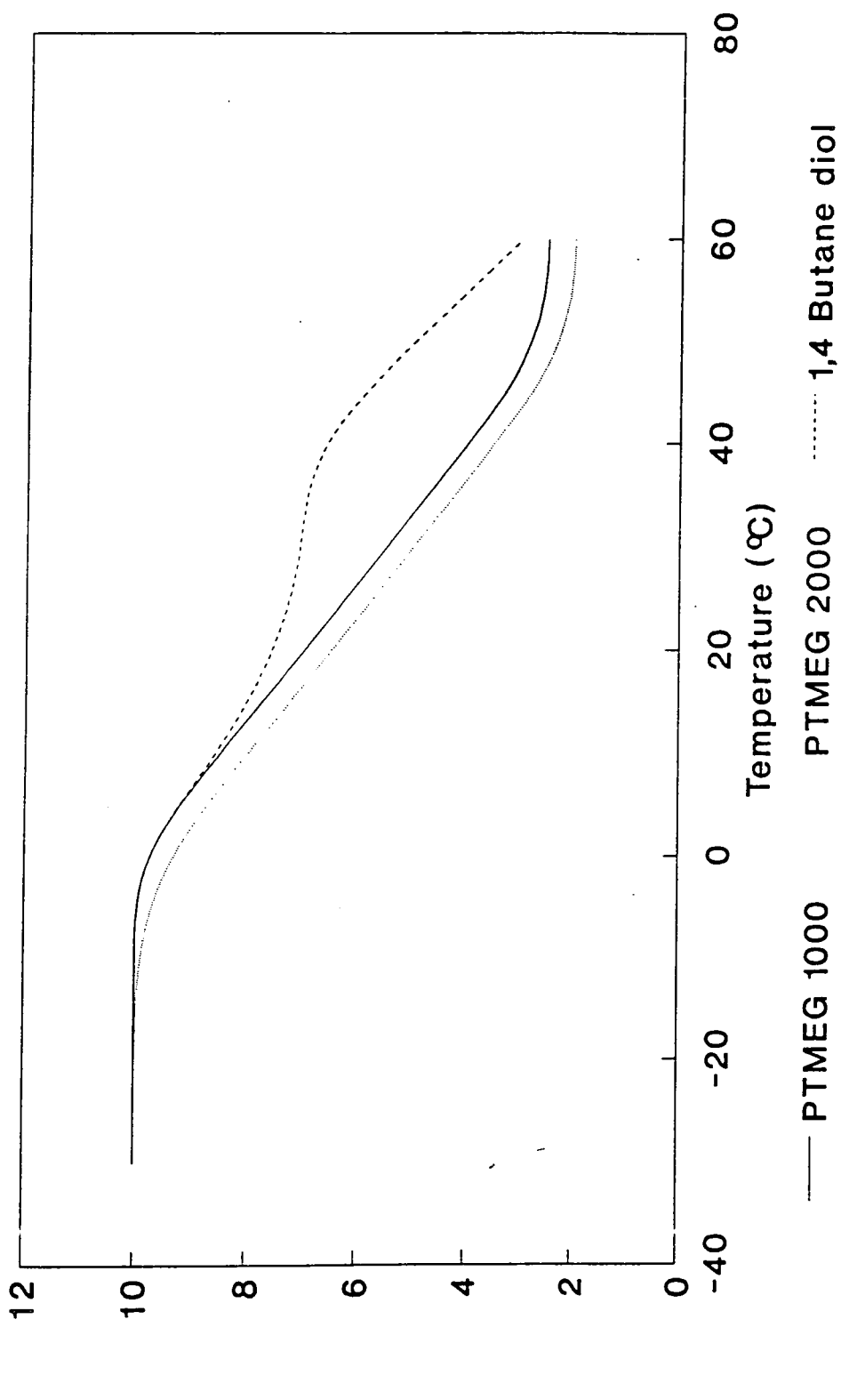
The large decreases in elastic modulus for the Tecoflex polymers were so significant that Thermedics, the manufacturers were contacted. Their own test results for 80°A and 60°D (equivalent to 105°A) grades indicated smaller changes (shown on figure 3.3a) but no record of their strain rates was available. It was anticipated that at lower strain rates, a smaller change in properties would be apparent. 'Aromatic' polyurethanes such as Pellethane and Estane, the tag being based on the Isocyanate component, showed less softening than the harder grades of the Tecoflex 'aliphatic' materials. Polyurethanes based on aliphatic isocyanate components possess increased UV stability, and increased resistance to hydrolysis and thermal degradation, but mechanical properties (ultimate strength and extension) may be inferior (Lelah and Cooper, 1986). The harder grades of Tecoflex use a lower molecular mass soft

segment (PTMO 1000) than the softer material, and this is combined with lower quantities of 1,4 butanediol to obtain the required mechanical properties. The effects of this can be shown schematically (figure 3.3b). Reductions in the quantity of 1,4 butanediol encourage temperature induced softening and the reduction in the molecular weight of the soft segments may be a reason for the glass transition temperature being higher (Lelah and Cooper, 1986 pp41) and closer to the testing range. In the region of the glass transition temperature visco-elastic properties become more important. Hydrogen bonding is present in the polymers as a link between the chains (a weak form of cross-linking) often between the ether and urea groups. The presence of water will modify this with the formation of a double hydrogen bond, increasing the distance between the polymer chains (Dawber and Healey, 1991). This explains the slight swelling, and if a force is applied to the assembly, it will tend to stretch both of these hydrogen bonds in the above example, leading to a measured modulus of approximately half of that if only one bond were present. Thermedics' results confirm the likelihood of this sort of mechanism with the largest changes in modulus occurring at high strains (> 200%), when the chains will tend to be relatively well ordered instead of in a tangled state.

Hydrogen bonds tend to be relatively long, with a bond length of 0.3nm and a bond energy of 60kJ/mole. This compares with 0.1-0.2nm and 800kJ/mole for a covalent bond. They also show an almost flat energy/distance curve, requiring little energy input to facilitate extension.

Using the results from both studies described in this Chapter it can be seen that most of the measured changes in elastic modulus occur as a result of polymer hydration and not an increase in temperature to 37°C. This confirms the theory that water molecules held between the chains are responsible for much of the change.

Figure 3.3b: A Schematic Diagram of the Change in Mechanical Properties of Polyurethanes with Temperature



3.3 Degradation of Polyurethanes

3.3.1 Introduction

The four polymers introduced in Chapter 2 were used to conduct *in-vitro* degradation studies. Tensile and cup samples were investigated through immersion in Mammalian Ringer's solution at 37°C. Hardness, elastic modulus and tribological properties were measured.

3.3.2 Materials and Methods

3.3.2.1 Hardness Testing

Two types of specimens were used to evaluate changes in hardness with time in Mammalian Ringer's solution. These were acetabular cups which were also evaluated for friction, and tensile test specimens used to evaluate elastic modulus. The method contained in the standard DIN 53456 was used which loads a 5mm ball into the surface to be investigated. A Hounsfield testing machine was used for the measurements which were made on at least 3 regions over each polyurethane surface.

3.3.2.2 Elastic Modulus

The Hounsfield testing machine was used to perform standard tensile tests on polyurethane specimens. The region over which loading was applied was 100mm in length with a cross section of 10mm width and 4mm thickness. The ends of the specimens were 25mm in width to withstand the contact stresses applied by the grips used for tensile testing. A rate of extension of 2.5mm/s was used and the maximum load to which each sample was subjected was 100N. This represented a stress level of 2.5MPa which was calculated to be similar to the stresses developed in an elastic layer bonded to a rigid backing undergoing loads similar to that of a walking cycle (Chapter 6). The samples were tested over 5 cycles to account for any initial slippage and elastic modulus was calculated from the final cycle.

3.3.2.3 Hip Function Simulator

The measurements of friction factor of the joints were made in the Durham Hip Function Simulator. Loading cycle I was used to represent walking (Chapter 5).

3.3.2.4 Materials

Pellethane, Estane 5714F1, Estane 58271 and Tecoflex polyurethanes were investigated. Two grades of the Tecoflex material were investigated as its Hardness when measured using the DIN test was less than predicted from the Shore Hardness values. Grades of 85°A and 93°A Shore Hardnesses were investigated thoroughly with grade EG100°A obtained later in the study, tested for tribological performance only. Its chemical constituents were very similar to the 93°A grade and being harder it is likely to be more resistant to degradation (Lelah and Cooper, 1986). Four injection moulded tensile dumbbell samples of each polyurethane were used in the degradation studies. The studies began at different times as the polymers were obtained and the results were designated groups a - d, which is how the graphical output is displayed.

The acetabular cups were produced to give 0.25mm radial clearance. However, swelling of some of the polyurethanes caused this clearance to be reduced resulting in grabbing. A second femoral head of 31.00mm diameter was made and subsequently used in the simulator tests where conditions warranted. Four samples of Estane 5714F1 and Estane 58271 were used in the construction of graphs 3.7a and 3.8. Three samples each of Tecoflex EG85°A, Pellethane and Estane 5714F1 were used in the second study. The results for this are displayed in figures 3.7b and 3.9.

3.3.2.5 Methods of Testing

All the specimens were immersed in Mammalian Ringer's solution at 37°C. Before testing, the specimens were removed from the fluid, dried, weighed and then left for 60 minutes to equilibrate to the laboratory temperature. Hardness, elastic modulus and mass of the tensile specimens and friction and hardness of the acetabular cups were measured.

3.3.2.6 Frictional Tests

An aqueous solution of carboxy methyl cellulose (CMC) was used as the lubricating fluid in the simulator. This has similar rheological properties to those of synovial fluid (Cooke *et al*, 1978) (figures 5.27a and 5.27b) and does not carry a health risk to the research staff. Viscosities from 0.002-0.071Pa s were used to cover the range normally associated with arthritic fluid (circa. 0.010Pa s).

3.3.3 Results of the Strip Samples

Individual values were omitted from figures 3.4-3.6 for clarity. The range of hardness and elastic modulus values after 0 and 500 days in solution were as follows:

For Estane 5714F1 elastic modulus (MPa) was initially 7.40 (7.16-7.63) which decreased to 5.20 (4.85-5.65) and hardness (N/mm²) changed from 3.75 (3.21-4.25) to 2.50 (2.18-2.97). Estane 58271 showed greater changes, elastic modulus (MPa) decreasing from 12.2 (11.56-12.7) to 7.35 (5.85-7.87), and hardness (N/mm²) from 4.80 (4.45-5.06) to 2.20 (1.76-2.48). The greater change in hardness values being due to plastic (irrecoverable) deformation under the indenter in the degraded sample. Tecoflex EG85A samples showed values of 5.06 (4.38-5.71) and 4.98 (4.01-5.65) for elastic modulus (MPa) [13.3 (12.3-14.2) and 13.4 (12.1-14.7) for Tecoflex EG93A] after 0 and 500 days in solution respectively. Hardness (N/mm²) was constant at 2.39

(2.29-2.48) and 2.36 (2.19-2.48) [3.26 (2.97-3.52) and 3.60 (3.13-3.93) for Tecoflex EG93A] over the same period. Pellethane showed a small range of values, with elastic modulus (MPa) decreasing from 14.6 (15.4-14.06) to 12.1 (11.6-12.8) and hardness (N/mm²) changing from 4.75 (4.6-4.95) to 3.90 (3.35-4.07) over 500 days in Mammalian Ringer's solution.

These ranges seemed very low, especially for the hardness tests. In these tests the ranges were based on 12 readings for each material (measurements at three points on the surface of each polyurethane sample). This indicated the good reproducibility available with this technique.

3.3.3.1 Elastic Modulus

The changes in elastic modulus with time in solution can be seen from figures 3.4a-d. All of the polyurethanes showed an initial decrease in modulus as water was taken up by the polymer. As the study progressed gradual decreases in elastic modulus were apparent in Estane '57' with little subsequent change for Pellethane and a slight increase in elastic modulus for Tecoflex. Estane '58' showed the largest initial decrease in modulus and steady properties up to 200-400 days. However, from this time a marked reduction in modulus was noted, in conjunction with a change in the appearance of the polymer surface. A short time after the initial reduction in modulus the tests had to be curtailed due to specimen breakage under the applied loading.

3.3.3.2 Hardness

Similar results were obtained from hardness measurements on the samples (figures 3.5a-d) with initial decreases after the first two days and a slight decrease thereafter for Estane '57' and stable properties for Tecoflex samples. Estane '58' again

Figure 3.4a : The Change in Elastic Modulus of Samples placed in Mammalian Ringers' at 37°C

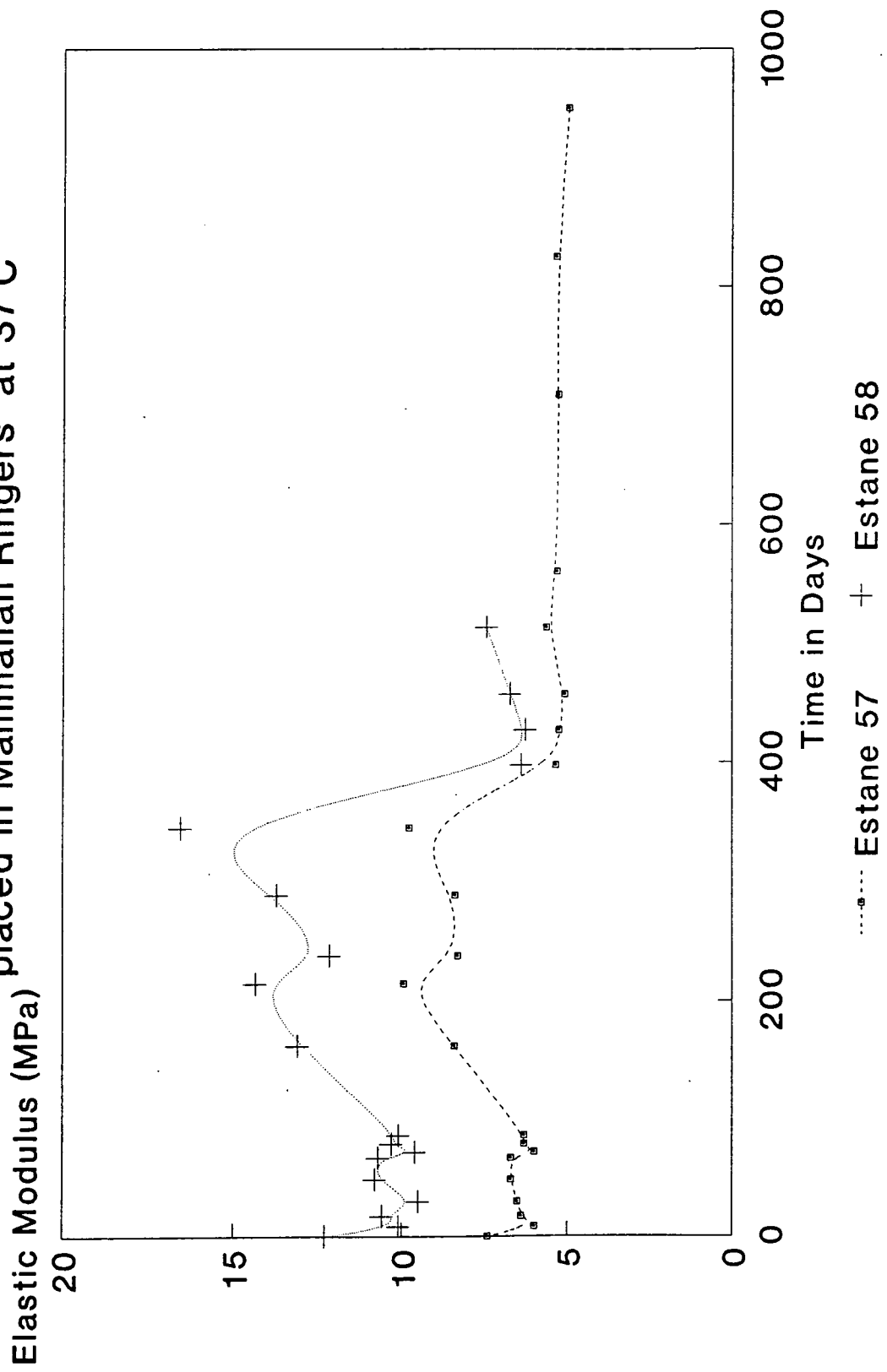


Figure 3.4b : The Change in Elastic Modulus of Samples placed in Mammalian Ringers' at 37°C

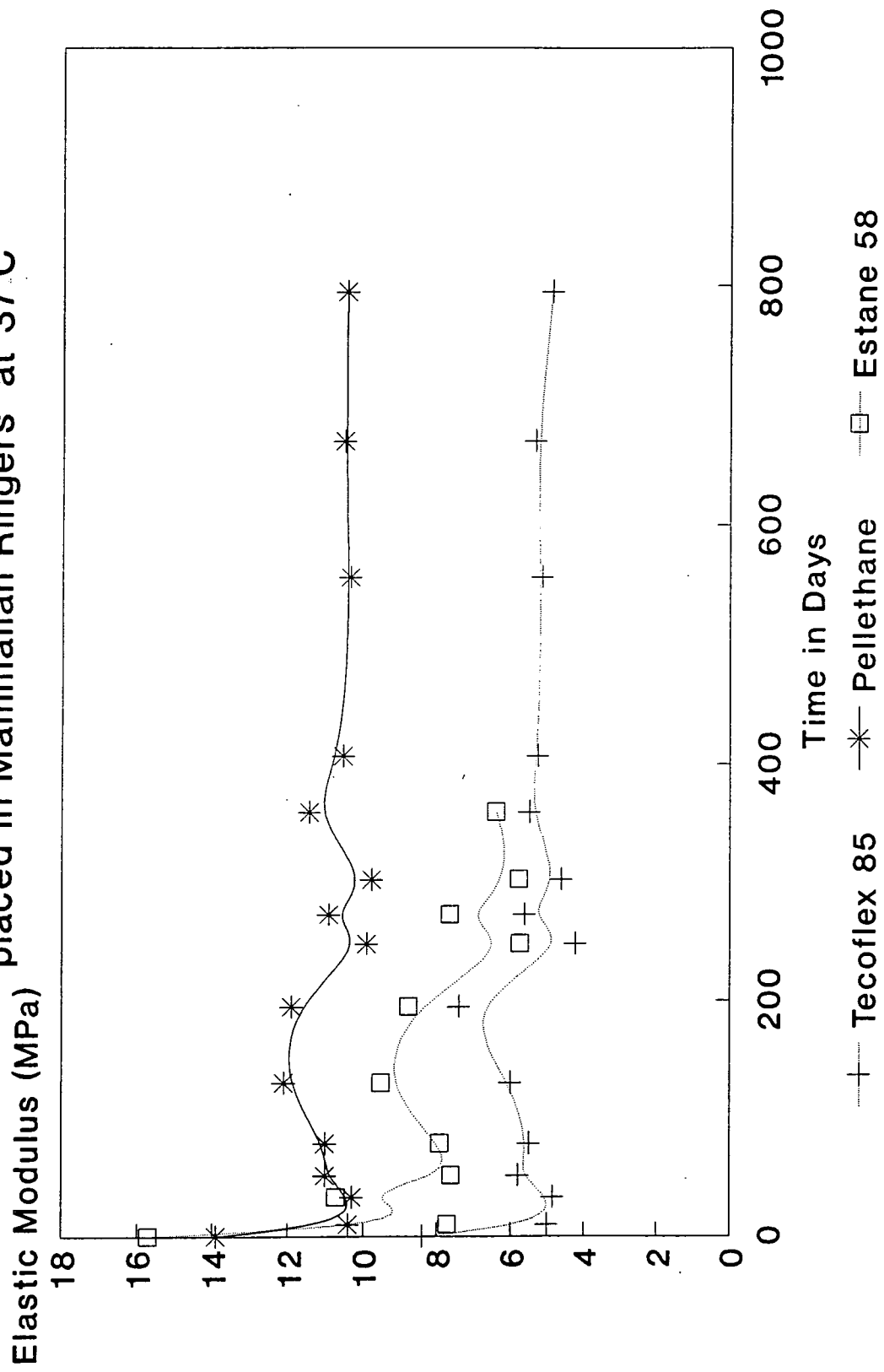


Figure 3.4c : The Change in Elastic Modulus of Samples
Elastic Modulus (MPa) placed in Mammalian Ringers' at 37°C

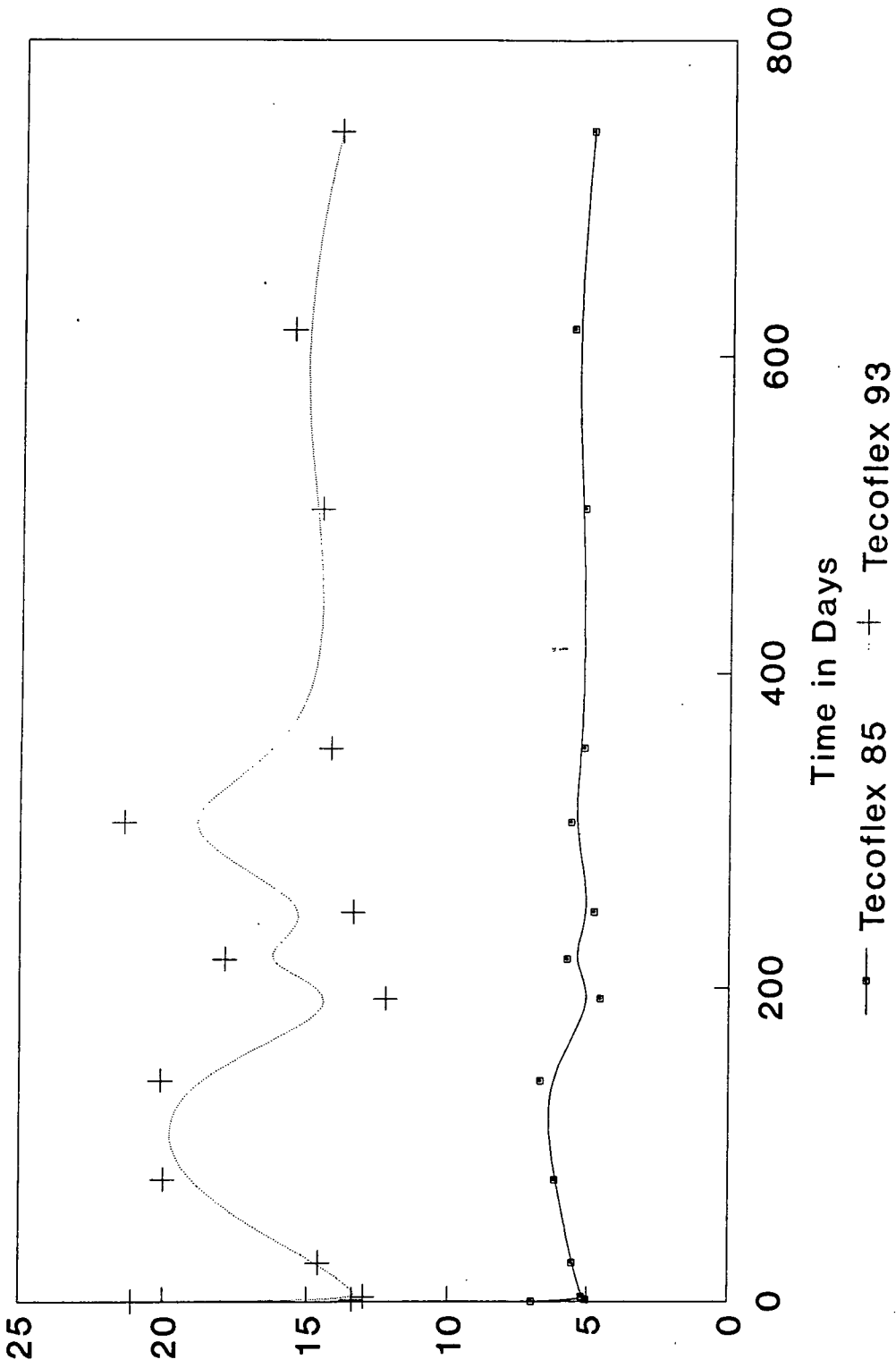


Figure 3.4d : The Change in Elastic Modulus of Samples placed in Mammalian Ringers' at 37°C

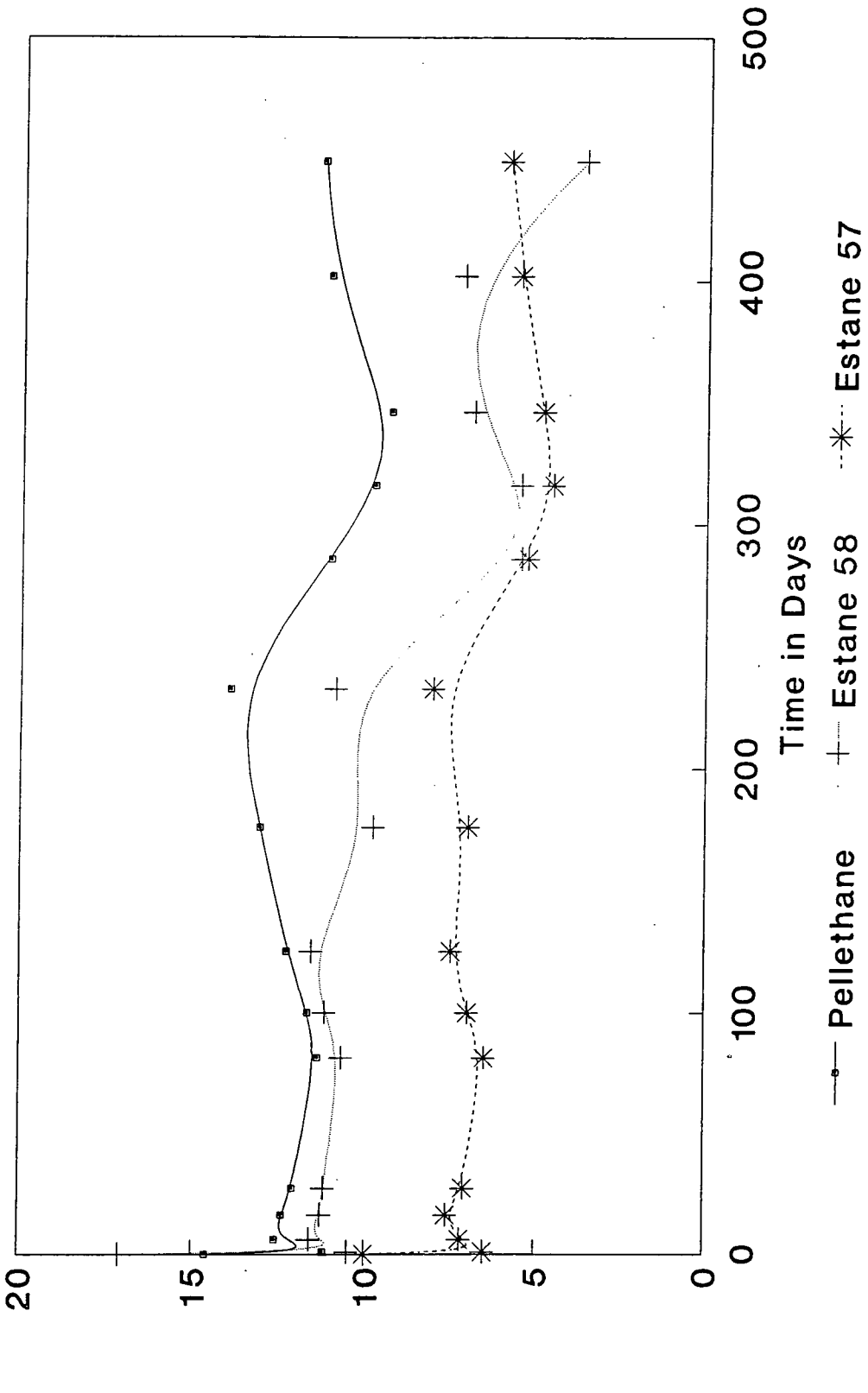


Figure 3.5a : The Change in Hardness of Samples placed
in Mammalian Ringers' at 37°C

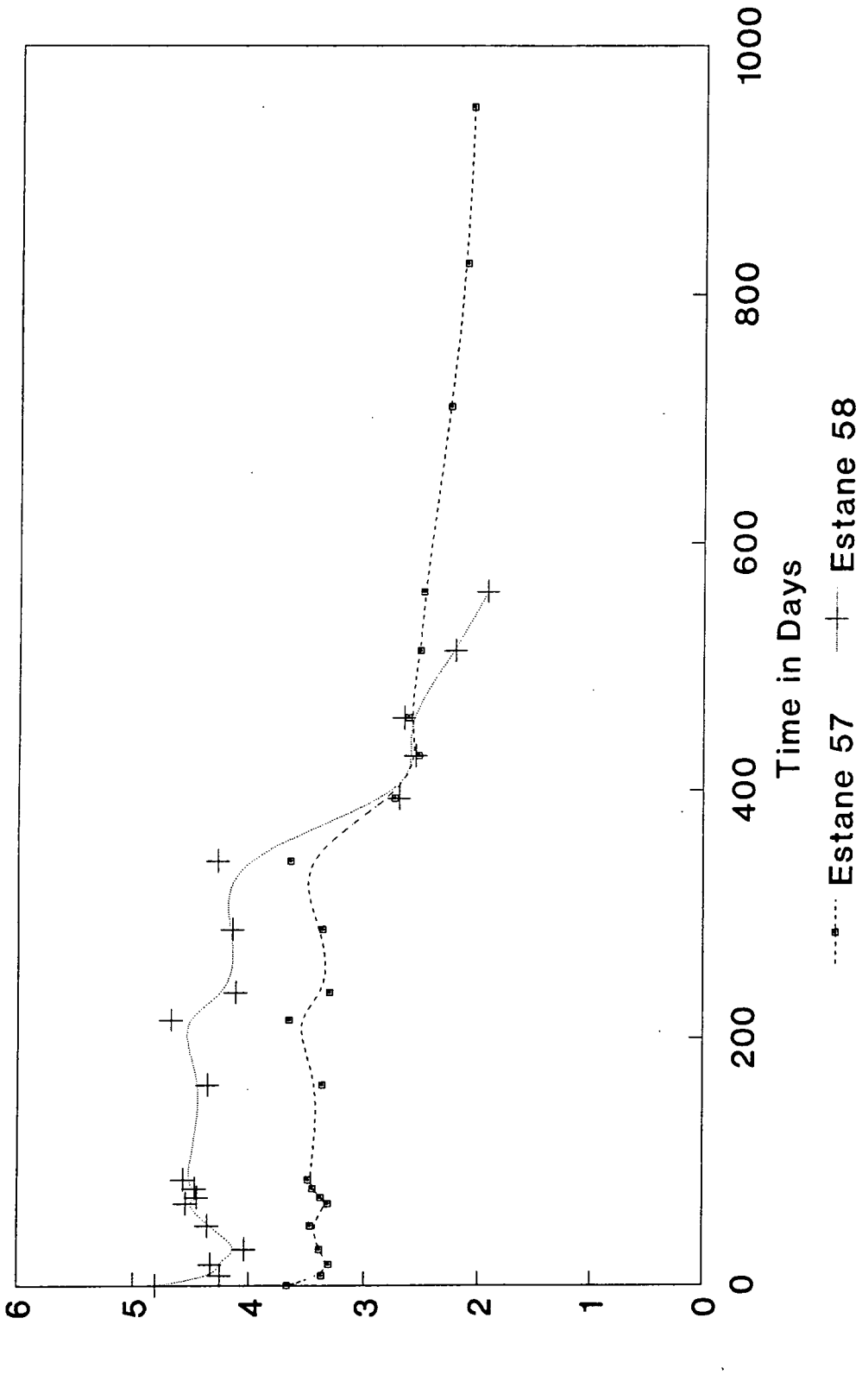


Figure 3.5b : The Change in Hardness of Samples placed in Mammalian Ringers' at 37°C

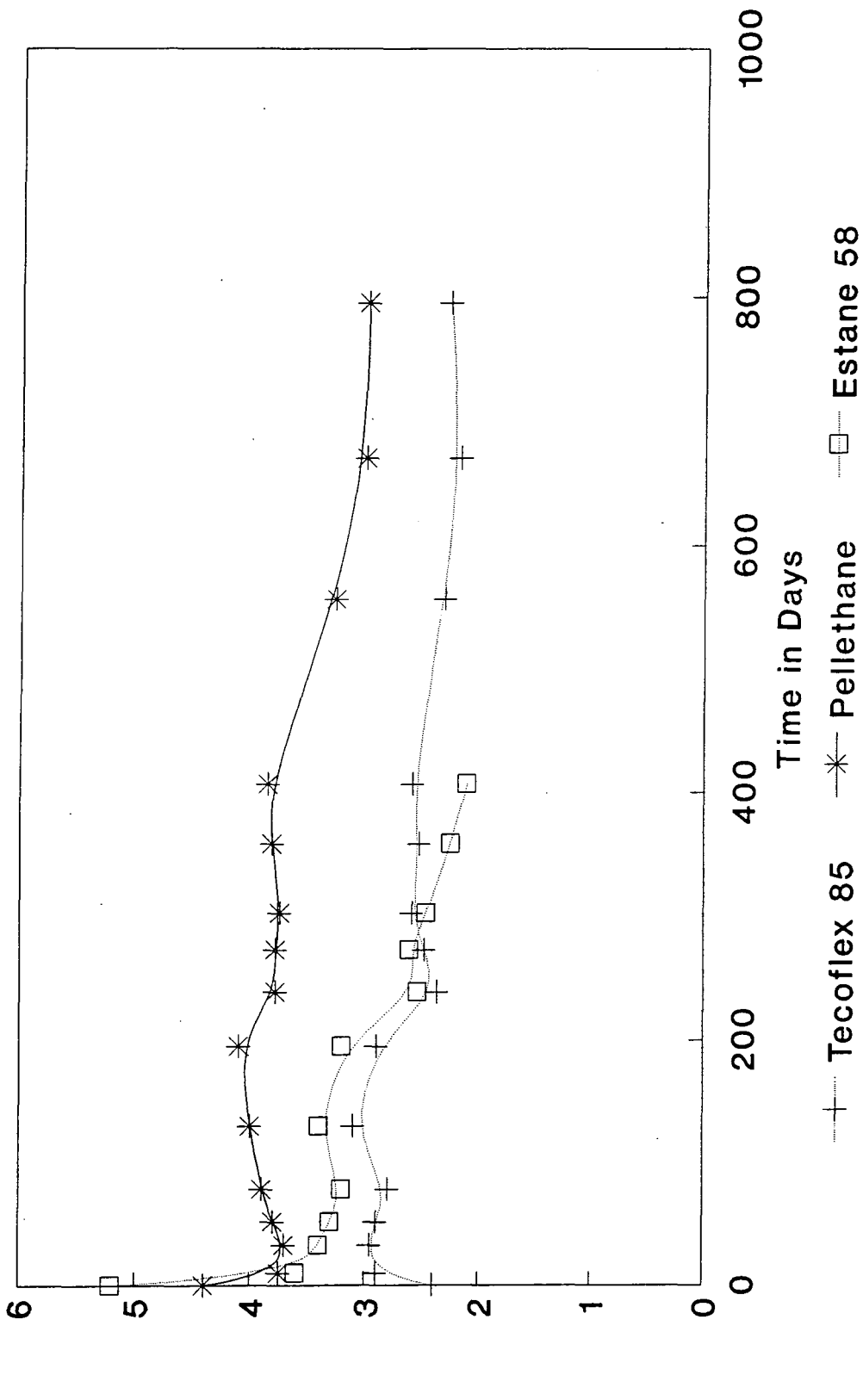


Figure 3.5c : The Change in Hardness of Samples placed in Mammalian Ringers' at 37°C

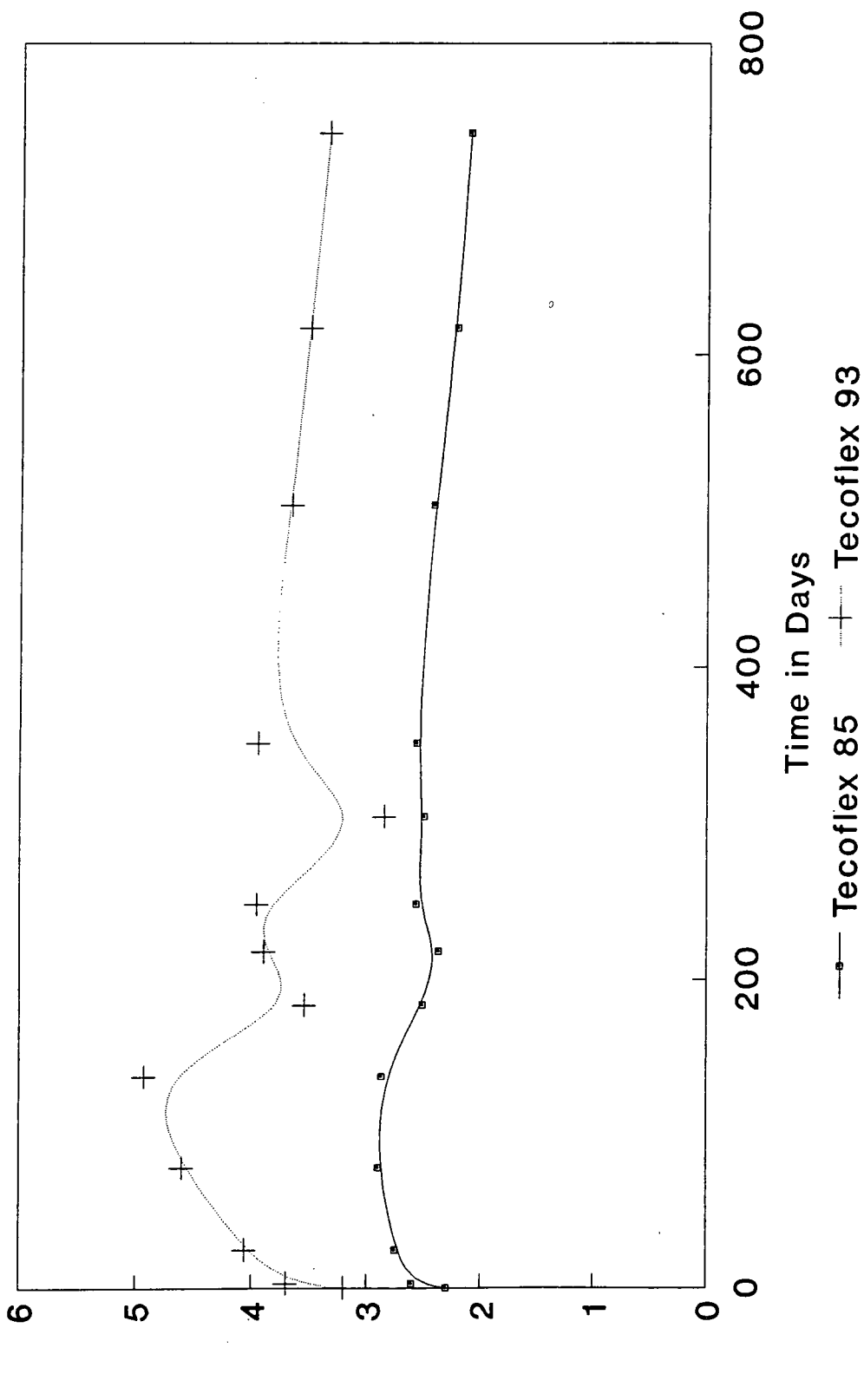
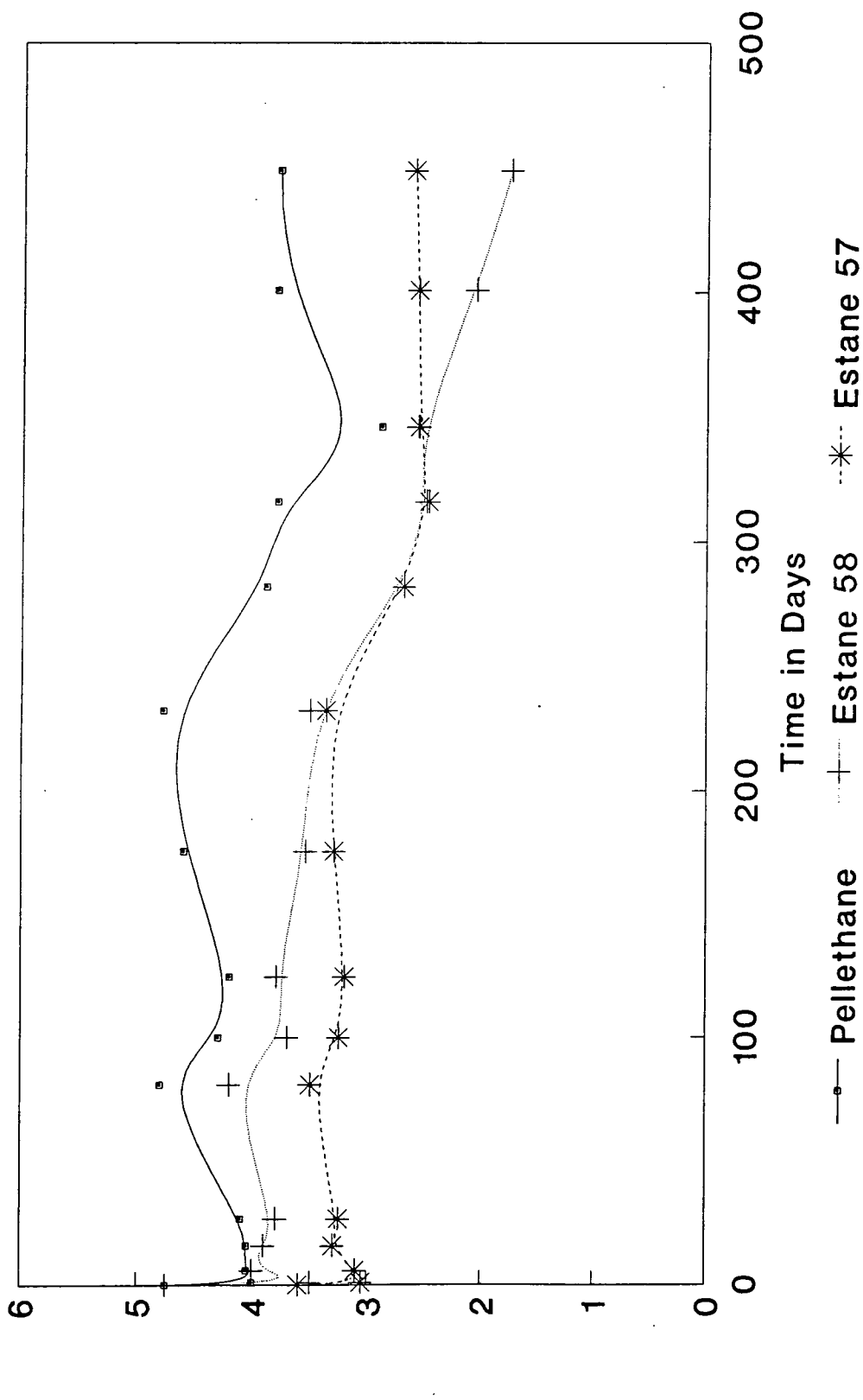


Figure 3.5d : The Change in Hardness of Samples placed
in Mammalian Ringers' at 37°C



showed early properties similar to the '57' material followed by a steady decrease after 200-400 days of 25%/100 days. However, some Pellethane samples have shown decreases in hardness of 20% from 400-800 days soaking time. It was noted that the initial values of hardness did show a large variation between polymers. The EG85°A and EG93°A grades of Tecoflex, which company literature suggested to be the hardest material, provided the lowest initial values of elastic modulus and hardness. However, towards the end of the study the material properties were much more evenly matched.

3.3.3.3 Mass Increase

The increase in the mass of the specimens was monitored and a fluid uptake equal to approximately 1.5% by mass of the polymer was noted during the early stages of the experiment (figure 3.6a-d). This increase is less than the thin samples tested in section 3.1 due to the decrease in the ratio of surface area/volume and the low permeability of these materials. The Tecoflex and Pellethane polyurethanes have maintained a fairly steady mass over the course of the study, indicating little polymer/environment interactions. However, Estane '58' showed increases in mass after 200-400 days reaching 6-12% by mass which suggests interaction with the Mammalian Ringer's solution. The appearance of the strips and cups (figure 3.7c) was white and flakely indicating hydrolysis of the material. Estane '57' showed a steady mass up to 600 days and then a steady increase of about 0.25%/100 days up to 950 days.

3.3.4 Results of the Cup Samples

3.3.4.1 Hardness

The cup samples showed a wide variation of hardness values (figure 3.7a and 3.7b). The values obtained were higher than the results from the strips because of the effect of the backing material (section 2.6.3). However, the changes which occurred

Figure 3.6a : The Change in Mass of Samples placed in Mammalian Ringers' at 37°C

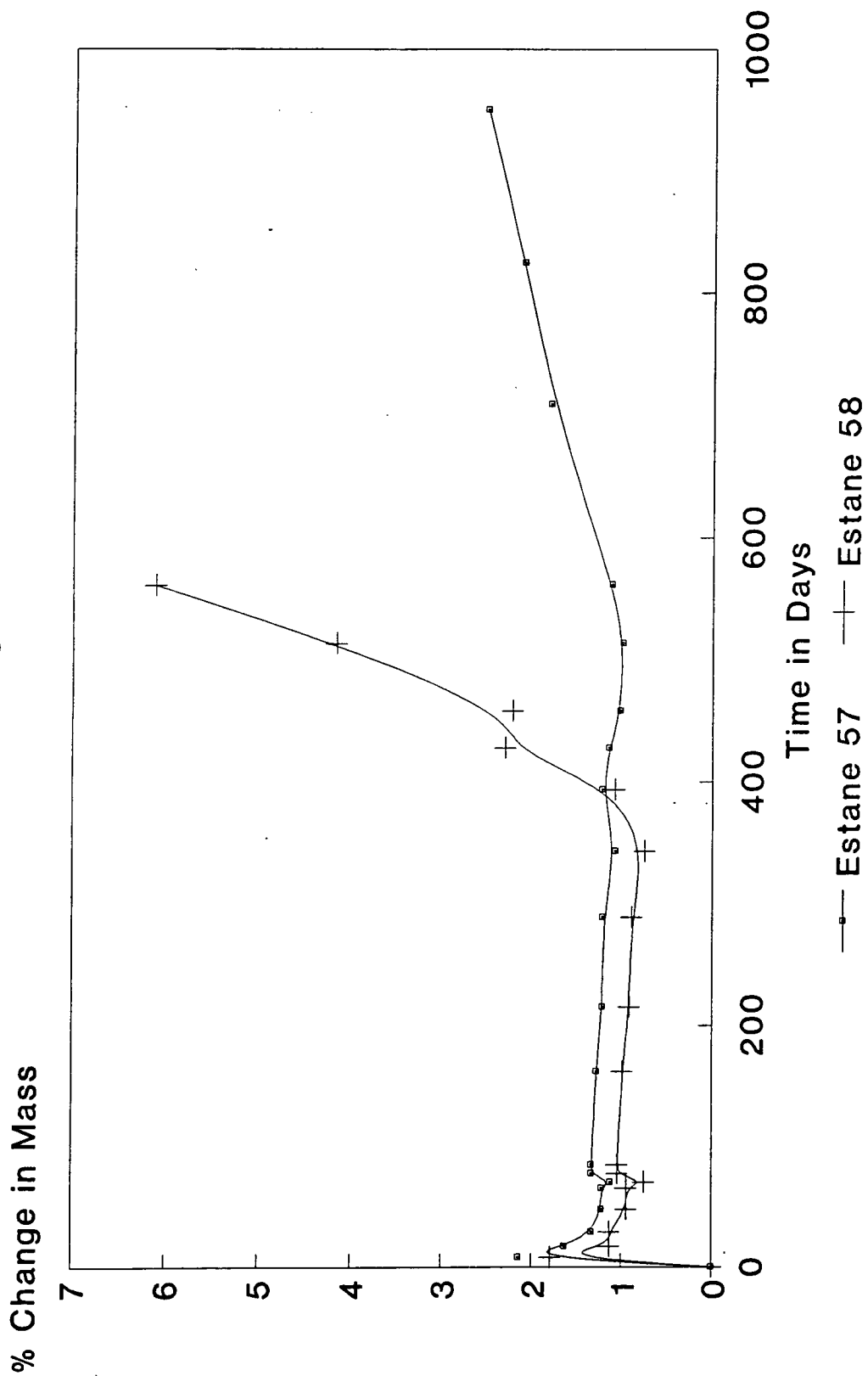


Figure 3.6b : The Change in Mass of Samples placed in Mammalian Ringers' at 37°C

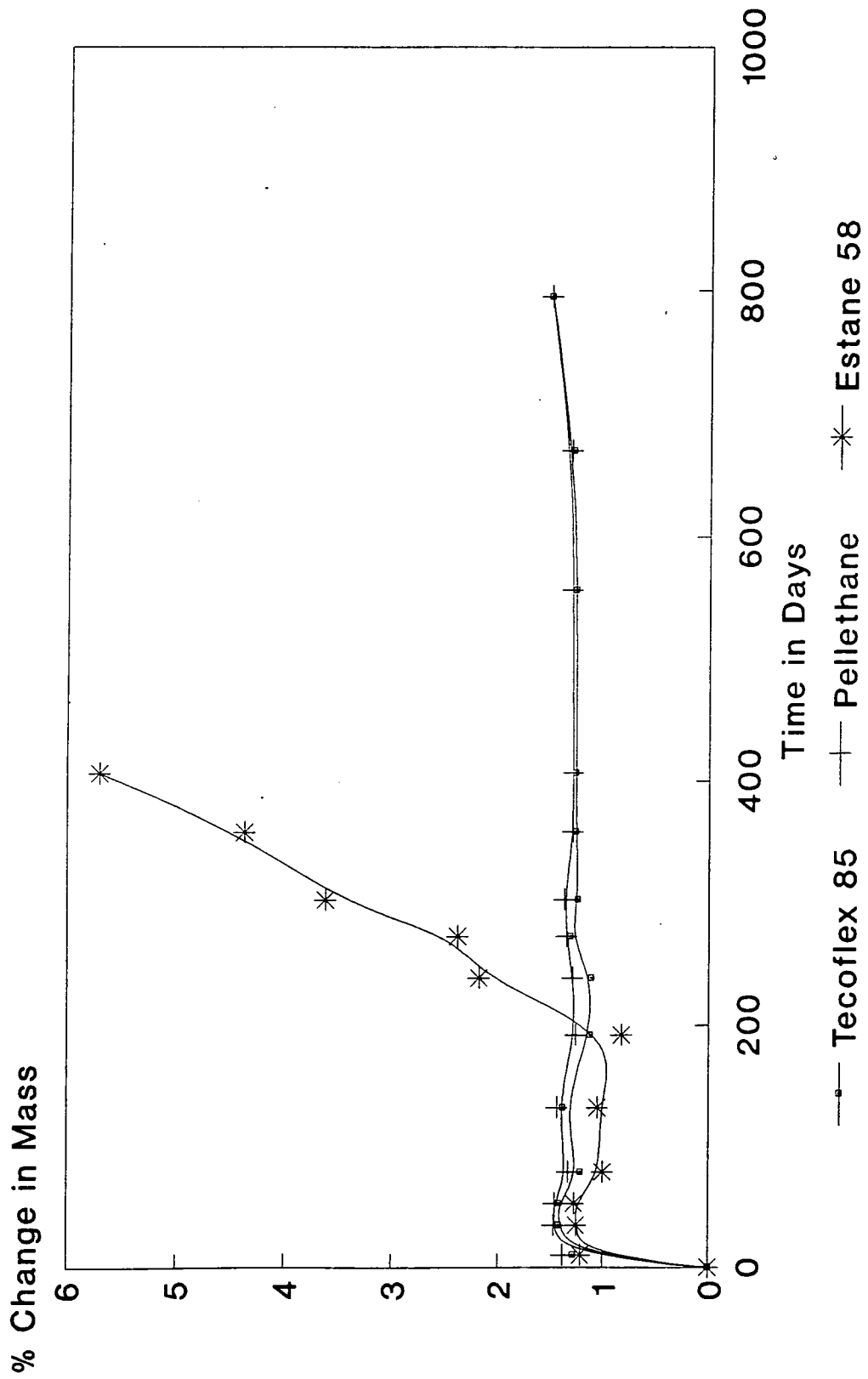


Figure 3.6c : The Change in Mass of Samples placed in Mammalian Ringers' at 37°C

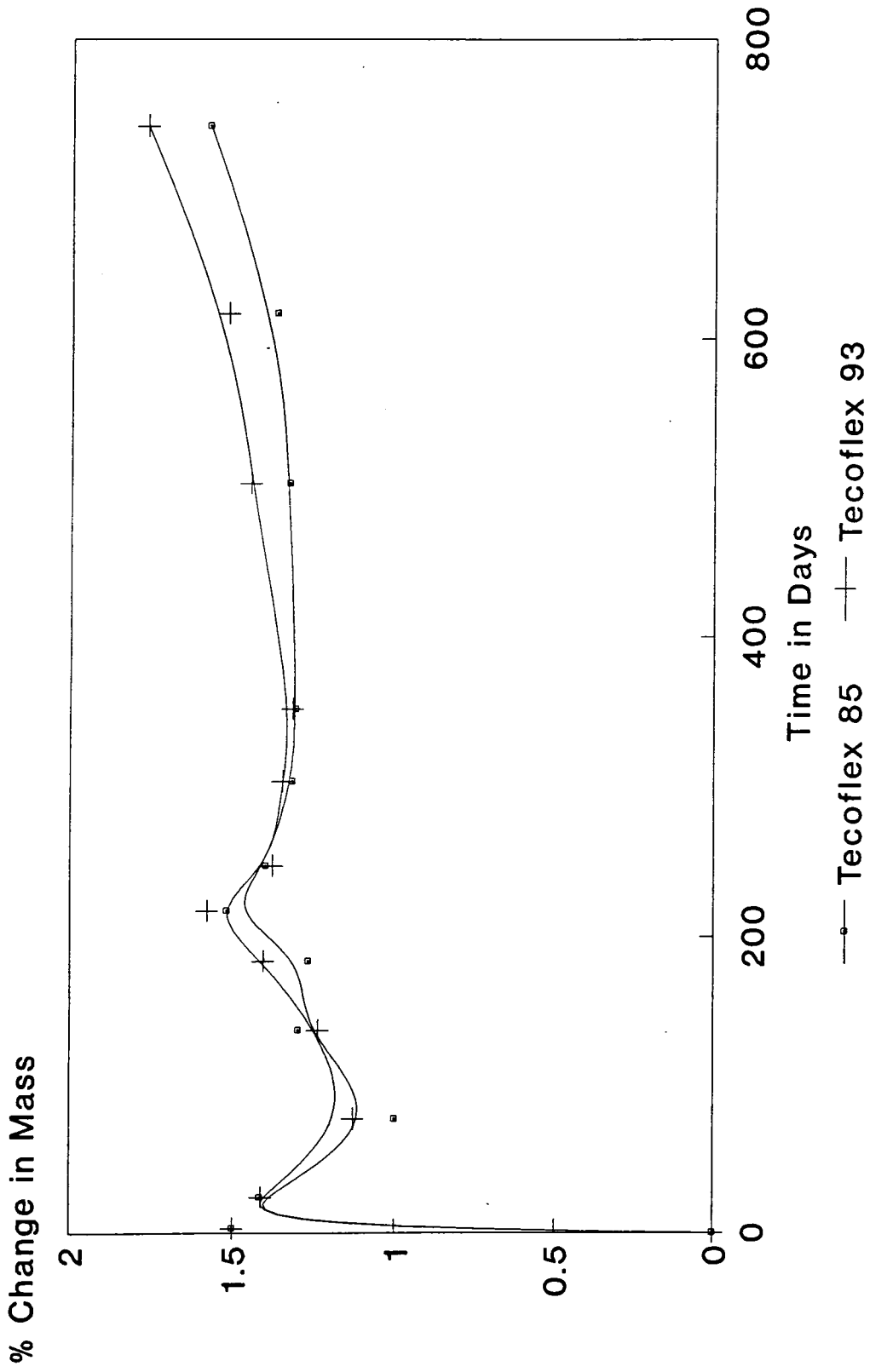


Figure 3.6d : The Change in Mass of Samples placed in Mammalian Ringers' at 37°C

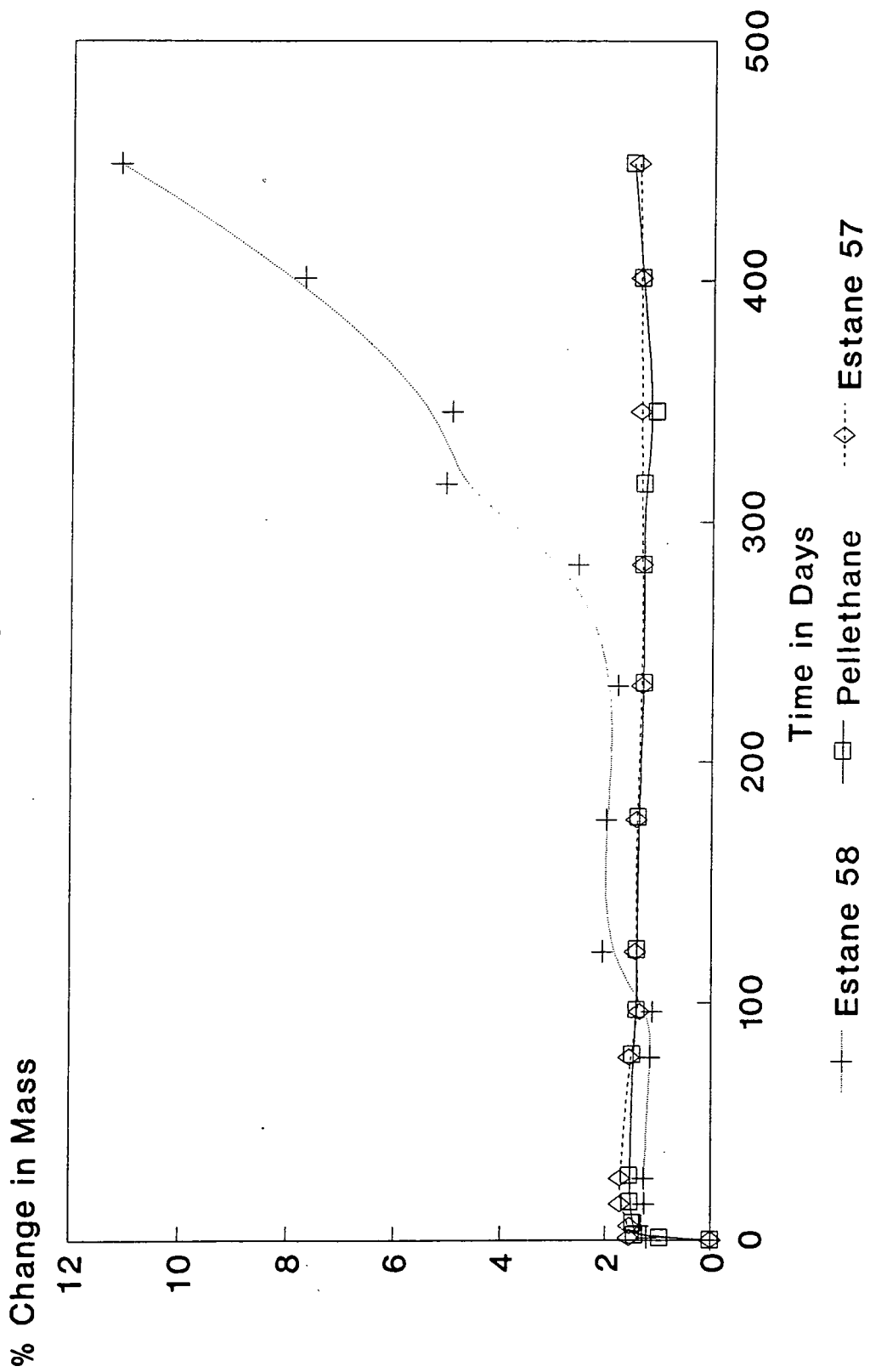


Figure 3.7a : The Change in Hardness of Estane cup samples placed in Mammalian Ringer's at 37°C

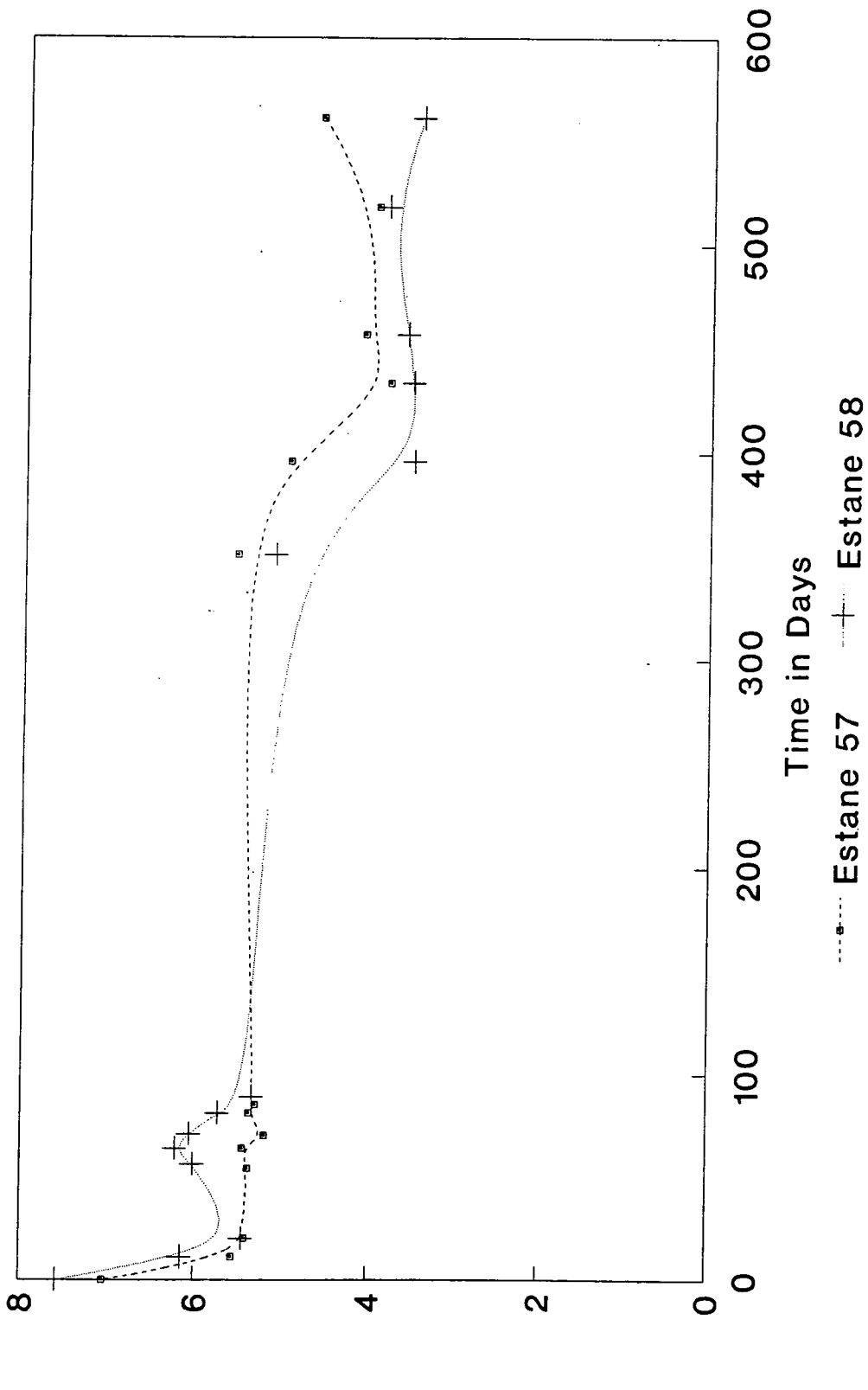


Figure 3.7b: The change in Hardness of Pellethane, Tecoflex and Estane '57' cup samples placed in Mammalian Ringers' at 37°C

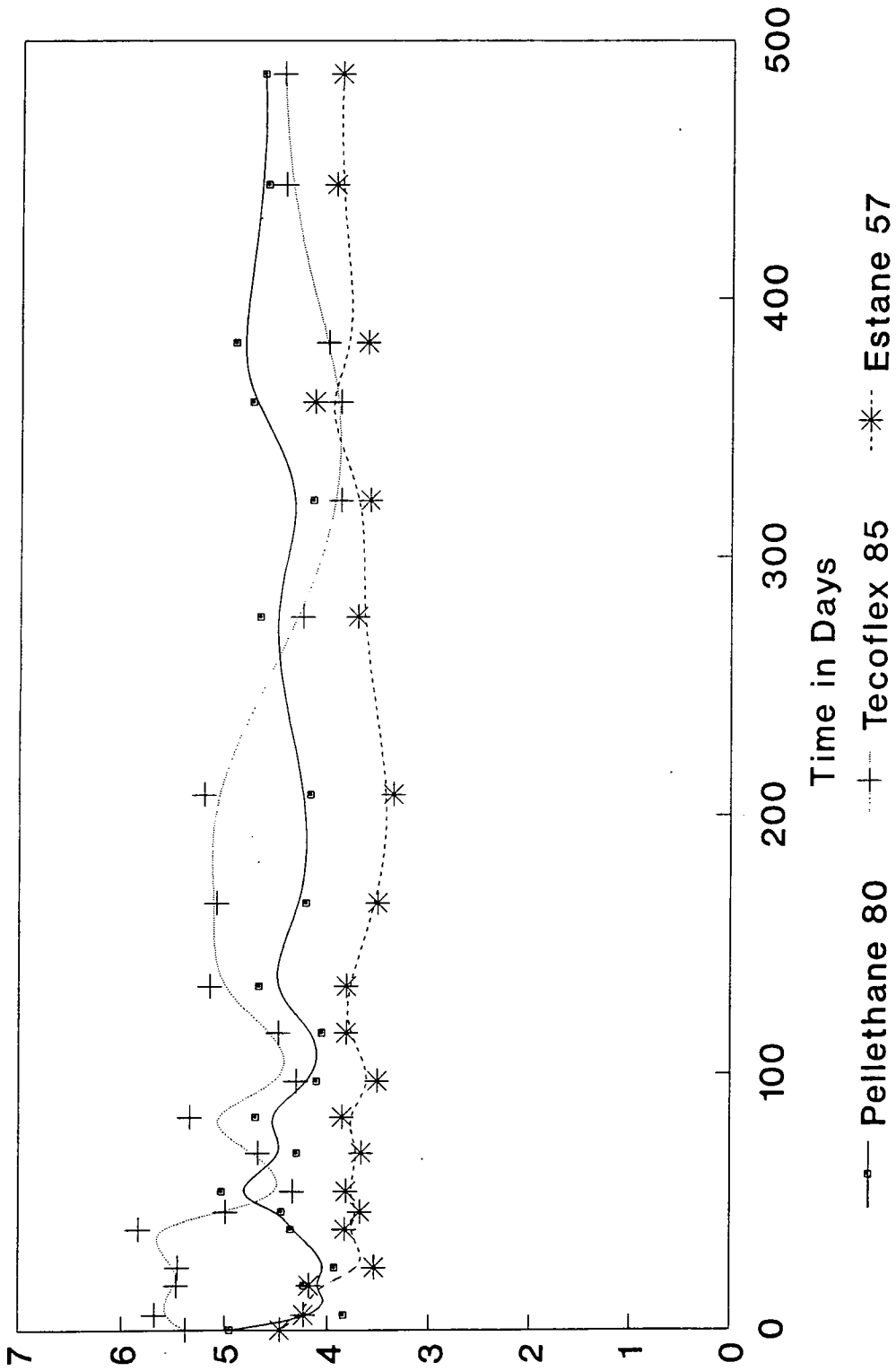


Figure 3.7c : The appearance of Polyurethanes following *In-vitro* degradation



Pellethane Estane 57 Estane 58

were similar to the strip samples with an initial sharp decrease for samples Estane '57' and '58' followed by a continued decrease in the property over the course of the degradation study amounting to a total reduction of 20% for Estane '57' and 50% for Estane '58'. Tecoflex 85°A showed a reduction in hardness of 22% and Pellethane showed little change over the entire course of the study. The Estane '58' cup sample showed a highly degraded surface which could not be tested at the completion of the study (figure 3.7c) after 760 days in solution. Estane '57' also showed changes with crazing of the surface noticeable between the individual granules used to produce the cup samples.

3.3.4.2 Frictional Measurements

The friction factors were measured for each polyurethane layer, lubricated with the range of differing viscosity CMC fluids. The results are displayed in figures 3.8 and 3.9, with the friction factor using the 0.010Pa s CMC fluid shown (this fluid behaves in a similar manner to diseased synovial fluid - section 5.6). All of the materials showed low values of friction at the beginning of the study with a rising tendency as the value of the viscosity of the fluid increased in magnitude, representative of fluid film lubrication. The values of friction factor were also very low, at approximately 0.008 over the range representative of *in-vivo* conditions.

Following immersion in Mammalian Ringer's at 37°C, Estane '57' and '58' both showed increased values of frictional torque at all viscosities at some stage during the soaking process with rises of up to 300% in the physiological range expected from osteo-arthritic synovial fluid. After 400 days the friction of the Estane '58' samples increased substantially, and the material surface changed to reveal deepening cracks on a white surface (figure 3.7c). Although Tecoflex 85°A and Pellethane acetabular cups have shown changes in friction factor during some periods of the testing, values

Figure 3.8 : The Friction Factor of Polyurethane Cups tested
Friction Factor (x1000) in the Hip Simulator with 10cP Lubricant

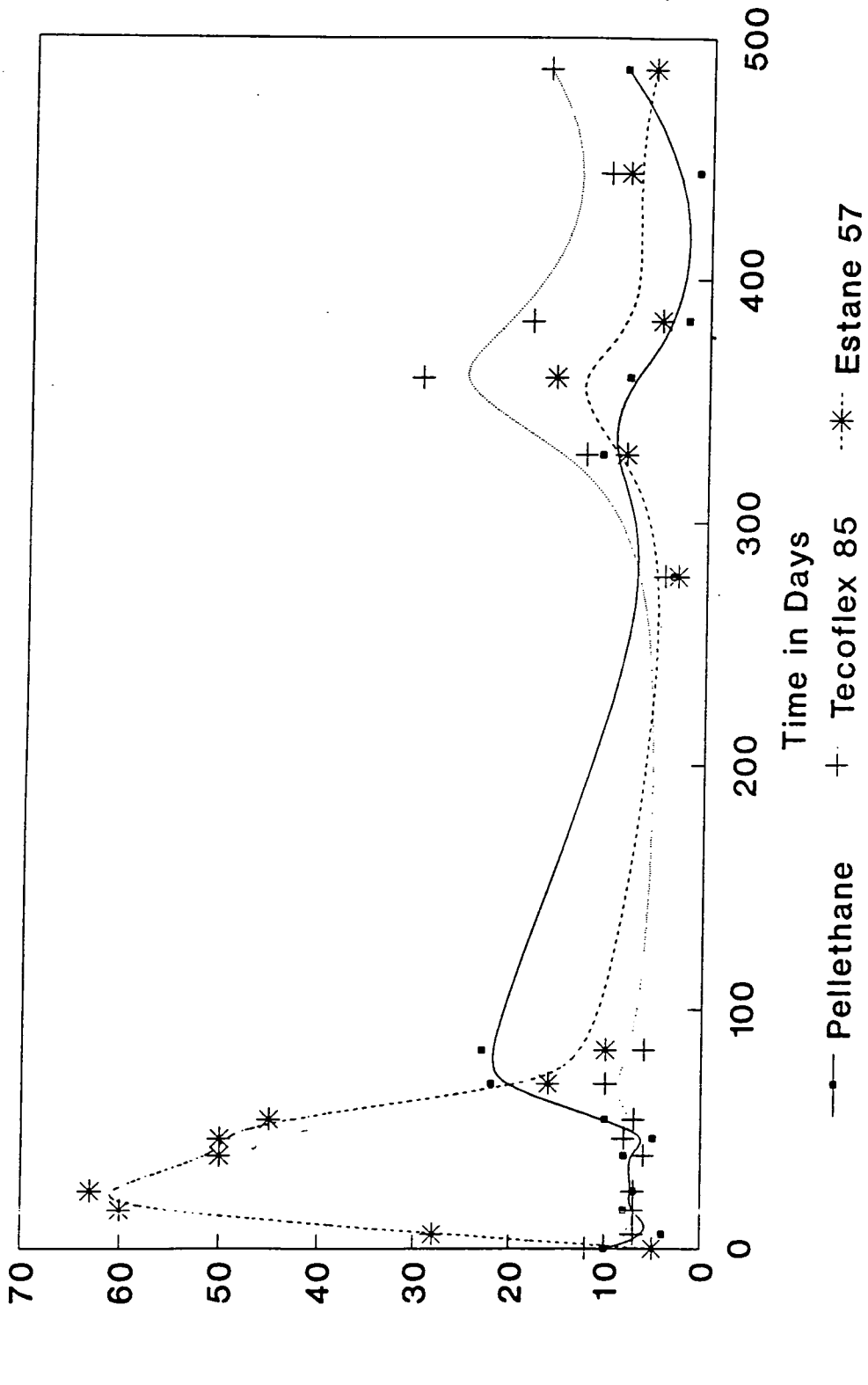
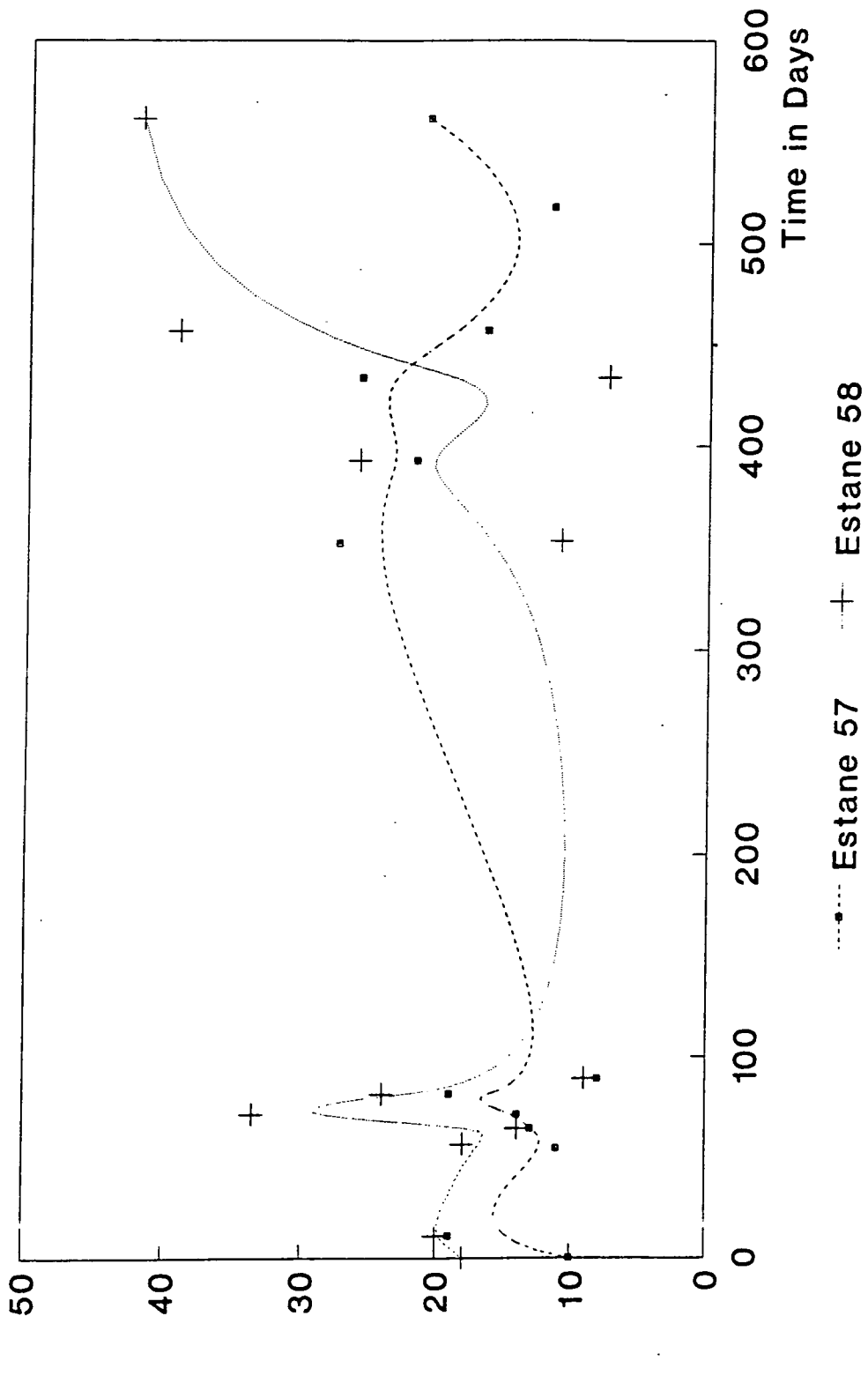


Figure 3.9 : The Friction Factor of Polyurethane Cups tested in the Hip Simulator with 10cP Lubricant



of friction factor did not rise above 0.030. However, grabbing may be the cause of the increase. For comparison a new Charnley Prosthesis has a value of about 0.050 (section 6.4.2). At present the Pellethane samples are showing the lowest friction.

3.4 Discussion

There are five modes of degradation which have been identified in polyurethanes (Lelah and Cooper, 1986):

Random chain scission occurs because of bond breakage leading to decreases in chain lengths and a slow gradual decrease in strength and a measurable decrease in a polymer's resistance to wear.

De-polymerisation can also occur and results in the polymeric material being transformed into monomeric units owing to the breakage of weak C - C bonds normally in the presence of strong C = C bonds.

Bond changes often linked with de-polymerisation, can lead to the formation of C = C bonds from the single bond leading to by-products and tending to weaken the other bonds in the chain of material.

Cross Linking is a phenomenon which is sometimes induced to increase the wear resistance of polymers and involves linking chains together along their length. However, it often causes hardening and embrittlement of the polymer, which is important for polyurethanes under conditions of large deformations, leading to premature mechanical failure. In addition hardness changes can lead to changes in the lubrication mode which is operating.

Side Chains may also be attacked (e.g. acid and alcohol groups) leading to a total change in the chemical properties of a molecule and hence the mechanical properties of the material.

The polyurethanes which were investigated had a number of differing material structures:

Estane '58' was a polyester urethane. The -ester group responds to an aqueous environment by hydrolysing and causing breakage of the chains. This was noticed by the large decreases in hardness and elastic modulus. The increase in mass of the specimens after about 300 days in solution may be due to the structure becoming more porous thus allowing a larger mass of fluid to be held in the polymer chains. At this stage it would be advantageous to measure the average molecular masses of the chains in each of the polyurethanes. Hydrolysis may have been limited to a fairly small region at the material surface initially, but may now have spread more deeply into the matrix. Hydrolysis involves a form of de-polymerisation and it is likely that the resultant surface damage caused breakdown of the fluid film and thus increased friction. Chemical Analysis using Reflected Infra-red (Appendix IV) revealed no differences between degraded and virgin material. This indicates that any structure change applied to less than 5% of the material.

Estane '57', a polyether urethane, showed stable specimen mass initially, but also indicated gradual decreases in hardness and elastic modulus. The ether linkage is not so easily broken by the action of hydrolysis. However, chain scission may be occurring at other points leading to a lower proportion of long chain molecules, thus increasing the number of soft segments and reducing the material hardness and elastic modulus. It is likely that this may also be a surface phenomenon leading to the changes in tribological properties of the layer.

The generation of a fluid film between two articulating surfaces is compromised by degradation of the polymeric surface. Estane '57' and '58', which showed the largest decreases in both hardness and elastic modulus, also showed higher friction factors measured in the hip function simulator following immersion in Mammalian Ringer's solution for 550 days. These results indicate a change in the mode of lubrication away from fluid film towards a 'mixed' mode, where part of the load is carried by direct solid contact.

Pellethane and Tecoflex showed little changes in any of the measured quantities and following initial fluid uptake there was no change in fluid content over the course of the study. Tribological properties were consistent at very low values of friction factor of 0.005-0.015 indicating little change in the material surface.

Pellethane and Tecoflex both showed consistent hardness and elastic modulus values as well as frictional torques which changed little over the course of the study. Frictional torques were at least an order of magnitude less than the best currently available prostheses showing a friction factor of 0.005-0.015 for fluid viscosities representative of osteo-arthritic synovial fluid. These low values and the shapes of the Stribeck plots indicate fluid film lubrication. When this regime is operating the surfaces are completely separated and so wear should be extremely low.

3.5 Fatigue of Polyurethanes

3.5.1 Introduction

Elastomers made of polyurethane with elastic moduli of 5-20MPa commonly have maximum tensile stress values of 10's of MPa coupled with ultimate elongations of 500% or more. Therefore the stresses and strains applied to a soft layer prosthesis

in-vivo will not cause failure in a single application. However repeated cycling will introduce fatigue loading to the polymer which must be studied before the materials can be considered for clinical use in this application.

The mechanical properties of polymers are highly dependent on external conditions with increases in temperature and the presence of a hydrating medium leading to large reductions in elastic modulus and ultimate tensile strength (sections 3.2 and 3.3). It is for this reason that the effects of fatigue stresses must be measured in a representative environment.

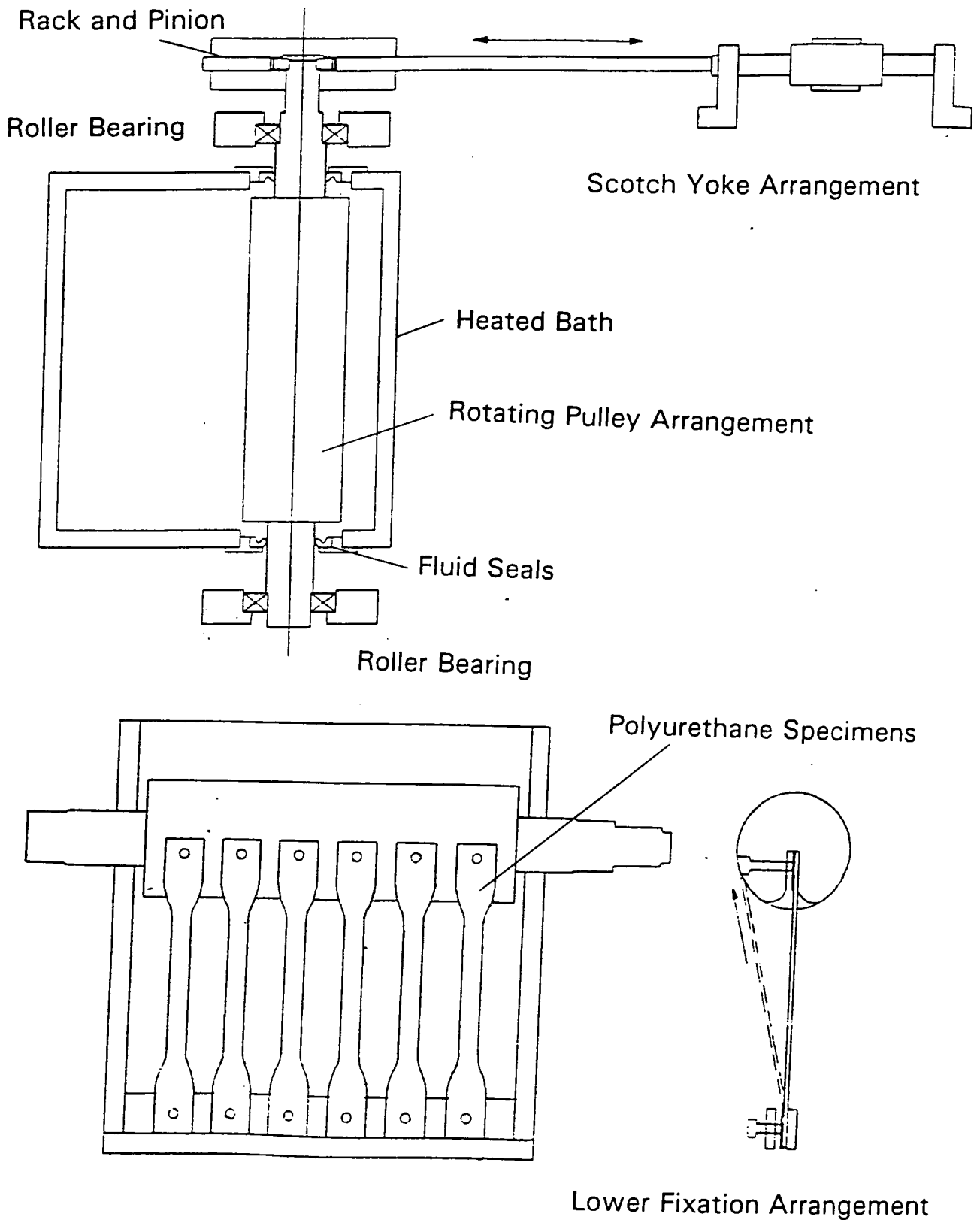
3.5.2 Methods of Measurement of Fatigue Response

During walking, loads of up to 2500N are developed (Paul, 1967) for short periods (figures 5.26a and 5.26b). Calculations and experimental results in chapter 6 show that pressures of up to 3.5MPa are produced with maximum compressive strains of the material in the cup of about 15%.

Because of the difficulty in assessing changes in compressive properties, especially of thin layers moulded to a bonding material, tensile stresses and strains were used since this would represent a more secure test of the fatigue properties of the material. Under fatigue analysis some metals exhibit a fatigue limit for developed stresses below which the component life is infinite. However polymers and other non-metallic materials do not exhibit a fatigue limit and even at low stresses there will be failure after a large number of cycles.

A fatigue machine was designed and built at Durham (figure 3.10), which allowed a sinusoidal strain to be applied to a maximum of 6 samples through a scotch yoke mechanism. The assembly was housed in a circulated bath of saline maintained at

Figure 3.10 : The Tensile Fatigue Rig



37°C to mimic *in-vivo* conditions. Studies of the variations of the mechanical properties of these elastomers indicated the importance of using the hydrated samples at 37°C (section 3.3). Samples were standard tensile dumbbells of 1.5-2.0mm thickness, working length 65mm and total length 150mm and were produced by compression moulding of flat sheets.

Initial studies were stress controlled, with extensions of 50 and 60% being required to produce the stresses developed in the acetabular cups which had previously been calculated as circa. 3.5MPa.

Tests on Tecoflex 85°A indicated failure after only 10,000 cycles. Similar experiments were conducted with Tecoflex 93°A, but failure was observed after relatively few cycles (circa. 100,000). Tests performed in the hip function simulator under conditions of lubricated motion and dry rubbing (where large shear stresses are developed on the surface of the polymer due to large frictional forces of up to 400N) indicated that fatigue damage was not evident after 120,000 cycles (section 6.8). A better indicator of conditions in the body might be maximum strain rather than stress, so strain was used as the limiting condition for the fatigue cycle. Tests on elastomeric acetabular cups indicated that loads of 2500N applied through a stainless steel ball resulted in penetrations in the region of 0.300mm. This corresponded to a 15% strain on a 2mm thick layer. Therefore, strains of 15% were used with a loading cycle which was similar to the hip loading cycle with 0.6 seconds under load and a recovery phase of 0.55 seconds. The frequency of the cycle was 0.87Hz.

3.5.3 Results

Initial results with Tecoflex 85°A showed a vast improvement in fatigue life with little change after approximately 400,000 cycles. Elastic modulus of the samples

was measured at 200,000 cycle intervals and little change was noted between the fatigue loaded samples and the control samples.

Samples of Tecoflex 93^oA were then investigated as these had shown improved fatigue properties during the earlier studies. The samples performed well and on completion of 9.5 million cycles were removed and tested to failure. In a similar way Pellethane 2363-80^oA samples were tested. Elastic modulus tests were conducted periodically. The samples were removed from the saline solution and left at 21^oC for one hour prior to testing. The mass of the samples was measured before and after testing to ensure that similarly hydrated samples were tested owing to the change in mechanical properties with hydration (section 3.2).

The test group consisted of 3 samples undergoing active fatigue with three identical samples as controls placed in the same saline bath. Because of large changes in measured Elastic modulus from small differences in degree of hydration it was decided to base the results on comparisons between fatigued and control samples as opposed to absolute values of modulus.

Some plastic deformation of the fatigue samples was apparent with increases in length tabulated (table 3.1), although a proportion of the deformation was recovered at the end of the study following two months under no load. The deformation obviously had to be taken into consideration when measurements of elastic modulus were made.

The results of the elastic modulus measurements are shown in figures 3.11a and 3.12a with comparisons between the fatigue and control samples shown as a percentage value. The mass of the samples was monitored and displayed on figures 3.11b and 3.12b. For the Tecoflex 93^oA samples it can be seen that following a difference of

Figure 3.11a: The Elastic Modulus of Samples of Tecoflex 93A undergoing fatigue in Mamalian Ringer's at 37°C

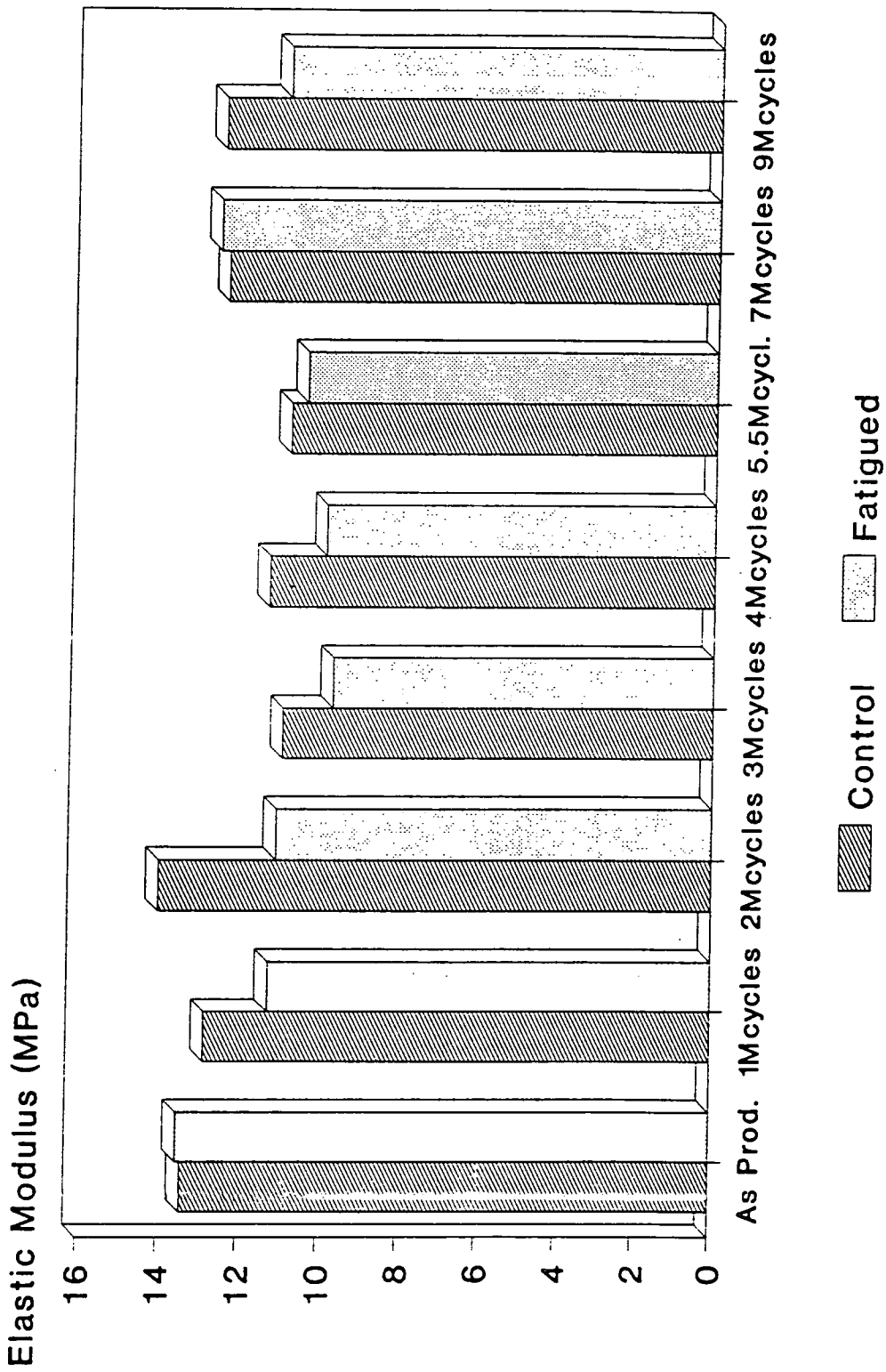


Figure 3.11b: The Mass of Fluid Contained in Samples of Tecoflex 93A undergoing fatigue in Mamalian Ringer's at 37°C

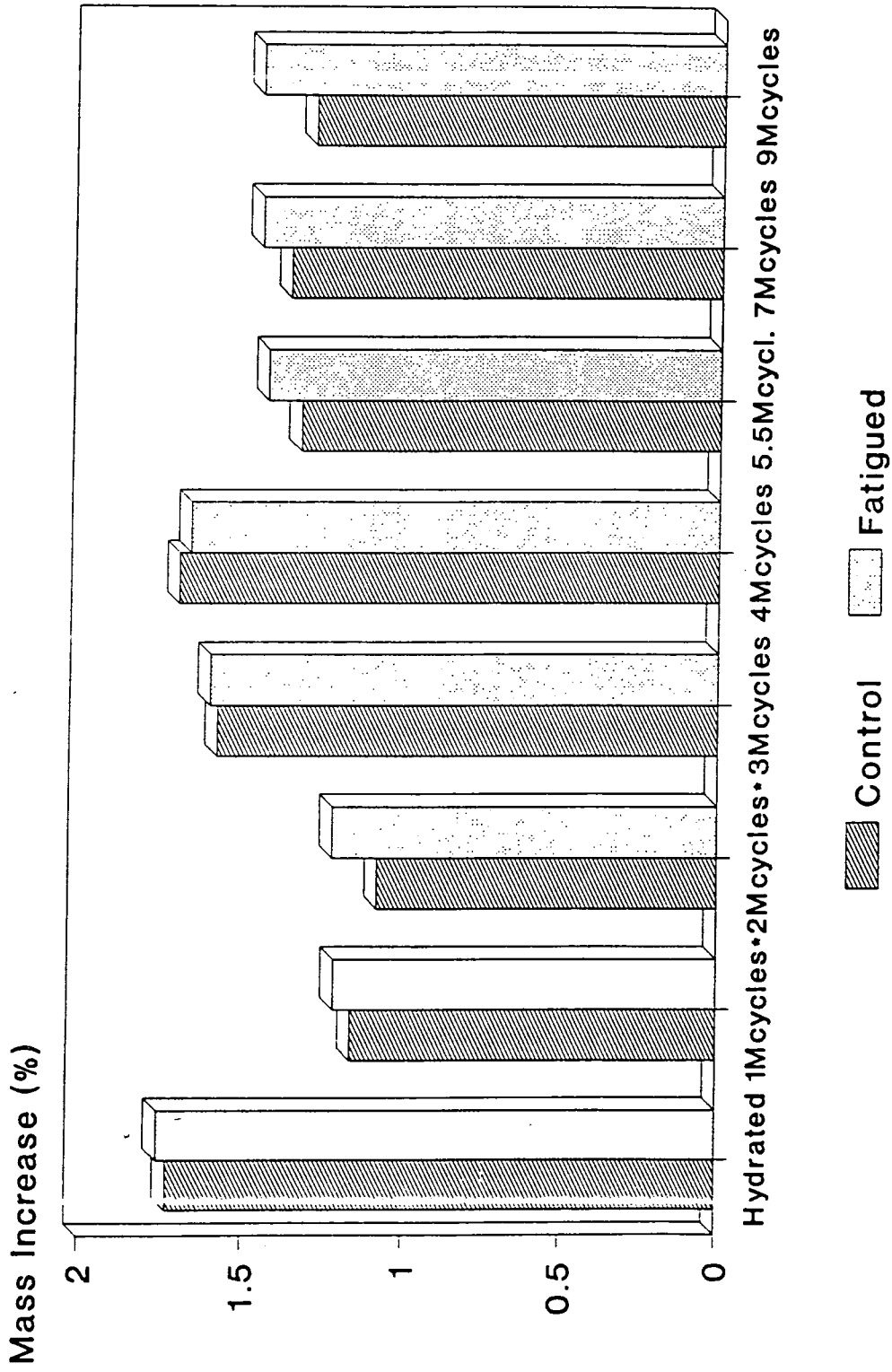


Figure 3.12a: The Elastic Modulus of Samples of Pellethane undergoing fatigue in Mamalian Ringer's at 37°C

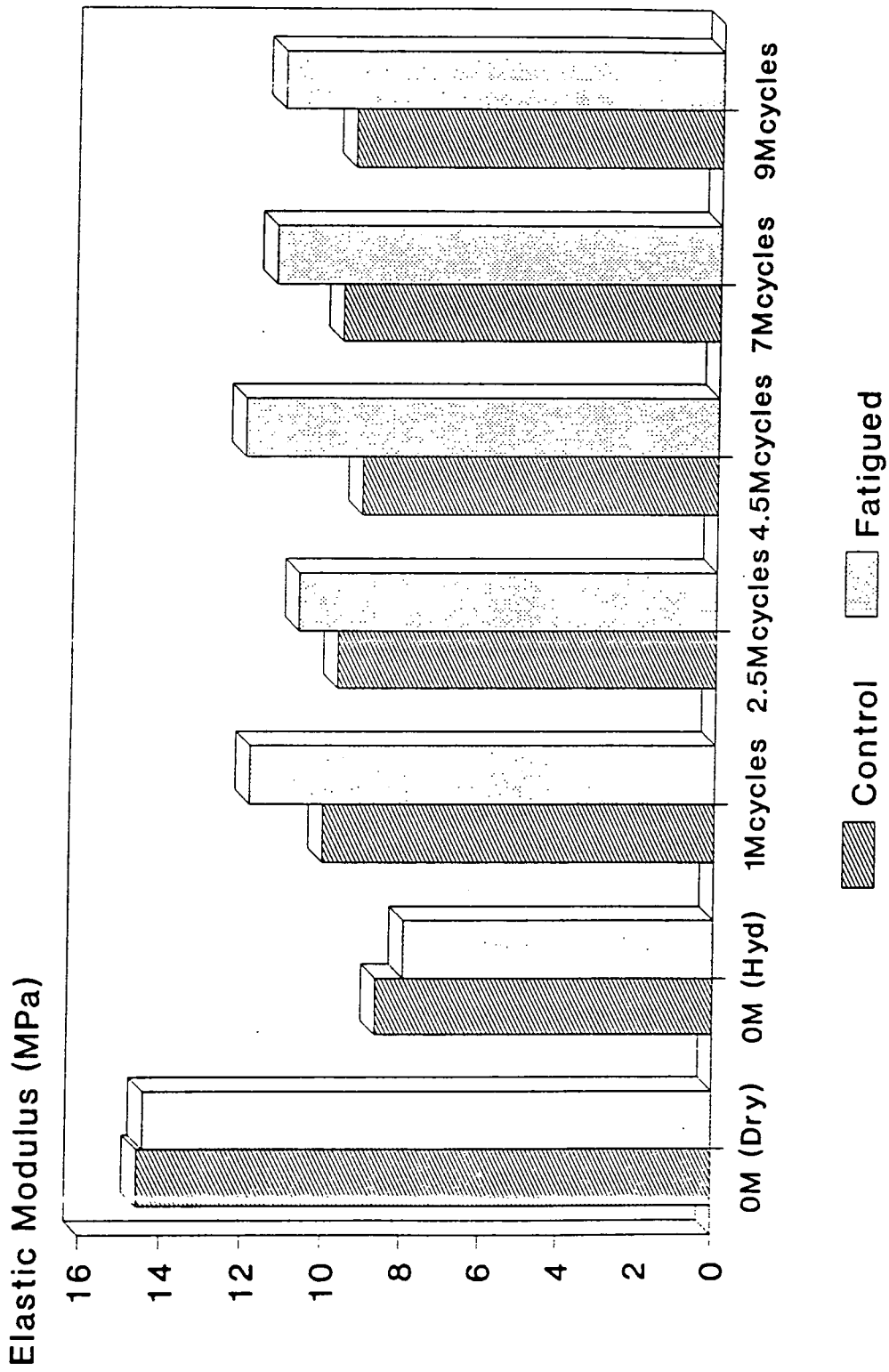
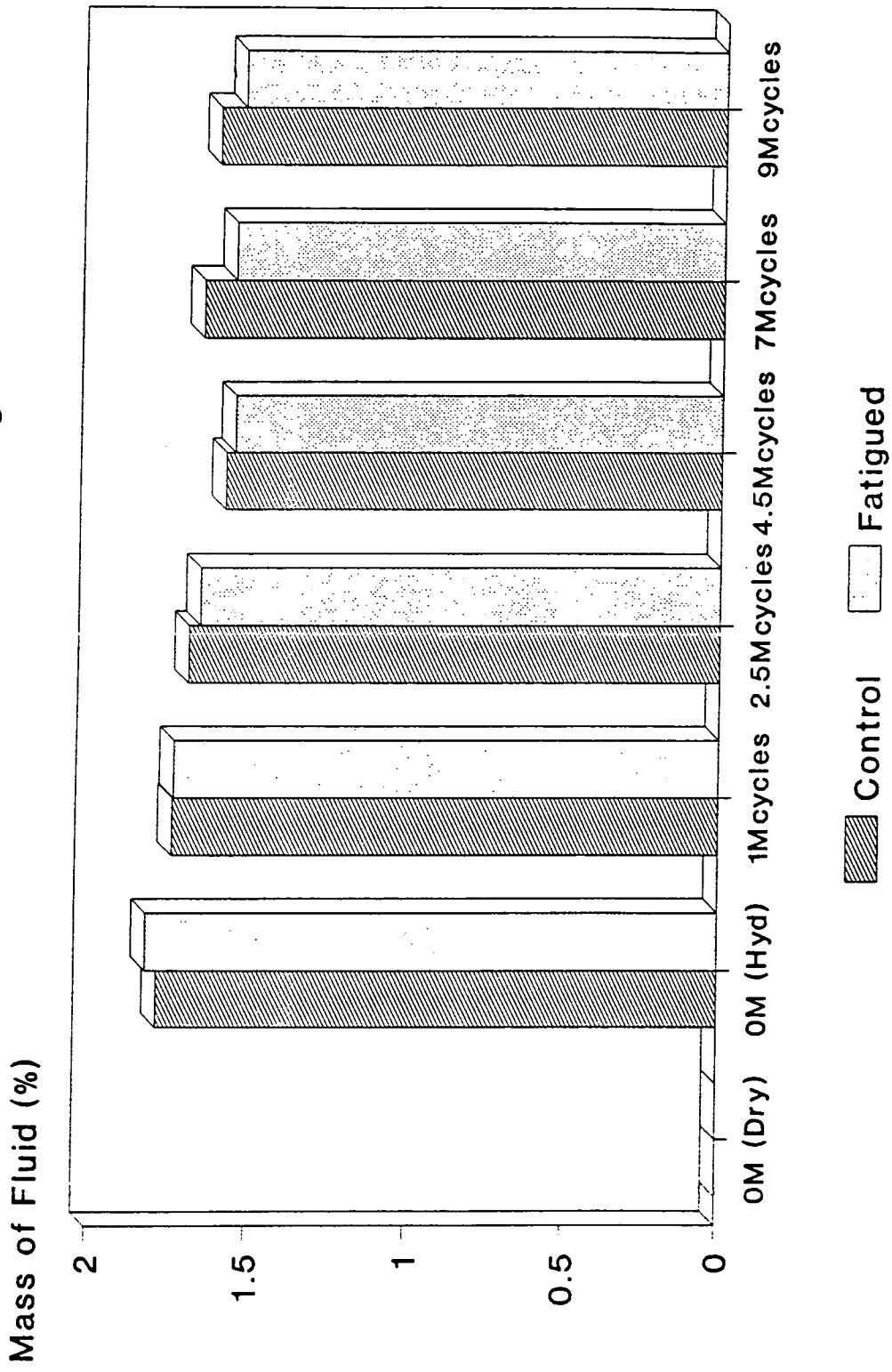


Figure 3.12b: The Mass of Fluid Contained in Samples of Pellethane 80A undergoing fatigue in Mamalian Ringer's at 37°C



20% measured after 2 million cycles the values of elastic modulus had returned to a 12% difference after 4 million cycles. Tests carried out after 5.5 million cycles show the values of modulus for the fatigue and control samples to be very close, with a 2% difference, which is less than experimental error. This difference was maintained at a low level to 7 million cycles but a drop in modulus of the fatigued samples of 8% was noted at 9 million cycles. The mass of the fatigued samples was consistently higher than the controls (about 0.1% greater uptake of fluid). Pellethane samples showed consistently that the elastic modulus of the fatigued samples had increased over the controls, although the mass of the two groups of samples were very similar.

Table 3.1: Plastic Deformation of Fatigue Samples

Cycles	Tecoflex EG93 ^o A		Pellethane 2363-80 ^o A	
	Length (mm)	% Increase	Length (mm)	% Increase
0	100.0		99.6	
1M	104.1	4.1	104.3	4.9
2M	105.8	5.8	103.1	3.5
3M	107.4	7.4	105.2	5.4
4M	108.9	8.9	106.0	6.4
5.5M	109.7	9.7	105.8	6.2
7M	109.8	9.8	105.7	6.1
9M	110.7	10.7	106.2	6.6
Recovered	106.8	6.8	-	-

3.5.4 Discussion

At this stage both of the polyurethanes are indicating favourable fatigue properties with relatively small decreases in modulus evident after nine million cycles.

This represents approximately 9 years activity as an implant, which is similar to the average lifetime of a current prosthesis (circa. 10 years).

Ultimate tensile stress was measured at a loading rate of 5mm/s. The results were based on sample groups of three for the fatigued and control samples and four for the unused samples of each polyurethane. Both Engineering (**Eng.**) and True Stresses were used to calculate values of modulus and failure stress.

Table 3.2a : Tensile Testing of Fatigued, Control and Unused Polyurethane Samples

Material	Tecoflex EG93 ⁰ A			Pellethane 2363-80 ⁰ A		
	Fatigue	Control	Unused	Fatigue	Control	Unused
0-100% Modulus (MPa) - Eng.	9.33	9.84	9.06	6.26	5.88	5.83
0-200% Modulus (MPa) - Eng.	8.22	7.76	7.49	4.15	4.02	4.12
0-300% Modulus (MPa) - Eng.	-	-	6.81	3.55	3.39	3.47
0-400% Modulus (MPa) - Eng.	-	-	-	3.42	3.24	3.31
Max. Stress (MPa) - Eng.	23.0	14.1	25.8	23.6	20.3	24.5
0-100% Modulus (MPa) - True	14.0	14.8	13.6	9.4	8.8	8.75
0-200% Modulus (MPa) - True	16.44	15.52	15.00	8.30	8.04	8.24
0-300% Modulus (MPa) - True	-	-	17.03	8.88	8.48	8.68
0-400% Modulus (MPa) - True	-	-	-	10.26	9.72	9.93
Max. Stress (MPa) - True	86.0	41.5	121.8	158.8	131.8	182.0
Max. Elongation (%)	274	194	372	573	549	643

The fatigue samples of both materials had Engineering and True moduli from 0-100 and 0-200% extension (and 300 and 400% extension for the Pellethane samples)

which were similar to the control and unused samples. Failure was initiated in the Tecoflex control and fatigued samples from the holes at the sample ends, used for fixation in the tensile testing machines. Wedge grips were used for the rest of the tests and the gauge length reduced to 75mm to remove the holes from the loaded region. However, maximum engineering stresses of 23.0MPa for the Tecoflex EG93^oA fatigue samples and 14.1MPa for the control samples were recorded, which correspond to true stresses of 86.0 and 41.5MPa respectively. The unused samples had slightly lower values of elastic modulus throughout, but the fact that failure was not initiated from the fixation holes meant that a higher value of ultimate tensile stress (25.8MPa) and elongation (372%) were recorded. These values represented a true stress of 121.8MPa. The close correlation of the mechanical properties of the Pellethane samples showed the resistance of the material to both degradation and fatigue.

3.6 Bonding of Polyurethanes to a Rigid Backing Material

3.6.1 Introduction

The use of soft elastomeric layers in hip prostheses poses problems with fixation of the acetabular cup to the bone of the pelvis. It must be supported by a rigid backing to maintain dimensional stability under high loading. This backing material must be bonded to the elastomeric surface to eliminate problems of the acetabular component grabbing the femoral head owing to the high Poisson's ratio of the material. If no bond were present, the layer would separate from the backing material and wrap around the ball, leading to greater frictional resistance. When correctly bonded, the rigid backing will reduce the tendency of the layer to grab onto the femoral head due to the geometrical arrangement. This may allow smaller clearances to be used between the femoral head and the acetabular cup which will improve the tribological properties since lower contact pressures are developed.

The use of adhesives in this application poses problems with bio-compatibility, bio-stability, hydrolysis, fatigue and creep response. In addition there is a requirement for a flexible bond due to the low elastic modulus of the polyurethane adherand.

3.6.2 Theory of Joint Design

Joints should be specifically designed to facilitate several bonding criteria:

1. Allow application of the adhesive
2. Allow the adhesive to cure
3. Put the adhesive under acceptable loading

Bonding of the elastomeric layer to the rigid backing would take place in a controlled environment, i.e. not *in-vivo* and so the first two criteria may be assumed. However ensuring that the loading is not too high for the adhesive requires thorough stress analysis and possible redesigning of the interface. Forces is transmitted between the substrate and the surface layer through the adhesive bond which consists of many minute adhesion sites. If enough of these sites are sharing the load then a successful joint can be formed. A number of loading geometries may be applied to the joint:

3.6.2.1 Tensile/Compressive Loading

In their idealised form, these joints have the highest strength when stress is being distributed over the entire bond area (figure 3.13a). However deflection of the joint components can lead to non-uniform loading and give rise to cleavage stresses (figure 3.13b) which reduces the load carrying capacity of the joint with stresses concentrated over a small cross-section of adhesive.

3.6.2.2 Shear Loading

Joints which include shear loading of the adhesive, apply stress over the entire bond area, but higher stresses may be concentrated at the ends of the bond (figure 3.13c). The strength of this form of joint is typically $1/10$ of that of a bond loaded in

Figure 3.13a: Tensile Loading of an Adhesive Bond

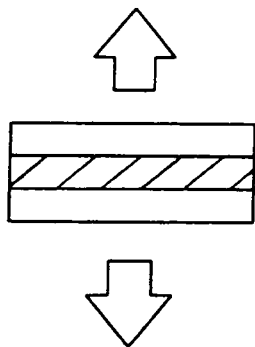
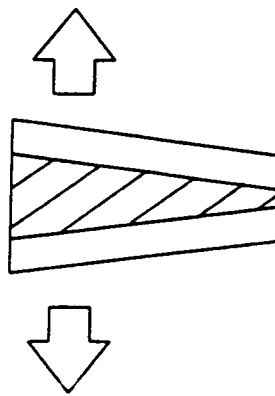


Figure 3.13b: Cleavage in tension on an Adhesive Bond



 Adhesive

Figure 3.13c: Shear Loading of a Lap Joint

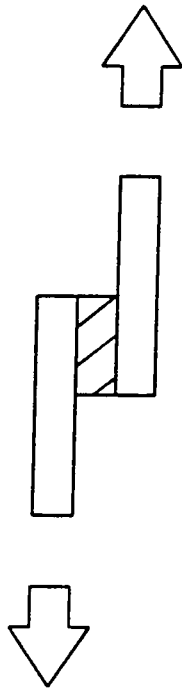
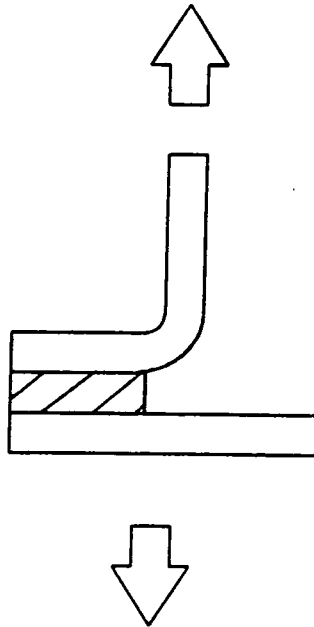



Figure 3.13d: Peel of an Adhesive Joint



 Adhesive

compression (with no cleavage). In-service conditions are normally limited to situations where shear stresses are less than 20% of the ultimate shear stress of the adhesive (Lees, 1984).

3.6.2.3 Peel Loading

The peel strength is usually the weakest property of a joint, and toughened adhesives are the only types capable of maintaining reasonable peel strengths. This property is normally assessed with a similar arrangement to that shown with a peel angle of 90 to 180° (figure 3.13d). Values of only $1/1000$ of those obtained in compressive loading and $1/100$ of the strengths obtained in shear loading are typically measured under peel tests.

3.6.3 Materials

Initially metal backed cups were used in the assessment of the performance of soft layers with the layer bonded directly to the backing by compression moulding. The bond was found to be extremely weak and holes had to be drilled in the stainless steel backing material to provide a mechanical interlock and allow the layers to be tribologically tested (figure 3.14).

This would be unsuitable for an *in-vivo* model and does not maximise the potential of the layers, requiring large clearances to limit the grabbing during use. Also if there were problems with the elastomeric layer during service and failure of the lugs occurred (as has been noted during long term *in-vitro* studies), the resulting metal on metal contact would necessitate immediate revision surgery.

Polyethylene, in its ultra high molecular weight (UHMW) form has been widely used in knee and hip prostheses since Charnley re-engineered his hip prosthesis to make use of it. Since this time its biological response has been well documented, with little

Figure 3.14 : Stainless Steel backed Acetabular Cups

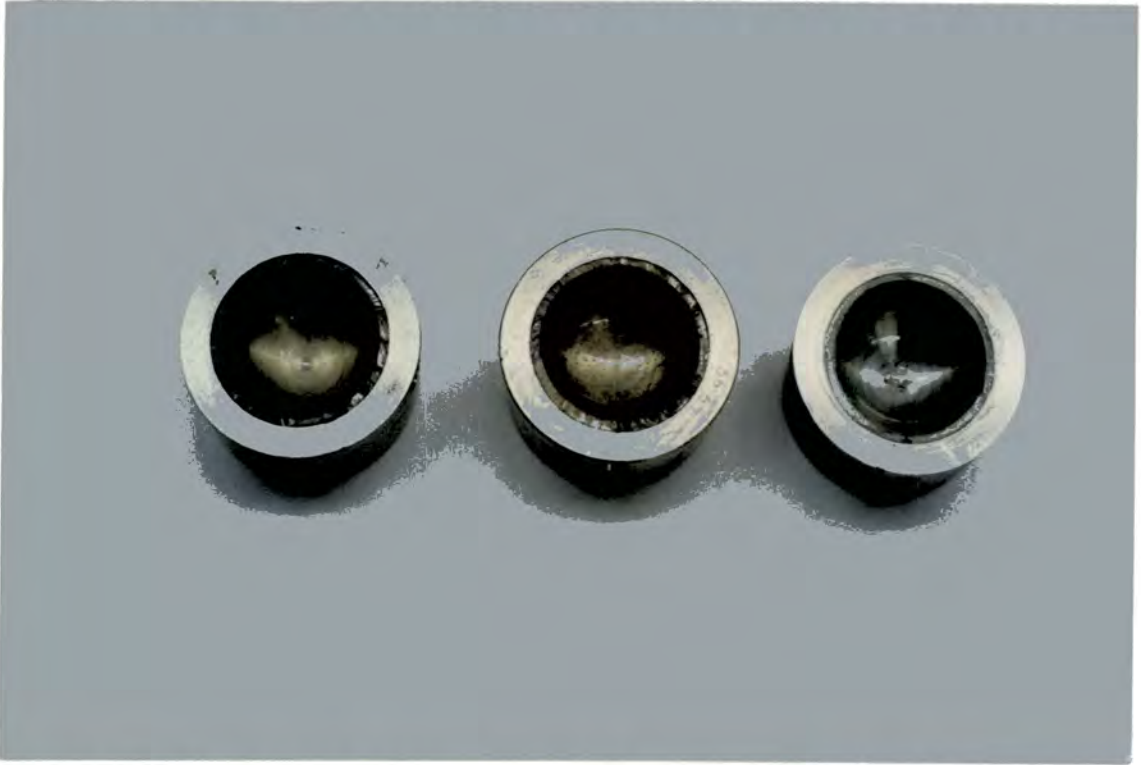


Figure 3.15 : A Customer Cup showing signs of Degradation



tissue reaction and minimal polymer degradation (Gibbons, 1978 & Hastings, 1978). Therefore, it would seem to be a good material to act as a backing for the elastomers. In the event of failure of the elastomeric layer this would lead to a UHMWPE/metal contact which shows reasonable friction of about 0.05 - 0.06, which is much lower than a metal-on-metal contact.

A further reason for using UHMWPE can be understood by considering the fixing arrangements for many currently available prostheses. Cementless, porous and hydroxyapatite coatings on metallic surfaces have become popular for improving bone fixation with the polyethylene acetabular component a "snap-fit" into a metallic shell. The Durham prosthesis could easily be incorporated into many of the currently available systems. This would allow a direct comparison to be made between the performance of soft layers and UHMWPE in a prosthesis with no other variables.

3.6.4 Adhesive Theory

The performance of an adhesive is highly dependent on the adherands. Surface cleanliness is important with de-greasing often mandatory prior to the application of the cement. However, some adherands are generally considered to produce poor bonds and polyethylene is amongst these. This is because of its waxy hydrocarbon surface which does not allow the polar active adhesive to bond well. This material requires oxidation of the surface, replacing the hydrogen ions (H^+) with oxygen ions (O^{2-}) to exhibit a polar surface for improved adhesion. Even with such modification there are only a few adhesives which are suitable.

3.6.4.1 Hot-melt Adhesives

Thermoplastic polymers are used in a liquid form at an elevated temperature to cover the surfaces prior to pressure and cooling to complete the bond. Problems can

occur because full wetting of the surface may be poor if a material of low surface energy such as polyethylene is used. In addition elevated service temperatures will lead to weakening of the bond through adhesive softening. This may be a problem in the body (37°C) if a low temperature adhesive were used. Bio-compatibility should be good, assuming a compatible thermoplastic were to be used. Bond strength is highly dependent on suitable adherands and a polar surface which may also be roughened.

3.6.4.2 Polyurethane Adhesives

Base materials of isocyanate and an amine or glycol are mixed to form a liquid material with quite a high viscosity which is then cast onto the surfaces to effect a bond. The castomer resin (non bio-compatible) which was used during the early phases of soft layer work (Unsworth *et al*, 1987) was moulded *in-situ* through this reaction. The bonds produced can be of good strength, especially in peel and impact loading but they are often the result of cross-linking of the polyurethane which can render it non bio-compatible. Also problems can occur in hot wet environments due to hydrolysis. This was observed with the castomer material following studies at 80°C in saline, with cracks appearing on the surface (figure 3.15).

3.6.4.3 Solvent Cast Systems

These range from low viscosity liquids to pastes and consist of a thermoplastic polymer (or polyurethane) carried by a suitable solvent. These can be bio-compatible, for example Tecoflex resins carried in Tetrahydrofuran solvent have been successfully used in the body (Brown, 1988). Cross linked materials tend to give the greatest strength with only light loading possible with non-cross linked adhesives. Precise placement is mandatory as there is an instantaneous "grab". Curing is often required to remove all of the solvent. The adhesive layers can be quite thick and so surface

roughening can be effected and because of their bond thickness adhesives are suitable for fatigue applications.

3.6.4.4 Alternative Systems

Other possible adhesives include Nitrile and Silicone rubbers. Although both are highly resistant to bio-degradation and they are obtainable in a variety of hardnesses, the strength of bonds obtained with the two adherands would be questionable. Toughened acrylics, a family which includes bone cement, show good bio-compatibility, but are often of high elastic modulus and as such are not suitable for bonding such a flexible material as polyurethane.

3.6.4.5 Contributing Considerations

Considerations such as bio-compatibility and minimal degradation in a hostile liquid environment at an elevated temperature are necessary for all biological adhesives. However, to improve the adhesive process the adherands should have elastic moduli close to or straddling that of the adhesive. Thus the adhesive acts as a stress reliever at the interface. Also if a large amount of motion is required, high values of ultimate elongation for the adhesive are essential.

Roughening of a surface is a good method of improving a bond and many successful bonds rely on mechanical interlock. In this application this would be an important consideration as many of the bio-compatible adhesives are only capable of withstanding nominal loads with all but the polyurethane systems incapable of supporting shear stresses above 3.5MPa for prolonged periods.

3.6.5 Bond Analysis

Tests by Unsworth *et al* (1987, 1988) indicated that layer thicknesses of 2mm or larger were required for optimum tribological properties. Armstrong (1986) studied the interface between cartilage and bone and obtained the following simplified expression for shear stress:

$$\tau_{\max} = \left[\frac{\delta P}{\delta x} \right] y \quad 3.1$$

This analysis assumed an incompressible ($\nu = 0.50$), flexible layer on a rigid backing material. The maximum shear stress applied to the bond can be seen to occur at the interface between the two layers beneath the point of maximum pressure gradient. Reductions in shear stress thus require a thinner layer and lower value of the pressure gradient. Eberhardt *et al* (1990) expanded this work and obtained similar expressions with normal stresses (representing compressive loads) reaching $1.92 P/\pi a^2$ at the interface between soft and hard layers. For the soft elastomeric joints this represents 3.5-6.3MPa. Shear stresses reach a maximum at a distance approximately 10-14mm from the central point, measured along the bond line. Values of 0.67MPa were calculated for b/t values of 5.0. At first this would seem to be too high a value of b/t. Previously layer thicknesses of 2mm had exhibited good tribological properties. However mechanical interlock has been suggested as being paramount to a successful bond. This would require an average value of t of 3-4mm to allow at least 2.0mm of unmodified elastomeric layer. This corresponds to b/t values of 6.1-4.6. Armstrong (1986) suggested shear stresses of 0.68-0.90MPa for these values of layer thickness.

Jin *et al* (1991) used finite element and finite difference methods to investigate the shear stresses in the layers. Results confirmed the above studies under normal operating conditions, with the maximum shear stress at the soft layer/hard substrate

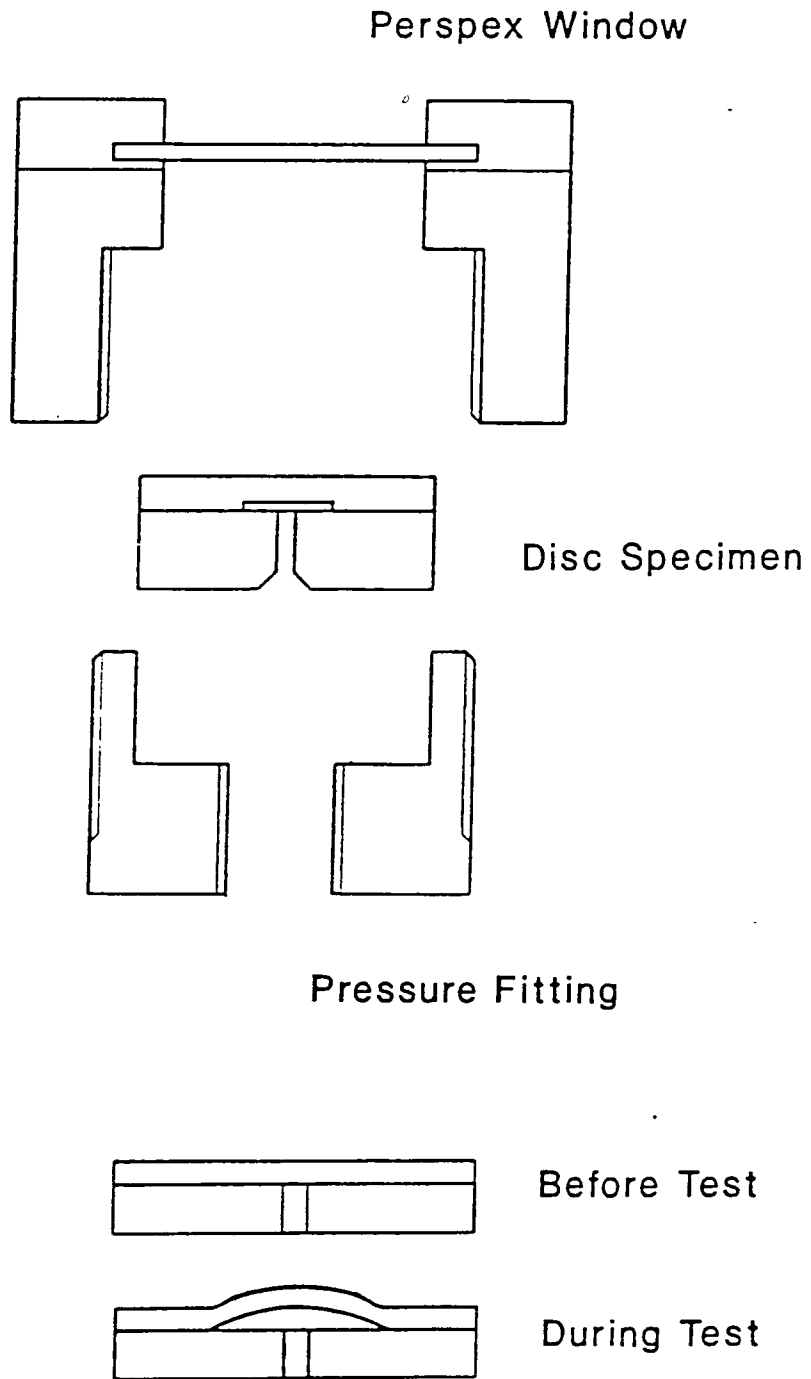
boundary. However, the incorporation of high frictional values (i.e. dry rubbing) increased shear stresses four fold, with maximum values at the layer surface. Increased clearance and hence reduced contact areas resulted in a six fold increase in shear stress.

Lees (1984) stated that for fatigue applications, the proof stress of the adhesive in the mode of expected stress should be five times that expected under the loading to give a good bond life. This means that the strength of the bond must be above 18MPa in compression and 4.5MPa in shear. Although this value of compressive stress should not cause a problem to many adhesives, because of the non-uniform loading, cleavage stresses will be introduced. These will probably be a maximum at the edge of the contact area.

In any bond, regions of low bond strength or pores within the adhesive layer are expected. The ability of an adhesive to limit crack growth from regions of high stress concentration is difficult to quantify, since it can depend on many inherent properties of the adhesive and adherands. However, most joints fail because they cannot meet peel and cleavage overloads with shear overloads being rare. The measurement of this property which may be related to peel strength is also a problem with many potential tests. Peel tests have been previously introduced and a range of specimen geometries exist as no peel test can fulfil the requirements of all cases (British Standard 5350 Pts C9-C14). However blister tests, where the interface is expanded using a pressurised fluid where the bonding has been interrupted, can also be used (figure 3.16).

This test indicates the resistance of an adhesive to crack growth in a cleavage configuration and the fluid used (which should be relatively incompressible) can mimic a degrading service environment. Fracture mechanics for the blister test arrangement can be simplified by a number of assumptions (Timoshenko and Goodier, 1970):

Figure 3.16 : The Blister Test Arrangement



Opening Loading: Tensile loads are applied perpendicular to the plane of the crack, leading to opening. This is Mode I loading as there are no shear stress components parallel to the crack.

Plane Strain conditions also apply, as the crack is internal.

For adhesive cases the following equation was derived (Andrews and Stephenson, 1978).

$$\theta = \frac{P_c^2 b}{E (1-\nu^2)} \left[\frac{3}{32} \left(\left[\frac{b}{t} \right]^3 + \left[\frac{c}{t} \right] \frac{4}{(1-\nu)} \right) + \frac{2}{p} \right]^{-1} \quad 3.2$$

3.6.6 Methods of Sample Preparation

Much of the current research concentrated on the preparation of hot melt processed components. Essentially these consisted of test pieces formed in moulds which were compressed between the heated platens of a compression moulding machine. Temperature control allowed the platens to be adjusted independently and loads of up to 45 tonnes could be applied. Three moulds were used for the majority of specimens and these were shown schematically in figure 2.2a and described in section 2.5.2. Typical bonded samples are shown in figure 3.17, with the bond line displayed in figure 3.18.

Figure 3.17 : Typical Bonded Samples

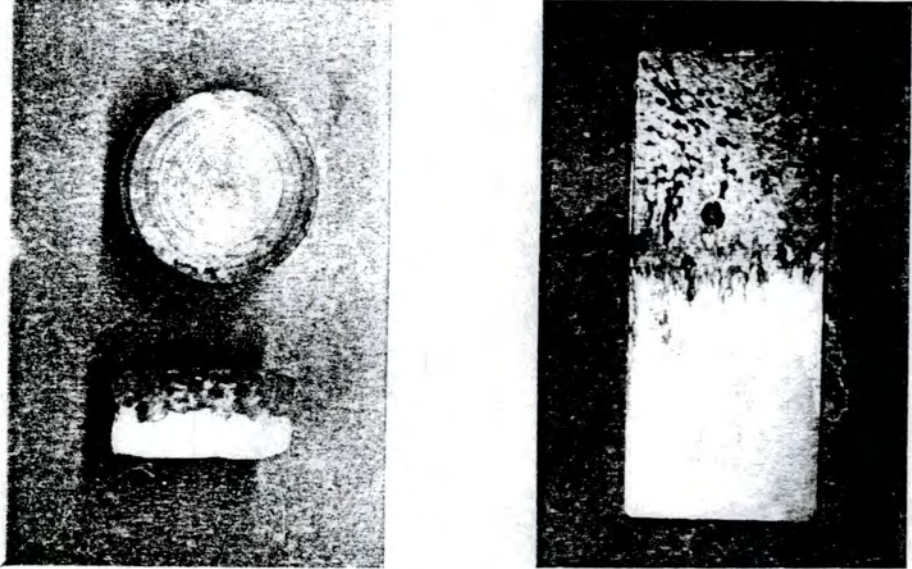
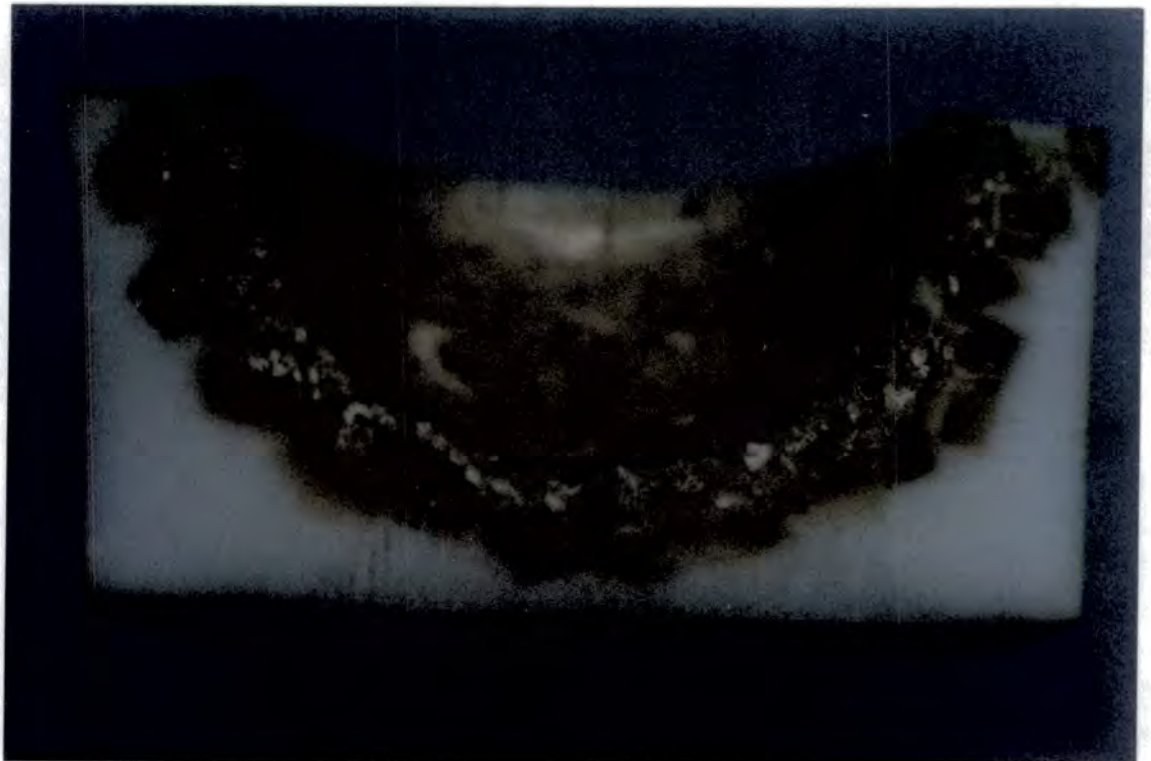


Figure 3.18 : The Polyurethane/Polyethylene Bond Line

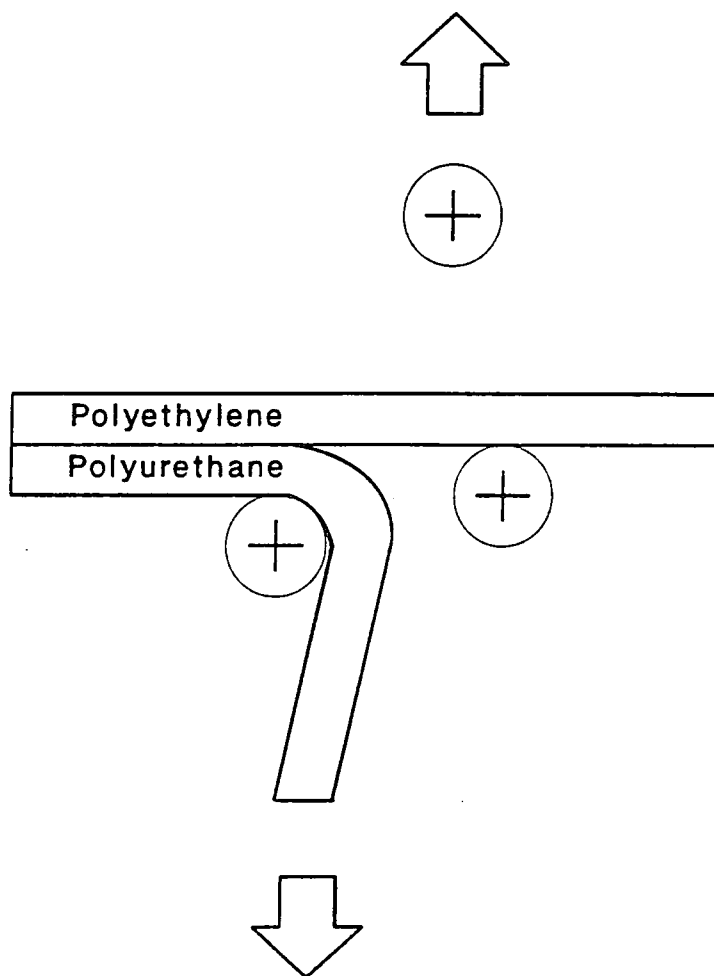


Three bio-compatible polyurethanes were investigated. All had been previously assessed for degradation resistance (section 3.3) and all are currently being used in medical applications. The processing temperatures of the materials were in the range 155-170°C, although lower temperatures could be employed if high compaction pressures were used. The use of very high temperatures led to bubble formation, whilst lower temperatures meant incomplete melting and inter-granular pores. Estane 5714F1 (77°A), Pellethane 2363 (80°A) and Tecoflex EG (85 & 93°A) were used. These were all polyether urethanes. The materials were in the form of pellets of typically 3-4mm diameter. Pellethane was of regular angular particles and Tecoflex of spheroids. Estane was in the form of irregular chips. The reliance of the bond on the mechanical interlock meant that the shape of the polyurethane particles was likely to have a substantial effect on the mechanical strength of the bond.

3.6.7 Methods of Peel Testing

A floating roller arrangement was used as it produced more constant numerical data than other methods (BS 5350 C9-14) with a bond formed mainly on mechanical interlock. The chemical bond was found to be relatively weak as specimens with little or no interlock could easily be pulled apart by hand. It was likely that a large spread of results would be apparent and so the test had to produce as consistent results as possible. The geometry of the arrangement (figure 3.19) was to BS 5350 Part C9 (1978) and a computer controlled Hounsfield tensile testing machine was used to apply the loading at a constant strain rate of 0.4mm/s. Estane '57' was used as the polyurethane component for a complete study but pilot studies were conducted with Pellethane and Tecoflex elastomers. Similar results were expected for all the elastomers as the bond strength was largely dependent on the mechanical interlock. The effect of soaking in saline at 37°C for 48 hours prior to testing was investigated. The polyurethane would be fully hydrated at this stage (section 3.1.2).

Figure 3.19 : The Floating Roller Peel Test Arrangement



Specimens were prepared in widths of 10 and 19mm and a cut was introduced along the adherence line using a 0.5mm width saw blade. At least 15mm of the bond line (10mm wide samples) and 25mm of the bond line (19mm wide samples) was failed and a graph of load/time obtained which allowed the bond strength to be calculated as load/unit width of bond line.

3.6.8 Results of Peel Testing

The results of peel testing are displayed in table 3.3 and the strength values compare favourably with results for adhesives. For comparison the peel strength of a toughened epoxy is 5.2N/mm. However, this is a pure chemical bond with no mechanical interlock. The reduction in strength of 25% when the samples have been hydrated in saline is acceptable and will be due to the softening of polyurethanes when hydrated (Blamey *et al*, 1991). This leads to increased deformation and failure at the mechanical interlock.

Table 3.3 : The Results from Peel Testing of the Polyurethane/UHMWPE Bonds formed by Compression and Vacuum Moulding

Polymer	Hardness (MPa)	Bond Strength (N/mm)	Sample Width (mm)
Estane 57	2.85	9.75	10
Estane 57 (saline)	2.42	7.25	10
Pell 2363	3.21	13.9	10
Teco 85	2.15	15.0	10
Teco 93	3.35	12.2	19
Teco 93 (vacuum)	3.42	6.8	19

The improvements in strength with Pellethane and Tecoflex may be due to the higher elastic modulus or more regular granules which form the interlock. However, a larger sample group is required before conclusions may be drawn, as these results were drawn from testing 6-8 samples of each material.

It can be seen that vacuum formed Tecoflex layers (which are then compression moulded to the polyethylene backing in a two stage process) are much less strong. This is because of the inferior mechanical interlock.

3.6.9 Methods of Blister Testing

Specimens were prepared in mould 1 with a PTFE disc incorporated into the interface. In fact the disc was often above the interface because of the rough nature of the bond with granules of up to 5mm diameter forming the interface. This moves the geometry to one which favours cohesive rather than adhesive failure (Andrews and Stephenson, 1978).

A PTFE disc of 11mm diameter and a nominal elastomeric layer thickness of 4mm were used. The disc was cut from a sheet using a simple punch. Although this method can produce imperfect cracks, with sharper edges than specified (Andrews and Stevenson, 1978) in this case this was thought to be unimportant because of the irregular nature of the bond. A countersunk hole was drilled in the specimens to transfer the pressurised oil to the crack thus forming the blister. The sample was mounted in a brass fitting which contained a perspex window so that failure could be seen as the crack extended. A dye was added to the oil to allow easier identification of the crack front.

3.6.10 Results from Blister Tests

The movement of the crack front was monitored and from the propagation the failure energy could be calculated from the pressures required with values of 2.9-8.5kJ/m² being typical. These values compare favourably with results obtained from epoxy/brass bonds of 0.4kJ/m². Failure was adhesive at the polyurethane/polyethylene bond in five of the six Estane '57'/UHMWPE samples tested. Although this was not an extensive study, it did give the comparative strength of the bond in relation to a purely chemical bond (epoxy/brass). However, a large scatter of results was noted, with the failure pressure also dependent on the time under load.

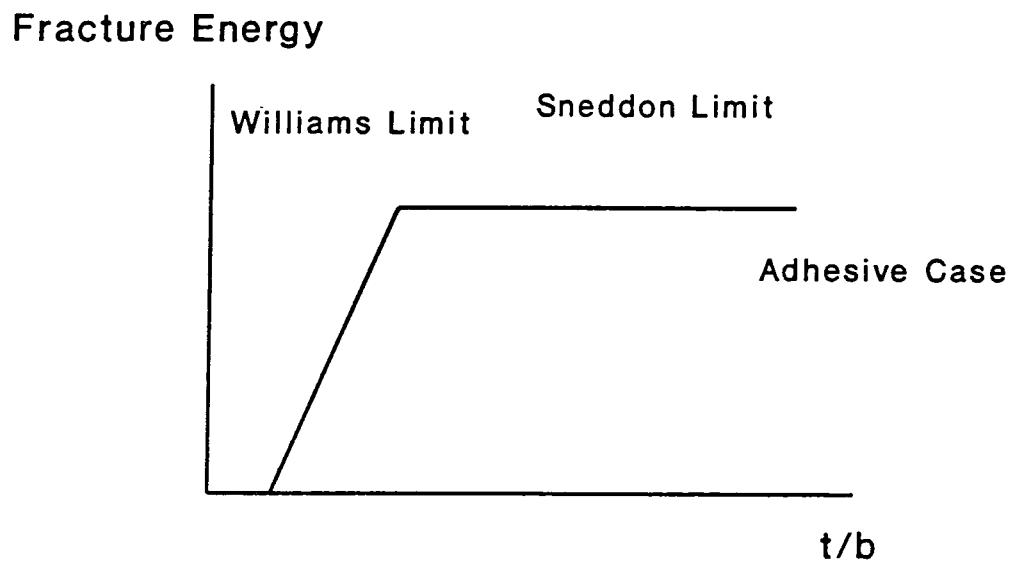
For the blister test the thickness of the elastomeric layer and the initial crack size both govern the failure pressures. At low values of t/b the elastomeric material will undergo plate like deflection. This causes larger destructive forces than for a high value of t/b which acts as an infinite medium with deflection within the material giving a "near field" only analysis. This can be seen from calculations of the adhesive fracture energy which increases as t/b increases (figure 3.20) and the results of Andrews and Stevenson(1978) which showed a many fold increase in the failure pressure as the thickness of specimen was increased.

3.6.11 Discussion

The results from the peel tests showed a low scatter, even with such low failure lengths, which was surprising with the irregular nature of the bond. However, much longer specimens should improve the accuracy of the results further.

The specimens which had the bond tested in shear by tensile loading of the polyurethane showed very high bond strengths as failure was always of the

Figure 3.20 : The Change in Adhesive Fracture Energy as t/b (thickness / blister radius) is altered



polyurethane, and not at the bond. This means that the failure shear stress of the bond is in the region required for the application.

The use of the blister test in this application is still at an early stage and much work is required in this area. Widely scattered results of other researchers have been found to be the result of imperfect PTFE discs leading to very sharp cracks. This should not be so critical in this application owing to the compliant nature of the materials blunting the crack tips and the very irregular bond.

A full analysis of the acetabular cup using finite element techniques is introduced in section 8.6. This should give an accurate description of where failure is likely to be initiated and which form of adhesive testing is most appropriate. The movement of the contact region from the pole of the acetabular cup (figure 6.16) may introduce cracking at the edge of the bond which could cause failure.

3.7 Fatigue of Polyethylene/Polyurethane Cups

3.7.1 Introduction

To complement the tensile fatigue experiments, fatigue testing of cup samples produced through bonding of polyurethanes with polyethylene was initiated. To mimic *in-vivo* conditions the use of femoral heads to apply loading representative of walking in a Mammalian Ringers' environment at 37°C was envisaged. Two other researchers provided some of the experimental data for this part of the study. They were Debbie Walker, who was studying for an MSc and Ian Howard, who investigated these effects during the final year project of his BSc.

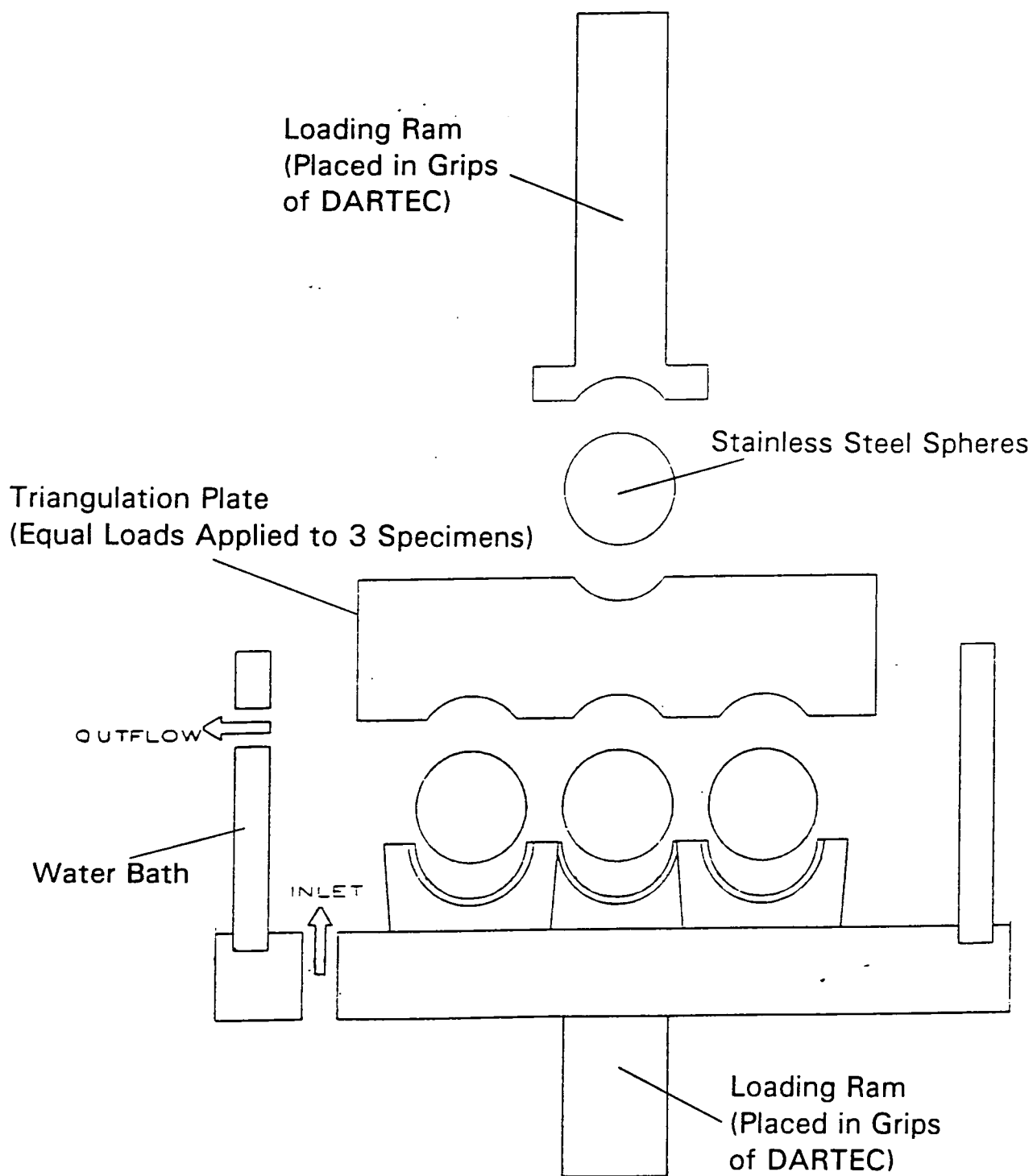
3.7.2 Methods of Measurement of Fatigue Response

A rig was designed and built to facilitate compressive testing of cup samples (figure 3.21). The rig which tests 3 specimens at once, fitted into the jaws of a DARTEC fatigue testing machine and was cycled at 120 cycles/minute to a maximum load of 3000N on each cup sample. This was to represent the loading applied to a prosthesis *in-vivo* where there are two load peaks for each cycle (figure 4.4b). One occurs at heel strike and one at toe off, with a reduction in loading to 1000N during the stance phase. The period of the loaded and recovery phases is equal at 0.25s. Therefore a sinusoidal loading was chosen with an amplitude of 1500N about a load of 1500N and a period of 0.5s. Using a minimum load of 0N led to a more severe test than a minimum load of about 700N (load during the stance phase). The samples tested were of two types, metal backed and polyethylene backed and were situated in a saline bath maintained at 37°C using a circulating pump and heater. The loads were applied through 31.76mm stainless steel balls to give a radial clearance of 0.25mm. These tests were to assess the fatigue life of both the bulk elastomer and the polyurethane/polyethylene bond (section 3.6). The response of the bond and polyurethane material to the fatigue was monitored using hardness testing and measurements of the frictional torque of the joints. Hardness testing (DIN 53456) was detailed in section 2.6.

3.7.3 Results

Metal backed cups, with the bond formed from direct bonding with the metal and a mechanical interlock through lugs, failed after about 300,000 cycles. The polyurethane/polyethylene bonded samples produced by vacuum moulding failed after 2-3 million cycles. Hardness testing proved to be good at indicating bond failure for the polyurethane/polyethylene bonds. Bond failure could be confirmed by visual analysis. However, due to the metal backed cups being totally reliant

Figure 3.21 : Compression Fatigue Rig for DARTEC used in testing Acetabular Cup Samples

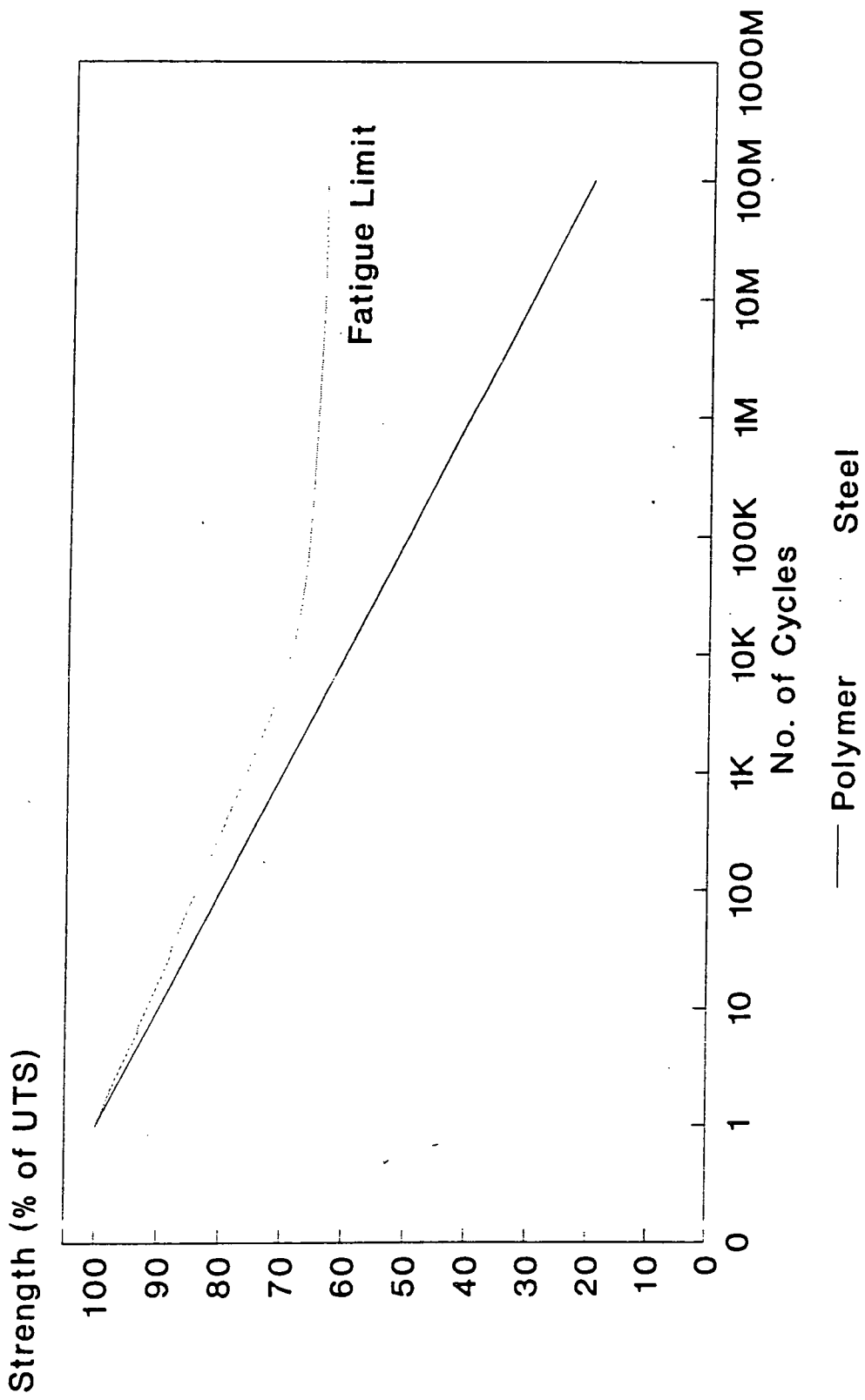


on the lugs around the periphery, the change in hardness during bond failure was minimal.

3.7.4 Discussion

To be viable within the body the soft layer joints will have to withstand at least 20-30 million cycles under double peaked maximum loads of 2500N. The vacuum moulded samples will only withstand 1.5 million double peaked cycles. However, peel tests of compression and vacuum moulded samples have indicated that loads at least 100% higher are carried by compression moulded samples. If a fatigue curve for a typical polymer is considered (figure 3.22) it seems possible that compression moulded samples will maintain the bond. Unfortunately, time has precluded the fatigue testing of such joints.

Figure 3.22 : Typical Fatigue Curves for Steel and Polymers



Chapter 4 : Introduction and Literature Review for Section 2

4.1 Basic Lubrication Theory

4.1.1 Lubrication Regimes

Lubrication is defined in Collins Dictionary of the English Language (1986) as:
" to cover or treat with a ... substance so as to lessen friction ".

With this in mind three lubrication regimes can operate between two surfaces moving relative to each other and carrying a load normal to this motion. These are fluid film, mixed and boundary lubrication and are characterised by changes in coefficient of friction as the speed, load or lubricant viscosity of lubricant is altered.

4.1.1.1 Fluid Film Lubrication

Fluid film lubrication occurs when a film of fluid is present at all times between two surfaces. This film has to be thick enough to prevent contact of the surfaces, even at the highest asperity peaks. The surface of a material can be characterised by its surface roughness value, R_a , which is also referred to as the centre line average. The R_a value is equal to the twice the average distance from the asperity peaks to the surface centreline. For a long component lifetime, an average film thickness of twice the sum of the R_a values of the two surfaces is desirable (Higginson, 1977). Jin (1988) indicates the use of a dimensionless parameter, Λ , which is > 3 for fluid film and < 1 for boundary lubrication.

$$\Lambda = \frac{h}{\sqrt{\Delta_1^2 + \Delta_2^2}} \quad 4.1$$

In an UHMWPE/metal prosthesis the surfaces have R_a values of $0.05\mu\text{m}$ (Isaac *et al*, 1992) (BS 3531/13) and $0.50\mu\text{m}$ respectively (as measured), leading to minimum film

thicknesses for fluid film lubrication of $1.10\mu\text{m}$ from Higginson's recommendations and $1.50\mu\text{m}$ from Jin.

The resistance to rolling or sliding is extremely small when a full fluid film is present as the frictional force is due to the shearing of the fluid only. This is dependent on the viscosity of the fluid and the shear rate applied to the fluid film. Coefficients of friction, when a full fluid film is present, are usually 0.010 or less. Shear rates under hydrodynamic conditions are calculated from the relative sliding velocity of the two surfaces and the thickness of the lubrication film. In externally pressurised systems the rate of squeeze of the fluid from the contact enables the shear rates to be calculated.

The wear of surfaces is also very low when a full fluid film is operating. Ideally there would be no wear, but with a fluid passing over a surface the solid particles present within the fluid will cause some three body wear or surface erosion to take place. The statistical nature of the surfaces, which will include some asperities much larger than the norm will also cause some degree of wear unless the fluid film thickness is many times greater than the surface irregularities.

4.1.1.2 Boundary Lubrication

Direct contact of two articulating surfaces can be avoided by the introduction of a boundary lubricant. This form of lubrication is better than direct surface to surface contact but the wear rate is higher than with either fluid film or mixed lubrication. Boundary lubrication is dependent on the ability of the fluid, or an additive within it, to bond to the surfaces by molecular action and thus offer protection against strong adhesion and scuffing of the solids themselves. The coefficient of friction normally obtained with boundary lubrication is highly variable, but often in the range 0.1 - 0.5.

Not specifically a boundary lubricant, but an important surface modification in artificial joints, is the use of hardened surface coatings for femoral heads, especially titanium nitride (Davidson, 1992). These coatings often reduce friction slightly, but their main role is to limit wear of the surfaces.

4.1.1.3 Mixed Lubrication

This is a form of lubrication common to the majority of bearings under certain circumstances. It involves a portion of the load being carried by the fluid film and the remainder by the boundary lubricant. Although many engineering bearings are designed to run with fluid film lubrication, there are times during start up and very high loading when some degree of mixed lubrication will be taking place. The mixed regime covers a wide range of possible friction coefficients and wear rates. The physical properties of the bulk lubricant (for example its viscosity) and the properties of the boundary lubricant are important during this form of lubrication.

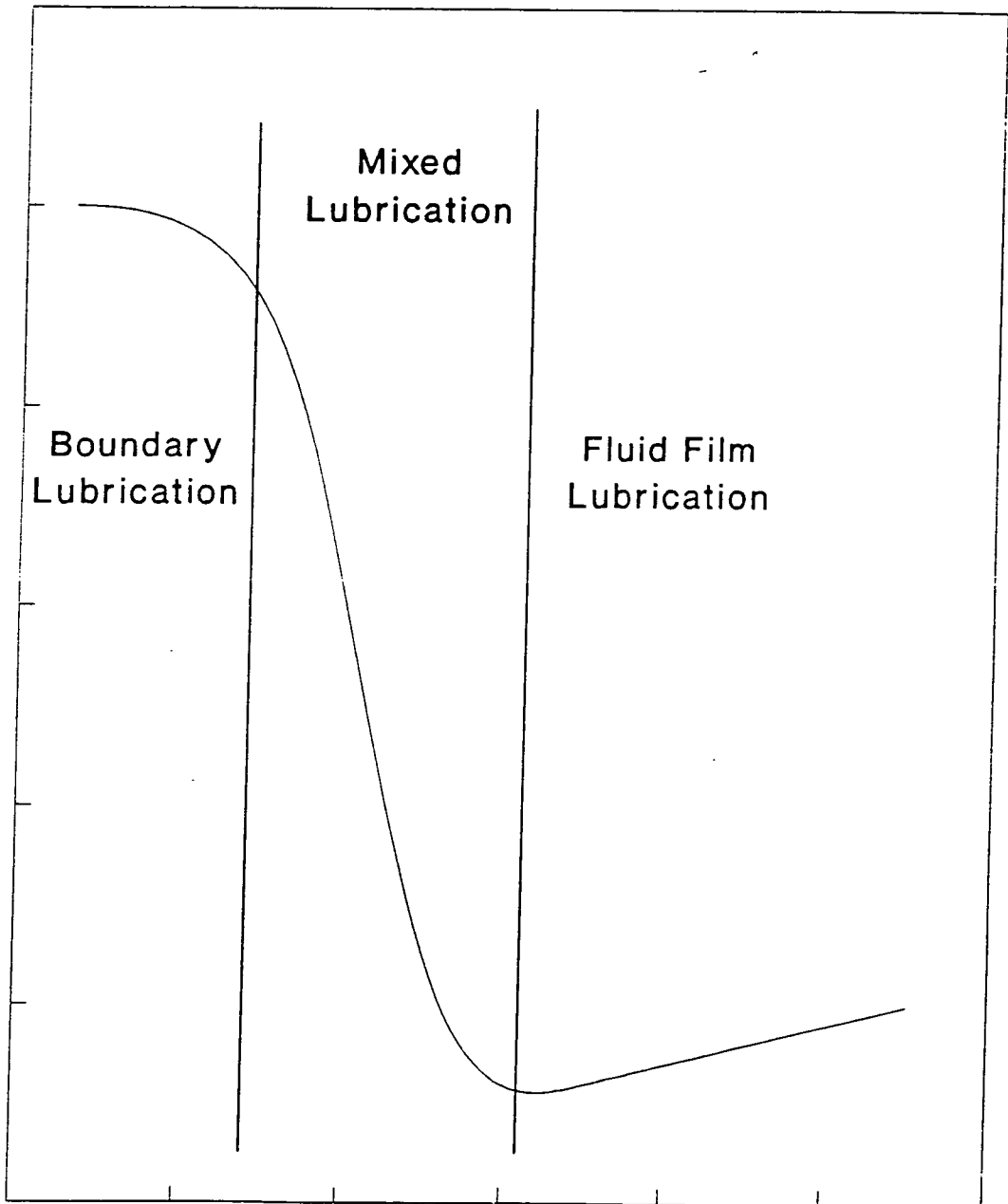
4.1.1.4 Analysis of the Lubrication Regime

One commonly used method to analyse lubrication problems is to construct a plot of two non-dimensional parameters, with the coefficient of friction or friction factor as ordinate and viscosity * speed * radius / load (the Z term) as abscissa. This is known as a Stribeck plot.

The curve can be split into three sections as shown in figure 4.1. The left of the plot has a region of constant coefficient of friction as Z increases, indicating that the frictional torque is independent of viscosity, speed and load. This corresponds to boundary lubrication, which is dependent only on the chemical properties of the boundary lubricant. The centre section of the curve shows the friction factor falling sharply as the Z term increases. This is exhibited by a mixed lubrication regime. As the

Figure 4.1 : A Stribeck Plot of Lubrication Mechanisms

Coefficient of Friction



$\text{Viscosity} \cdot \text{Speed} \cdot \text{Radius} / \text{Load}$

viscosity or speed increases or the load decreases, more of the load is carried by the fluid film with less reliance on the boundary lubricant. Hence the frictional torque of the joint is reduced. The right hand section of the curve shows a slight rising tendency which corresponds to full fluid film lubrication. The only force resisting motion is due to the shearing of the lubricating fluid. If the film thickness is calculated using Elastohydrodynamic theory (Hamrock and Dowson, 1977).

$$h \propto (\eta)^{0.65} \quad 4.2$$

When a full fluid film is present the frictional force can be related to the other parameters as:

$$\mu \propto \eta/h \quad 4.3$$

Therefore,

$$\mu \propto (\eta)^{0.35} \quad 4.4$$

This leads to the rising tendency in the curve as viscosity is increased.

It is possible for a joint or bearing to exhibit fluid film lubrication at high values of the Z term, but mixed or even boundary lubrication at low values of Z. In this case the plot may follow part or all of the shape of the theoretical curve in figure 4.1.

4.2 Lubrication Mechanisms

The mechanisms which allow and encourage the formation of a film of fluid between two surfaces rely on factors concerning the entraining velocity of the surfaces, the viscosity of the lubricant, geometrical considerations and the magnitude and steady or

transient nature of the loading on the device. Reynolds (1886) introduced these mechanisms:

$$\frac{\delta}{\delta x} \left[\frac{h^3}{12 \eta} \frac{\delta p}{\delta x} \right] = \frac{\delta}{\delta x} \left[\frac{(u_1 + u_2) h}{2} \right] + \frac{\delta h}{\delta t} \quad 4.5$$

4.2.1 Squeeze Film

Squeeze films rely on a load of varying magnitude or direction to allow the fluid reservoir between the surfaces to be replenished prior to the next period of loading. On application of a load, as Higginson (1978) explained, "the only deterrent to the solids coming into contact is the viscous resistance of the fluid to being squeezed out of the gap between them" (figure 4.2a). Examples of this are gear teeth meshing and journal bearings, with dynamic loading applied to the contacts. During the period under no load the fluid film is replenished. The cases above deal with rigid materials in general and early theoretical work concentrated on solutions for 'stiff' solids (Christensen, 1962). However, more recent work has indicated that in these cases elastic deformation of metal surfaces may be taking place at highly loaded contacts. However, under these conditions the pressure / viscosity properties of the lubricant become important.

Human joints and the soft layer prostheses are constructed from much softer materials, which undergo large elastic deformations under low pressures (circa. 5MPa). Even the UHMWPE acetabular components of commercial prostheses will undergo some deformation under the physiological loading carried by the joints. Theoretically Higginson (1978) confirmed the results of Herrebrugh (1970), stating that for two approaching cylinders:

$$\frac{h}{R_x} = 4.032 \left[\frac{\omega}{E' R_x} \right]^{1/4} \left[\frac{\eta}{E' t} \right]^{1/2} \quad 4.6$$

Figure 4.2a: The Squeeze Film Lubrication Mechanism

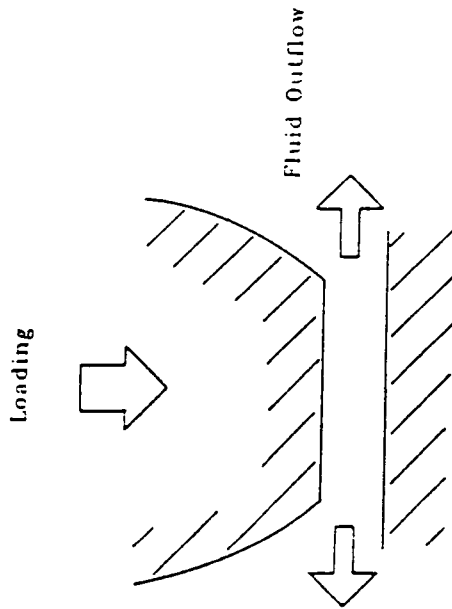


Figure 4.2b: The Hydrodynamic Lubrication Mechanism

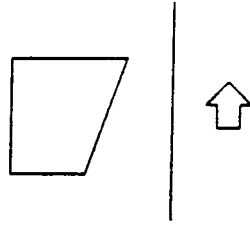
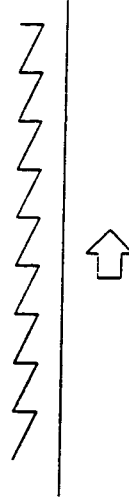


Figure 4.2c: The Effect of Asperities on Lubrication : Micro-EHL



and the results of Fein (1967) for spherical contacts (assuming a Hertzian pressure distribution):

$$\frac{h}{R_x} = 2.011 \left[\frac{P}{E' R_x^2} \right]^{1/6} \left[\frac{\eta}{E' T} \right]^{1/2} \quad 4.7$$

which can be written in terms of the contact radius, a ,

$$h = a^2 \left[\frac{3 \pi \eta}{4 P T} \right]^{1/2} \text{ for large initial film thicknesses} \quad 4.8$$

The squeeze film times can then be calculated:

$$T = \left[\frac{3 \pi \eta a^4}{4 P} \right] \left[\frac{1}{h_s^2} - \frac{1}{h_0^2} \right] \quad 4.9$$

$$T \sim \left[\frac{3 \pi \eta a^4}{4 P h_s^2} \right] \text{ for large initial film thicknesses} \quad 4.10$$

The squeeze film effects are enhanced with soft materials where there is a large area over which the load is carried due to local deformation of the material. Experimental support of spherical contacts by Fein (1967) and Gaman *et al*, (1974) showed excellent agreement with the theoretical solutions. However, experimental work by Roberts (1971) did not agree, although he made use of extremely viscous silicone fluids (1,000 Pa s). This may be where the theoretical results break down.

A more complex solution was available from Pinkus and Sternlicht (1961). They equated the time dependence for a hemispherical seat by looking at the fluid passing a conical element of a surface.

$$T = \frac{3 \pi \mu R_x^2}{(c/R_x)^2 P} \left[\frac{\varepsilon_2 - \varepsilon_1}{\varepsilon_2 \varepsilon_1} + \frac{1 + \varepsilon_1^2}{\varepsilon_1^2} \ln (1 - \varepsilon_1) - \frac{1 + \varepsilon_2^2}{\varepsilon_2^2} \ln (1 - \varepsilon_2) \right] \quad 4.11$$

$$\text{Initial Eccentricity, } \varepsilon_1 = c - h_o$$

$$\text{Final Eccentricity, } \varepsilon_2 = c - h_s$$

Additional theoretical work (Shukla, 1978) has shown that the load capacity, and hence the efficiency, of the squeeze film rises as the surface roughness is increased.

Squeeze films between porous materials have also been under investigation (Wu, 1971 & 1978). This required the introduction of a permeability factor, ψ ,

$$\psi = \frac{\phi t}{h_o^3} \quad 4.12$$

with the effects of porosity only becoming noticeable if the value of ψ rises above 0.001.

One important observation (Wu, 1971) was the reduction in the performance of the squeeze film if translational motion acted, although the effect was small. Gupta and Patel (1975) and others introduced axial flow by electromagnetic means and showed an increased load carrying capacity, which seems to agree more closely with classical theory. It was noted that load could be carried with no squeeze, showing hydrodynamic effects.

Squeeze film analysis was subsequently extended to include surface roughness on the porous coatings and elastic deformation of the layers (Ting, 1975) although in a simplified case. Wu (1978) indicated that the non-isotropic nature of the surfaces and the

possibility of air entrapment within the porous matrix would be important and suggested that a more complex model was needed.

4.2.2 Hydrodynamic Lubrication

Hydrodynamic lubrication relies on the movement of the surfaces parallel to the plane of their general surfaces to generate the pressure. Fluid is entrained between the two surfaces and a pressure is generated if the surfaces form a converging wedge. The true hydrodynamic mechanism must be modified for soft, compliant surfaces of finite roughness into two mechanisms for generation of the fluid film. Elasto-hydrodynamic lubrication (EHL) (figure 4.2b) and Micro-EHL (figure 4.2c) can generate films, enhanced by the elastic deformation of the bearing surfaces under the applied loads.

4.2.3 Elastohydrodynamic

In order to calculate the thickness of the lubricant film generated, simultaneous solution of Reynolds equation and the elasticity equations is necessary. For a semi-infinite solid Hamrock and Dowson (1978) developed a solution, with the lubricant assumed to be incompressible and isoviscous. The first of these assumptions is valid, but due to the non-Newtonian characteristics of synovial fluid (Section 4.2.7 and 5.6) the second assumption may be in doubt for human joints and prostheses.

$$\frac{h_{\min}}{R_x} = 2.789 \left[\frac{\eta u}{E' R_x} \right]^{0.65} \left[\frac{P}{E' R_x^2} \right]^{-0.21} \quad 4.13$$

This assumes the use of an equivalent model, which consists of an elastic sphere upon a rigid plate. For a high conformity joint such as the hip, this can cause problems (Chapter 6). The existence of thin soft layers attached to rigid backing materials, both in

the human joint and the soft layer prosthesis encouraged Dowson and Yao (1991) to modify the formula:

$$\frac{h_{\min}}{R_x} = 1.37 \left[\frac{\eta u}{E' R_x} \right]^{0.56} \left[\frac{P}{E' R_x^2} \right]^{-0.19} \left[\frac{t}{R_x} \right]^{0.37} \quad 4.14$$

The constrained column model was adopted for the analysis, which limits the use of the equation to Poisson's ratios of less than 0.4 (Hooke *et al*, 1967; Zhang, 1987; Strozzi, 1992). Dowson *et al*, (1991) recognised the problem as the Poisson's ratios of cartilage and polyurethanes are closer to 0.500 (Strozzi, 1992) and suggested that adjustment of the effective elastic modulus of the elastomeric layer by factors of 1.5 to 7.0, depending on the value of a/t . However, no theoretical analysis for the determination of the size of the adjustment was available. Strozzi (1992) indicated that although the elastic moduli of polyurethanes were low (circa. 8.5MPa) bulk moduli were much higher (circa. 1500MPa). In the partially constrained geometry of the hip prosthesis, this may be important, especially with a good bond between soft layer and rigid backing.

The most favourable option seems to be the experimental measurement of the contact radius of the prosthetic device followed by calculation of an effective elastic modulus. This modulus can then be used as if for a semi-infinite solid.

4.2.4 Micro-EHL

The expected film thickness existing between the articulating surfaces of healthy human joints and soft layer prostheses (Dowson *et al*, 1991) is of the same order as the asperities on the articulation surfaces (Section 4.1.1). The inlet side of the asperities will act as a wedge, generating lift, with the outlet side generating drag. Because of this, local deformation of the asperities on the articulating surfaces was indicated (Jin, 1988), giving

rise to a modified asperity shape, with the possibility of cavitation at outlet. This will generate a pressure to improve the film of fluid between the articulating surfaces.

This mechanism has been shown to improve the thickness of the lubricating film, with increased pressure generation for both rigid (Chow and Cheng, 1976) and elastically deformed asperities (Dowson & Jin, 1986). Kodnir and Zhilnikov (1986) showed almost total squashing of the original roughness for asperities of large wavelength. Jin (1988) calculated surface roughness reducing by 88-97% for asperities initially $1\mu\text{m}$ in height, which backed up research by de Silva & Sayles (1986), who indicated that the film thickness parameter, Λ , could be as low as 0.5, without breakdown of the film. Deformation of the asperities is described by the equation:

$$\delta = \frac{(1 - \nu^2) \lambda p_a}{\pi E} \quad 4.15$$

Jin (1988) referenced Jackson and Cameron (1976), who showed that micro-EHL effects were particularly important at low sliding speeds and small values of film thickness (in relation to asperity height), both of which are representative of prosthetic conditions. Moore (1978) indicated that the local pressure distributions at the asperities within the contact area may affect the simultaneous solution of Reynolds' and the elasticity equations.

4.2.5 Weeping and Boosted Lubrication

Although pure hydrostatic lubrication relies on an external source of pressurised fluid to support the load, this can often be accomplished by pockets of lubricant on or just below the articulating surfaces. The mechanism has been in use in vacuum environments (eg. space) for extended (> 5 years) running. Sandblasted surfaces, for which R_a values are typically $1-8\mu\text{m}$, produced a good weeping mechanism, with lubricant contained within the surface pores, under conditions in which smooth surfaces produce little effect (Fote *et*

al, 1978). The permeability of the surfaces and their porosity seem to be important in determining the final effect. Boosted lubrication, brought about by non-Newtonian properties of the lubricating fluid, is uncommon in many bearings due to the Newtonian lubricants used. However, due to the increases in viscosity of the synovial fluid at low shear rates this mechanism increases squeeze times in human joints (Dowson *et al*, 1970).

4.2.6. Methods of Measuring the Thickness of Lubricating Films

The measurement of the small separations between lubricated solids (circa. 0.2-5 μ m) has prompted much research. Initial studies using interference techniques (Roberts, 1971) have proved successful at analysing squeeze films. The maximum accuracy of such techniques based on the fringes is 5nm, but this technique is not useable for dynamic systems with loading and reciprocating motion. In addition, Binnington (1991) quoting Olgar and Tavallaey (1987) stated the inaccuracy of this technique for film thicknesses of the same order as the surface asperities, indicating it is only accurate for films at least an order of magnitude larger than the surface roughness.

Resistance and capacitance techniques have been used for rotating seals and similar geometries. Resistance techniques run into problems as both surfaces have to be conductive, with the lubricant semi-conductive for quantitative analysis. In addition, the resistivity of the lubricant must not undergo substantial change under the action of shearing, pressure changes or in thin films. The transmission behaviour at the solid-liquid interface is also a cause for concern and this limits resistance techniques to largely qualitative analysis. Capacitance techniques have proved successful in the analysis of oil lubrication, due to the stable properties of oil as a dielectric.

Fluorescence methods have been successfully used since 1978 (Ford and Foord, 1978) and they are particularly applicable to very thin films. The use of a laser as the light

source simplifies the optical requirements. This technique has been used to show mixed lubrication in rotary lip seals made of an elastomer and this indicates the resolution of the technique is at least $0.8\mu\text{m}$ (Binnington, 1991).

An alternative technique based on neutron imaging has been investigated for oils. It relies on the large number of hydrogen atoms within the oil film. At present no information has been found to suggest that the technique will work with water based lubricants. In addition resolution seems limited to about $25\mu\text{m}$ (Spowart, 1978).

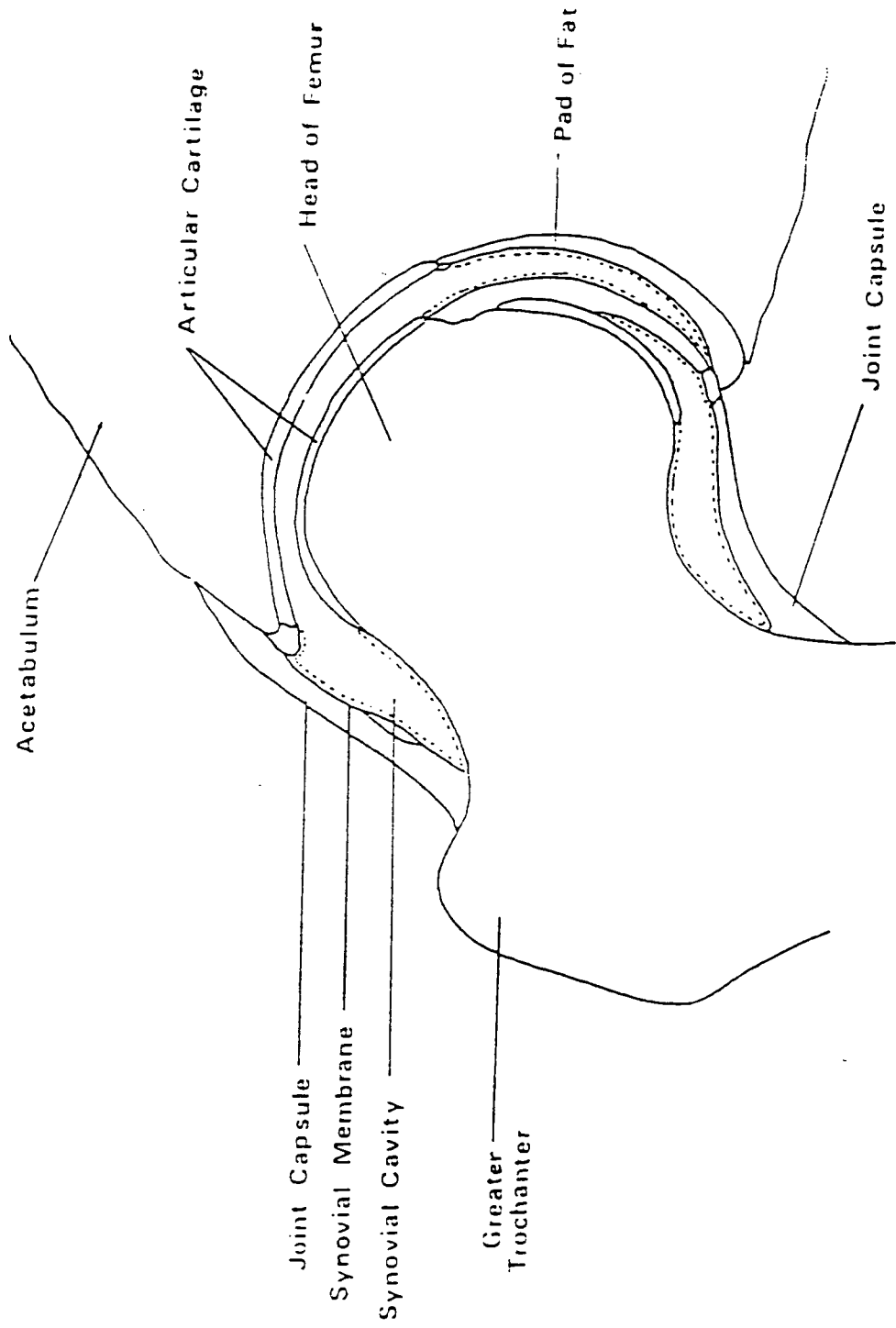
4.3 Human Joints

The joints of the body have proved themselves to be very effective in allowing the limbs of the body to articulate in relation to each other. They consist of a layer of cartilage covering the ends of the bones with a joint capsule containing a fluid enveloping the assembly (figure 4.3). The synovial fluid and the soft cartilage layers both have to be present to promote good performance of the joint, as can be seen from the condition of the articulating surfaces of diseased and arthritic joints. Many studies have been carried out on the modes of lubrication in healthy human joints (Unsworth *et al*, 1975, Mansour & Mow, 1977) and these have concluded that the two cartilage layers are separated by the fluid during the majority of joint activity. This explains the success of human joints in withstanding the loads and motion over their lifetime with little damage to the surfaces.

4.3.1 Cartilage

Cartilage in the hip joint has been measured at between 2 & 4mm in thickness on both the femoral head and on the acetabulum (Meachim & Stockwell, 1979; Swann & Seedhom, 1989). The higher thicknesses tended to be in the most highly loaded regions. Its modulus of elasticity is between 10 & 50MPa in unconfined compression (Johnson *et al*, 1977) but due to its relatively high Poisson's ratio of 0.42-0.47 (Armstrong *et al*,

Figure 4.3 : The Human Hip Joint



1984), under semi-confined compression, when bonded to a rigid substrate (e.g. bone), much higher values of layer modulus are apparent; 50 - 500MPa (Higginson and Snaith, 1979).

Cartilage does not have a perfectly smooth surface but a roughness value (R_a) of $2.0\mu\text{m}$ has been measured for healthy joints with much higher values for osteo-arthritic conditions (Jin, 1988; Sayles *et al*, 1979). Under loading however, the asperities are flattened due to the low modulus values of the surface (10 - 50MPa). Under disease conditions the cartilage becomes softer, less resilient and thinner (Freeman, 1979; Gore *et al*, 1983). Because of the decrease in thickness the underlying bone modifies the elastic properties to a greater extent than normal and may reduce the contact area of the joint by giving the effect of a harder material (Chapter 2). This influences the contact area and also the deformation of the asperities may cause the fluid film mechanism to break down.

The softening of the cartilage leads to a material more easily damaged by abrasive wear, a phenomenon it shares with many engineering polymers (Li and Hutchings, 1990), although softer rubbers have shown improved erosive wear over harder materials (Arnold and Hutchings, 1992). Wear of the surface increases the roughness and larger film thicknesses are required to prevent surface to surface contact. This is clearly a degenerative process and in human joints can contribute to arthritic conditions.

The weeping mechanisms discussed earlier may help to induce fluid film lubrication in the synovial joints. The high fluid content and porous nature of cartilage could lead to a pumping action on the synovial fluid in the open pore network. This has been indicated as important by a number of groups (McCutchen, 1962; Mak, 1986; Jurvelin *et al*, 1988; Farquhar *et al*, 1990). However, the permeability of the cartilage has been found to be too low to exhibit a substantial effect (Higginson and Norman, 1974).

4.3.2 Synovial Fluid (see also Section 5.6)

Synovial fluid is non-Newtonian. This means that its viscosity is not independent of shear rate. Under low shear rates its viscosity increases by several orders of magnitude from its level at high shear rates. This is due to the coiling of the long chain hyaluronic acid protein complex. At high shear rates the chains are straightened and thus provide little resistance to motion, reducing stresses within the joint, in particular at the cartilage-bone interface. This gelling helps to keep the cartilage surfaces separated under steady loading and when the joint surfaces are stationary, where squeeze film and EHL mechanisms respectively cannot operate. The hyaluronic acid complex, formed through protein action, has a chain length of 0.1-1.0 μm and also acts as a boundary lubricant by forming bonds with the cartilage surface (Davies and Palfrey, 1968; Walker *et al*, 1970). This was shown by the filtration of synovial fluid through cartilage, which led to the formation of a surface gel (Maroudas, 1967). This was viewed using scanning electron microscopy (Walker *et al*, 1970) with deposit thicknesses of up to 10 μm . The viscosity of synovial fluid does not change at high pressures (Cooke *et al*, 1978) enabling the lubricant to perform in heavily loaded contacts.

4.3.3 Loading and Motion Cycles

The loading developed in the hip joint and the angular velocities of the femoral component were derived by Graham & Walker (1973), utilising the results of Rydell (1966) Murray *et al* (1964) and Paul (1967). These calculations were based on force plate studies and gait analysis using goniometers and cine film and allowed the loading on the hip joint to be accurately determined during a range of activities. The results that they obtained for walking at a steady rate are shown in figure 4.4a. It can be seen that the highest loads are generated during heel strike and toe off, reaching three times body weight. Considerations of the angular velocities at these points (from the gradient of the

Figure 4.4a: Load Applied to the Hip (Paul, 1967)

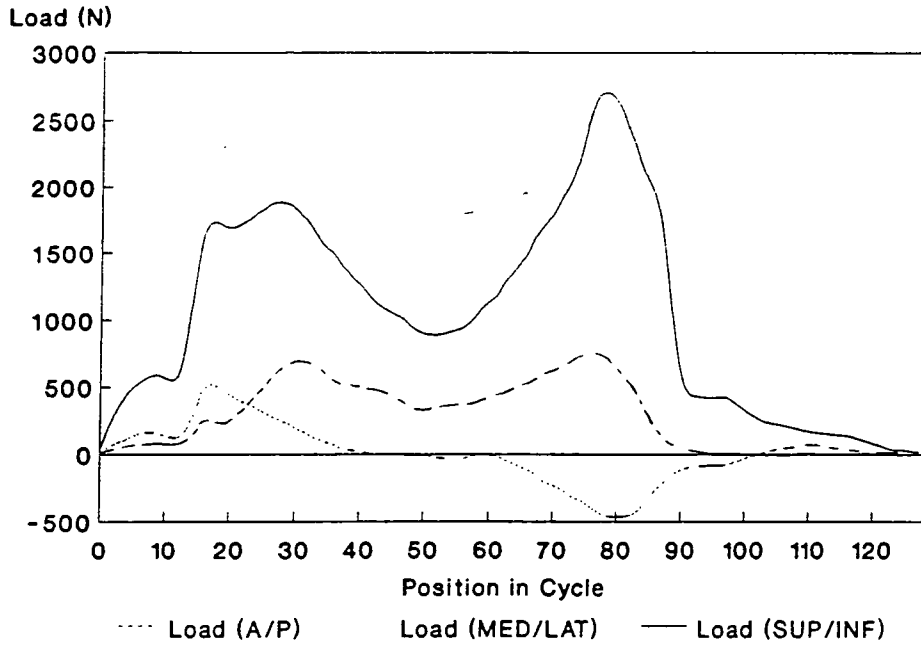
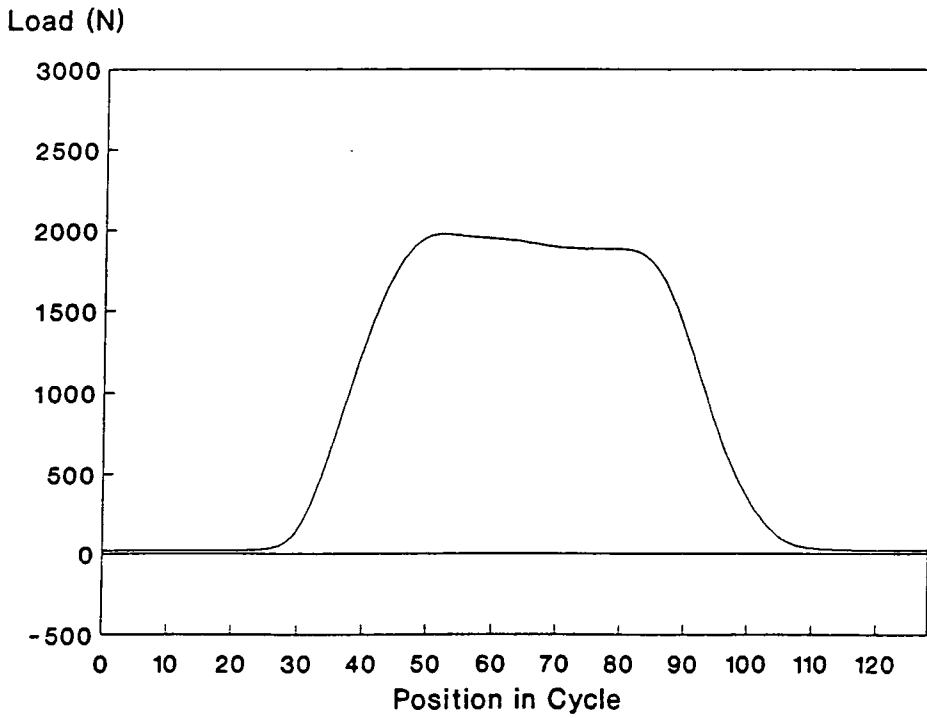


Figure 4.4b: Load App. to the Hip (after English, 1979)



curve in figure 5.2) show that the EHL effect may be small. However, during the stance phase of the cycle, loads decrease to 1.5 times body weight and the velocity increases to a maximum thus promoting the EHL mechanism, increasing the film thickness prior to toe off. The low loads during the swing phase of the cycle, when the forces are provided by muscular action, allow for replenishment of the film by EHL action prior to the next heel strike. English and Kilvington (1979) obtained similar values of loading with transducers implanted in the hip joint (figure 4.4b). The only difference was the maintenance of load close to its peak value during the stance phase of the cycle.

Following surgery and the implantation of prosthetic components, loads on the joints are modified due to muscular changes. Instrumented prostheses have been used by a number of research groups (Kilvington and Goodman, 1981) to reveal that the changes are small in magnitude and the points of maximum loading still occur during heel-strike and toe-off as in the normal gait pattern (Davy *et al*, 1988).

4.4 Soft Layer Joints

Section 4.2 outlined mechanisms of creating a lubricating film and the operation of these with reference to human joints was discussed in section 4.3. These are very similar to those thought to exist in elastomeric joints (Unsworth *et al*, 1987, 1988) with the film being generated by hydrodynamic, squeeze and EHL mechanisms. This had been shown previously by incorporating a soft lining to journal bearings (Bennett and Higginson, 1970) with a reduction in friction and wear noted.

The moulding of soft layers can be accomplished with much lower surface roughness values than human joints. Although in both cases the surface asperities will be substantially deformed under contact in the hip joint, it is likely that the film required for complete separation of a soft layer prosthesis will be less than for the human joint.

Therefore, the mechanisms for film generation in soft layer prostheses do not need to be as successful as the human joint. The joint size can be smaller, the layers harder to reduce the possibility of fatigue failure and less viscous lubricants (ie. rheumatoid and osteoarthritic synovial fluid) could produce successful lubrication.

4.4.1 Weeping and Boosted

One of the important differences between the materials of the human and soft layer prostheses is that cartilage has a high fluid content of up to 70% (Freeman, 1979), whereas polyurethanes have a low average fluid content of about 1.5-2.0% (Chapter 3). However at the surface, values of 10 - 15% are estimated from the fluid uptake of different thicknesses of polyurethane samples and the low permeability of the material. The low permeability will also reduce the possibility of a weeping effect of fluid within the material matrix onto the joint surface. One method of improving this is the addition of discrete pores on the articulating surface, which was investigated during the course of the study (Chapter 7).

4.4.2 Elastohydrodynamic

In both EHL and Squeeze film mechanisms the size of the contact and the pressures developed within this region will be important in determining the nature of the lubrication. The values can be measured and calculated and although the clearance and sizes of the natural and prosthetic joints are different, contact areas and pressures are similar. The smaller size of the prosthetic head (16mm radius) compared with 22-24mm for the human joint will reduce the EHL effect due to a reduction in surface velocity. However, the smaller R_a value of soft layers should counteract this. The deformation of the surface asperities of soft materials has been an area which has been extensively researched recently (Gardner, 1972). The pressures generated to maintain the load will certainly cause

deformation of the asperities, by as much as 90% (Jin, 1988), reducing the required film thickness in a similar way to the human joint.

However, the converging-diverging nature of the surface of the polyurethanes is thought to act in a similar way to articular cartilage in providing micro-EHL. Theoretical analysis of this condition has concluded that large roughness amplitudes and moderate wavelengths provide the largest effect (Jin, 1988), and that this effect may be significant.

4.4.3 Squeeze Film

The movement of two lubricated surfaces toward each other will cause the lubricant to be squeezed out. From Reynolds (1886) it can be shown that the restriction of this outflow will generate a pressure which can support load. The deformation of an elastomeric material under such pressure will produce a larger contact improving the squeeze film effect by reducing the required rate of fluid outflow.

Soft elastomeric layered joints will operate in the same environment as the cartilage covered human joint, with similar loading and motion. The only difference is that the synovial fluid of patients requiring surgery will tend to be of lower viscosity than that in a healthy hip. The use of a material which encourages lubrication in the same way as cartilage should produce the excellent lubrication characteristics which are sought.

4.4.4 Boundary Lubricants

Hyaluronic acid attaches to the surface of the articular cartilage through chemical bonding and acts as a boundary lubricant. The polyurethane surface is polar and so there is a chance of attracting the long chain protein molecules. However, lipids may be the key to a successful boundary lubricant, as these have been shown to attach to polyurethanes.

Lower coefficients of friction have been measured on soft layer joints when these are present. (Laberge *et al*, 1992)

4.5 Current Prostheses

The lubricating mechanisms which provide the fluid film during operation of the human and the Durham polyurethane joints, do not operate as successfully in currently available prosthesis. This is because the UHMWPE/Metal combination of articulating surfaces does not provide such favourable conditions as the soft elastic layers.

The use of a harder material (UHMWPE), rather than a soft elastomer or cartilage, reduces the area of contact under load (Chapter 6). As a result the thickness of the fluid film maintained by EHL and Squeeze film action is smaller. In addition, the deformation of the asperities on the polyethylene surface will be less than for the soft layers or cartilage, thus requiring a larger film thickness for full fluid film lubrication. Load carrying through micro-EHL will be severely reduced as the asperities will tend to resist deformation.

Previous studies have indicated mixed lubrication for Charnley and Muller based prostheses (Unsworth, 1978), which has been confirmed by wear particles in the vicinity of implanted joints (Mathieson *et al*, 1987) and the high frictional torques previously measured. The wear debris appears to initiate the formation of giant cells and bone necrosis, leading to prosthetic failure through loosening. Ceramic heads seem to reduce debris, but the mixed mode of lubrication remains unchanged. Ceramic/ceramic and metal/metal combinations show even smaller contact areas and although a small proportion of load will be carried by the film, direct contact will be the dominant mode of load carriage.

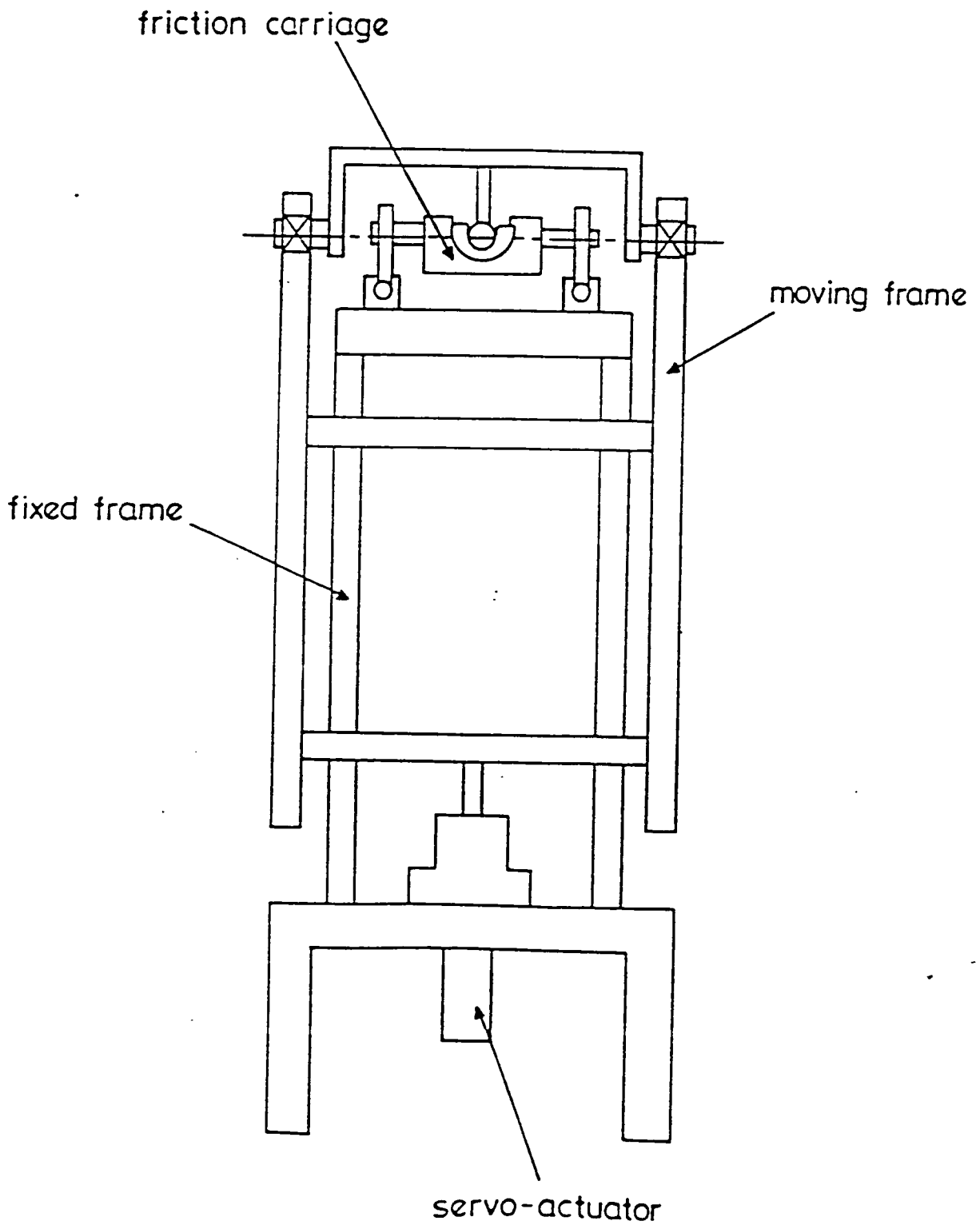
Chapter 5 : Design and Commissioning of the Simulator

5.1 Simulation of the Hip Joint

The requirements for any simulator are to follow the conditions a component would experience in-service as closely as possible (BS 7251/7). However, in many cases compromises must be made if important parameters are to be measured. The friction developed in the hip joint has an influence on the lifetime of the component. Measurement of the friction may be used to produce a Stribeck plot (Chapter 4), which suggests the mode of lubrication in operation, giving an indication of wear and possible loosening. The majority of the research conducted by the author over the past three years has concentrated on soft elastomeric layers, which require accurate measurement of friction due to the operation of a fluid film regime which promotes very low friction. The simulator which has been used for the majority of the tribological work was completed in 1985 and has performed successfully since then.

The existing simulator (figure 5.1) comprised a fixed main frame and a moving loading frame. The joint was inverted from the natural position so that the acetabular component was held in the low friction cradle which was mounted on the fixed frame through externally pressurised bearings. These relied on a thick film of oil to provide a coefficient of friction at least two orders of magnitude less than that of the hip joints under test. Small misalignments in the mounting of the prosthesis could be accommodated in the bearings without affecting the measured friction. The femoral component was mounted in the upper moving frame. A frequency of 0.8Hz was used throughout the study together with amplitudes of 28° in the anterior and 14° in the posterior directions. This simple harmonic motion was provided by a motor and variable speed drive through a toothed belt and scotch yoke mechanism.

Figure 5.1 : The Existing Hip Function Simulator



The friction generated by the prosthesis tried to rotate the cradle mounted in the pressurised bearings. This rotation was resisted by a piezo-electric transducer which consequently measured the frictional torque developed. The cradle was able to adjust for medio-lateral and antero-posterior misalignments through two further pressurised bearings. The lower sections of these were fitted with strain gauges so that the load applied by the servo-hydraulic ram could be monitored throughout the test period. The resulting signal was accessed by the computer and used as a feedback loop for the ram.

However, six years use has indicated some important limitations to the machine:

1. The maximum load which can be applied is 2000N. This corresponds to only 2.5 x body weight, whilst loads developed during walking can reach 3500N.
2. The 68000 based processor board and associated hardware are proving to be unreliable due to age.
3. The microcomputer was of 1983 vintage (NEC advanced personal computer) and was not able to support commercial data analysis software.
4. The hydrostatic bearings were showing some surface damage, which meant that pump pressure had to be increased to maintain the low level of friction.
5. The joint was inverted from the physiological position. Although theoretical calculations suggest that gravity should have little effect on the lubrication it would be advantageous if the joint could be tested in normal and inverted orientations to prove this.
6. The hydraulic system which activates the ram has shown signs of wear and some oil leakage has become apparent.
7. The incremental encoder (which measured the position of the motor) and the potentiometer (which measured the angle of the femoral component during the cycle) were in need of replacement.

It was decided that replacement of the processor boards to incorporate the Motorola 68020 processor, improving both speed of data acquisition and reliability, and the use of a RM Nimbus PC ("386" processor) would solve many of the problems. The boards and software were produced by the microprocessor centre in the University. The board provides command signals to the hydraulic system through a MOOG controller and valve and the software allows comprehensive data analysis. The details of the system are included in section 5.3.7.

In addition a new machine was required to increase the number of tests which could be performed. There were some important criteria that this machine had to satisfy over the existing simulator:

1. Increased load capacity to simulate heavier patients and asymmetric walking
2. Ability to use both inverted and physiological positioning of the prosthesis
3. Provide representative loading and motion within financial limitations

In addition the electronics hardware and data acquisition software had to be compatible with the old machine and the machine had to continue to measure friction accurately.

5.2 Currently Used Simulation Devices

There are a number of hip simulators in use throughout the field of bioengineering in both Universities and commercial research laboratories. Prior to deciding on the new design the options were looked at in detail. These machines can be grouped into wear machines, which are often multi-station, and friction measurement machines. Friction machines tend to provide a simplified motion and

loading to the joint as a fixed frame of reference is required for measurement. The Durham and early Leeds machines are based on the pendulum motion, using antero-posterior swing only. The motion in the hip can be seen in figure 5.2 to be primarily in the antero-posterior direction with an amplitude of $\pm 21^\circ$, but the small medial-lateral movements and internal-external rotation are likely to affect the lubrication performance of the joint. In addition the loading is applied vertically, with no horizontal component. Again this can be seen to be the dominant action (figure 5.3).

The wear machine, which tends to be favoured by industry, usually incorporates three dimensional loading and motion. Machines of this nature have been in use since 1965 (Stanmore mk.1) and the use of these "simulators" to test prospective artificial joints has increased since their introduction. Many of the successful prostheses were originally designed without such research aids (for example the Charnley Prosthesis) but modifications, in particular to materials, have normally been made as a result of simulation. The limitations of metal-on-metal prostheses has tended to be seizure and metal-on-plastic suffer from wear and the effects of wear debris (Mathieson *et al*, 1987). Therefore, the measurement of friction was not thought to be of importance in comparison with accurate physiological simulation of the complete cycle. However, reduction in wear debris has become increasingly important due to the formation of giant cells and loosening of the femoral stem, both of which are thought to be as a result of UHMWPE particles (Section 6.1). The production of wear debris indicates that fluid film lubrication is not taking place. Because of this, the analysis of the tribological performance of the joints has become more important in order to reduce debris and friction measuring devices have gained acceptance.

Thus, measurement of friction was a primary consideration. Three dimensional loading would have provided a superb tool for the analysis of the hip prostheses, but

Figure 5.2 : The Motion of the Hip Joint

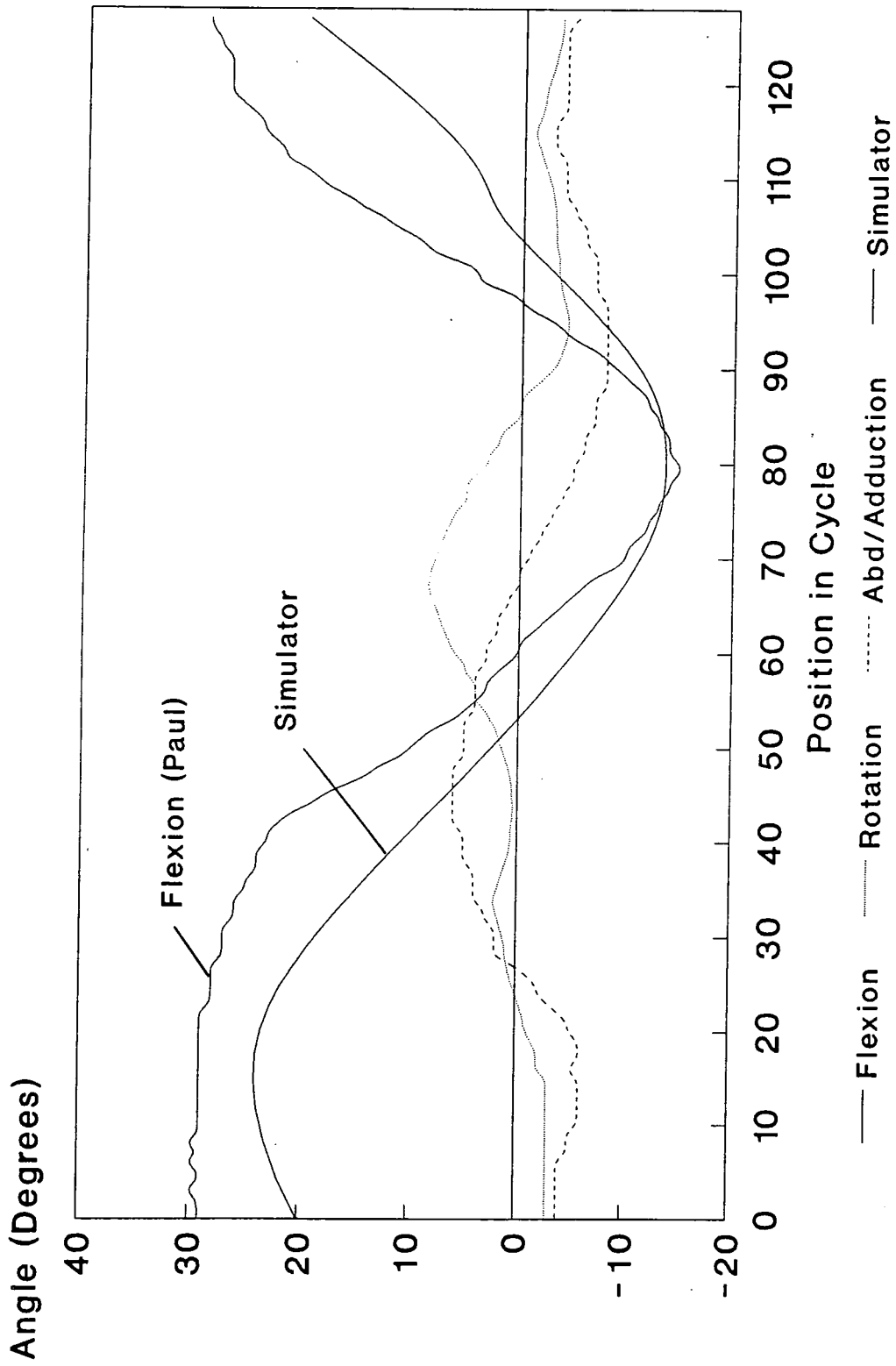
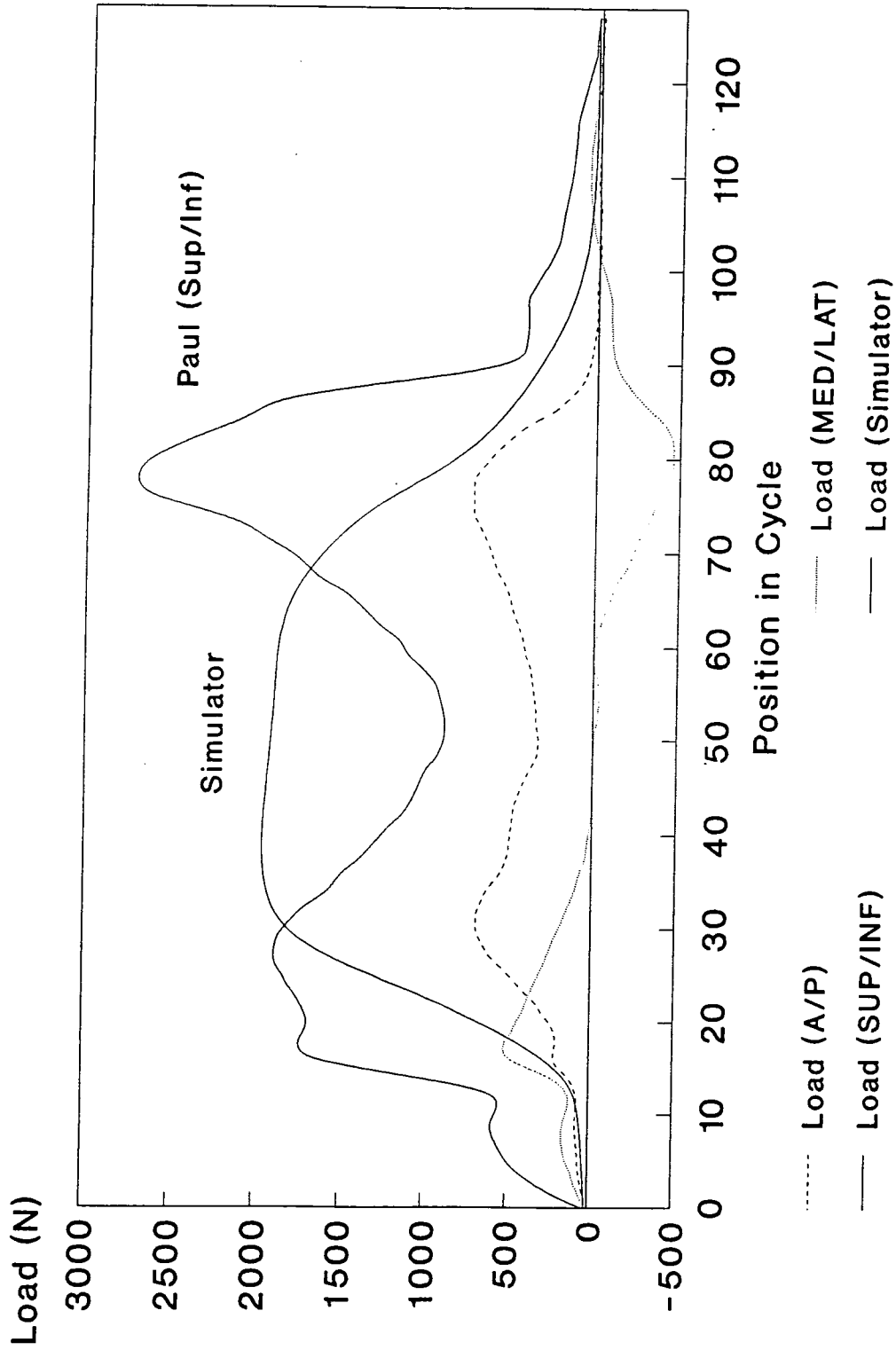


Figure 5.3 : The Loading Applied to the Hip



due to time limitations and the vastly inflated costs of such a device (three actuators and sets of hydrostatic bearings per head) a simplified machine was designed.

5.3 Design of the New Simulator

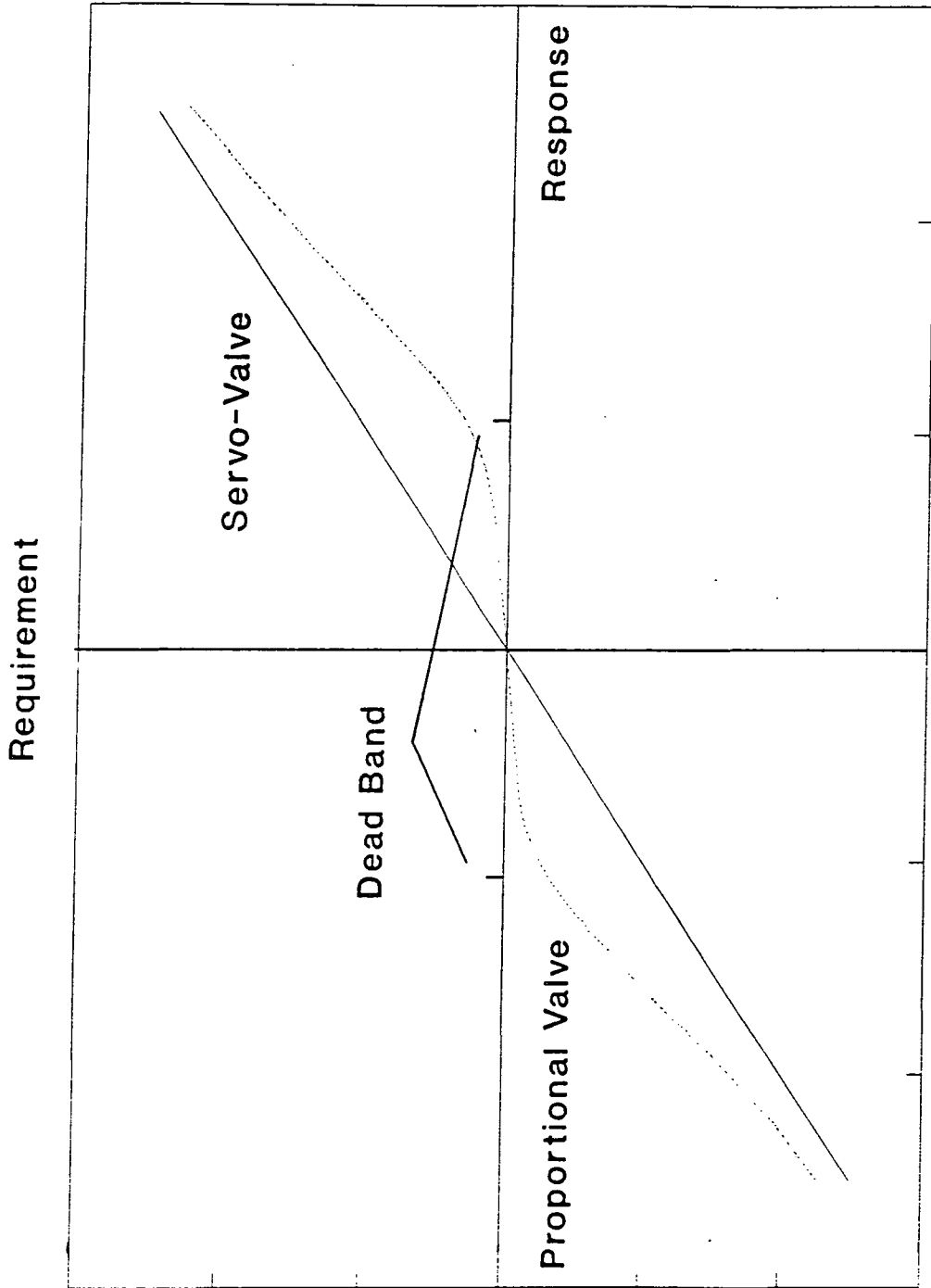
5.3.1 Application of the Load

The use of mechanical cams and weights to simulate the loading applied to the joints of the body during walking has largely disappeared as it has become critical to monitor the performance of prosthetic components during all stages of the walking/loading cycle. It has become important to be able to change the loading patterns in order to isolate the conditions in which the joints perform best and to improve any weaknesses. As a number of lubrication mechanisms are acting to produce the lubricating film these must be isolated and studied alone. In this way improvements can be made.

Hydraulics were chosen to apply the force to the simulator due the accuracy and precise control which could be attained. The current Durham friction measuring machine and the Leeds wear machine make successful use of servo-valves to control the hydraulics. The use of a similar hydraulic system to the old machine had the added advantage of spreading the development cost for the software and microprocessor control system over two machines.

In the past, servo-valves have been extensively used for the application of loading to simulators for both the hip and knee joints. This is due to the feedback circuit which until recently was only available with these valves and allowed close control and high accuracy of the loading cycle. Servo-valves provide linear flow output with displacement of the spool and a very small null-point which contrast with early proportional valves which showed a large dead-band (figure 5.4). In addition the

Figure 5.4: The Large Dead-Band in Early Proportional Valves

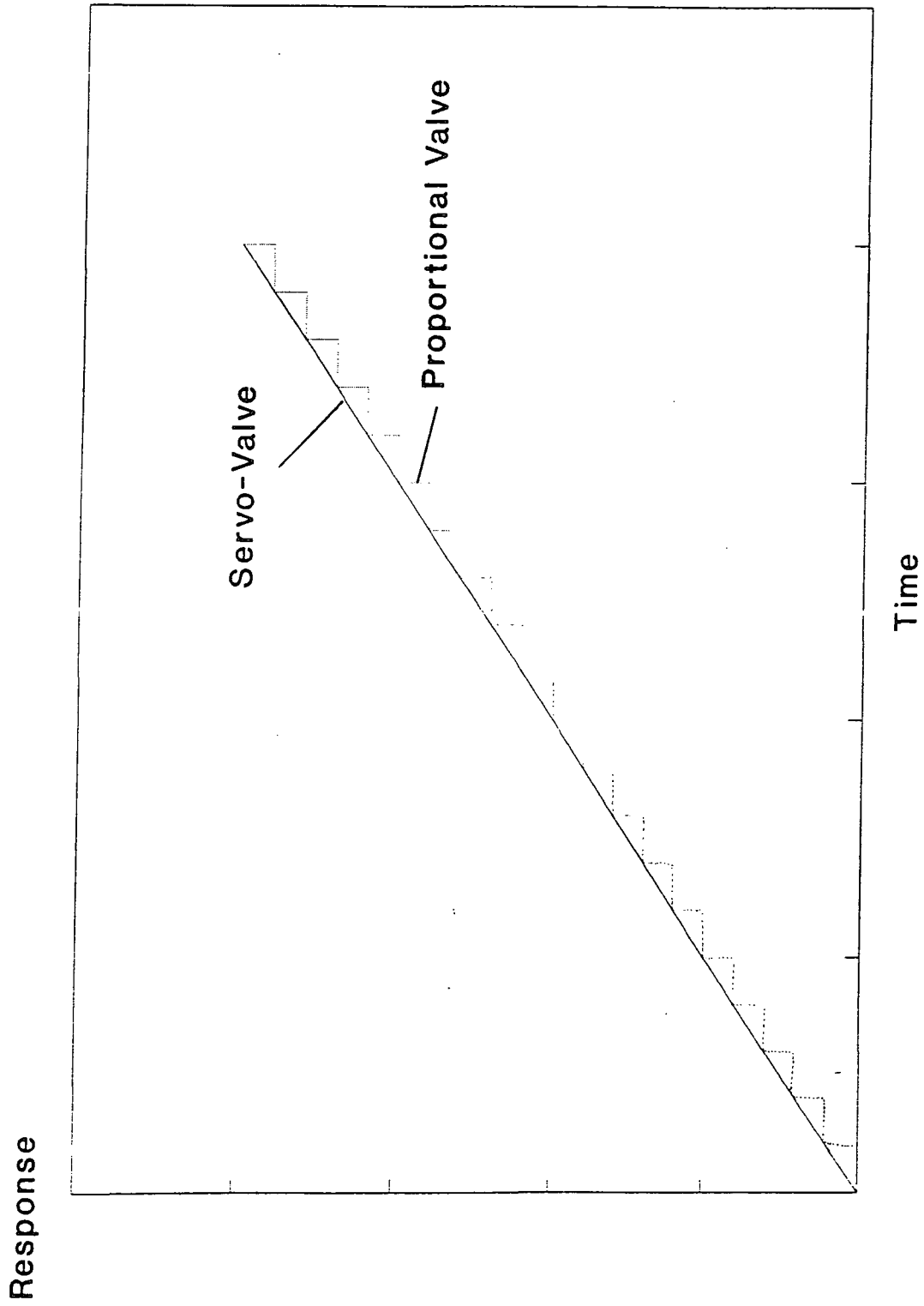


early proportional valves showed a stepped output response in contrast to the smooth output of the servo-valve (figure 5.5). However, recent advances in proportional valves and the application of feedback to facilitate a closed loop system has closed the performance gap between the two systems, and with proportional valve systems costing up to 50% less than a similar servo system they represent a good alternative.

In order to simulate the loading applied to the hip during a range of motions, but specifically walking, a number of criterion were set out. A fast response to the command signal was important (0-5000N in 100ms) and so a Vickers system with a KSDG4V proportional valve was chosen. This valve exhibits both high dynamic performance and very low hysteresis ($< 0.5\%$) and through a PID card module a feedback signal from the load cell could be used. The working environment was not particularly hostile. The laboratory is clean (in comparison to many industrial environments) and kept at a reasonably constant temperature (15-25°C), therefore requiring no additional filtration requirements. As well as a swift ramping of the load, removal had to be accomplished in a similar time (to mimic the *toe-off* condition of walking). To facilitate this a pressure of 140 bar was chosen to act through a 2" bore ram. A double ended ram was used to equalise the pressurised areas and simplify control. A short stroke of ± 5 mm was used to ensure maximum stability of the ram under load.

The maximum flow rate of the pump was 8 litres/minute, and a 40 litre tank was used to allow a 5 minute rest time at maximum flow rate. Rest time is important to disperse the air bubbles which tend to form in such systems. The bubbles can account for substantial heating effects as they are compressed in the pump with a loss of performance of the servo or proportional valve. A water fed oil cooler was also incorporated into the system to maintain performance during long term fatigue testing

Figure 5.5 : Comparative Response for Servo and Proportional Valves



of prostheses (10 million walking cycles will take 140 days of continuous running to complete). A schematic diagram of the hydraulic system is shown in figure 5.6.

The valve was controlled by an electronic card module. This communicated with the proportional solenoid and relied on signals from the 68020 based microprocessor board produced in-house and the feedback signals from the strain gauge based load cell. This card performs a similar job to the MOOG controller used on the current machine. The card is a PID module, which means that the signal can be modified by adjusting the proportional, integrating and derivative potentiometers to ensure the speediest and most accurate response. During setup the P, I and D controllers were set to zero and then adjusted to give the optimum response. Figure 5.7 shows how changes in the three signals vary the response. Use of the Integral term can slow the speed of response slightly but the steady state error can be removed completely. Increases in the derivative term can be used in conjunction with raising the proportional signal to improve the speed of the response. This is accomplished by the derivative term damping out the oscillations brought about by the higher P value. However, incorrect adjustment can give rise to violent oscillation. The normal procedure is to use Integral control for steady state systems and Derivative control to adjust transient response. In this system the loading cycle includes periods of steady load as well as rapid change. Therefore, both integral and derivative terms were used. However, in the interests of safety only a low value of P (underattainment) was used to avoid oscillation.

The general control circuit is shown in figure 5.8. The input signal, F_D , is through the 68020 processor based board. The loading patterns were generated through the software and are explained in Section 5.5. The standard program follows a similar loading pattern to that suggested by Paul (1967 & 1976). A load of 20-60N is applied

Figure 5.6 : A Schematic Diagram of the Hydraulic System

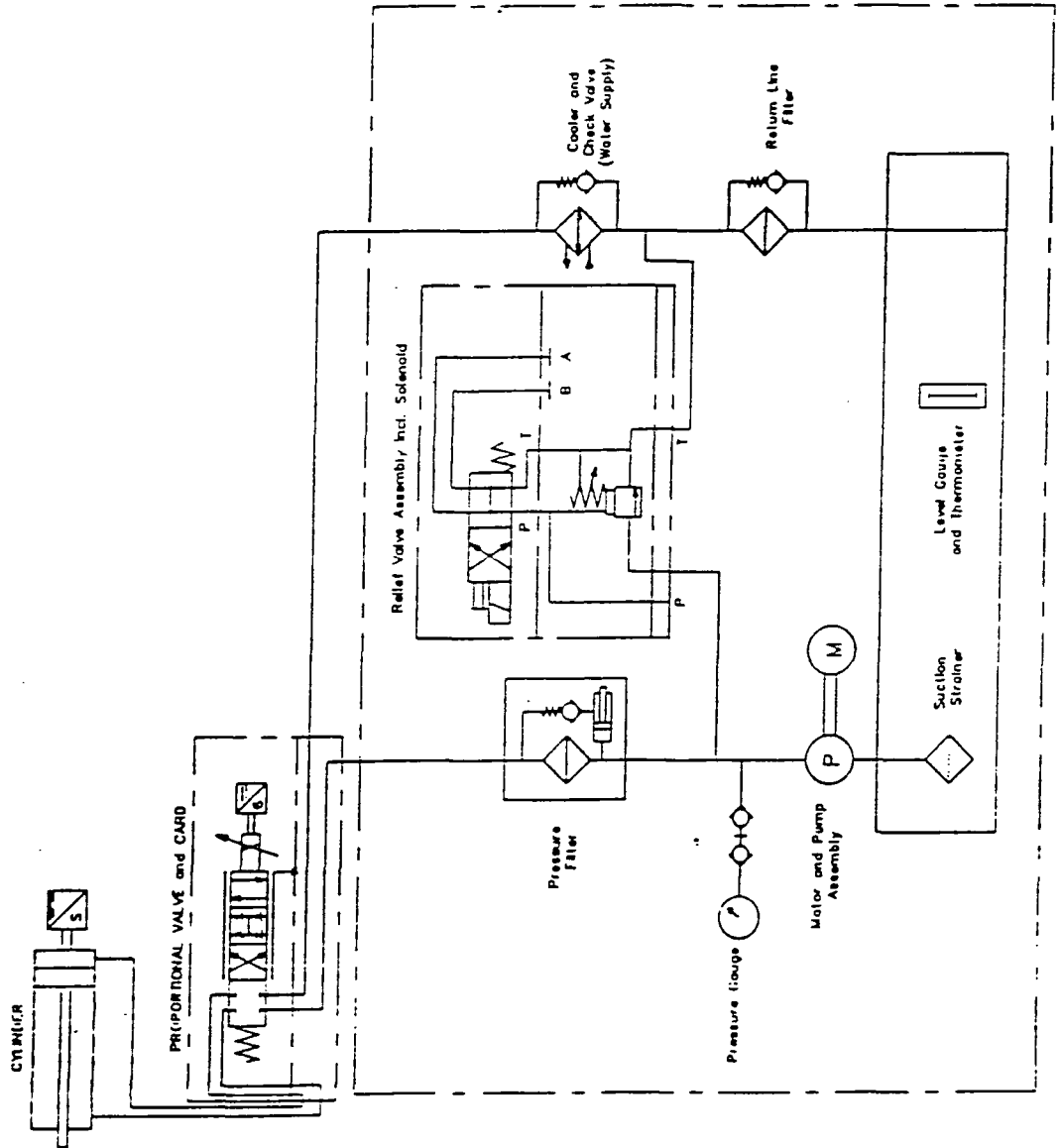


Figure 5.7: Response of the Proportional Valve following changes in the PID Module

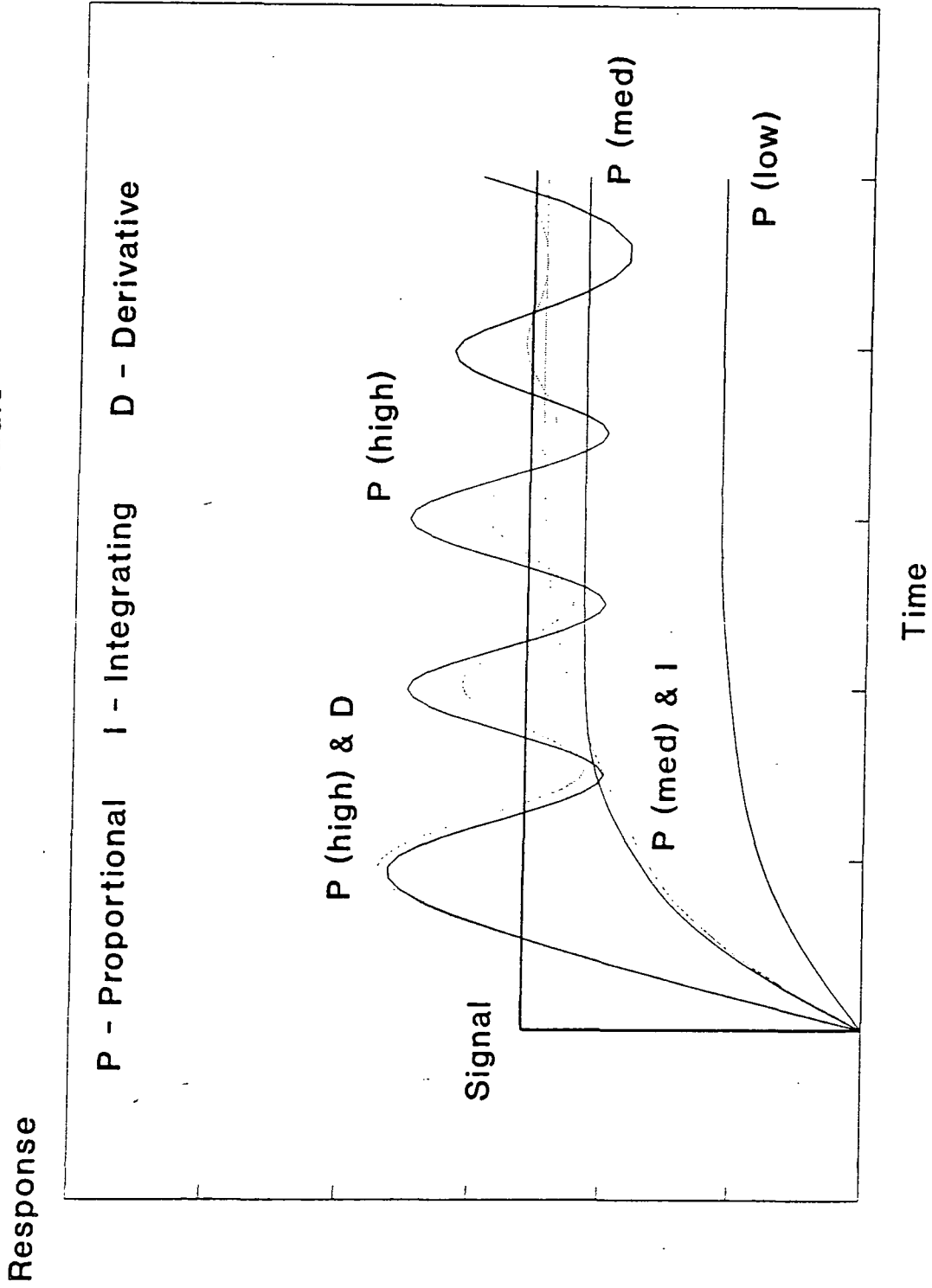
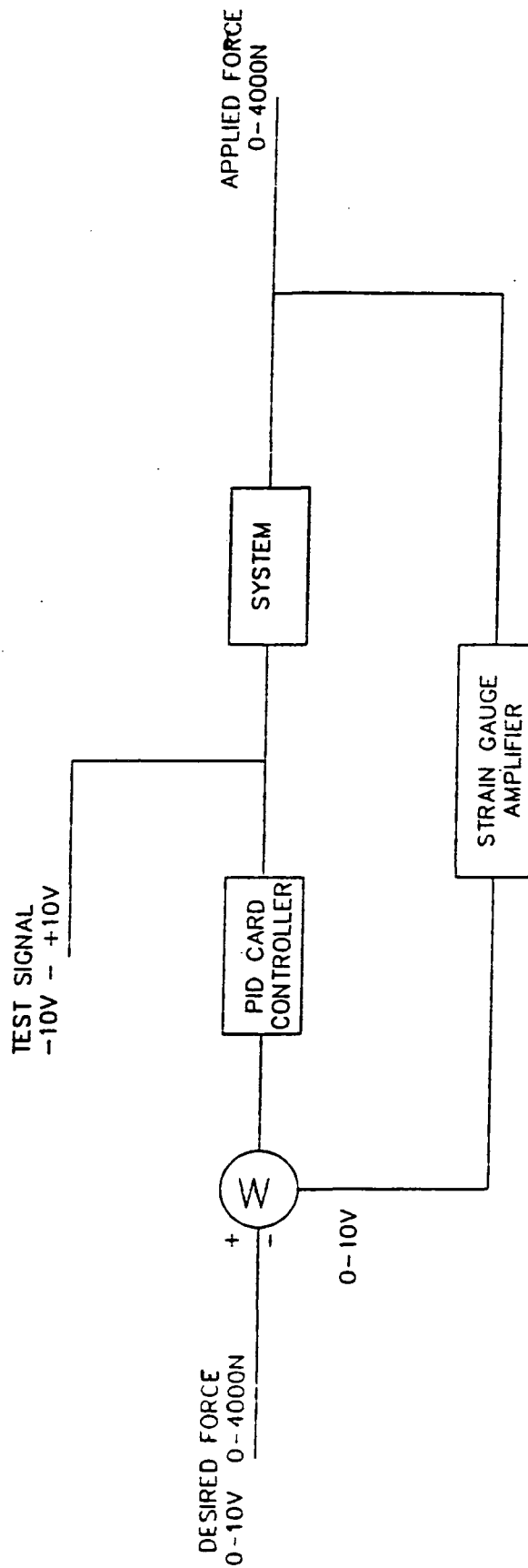


Figure 5.8 : The General Control Circuit



during the carry phase of the walking cycle, which is increased to 3000N at heel strike (figures 5.26a and 5.26b). This load is then maintained until toe off which was measured *in-vivo* by English and Kilvington (1979). The loading was increased from 2000N (the maximum possible with the older machine) to 3000N (4 times body weight) to allow further tribological analysis of the head sizes and the suitability of prosthesis for heavier patients. The loading cycle could also maintain a steady load throughout (to isolate EHL effects), mimic start up conditions following stance under load, and the minimum load could be increased to investigate the effects of surface modifications (Chapter 7). This is further discussed in Section 5.5.

The ram was mounted on the lower plate of the die set with the piston rod extended and attached to the upper plate. Motion of the die set was along four linear roller bearings (figure 5.9). The set was built in the workshops at Durham owing to the amount of machining required to the upper plate. However, for future machinery it would be advantageous to buy in the set and modify the machine design to take advantage of this. The reason for this is that slight mis-alignment of the bearings can cause high friction and failure of the components.

The lower plate was mounted on bars positioned on the vertical 'U' beams. A direct mounting was not needed and this method led to flexibility had the height of the die set required alteration. In addition this gave the option of fitting piezo-electric load transducers at a later stage if problems were encountered with the strain gauge load cell arrangement. The upper plate of the die set carried the beam arrangement, hydrostatic bearings (figure 5.10) and friction carriage. It acted as the oil return reservoir for the hydrostatic bearings with the addition of oil retainers and drain holes (figure 5.11). In this way the configuration of moving and fixed frames was also altered in order to simplify the machine and reduce the number of moving parts. The hydraulic actuator

Figure 5.9 : The Die Set Arrangement

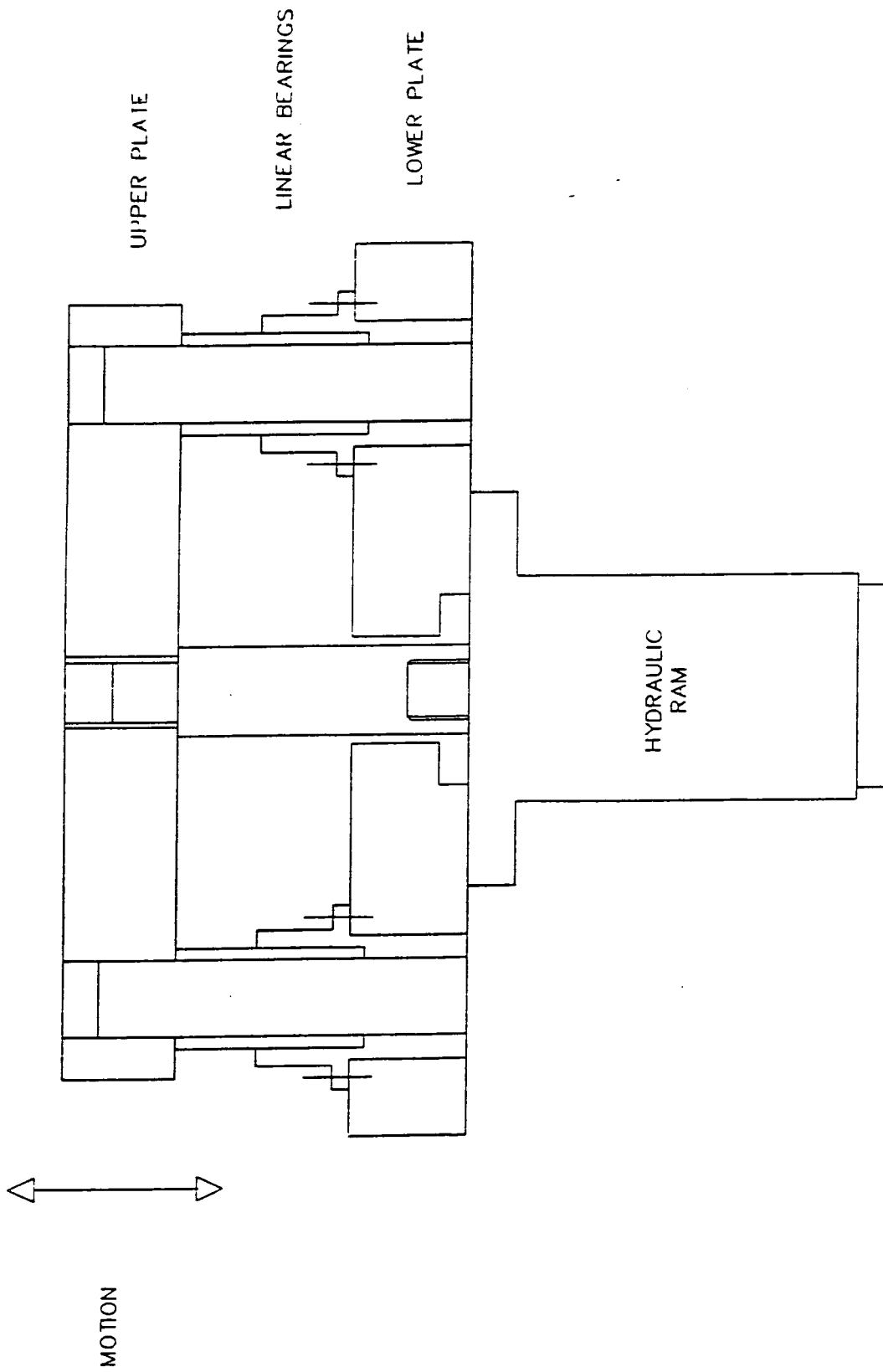


Figure 5.10 : The Hydrostatic Bearings mounted on the Strain Gauged Beams

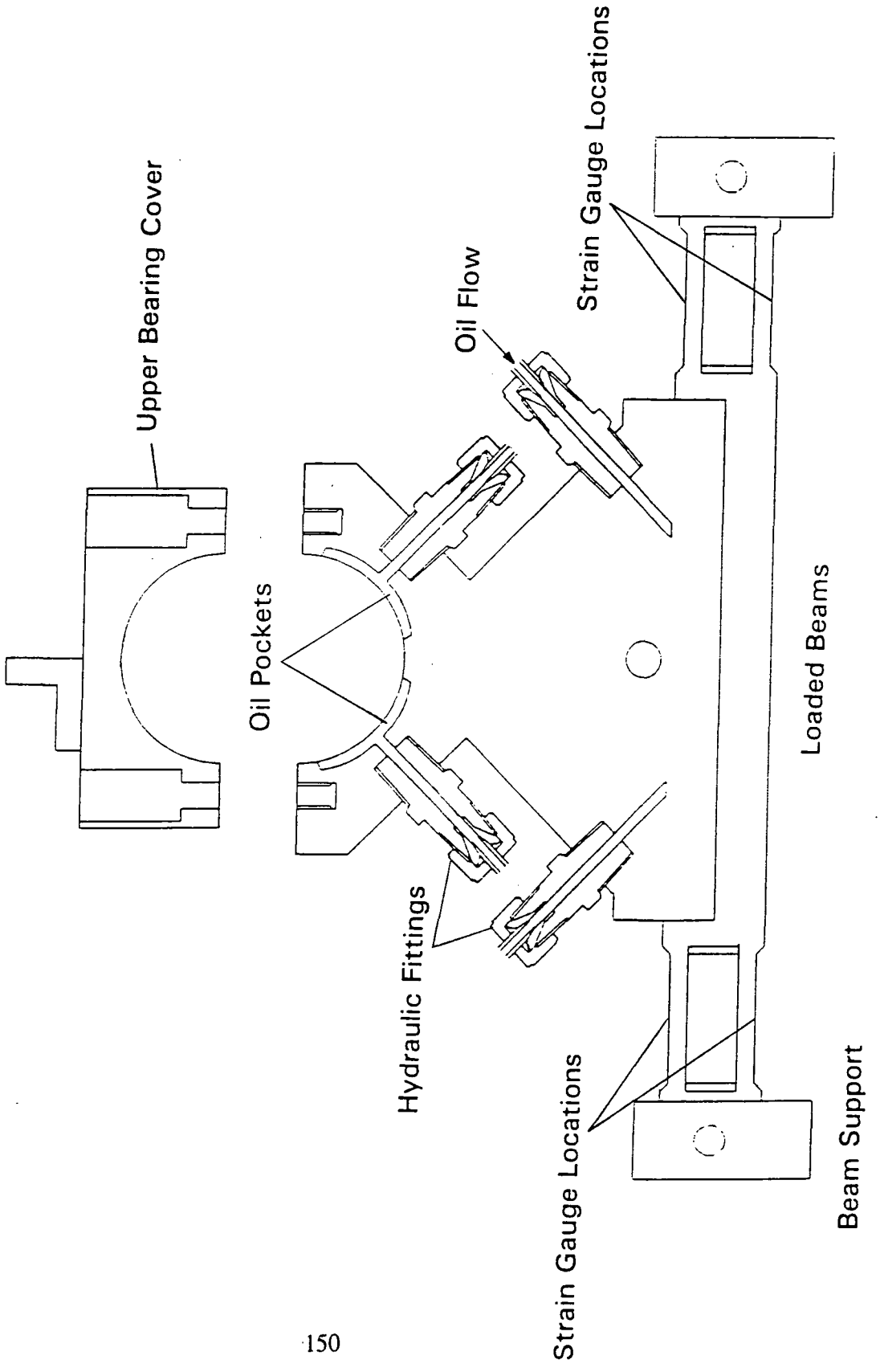


Figure 5.11 : The New Simulator

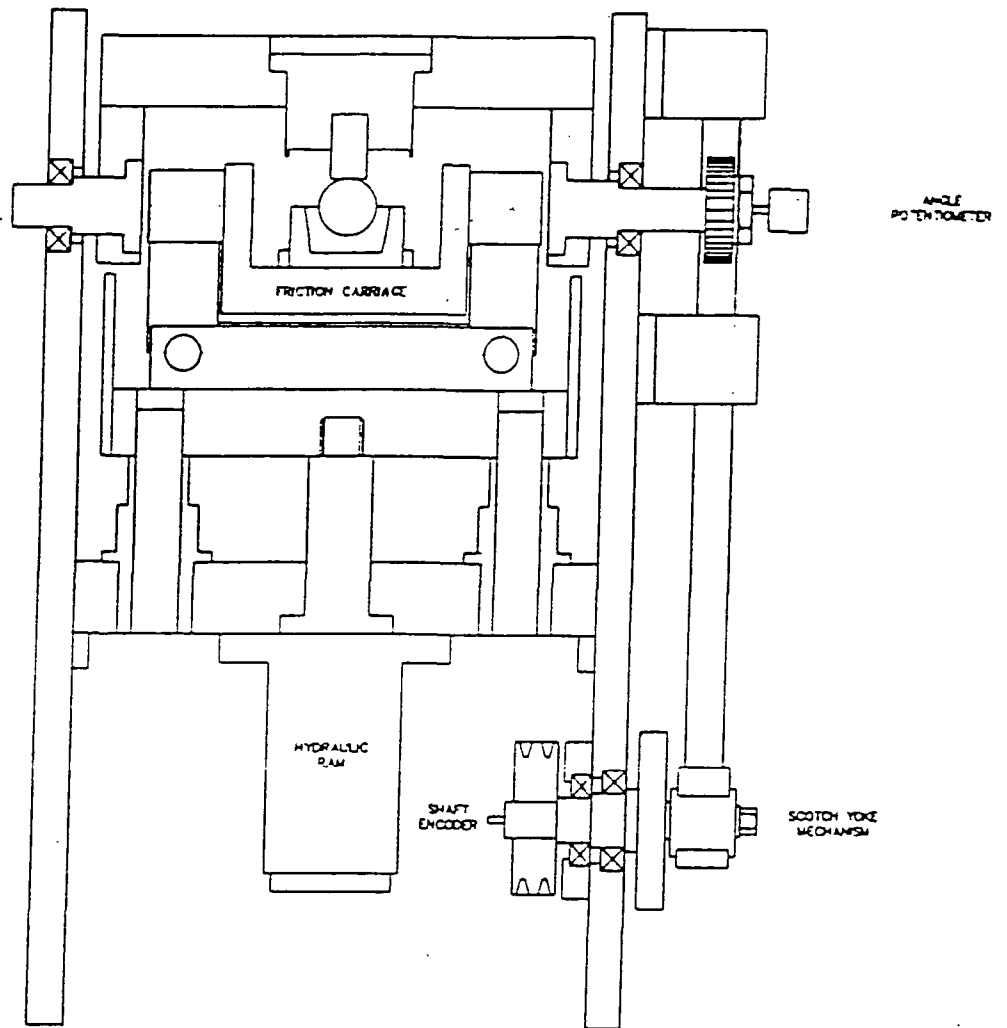
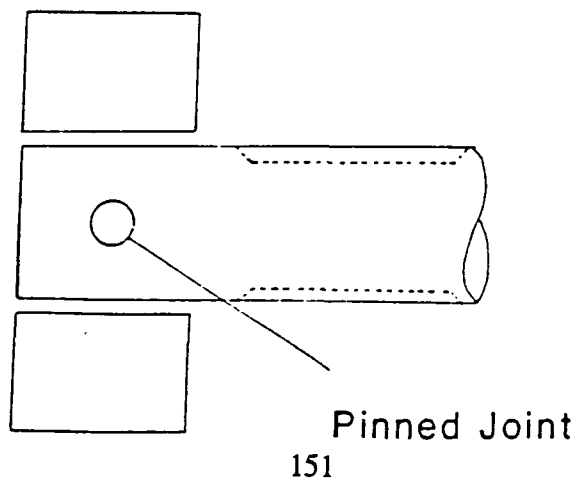


Figure 5.12 : The Simply Supported Beams

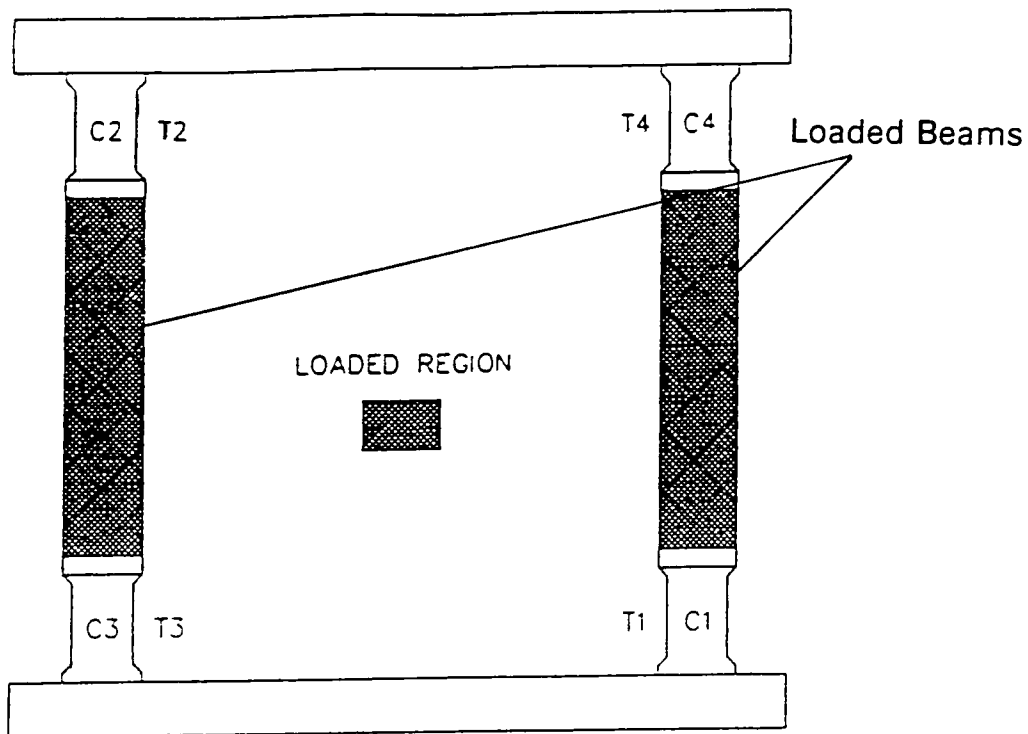


on the new machine moves the lower frame which ultimately carries the friction carriage, with the oscillating carriage mounted on a frame rigidly fixed to the lower base plate. This allowed the distance between the ram and prosthesis to be reduced substantially, lowering the deflection of the assembly (figure 5.11).

5.3.2 Measurement of the Loading Applied to the Prosthesis

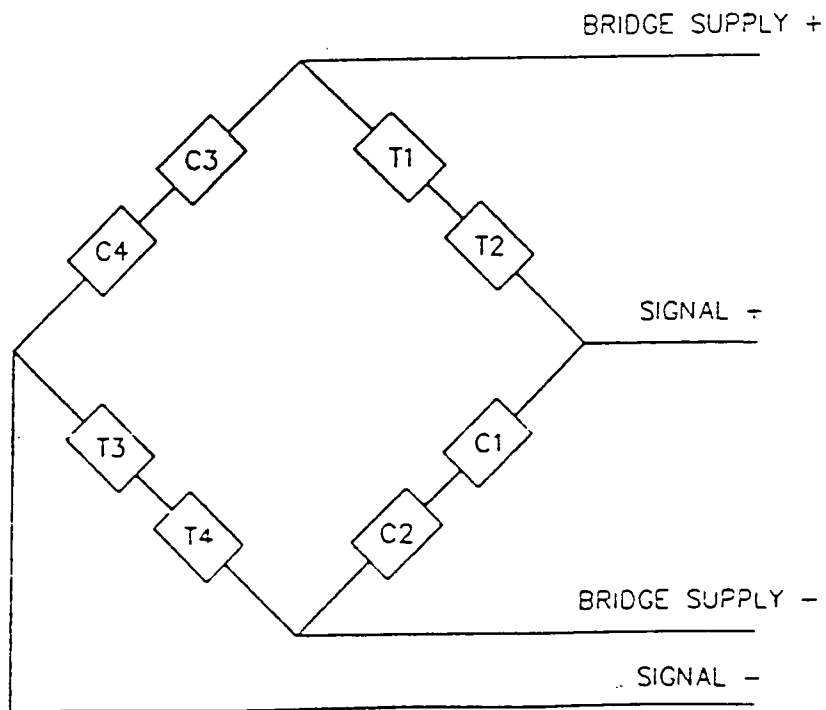
The measurement of the load applied to the prosthetic component was by means of strain gauges measuring the deflection of simply supported beams. The machine also had the capability of utilising piezo-electric load cells, but owing to the financial costs of such a system these were not used initially, but they may be incorporated at a later stage of the development of the simulator. The beams, which carried the hydrostatic bearings, were mounted on steel pins of 6mm diameter which located in fixing bars (figure 5.12). A large clearance between the beams and fixing bars eliminated the possibility of partly constrained support when the beam deflected. Eight gauges (with provision for two additional gauges centrally mounted on the tensile surface of the beams) were used to develop the largest possible signal from the deflections and these were connected in a full Wheatstone bridge circuit (figure 5.13). The Wheatstone bridge allows only the voltage change across the bridge to be amplified, and substantially increases the accuracy of the determination of deflection (or load). The gauges were from TML, of foil construction and temperature compensated for steel. Further temperature compensation was considered unnecessary due to minimal temperature changes encountered with the current machine. A gauge length of 5mm was chosen to give a reasonably sized signal within the spacial constraints. The resistance of the gauges was 120 ohms (+/- 0.3) and the gauge factor was 2.14. The gauges were fixed with cyanoacrylate (Mbond 200) and coated with nitrile rubber (Mbond B) on an acylic base (Mbond D). This was to eliminate shorting through the oil outflow from the hydrostatic bearings. The signals were amplified with

Figure 5.13 : The Strain Gauge Arrangement and Wheatstone Bridge Circuit



C1-C4 Strain Gauges
in Compression

T1-T4 Strain Gauges
in Tension



an RS 308-615 amplifier at a gain of 10,000. The gain used was large and noise was a potential problem, however this was necessary owing to the stiffness of the beams. These had been designed with fatigue life and minimal permanent deflection as primary considerations. As the machine was to be used for both long and short term testing it was expected to withstand at least 10^8 cycles. In the standard configuration a load of 4000N led to a strain gauge reading of $460\mu\epsilon$. The gauges were calibrated with a 0-10kN load cell and results were encouraging with minimal hysteresis compared with the old simulator, and good linearity ($< 0.5\%$) up to 4.5kN (figure 5.14). This corresponded to an output of 10 Volts above which there was a slight deviation, due to saturation of the amplifier.

5.3.3 Oscillatory Motion of the Simulator

Motion was provided by a 2.9kW four pole electric motor. This was geared to 56 revolutions per minute and drove a scotch yoke mechanism through a twin "V" belt arrangement which reduced the speed further to 48 rpm (0.8Hz). The input pulley to the yoke was connected through a flexible coupling to an absolute shaft encoder (figure 5.15). An absolute encoder was used to eliminate the possibility of a gross out of synchronisation of load and oscillatory motion which can be a danger with incremental encoders. The scotch yoke was adjustable and set to give an amplitude of 21° , the same as the old machine. The central point was set to $+7^\circ$, to give a maximum anterior displacement of 28° and posterior displacement of 14° . The scotch yoke drove a rack which was stabilised by the U beam (figure 5.16) and caused the upper cradle to oscillate through a pinion. The cradle was mounted in deep groove bearings for stability and by using a range of adapters (figure 5.17) was able to carry femoral or acetabular components from experimental or commercial prostheses. A range of experimental femoral heads of different radii were available to enable a range of

Figure 5.14: Primary Calibration of the Strain Gauge Load Cells of Old and New Simulators

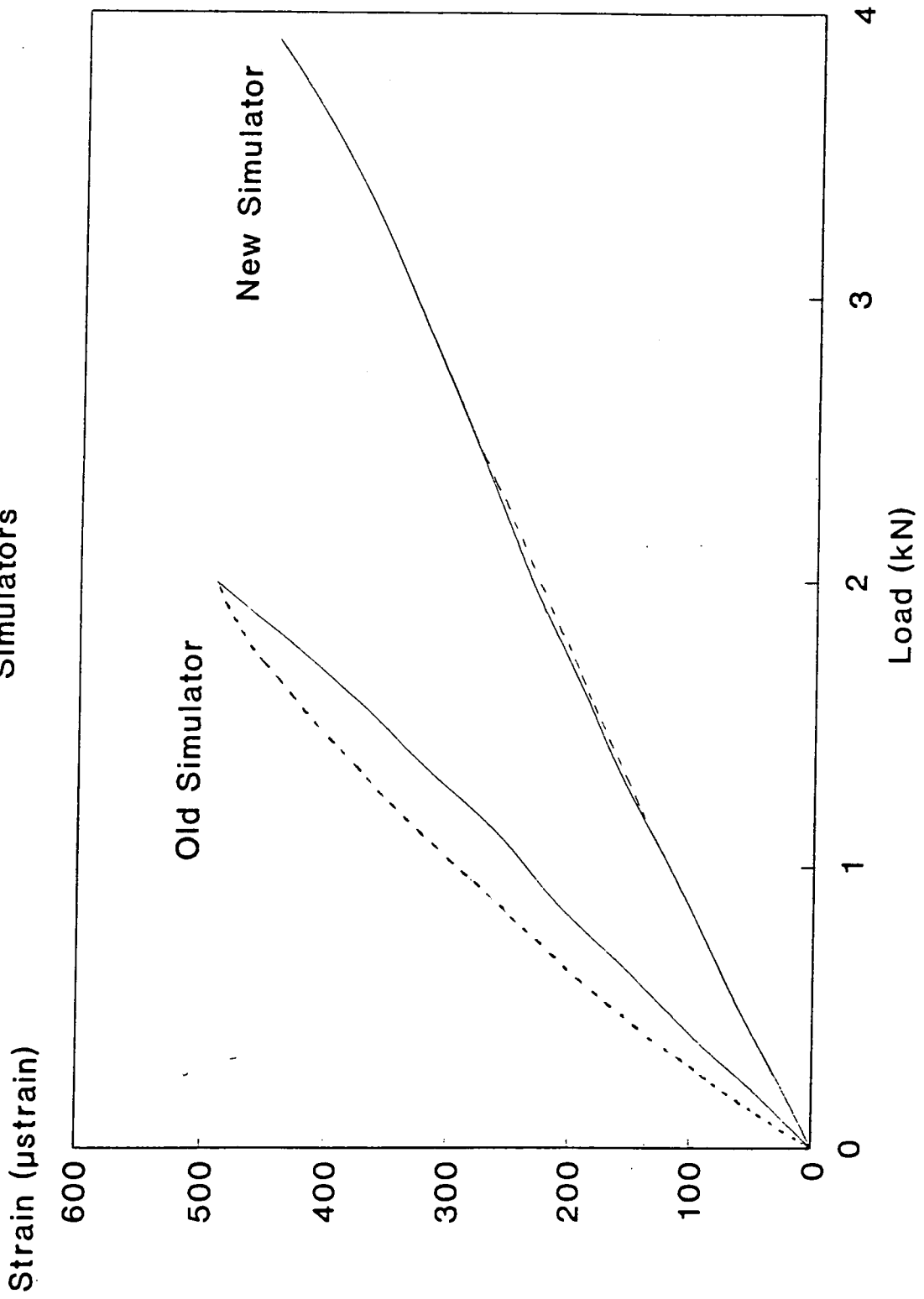


Figure 5.15 : The Encoder Position on the Input Shaft to the Machine

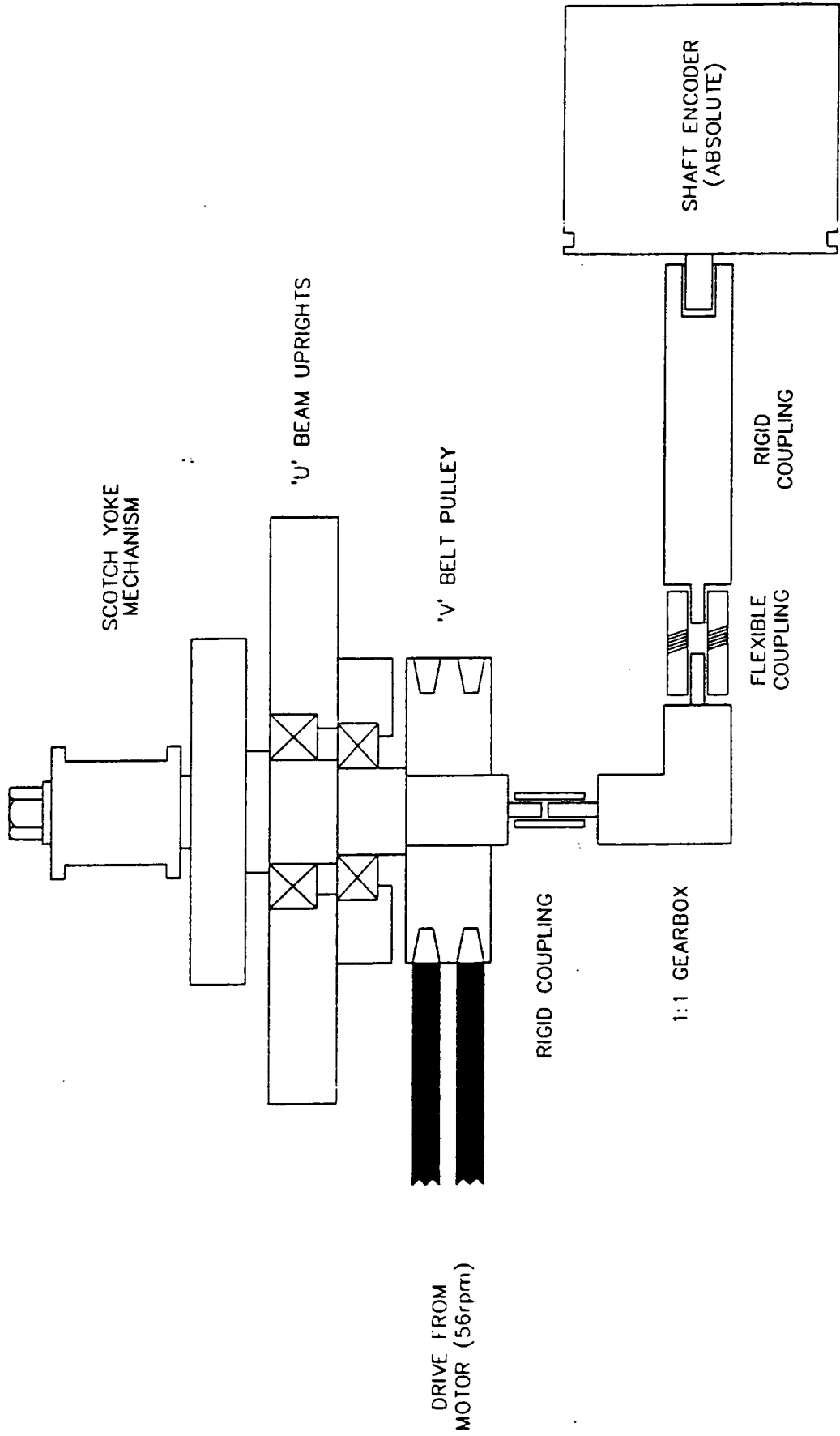


Figure 5.16 : The Scotch Yoke and Rack Arrangement

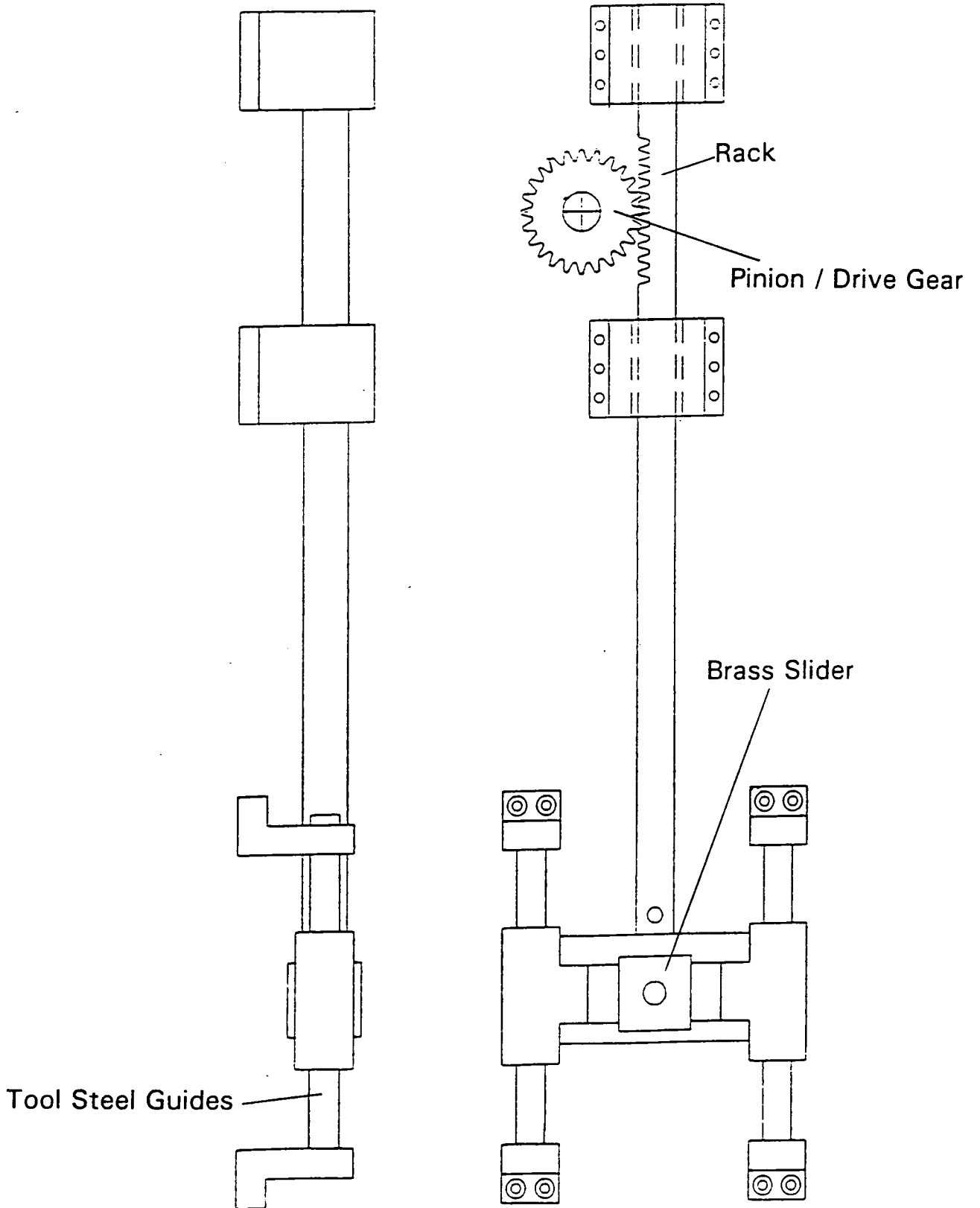
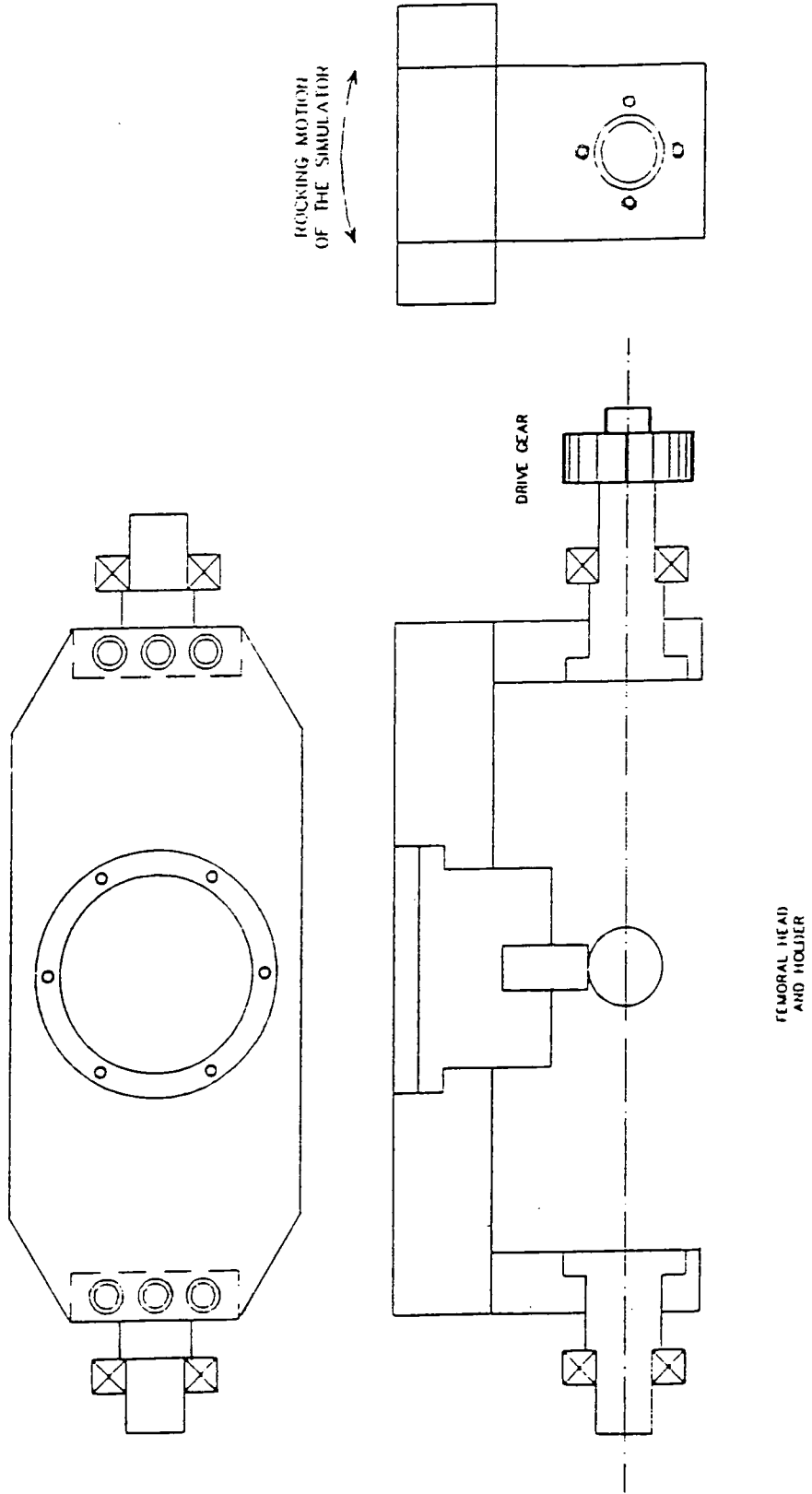


Figure 5.17 : The Upper (Oscillating) Cradle



clearances to be investigated. The explanted prostheses were mounted in plaster of Paris or polymethyl-methacrylate (PMMA) bone cement.

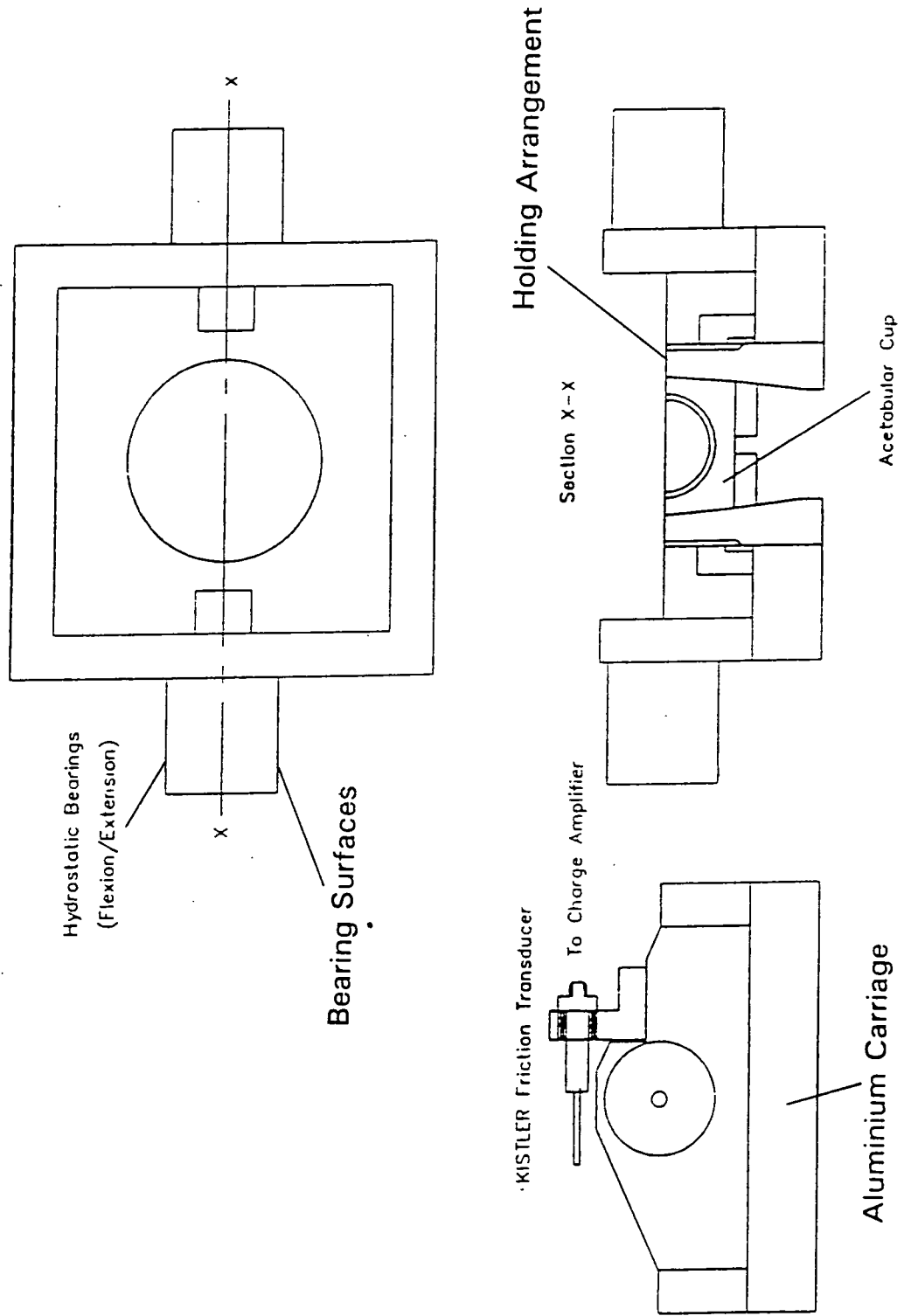
5.3.4 Measurement of the Frictional Torque Developed in the Joint

The torque resisting the motion of the femoral head within the socket was measured using a cradle arrangement (figure 5.18). Hydrostatic bearings (friction typically two orders of magnitude less than a commercial hip prosthesis) allowed for small movements of the cradle. This was resisted by a Kistler piezo-electric transducer. This model was chosen in preference to the TML device, in spite of higher costs, because of the faultless performance of the transducer mounted on the existing machine. The range of the transducer is 0-500N (which corresponds to a maximum friction factor of 0.2 with a maximum load of 2500N), with linearity better than 0.3% over this range. The electronic signals were processed using a Kistler 5039A charge amplifier and the voltages downloaded to the processor. Once in the PC the data was converted into real frictional torque values from which friction factor was calculated. As with the load, periodic calibration of the transducer was made. This was accomplished both *in-situ* or with the device removed from its assembly. Any discrepancy between the two readings indicated problems with the hydrostatic bearings.

5.3.5 Prosthetic Mounting

Although the machine was designed to operate with the prosthesis in both the physiological and inverted positions, the inverted orientation was chosen for the majority of tests. The acetabulum could be mounted in the oscillating upper cradle for a number of tests to investigate the influence of gravity on the tribological properties of the soft layer prostheses and simulate the physiological geometry. Simple theoretical analysis suggested that the forces due to the weight of the fluid would be less than 1% of the squeeze film forces. This is ignoring the substantial adherence of the fluid to the

Figure 5.18 : The Friction Carriage showing the Transducer and Bearing Arrangement



articulating surfaces in such a thin film. Unfortunately, this introduces a major problem as the "contact" area is now moving over the inside surface of the acetabular cup, which differs from the physiological case where the "contact" moves around the femoral head. This suggests a change in the lubrication conditions as the deformed region is now undergoing cyclic instead of static loading during the stance phase. This may have the effect of boosting the fluid film due to a reduction in squeeze as a rolling condition is approached. However, changing the orientation should indicate any major changes in tribological performance due to gravitational effects.

The upper component was fixed in height by the use of standard femoral heads or mounting the prosthetic stem in plaster of Paris using a jig. This sets the centre of rotation of the system which must be concentric with the centre of rotation of the hydrostatic bearing and the friction transducer. This is to ensure that the action of loading does not apply a torque to the carriage which would interfere with the friction results. The standard polyurethane and polyethylene components were located on a tapered recess and height was adjusted by means of a locking ring. Commercial components were fixed using bone cement in the jig.

5.3.6 Data Acquisition and Analysis

The control of both simulators is now very similar. A computer built around the Motorola 68020 processor provides commands for the hydraulic system through a MOOG controller and servo-valve on the old simulator and a Vickers PID card and proportional valve on the new machine. Experimental parameters, such as the lubricant used, the loading specified and the cycles which are to be recorded are entered by the operator and stored in a unique data file. Through a parallel communication link the processor monitors the applied load through strain gauges mounted on the fixed frame, frictional torque through the transducer mounted on the friction carriage, the angle of

the prosthesis through a potentiometer and absolute shaft position through an incremental encoder. The loads measured by the frame are used in the feedback loop for the valve and ram. Processing of the raw data (in ADC units) into physical properties is accomplished using the calibration coefficients, which are obtained during calibration routines. The data is stored in ASCII format with each column representing a variable:

1. Position (Encoder)
2. Measured Load (Strain Gauges)
3. Measured Angle (Potentiometer)
4. Measured Frictional Force (Piezoelectric Transducer)
5. Friction Factor (Frictional Force / Applied Load)
6. Nuovload (Parameter comprising Viscosity x Radius x Speed / Load)

Columns 5 and 6 are calculated to enable the preparation of Stribeck plots. These give an indication of the mode of lubrication present within the two surfaces of the prosthesis (Chapter 4). A typical real data file is shown in figure 5.20.

The AVDAT routine can then be implemented to take the data from the loaded portion of the curve and average values to give five points representative of the lubrication conditions. These are used in the construction of the Stribeck plots to avoid overcrowding. A typical file is shown in figure 5.21. This file can then be viewed using one of the plot routines.

5.3.6.1 Calibration Routines

The use of electrical measurement equipment requires that devices be regularly calibrated. This can be facilitated with the simulator using the SETUP Routine. This

Figure 5.20 : The Real Data File Produced by the PC Following a Typical Run

```

jmb03SE1.x8 4.50
*jmb
*1
*09/03/91 18:38:42 /** Run **/
*x /** Machine **/
*15.88 /** Head Radius **/
*57.699997 /** Viscosity **/
*0.740200 -39.730000 /** DAC.CAL **/
*2000.00 80.00 /** MAX..MIN load **/
*/** Cycles Recorded **/
*1 21 41 -1
*/**/

-set 1
    0    122    3    14    115    375
    1    117    4    14    120    377
    2    124    6    10    81    375
    ...
    66   1758    7   115    65    260
    ...
    125    99    -4    11    111    388
    126    101   -2    12    119    387
    127    108   -1    13    120    381

-set 21
    0    126    1    10    79    374
    1    101    3    10    99    384
    2    126    4    10    79    374
    ...
    67   1751    6    82    47    260
    ...
    125    117   -4    6    51    381
    126    131   -2    7    53    376
    127    115   -1    9    78    378

-set 41
    0    103    1    10    97    383
    1    101    3    10    99    384
    2    101    5    10    99    384
    ...
    62   1770    12   78    44    263
    63   1775    11   75    42    263
    ...
    125    113   -3    8    71    382
    126    126   -2    10   79    377
    127    115   -1    10   87    378
    
```

Figure 5.21 : A Typical File Used to Construct a Stribeck Plot

-ciclono 1					
51	1866	19	82	44	1445
57	1866	13	92	49	1548
63	1856	7	98	53	1584
69	1842	0	107	58	1478
75	1818	-3	106	58	1202
-ciclono 21					
51	1888	19	73	38	1412
57	1880	13	83	44	1548
63	1862	7	89	47	1584
69	1848	1	98	53	1478
75	1816	-3	94	52	1202
-ciclono 41					
51	1886	19	82	43	1412
57	1872	13	90	48	1548
63	1862	7	94	50	1584
69	1848	1	103	56	1478
75	1820	-3	99	54	1202

allows loads and torques to be applied to the strain gauges and frictional transducer incrementally to form a calibration curve. The curve is then used to calculate the calibration coefficients which are inputted into the CALIB.DAT data file (below). This is accessed each time a test is performed.

Figure 5.19 : The Calibration Data File

```
2.318 -4746 load calibration (N){orig. N = 2.484 * a-d reading - 5085}
-0.192E-1 57.1 angle calibration (degrees)
3.965 -8595 friction calibration (Nmm) {trans sens = 46, 20 Mech unit/V}
{1.885E-1 -386 friction calibration (Nmm) {trans sens =45.9, 1 Mech unit/V}}
```

5.4 Commissioning of the Simulator

Three modules had to be optimised during the commissioning procedure and these were evaluated separately.

1. Hydrostatic Bearings
2. Proportional Valve
3. Data Analysis Software and Hardware

5.4.1 Hydrostatic Bearings

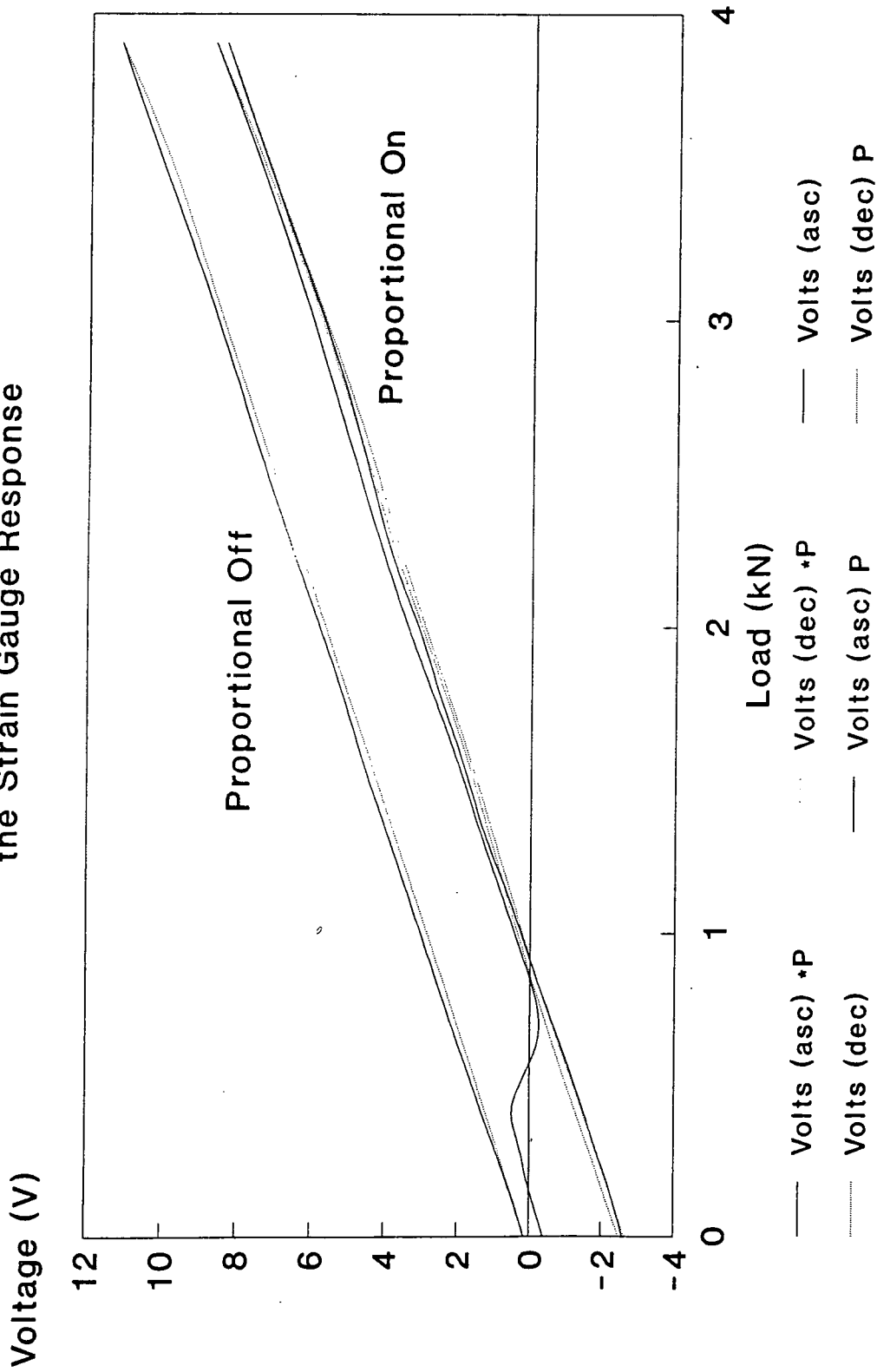
The hydrostatic bearings were modelled on the existing machine, but due to increased load capacity they had been redesigned. Pockets were machined in the bearings which provided motion in the lateral-medial directions and rotation (flexion/extension). Initially some tightness was noted, but this was alleviated by introducing a small clearance ($\sim 50\mu\text{m}$ radially). The beams which carried the strain

gauge load cells were left without pockets during the initial setup so that the pockets could be machined according to the initial performance of the bearings.

5.4.2 Proportional Valve

The increase in the load capacity of the machine required the use of 22mm diameter beams for the antero-posterior bearings. This meant that the deflection of the beams was less under the applied load and the signal from the strain gauge load cell was reduced in comparison with the old machine. The existing machine had beams that were partially constrained at the ends, as opposed to the pin joints on the new load cell and this may also have been a contributory factor. Actual deflections were $460\mu\epsilon$ for the system under a load of 4000N, approximately half that of the old system. The PID control circuit for the proportional valve required a signal of 10 volts (after amplification) from the load cell and a gain of 10-12000 was required for this. This led to a severe problem with noise and a DC shift. The shift was as a result of the high currents generated by the proportional valve (up to 1.7Amps) and the noise was mainly as a result of the current pulses required to move the solenoid. These effects were initially large (shift of 2.5V) (figure 5.22) but were reduced substantially by the elimination of earth loops and the use of filtering capacitors between the bridge supply and a common earth. Earthing of the screened cable and the connector box to the common earth of the PID card reduced the shift to 60mV. This reduced to 20mV at lower amplifier gains (approximately 1000), and at this stage the use of load washers was considered. These are strain gauge based devices which provide a large signal from relatively low loads. The strain gauge is mounted circumferentially on the outside of a machined washer. With 4 of these devices, occupying two arms of a full bridge, the output was ($16000\mu\epsilon$) at 4000N load. This means that the gain of the amplifier could be reduced to 250, reducing the DC shift and increasing the accuracy of the measurement. However, cost was prohibitive (£1300 for commercial devices), unless

Figure 5.22: The Effect of the Proportional Valve on the Strain Gauge Response



the washers were made in-house, and their resistance to the oil atmosphere was not guaranteed. Following testing of both devices it was decided that the increased cost could not be justified and the beam arrangement was maintained.

5.4.3 Data Analysis Software and Hardware

Much of the data analysis software had been in use for a number of months on the old machine and only a few small modifications had to be made to the system to make use of the proportional valve system (figure 5.8). The three input signals to the proportional card were:

- 0 - +10V Desired Force
- 0 - +10V Feed Back Signal from Strain Gauge Amplifier
- 0 - +/-10V Open Loop input to Position Cylinder

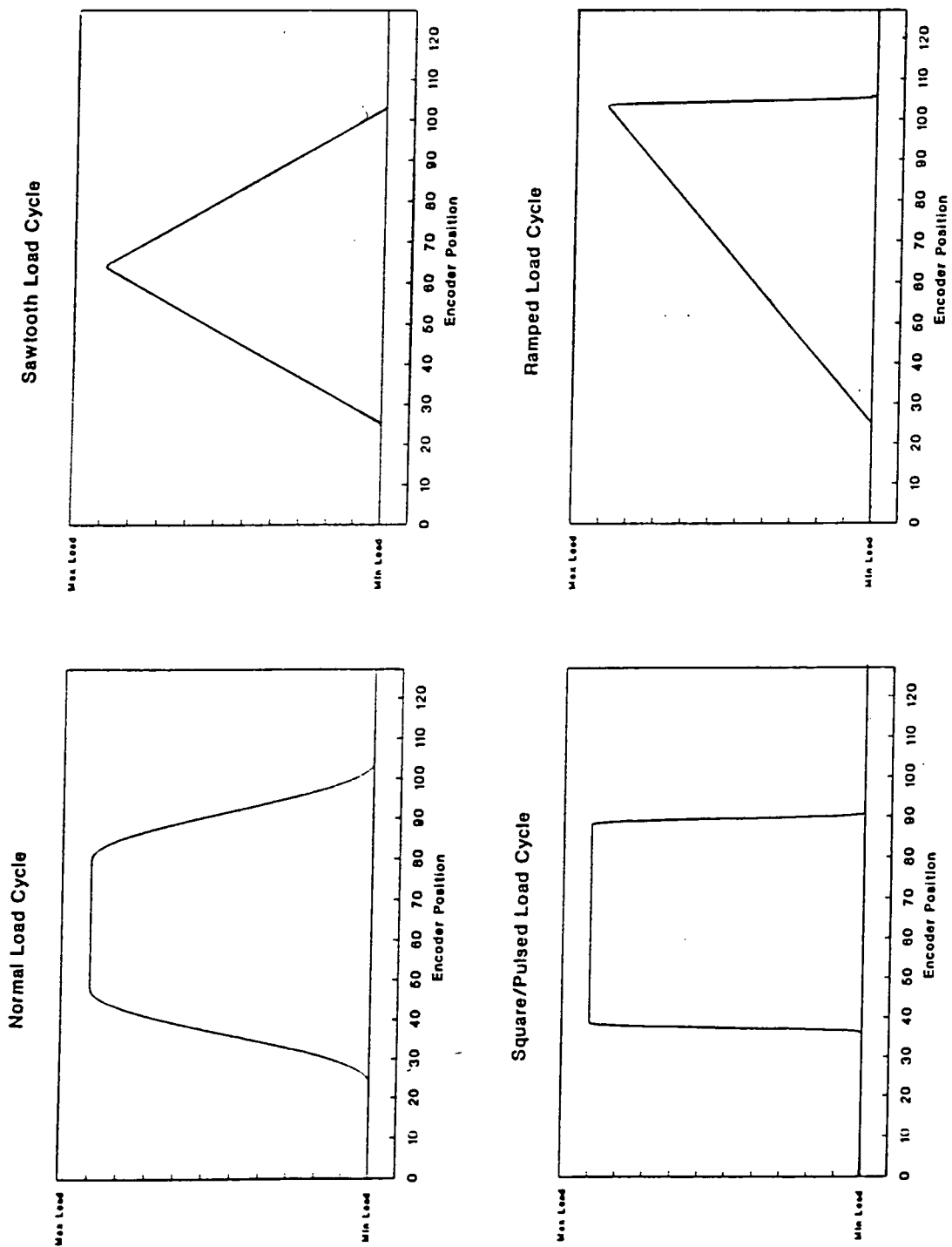
The rest of the 68020 based computer was identical, to allow for inchanging the boxes as an aid to fault finding. The PC used with the new machine was a Viglen "386".

A number of additions to the software were made to simplify and improve setting up of the simulator. Routines which allowed a number of load patterns to be specified (figure 5.23) and these to be time, and not encoder position, dependent were used to fine tune the PID module for the optimum response. In addition raw data from the simulator could be obtained to aid fault finding.

5.4.4 Calibration

Prior to calibration the scotch yoke mechanism was set to give an amplitude of 21° about a central position +7° from the vertical, in line with physiological

Figure 5.23 : The Load Patterns used for Fine Tuning of the PID Module



measurements in the anterior-posterior directions. Calibration of the machine was required to ensure that the loading and friction measurements were accurate and that the loading was synchronised to the angle of the head and the position of the encoder. Graphs were plotted (figures 5.24a,b,c) and from these the hysteresis of the arrangement was monitored and the calibration coefficients calculated. The SETUP routine allowed measured values of load (load cell) (figure 5.24a), friction (torque measurement) (figure 5.24b) or angle (goniometer) (figure 5.24c) to be input and calibration of the required load, measured load, frictional torque and head angle with respect to the ADC and DAC readings. Following this the encoder was positioned to match the potentiometer reading to ensure that the application of major load at heel strike was at the correct flexion angle. Calibration was conducted periodically during the course of the study with both machines, typically on a monthly basis or after a few weeks without experimentation.

5.5 Loading

5.5.1 Dynamic Loading

The loading cycle used for the tribological assessment of the experimental prosthesis was governed by the maximum and minimum loads. At heel strike the load was ramped quickly to its maximum value. This value was maintained during the stance phase of the cycle to toe off to give a loading pattern similar to that found by *in vivo* (English & Kilvington, 1979). The minimum load, which represents joint forces during the swing phase, was low.

The majority of the testing was carried out using the old machine with a maximum load of 2000N, 2½ times body weight, and a minimum load of 20N. This was Loading Cycle I (figure 5.25a).

Figure 5.24a: The Calibration of the Loading Applied by the Simulator

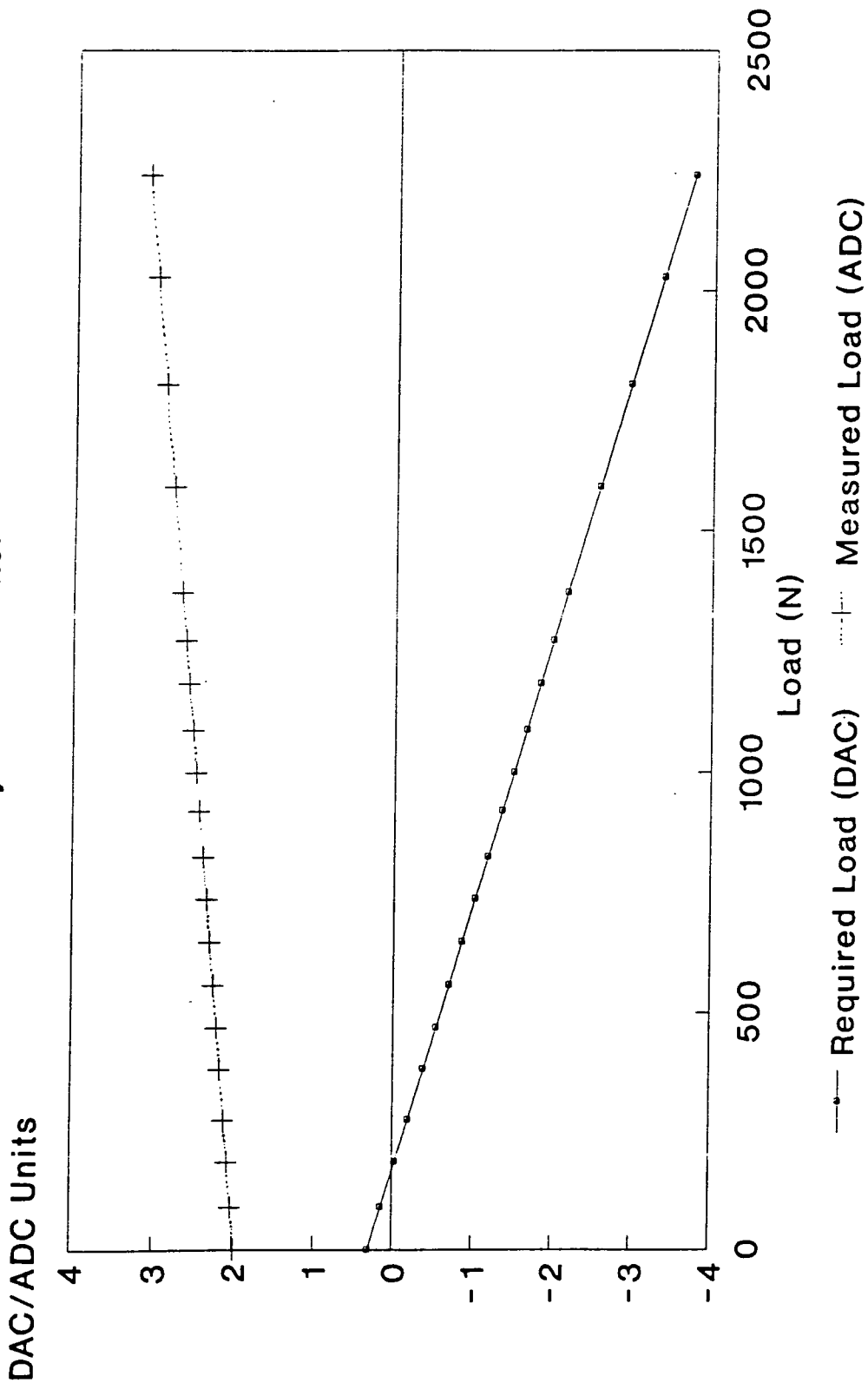


Figure 5.24b: Calibration of the Kistler Friction Transducer

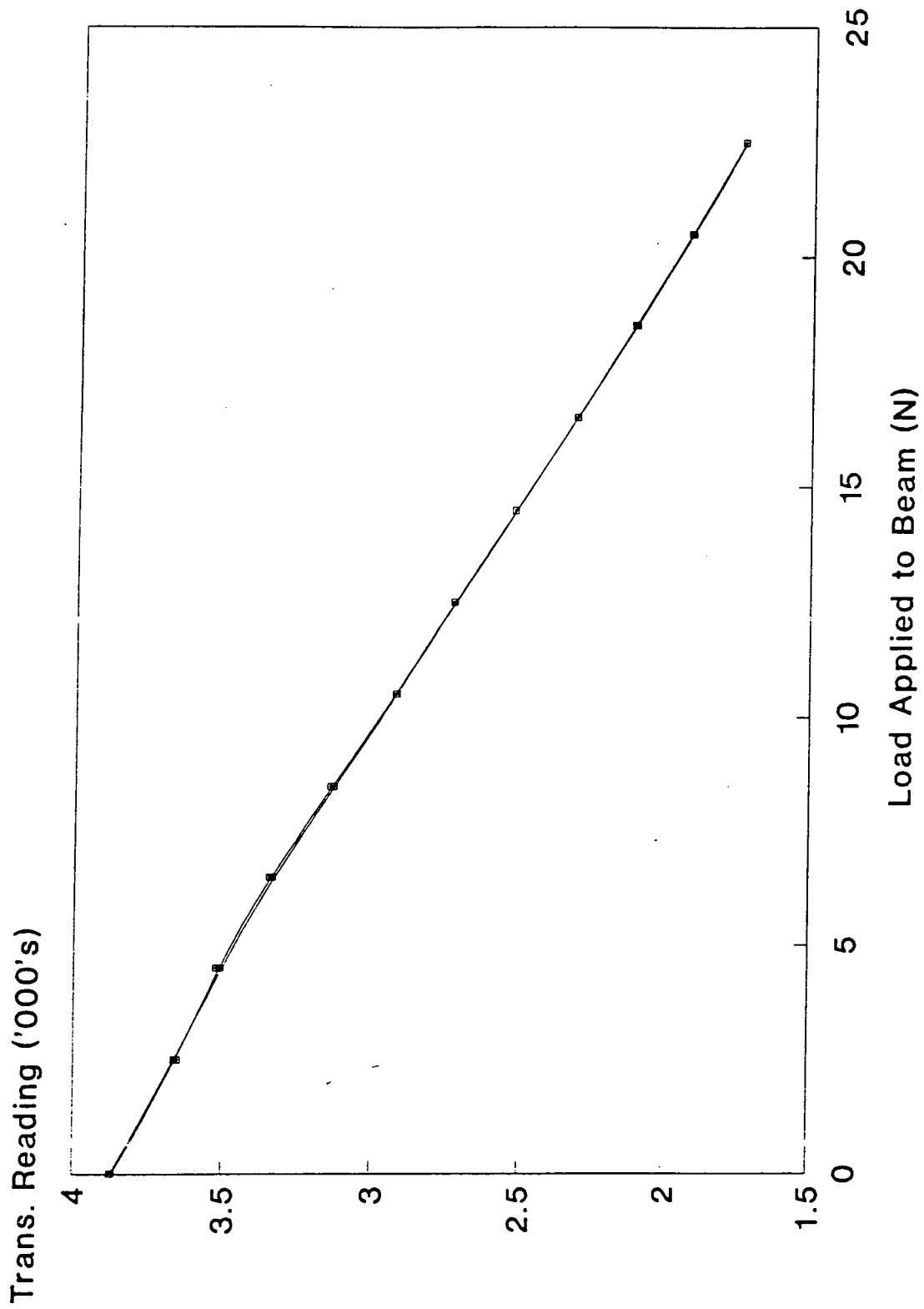


Figure 5.24c : Calibration of the Potentiometer

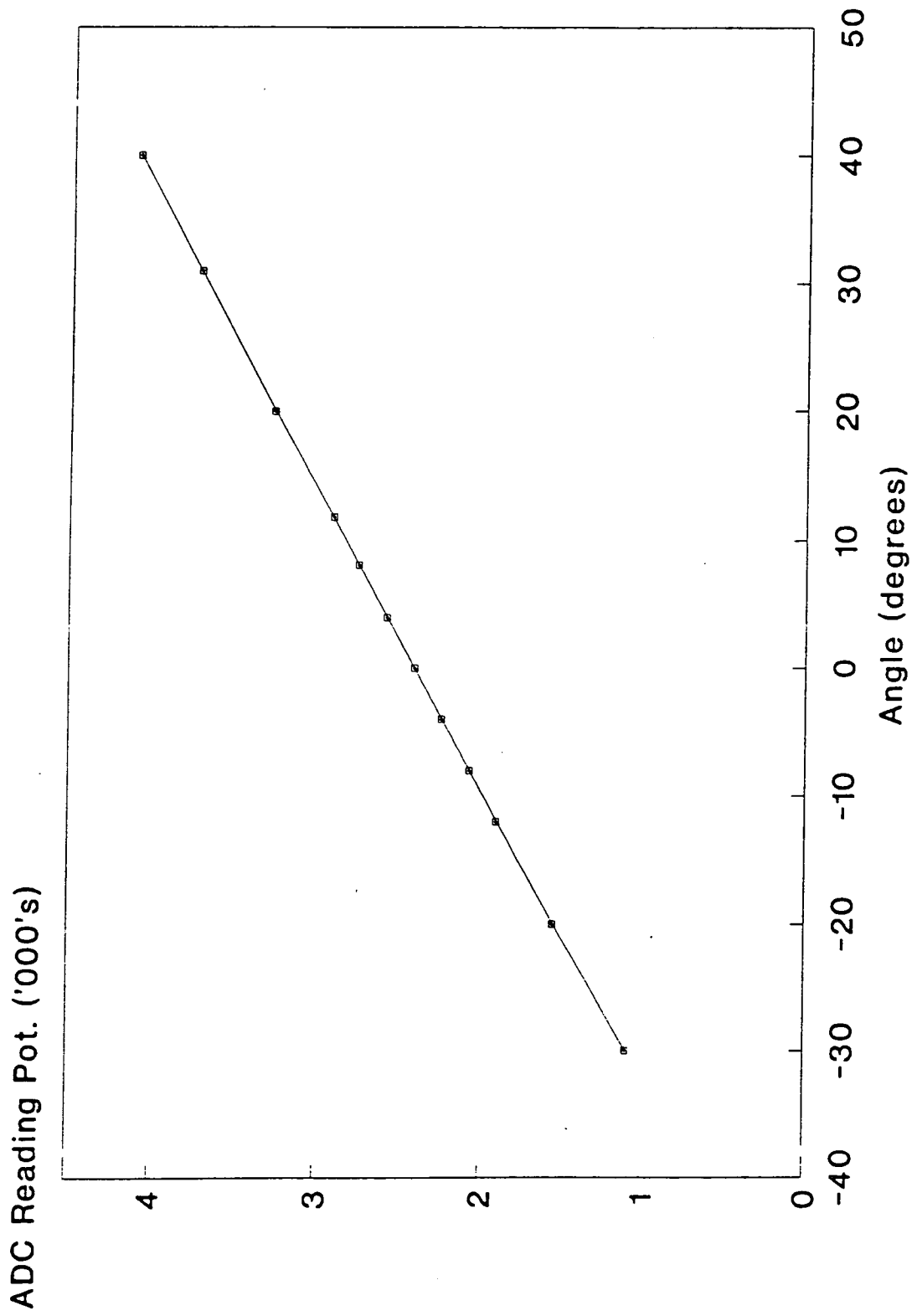
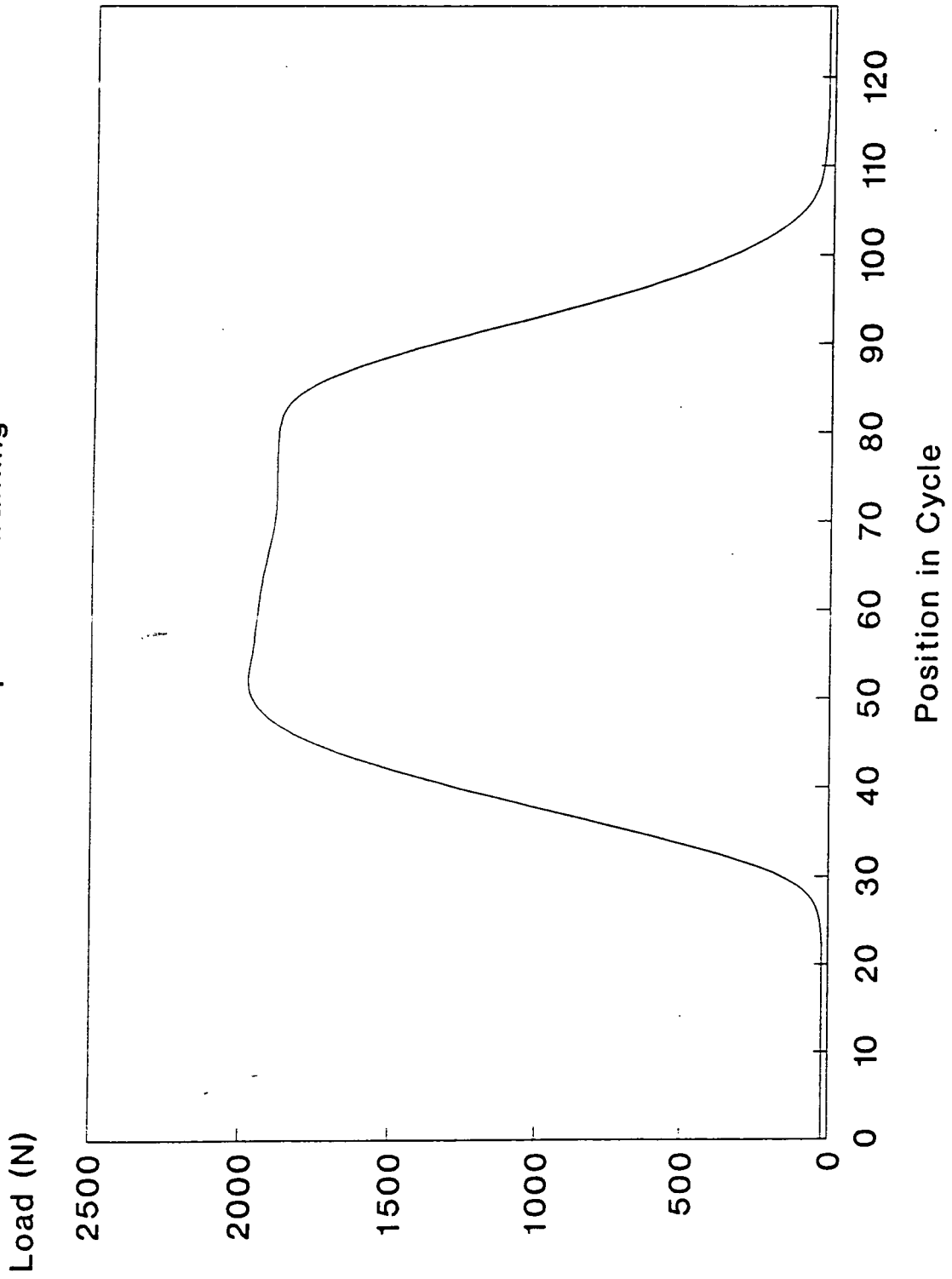


Figure 5.25a: Loading Cycle 1 applied by the Simulator to represent walking



5.5.2 Constant Loading

If the minimum and maximum loads were set to the same value, such as 1000N as detailed in Chapter 7, then a constant load was applied to the prosthesis. This eliminates the squeeze film effects and allows tribological assessment of the importance of this mechanism. Loading cycle II is shown in figure 5.25b.

5.5.3 The Minimum Load

The work on the laser modified cups (Chapter 7) also investigated increases in the minimum load to determine the value where replenishment of the fluid film would not be sufficient to maintain full lubrication. This was done in order to assess any advantage from the porous structure created by the laser modification. Loading cycle III used a minimum load of 1000N and an upper load of 2000N, as shown in figure 5.25c.

5.5.4 The True Walking Cycle Loading

The loads applied to the joint through the articulating surfaces were discussed in Section 4.2.8. Although the cycle used for the majority of the early soft layer work at Durham gave a more demanding tribological case than the loading cycle suggested by Paul (1967, 1976), the differences in tribological properties were small (Section 6.5). In addition the numerous peaks of the measured loading may lead to more severe fatigue conditions. Paul's curves were digitised and applied to the simulator through the proportional valve. Two loading cycles were available, applying the vertical component only (figure 5.26a) and the resultant force (figure 5.26b). The use of Paul's loading cycle and comparisons of theoretical and experimental results from it and the simplified cycle are further discussed in Chapter 6.

Figure 5.25b: Loading Cycle II applied by the Simulator

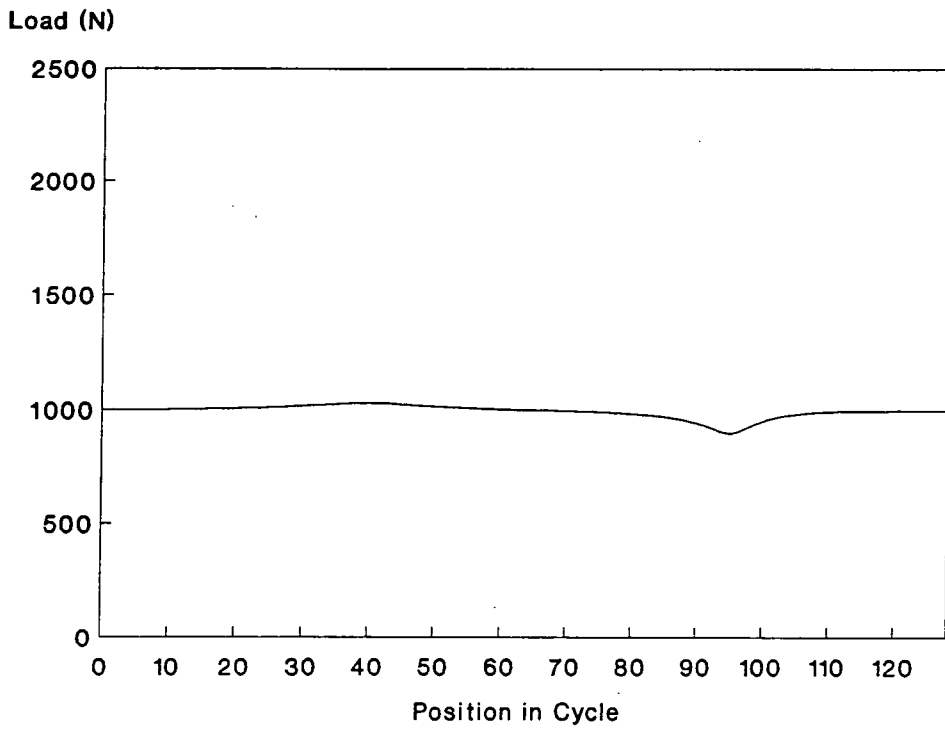


Figure 5.25c: Loading Cycle III applied by the Simulator

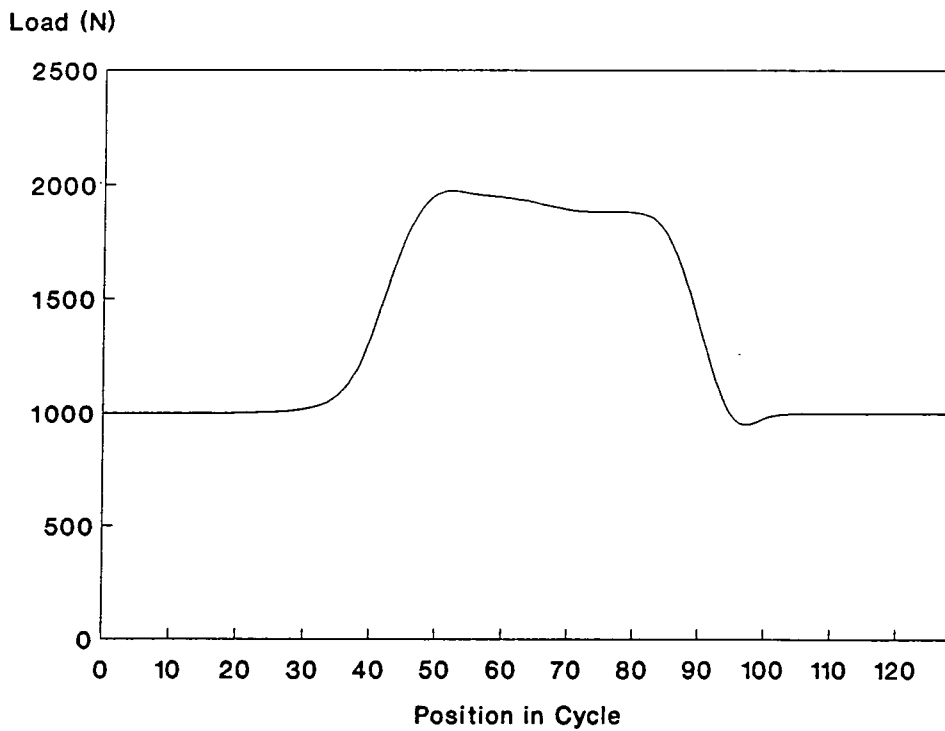


Figure 5.26a&b: The Vertical Component and Resultant of the Forces Applied to the Hip during Walking (Paul, 1967)

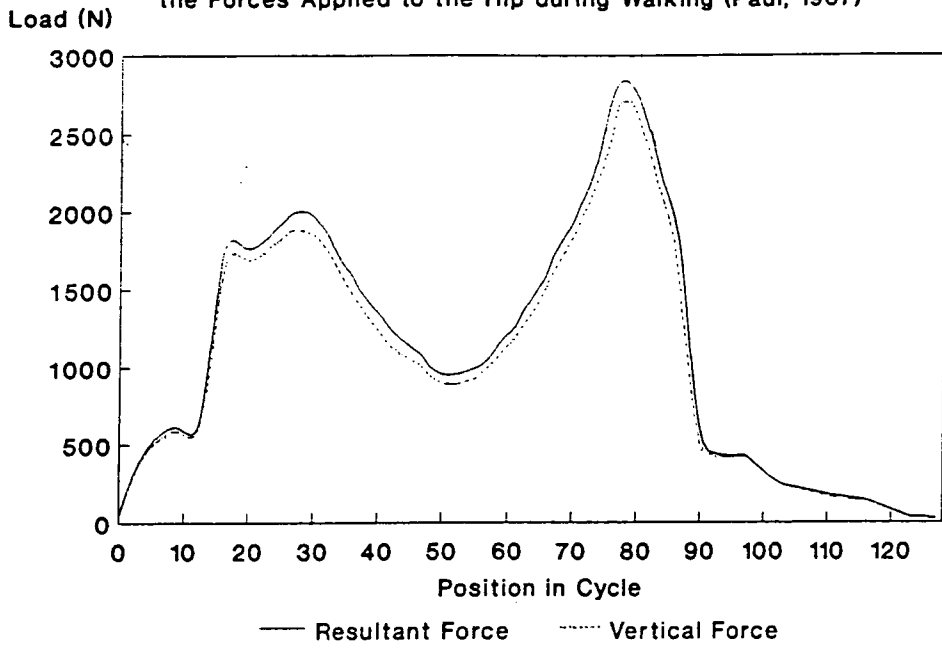
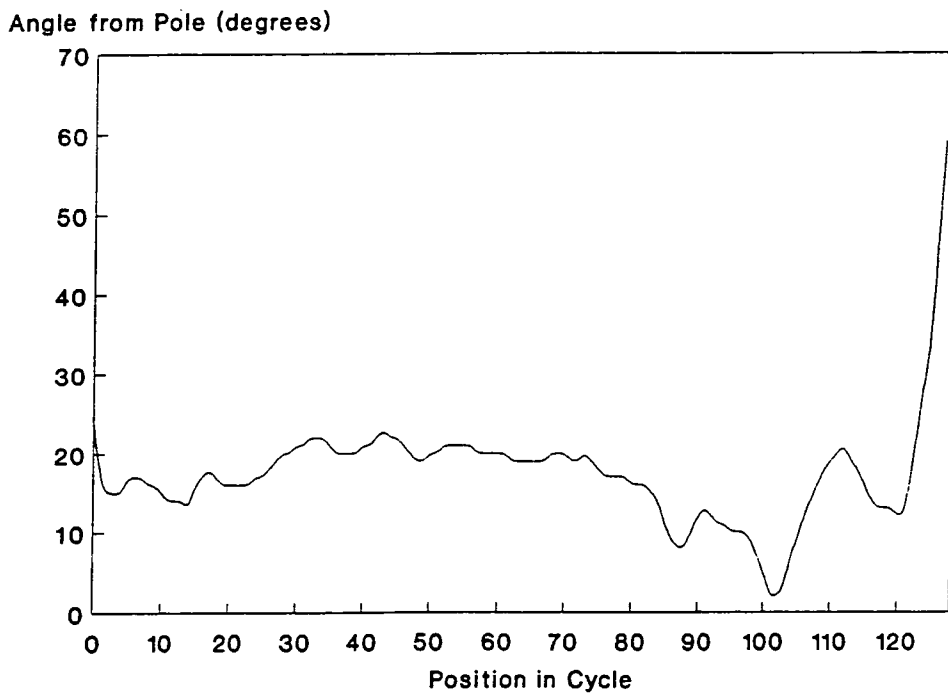


Figure 5.26c: Angle of Resultant Force Applied to the Hip (Paul, 1967)



5.6 Lubricants

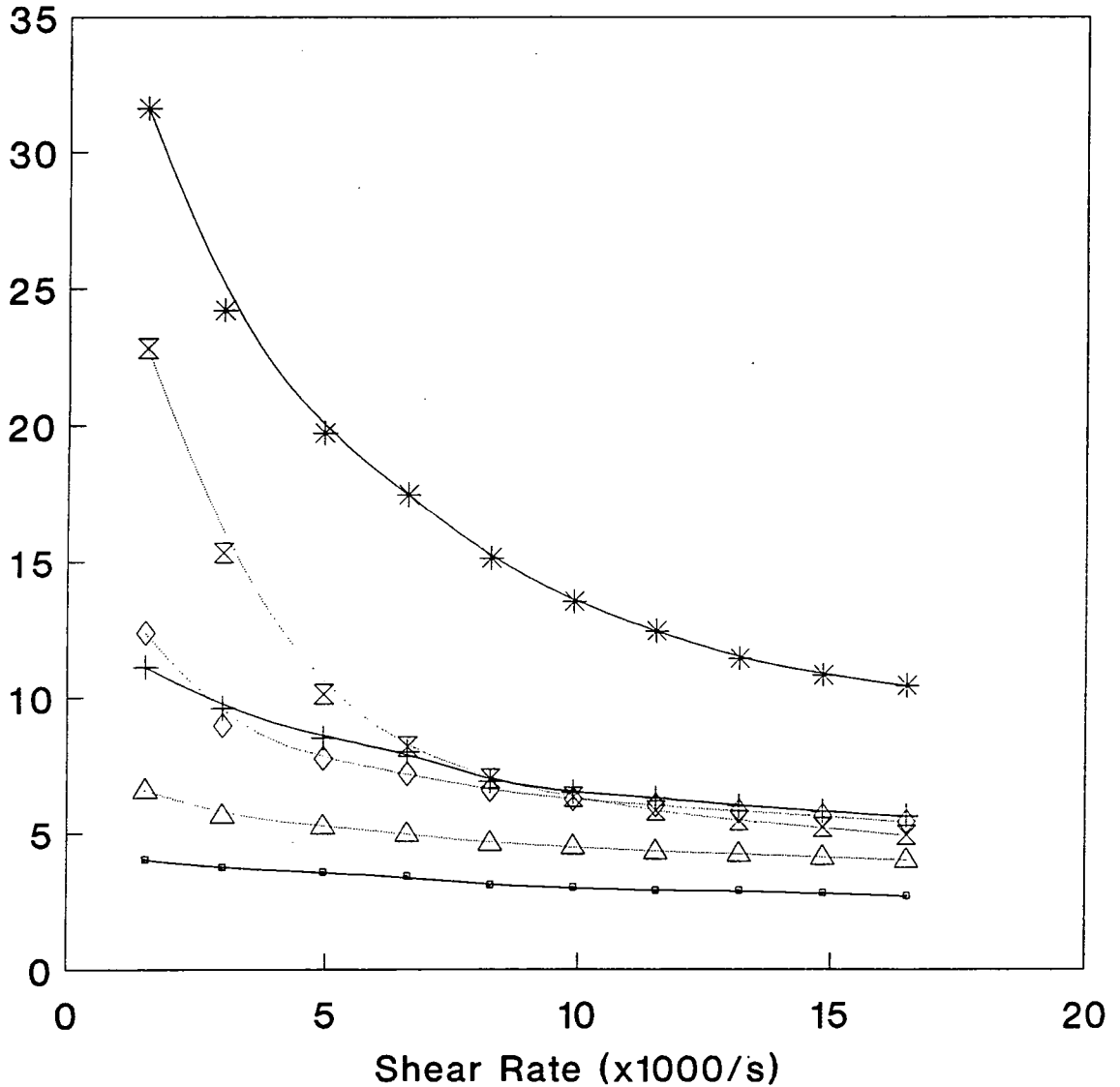
Artificial lubricants were used which closely followed the response of natural synovial fluid to pressure and shear rate, to allow the tribological properties of the prosthetic components to be measured without the risk of infection. Synovial fluid is highly non-Newtonian, having a viscosity which increases significantly with decreasing shear rate (Dintenfass, 1963). With normal synovial fluid this is due to the concentration of the hyaluronic acid-protein complex which forms a gel under low shear stresses. This helps separate the articulating surfaces when stationary. Rheumatoid and osteo-arthritic synovial fluids both exhibit viscosity increases at low shear rates but generally the viscosity of these fluids is less than that of healthy fluid. In addition, synovial fluid behaves as an elastic gel when rapid and transient stresses are applied (Gibbs *et al*, 1968). Aqueous Carboxy-Methyl Cellulose (CMC) was prepared to the required viscosity by mixing the CMC solid with distilled water in different proportions. A range was used to allow the tribological properties of the prostheses to be evaluated.

A Ferranti-Shirley Cone-on-Plate Viscometer was used to measure the fluid viscosities. Although this machine was able to generate shear rates of over 10000s^{-1} , fluctuations in the frictional torque reading limited measurements to shear rates of 5000s^{-1} . A shear rate of 3000s^{-1} was generally used for the measurements of the viscosity of the CMC fluids. Although this is less than values which may be present during some periods of the walking cycle, shear thinning was low at these rates (figure 5.27a).

Figure 5.27a shows a graph of viscosity against shear rate for osteo-arthritic, rheumatoid and aqueous CMC fluids and indicates how the lower range of artificial fluids resembles the lubricant properties likely to be encountered by any prosthesis.

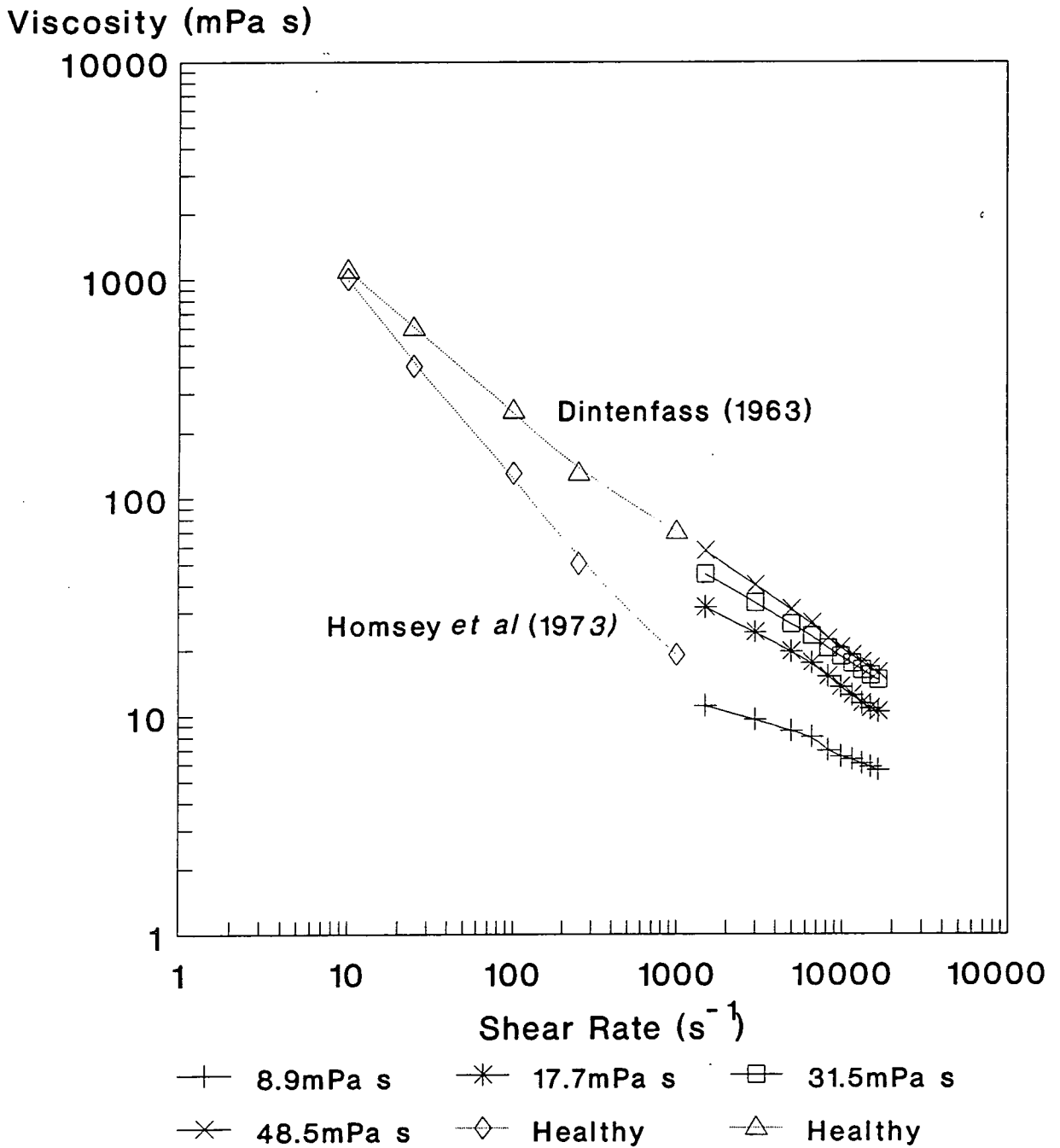
Figure 5.27a: A Plot of Shear Rate against Viscosity for CMC and Diseased Synovial Fluids

Viscosity (mPa s)



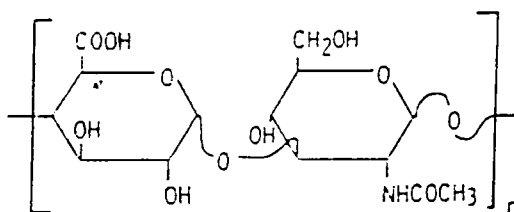
—○— 4.8cP Fluid —+— 8.9cP Fluid —*— 17.7cP Fluid
 -◇- Rheumatoid 3 -△- Rheumatoid 1 -⊗- Osteoarthritic

Figure 5.27b: A Plot of Shear Rate against Viscosity for CMC and Healthy Synovial Fluids

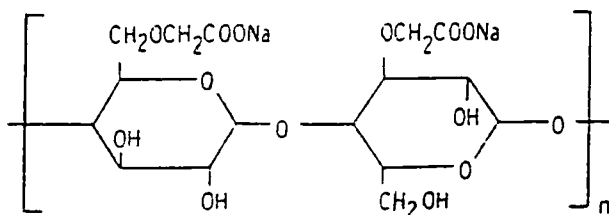


Although healthy synovial fluid could not be obtained the results of Dintenfuss (1963) and Homsey *et al* (1973) were used to construct figure 5.27b. Synovial fluid acts in a similar way to the 0.0177Pa s fluid at high shear rates with a higher viscosity at low shear rates. The reasons for this are because of the structural similarity of the hyaluronic complex and the CMC molecule. Chapter 6 indicates the positive effect of high viscosities on lubrication and the use of a range of CMC fluids seems to show this effect in the same way as natural fluid would.

.Hyaluronic Acid



Sodium Carboxymethyl Cellulose



Silicone fluids, which are Newtonian under shear rates generated in the artificial hip, were only used during the initial studies on UHMWPE joints where fluid film lubrication was being encouraged by the use of high viscosities. CMC solutions were only capable of reaching viscosities of 0.250Pa s (at 3000s⁻¹), with silicone fluids available up to 30Pa s. The non-Newtonian behaviour, which encourages gel formation in CMC and natural fluids and protects the cartilage layer (Section 4.2.7), was seen as less important with higher viscosity lubricants.

Chapter 6 : Tribological Studies and Contact Area Assessment of Hip Prostheses

6.1 The Importance of Tribological Properties

Current prosthetic components have been shown to exhibit low frictional torques under simulation of the forces within the hip. However, as was shown in Chapter 4, wear does occur due to the mixed lubrication regime which operates (Unsworth, 1978). Tissue disruption as a result of debris formed on the articulating surfaces has been linked to prosthetic loosening (Villacin and Bullough, 1978; Willert *et al*, 1976) and the chain of events is shown in figure 6.1 (Clarke, 1981). Even with the changes to cements, stem design and coatings, loosening is still the major source of failure. The formation of a film of fluid between the components of the hip will therefore have greater importance in the reduction of wear debris than lowering of the frictional torque. In order to understand the mechanisms of the lubrication a number of studies were made.

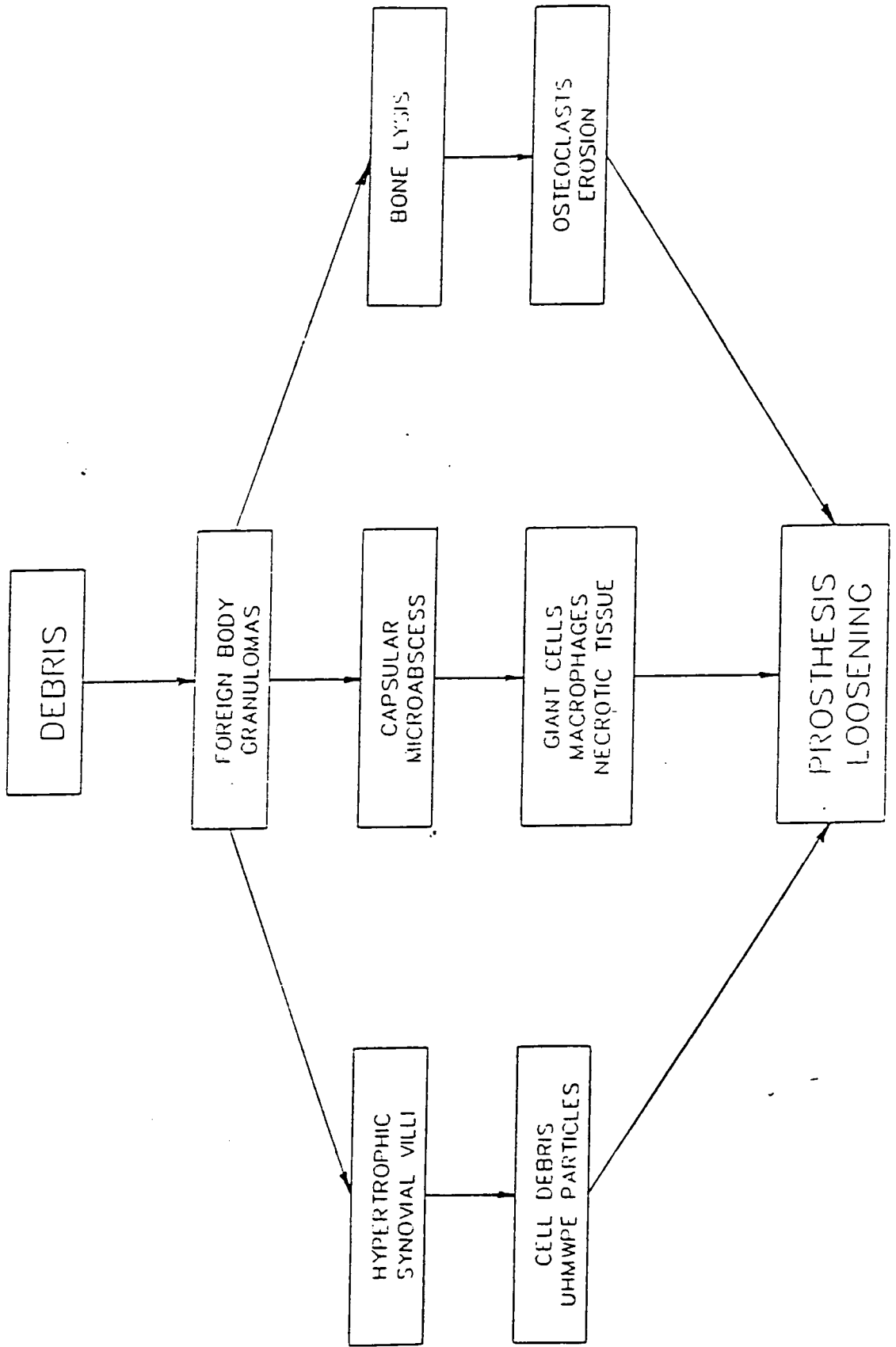
6.2 Contact Analysis of Currently Available Systems

6.2.1 Introduction

The tribological performance of a bearing is, to an extent, dependent on the magnitude of the pressures applied both through the lubricant and direct contact of the surfaces. In the hip joint, the elasticity of the materials, the geometry of the femoral and acetabular components and the forces applied to the joint are all important.

Transmission of force between two surfaces in contact or separated by an incompressible fluid, takes place across a finite area. The size of the contact area, which is dependent on the elastic deformation of the surfaces, determines the pressures which will be generated at the interface under the applied load. Tribological theory for

Figure 6.1 : The Pathway for Prosthetic Loosening due to Wear Debris



EHL and Squeeze Film mechanisms predicts that the lubricating film is enhanced by low peak pressures. Therefore, it is preferable to have as large a contact area as possible. Hertzian contact theory may be used to show that the peak pressures developed are about 50% greater than the average pressure (Timoshenko and Goodier, 1970). A typical pressure distribution is shown in figure 6.2. Sliding perpendicular to the vertical axis, which can be representative of flexion/extension of the hip joint, introduces only minor fluctuations to the pressures at the entry and exit of the "contact" (Chapter 4). Although Hertzian theory refers to a spherical indenter on a flat surface, the ball in cup arrangement can be investigated, with a model based on the equivalent radius (figure 6.3).

$$R_x = \left[\frac{1}{R_1} - \frac{1}{R_2} \right]^{-1} \quad 6.1$$

This radius R_x can be used to assess the area of contact.

$$a = \left[\frac{W R_x}{E'} \right]^{1/3} \quad 6.2$$

The equivalent elastic modulus is calculated from a combination of the values for the two surfaces.

$$E' = 2 \left[\left(\frac{1 - \nu_1^2}{E_1} \right) + \left(\frac{1 - \nu_2^2}{E_2} \right) \right]^{-1} \quad 6.3$$

For UHMWPE/metal prostheses there is little problem in determining E' , but this is not the case for the Durham elastomeric prosthesis, which consists of a

Figure 6.2 : The Typical Pressure Distribution for an Acetabular/Femoral contact from Hertzian Theory

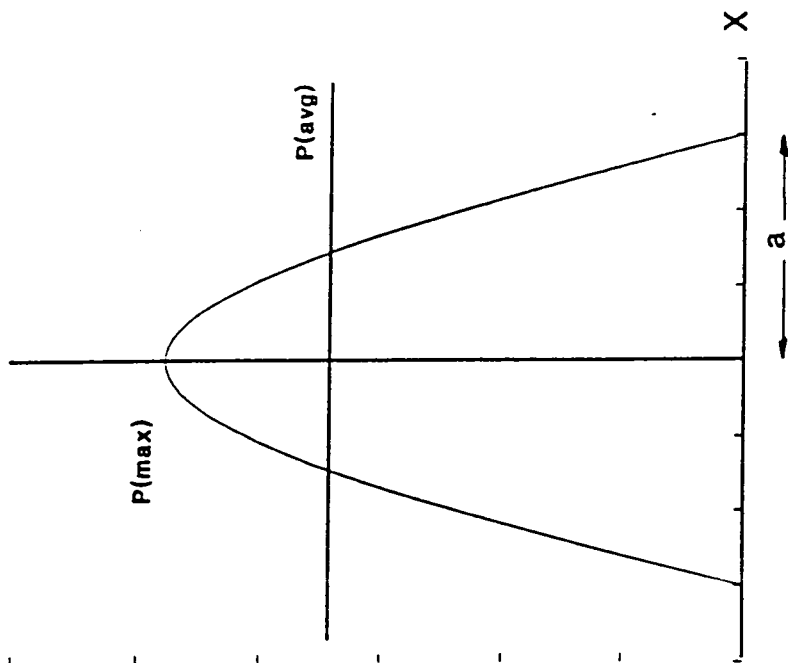
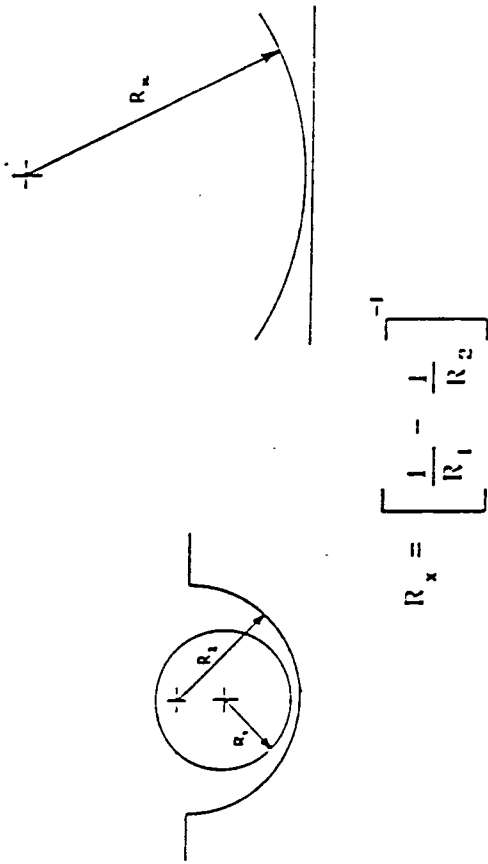


Figure 6.3 : The Ball-in-Cup to Ball-on-Plate Transformation



compliant layer of 2mm thickness bonded to a rigid backing material. The effective elastic modulus of the assembly is not easy to calculate as the effect of the backing material and the bond between it and the elastomer on the apparent mechanical properties of the device become important (sections 2.6 and 2.7). This is similar to the arrangement of the cartilage and the sub-chondral bone.

The calculated values of contact area and maximum pressure developed for a range of commercially available hip prostheses and for a healthy human joint are shown in table 6.1. Current prostheses have much smaller contact areas and hence higher contact pressures than the healthy human joint or the experimental Durham prosthesis.

At present implanted prostheses tend to be UHMWPE on metal or ceramic, which exhibit a larger contact area than the McKee-Farrar metal-on-metal prosthesis. The UHMWPE is responsible for the reduction in the value of E' and the use of titanium or ceramic femoral heads in preference to steel makes little difference to the contact. The effect of clearance on the contact radius and generated pressure (assuming a Hertzian pressure distribution) can be seen in figure 6.4. At very small clearances the contact area can reach similar values to the human joint which should improve tribological properties. Unfortunately, the nature of the biological environment precludes very small clearances due to deformation of the polyethylene under load, which could cause grabbing, and the inevitable presence of small particles of bone or cement which could cause seizure (Isaac *et al*, 1992). However, investigating the effects of contact area on friction factor will indicate the relative importance of micro-EHL and flattening of the asperity peaks within soft layer prostheses. Stribeck plots which cover the transition from mixed to fluid film could be obtained by using a broad range of lubricant viscosities. The effects of increasing the

Figure 6.4 : The Effect of Clearance on Contact Radius and the Maximum Pressure Generated

Pressure (MPa)

Contact Radius (mm)

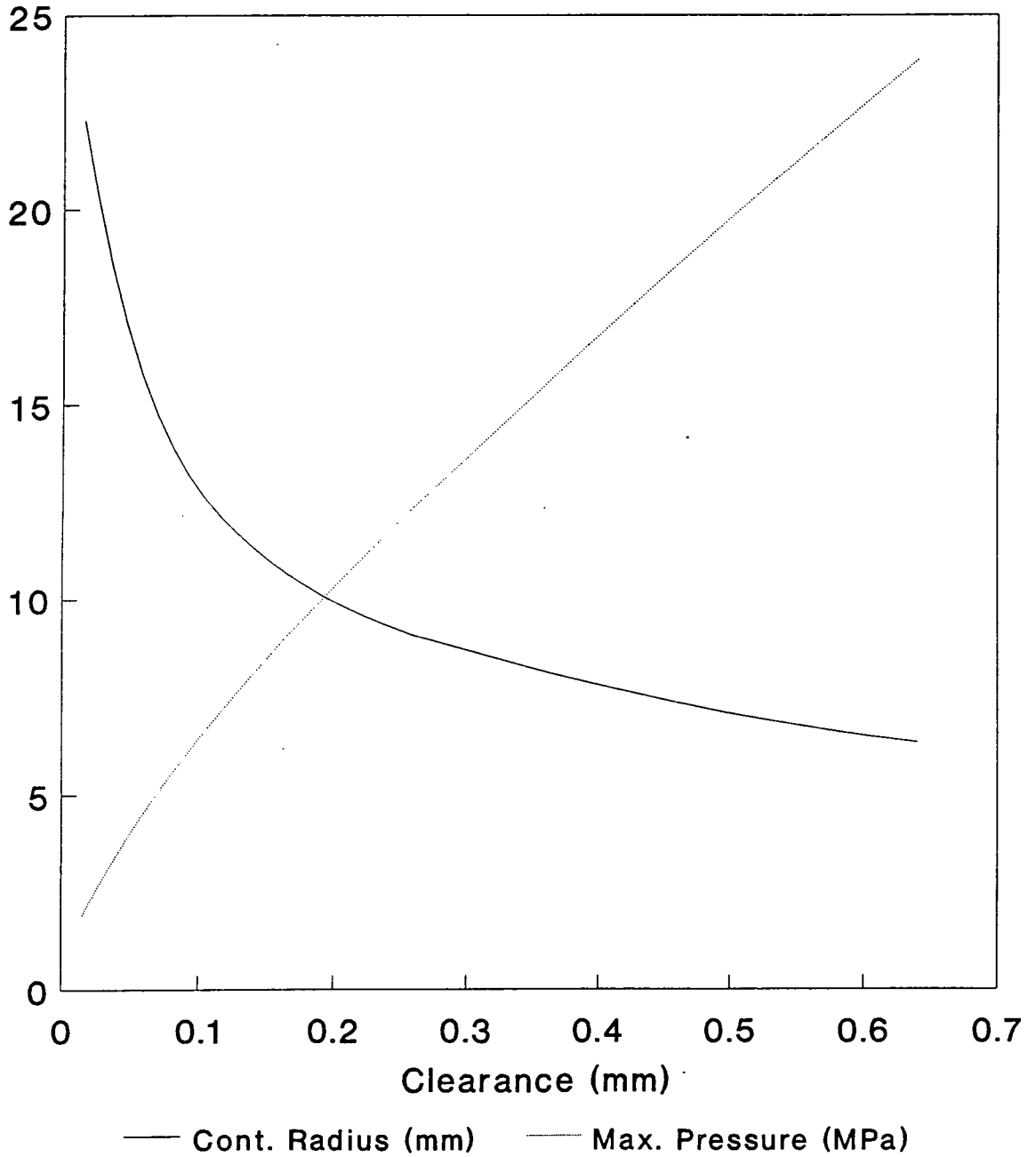


Table 6.1 : The Contact Radii and Pressures Developed under Loading (Maximum Load = 2000N) in a number of Commercial and Experimental Prostheses

	McKee-Farrar (a) Cobalt Chrome Molybdenum Alloy - Both Components	Muller (b) Chrome Cobalt Molybdenum Alloy /UHMWPE	Charnley (c) 316L Steel/ UHMWPE	Durham Soft (d) Layer 316L Steel/ Polyurethane	Natural Synovial Joint (e) Cartilage/ Cartilage
R (Femoral Head)	17.437	16	11	16	23 - 25
Clearance (mm)	0.076	0.25	0.125	0.250	>0.54
R _x (mm)	4118	1024	979	1024	1090
E (MPa)	2.1 x 10 ⁵ /2.1 x 10 ⁵	2.0 x 10 ³ /2.1 x 10 ⁵	2.0 x 10 ³ /2.1 x 10 ⁵	10/2.1 x 10 ⁵	10-100/10-100
ν	0.3/0.3	0.4/0.3	0.4/0.3	0.49/0.30	0.43
E' (MPa)	2.3 x 10 ⁵	4.71 x 10 ³	4.71 x 10 ³	80	24.5 - 245
Contact Radius (mm)	6.186/7.62*	7.58	7.46	33.7 [†]	23.7 - 37.7
Max. Pressure (MPa)	24.95/16.48	16.63	17.14		0.67 - 1.70

a. Data from Unsworth (1978) and contact area analysis using Engineering Blue.

* Two values of contact radius were obtained. The first was found using Hertzian Theory. The second was measured using Engineering Blue. The discrepancy was due to the stress relieved area at the base of the McKee-Farrar Cup, which resulted in the Load distributed around an annulus of internal diameter 8.4mm and external diameter 17.4mm.

b. Dowson *et al* (1991).

c. Dowson *et al* (1991) and measurements made by the Author at Durham.

d. Unsworth *et al* (1987, 1988) and Measurements made by the Author at Durham.

† The value of contact radius is not possible due to the geometry of the acetabular cup. The maximum permissible size would be 25.0mm.

e. Dowson *et al* (1991), Gore *et al* (1981).

contact area should be seen as a movement in the fluid film/mixed transition to lower values of Z ($\eta uR/W$).

6.2.2 Materials and Methods

Cups of UHMWPE were machined from solid using a CNC milling machine. This method of production is used for all commercial hip prostheses as injection moulding of UHMWPE is not possible due to its high viscosity in the liquid state. Initially two cups were produced, which coupled with femoral heads of 15.88mm and 15.48mm diameters gave four radial clearances of 0.125, 0.250, 0.525 and 0.64mm. Following a short study, the components were checked for damage and wear. Pitting was noticed on the 15.48mm ball, which was of tool steel and not 316L stainless steel.

With this problem in mind, thirteen cups were constructed from two UHMW polyethylenes, six from material I and seven from material II. Material I was supplied by Hoechst (GUR 415) and material II was obtained from the production facility at De-Puy (Thackrays). With the thirteen cups the 15.88mm stainless steel femoral head was used throughout to give the range of clearances shown in table 6.2:

Table 6.2

Material I

CUP NUMBER	RADIAL CLEARANCE (mm)
1	0.00
2	0.03
3	0.125
4	0.250
5	0.350
6	0.650

Material II

CUP NUMBER	RADIAL CLEARANCE (mm)
1	0.00
2	0.03
3	0.125
4	0.250
5	0.350
6	0.65
7	1.00

Calculations of the contact radii of the cup and ball combinations were made and showed a range from 4.85-24.94mm as shown in table 6.3, with corresponding maximum pressures from 40.6-1.53MPa. The tensile yield stress of GUR 415 is 21MPa.

Table 6.3

CUP NUMBER	CLEARANCE (mm)	CONTACT RADIUS (mm)	MAXIMUM PRESSURE (MPa)
1	0.00	24.94	1.535
2	0.03	15.29	4.083
3	0.125	9.52	10.54
4	0.250	7.63	16.41
5	0.350	6.82	20.5
6	0.650	5.57	30.8
7	1.000	4.85	40.6

6.2.3 Assessment of Cup Sizes

Although sizing of acetabular cups can be done by direct measurement deformation of the surface can cause inaccuracies. Therefore, casting techniques were used.

Three moulding resins were used to assess the size of the acetabular cups; Silicone (flexible), PMMA (rigid) and Polyester Moulding Resin (rigid). Resins tend to shrink upon curing and this was monitored by moulding 30 and 40mm diameter cylindrical specimens, treated in the same way as the acetabular cups, and with resin poured from the same mix. This allowed a percentage shrinkage to be used to calibrate the results (table 6.4a). The sizes of the cups could then be calculated (table 6.4b).

Table 6.4a

Mould Material	Shrinkage (mm) (30mm sample)	Shrinkage (mm) (40mm sample)	Avg. Shrinkage (%)
Silicone (Mat 1)	0.93	1.01	0.97
Silicone (Mat 2)	0.71	0.98	0.85
PMMA (Mat 1)	1.99	2.43	2.21
PMMA (Mat 2)	2.08	2.75	2.41
Polyester (Mat 1)	1.91	1.58	1.75
Polyester (Mat 2)	1.25	1.78	1.52

Table 6.4b

Cup No.	Silicone (mm)	PMMA (mm)	Polyester (mm)	Required (mm)
(I) 1	31.94	32.23	32.07	31.76
2	31.99	32.41	32.06	31.82
3	32.29	32.40	32.32	32.00
4	32.61	32.79	32.53	32.25
5	32.85	32.91	32.67	32.45
6	33.14	33.51	33.29	33.05
(II) 1	31.83	32.32	31.59	31.76
2	31.86	32.34	31.93	31.82
3	31.93	32.37	31.96	32.00
4	32.14	32.52	32.14	32.25
5	32.39	32.62	32.39	32.45
6	32.58	32.99	32.55	33.05
7	33.17	33.65	33.10	33.76
% Difference	+0.07	+1.10	+0.04	

The results show that the silicone and polyester casting resins can be successfully used to determine the sizes of the cups. The sizes requested by the operator of the CNC machinery can be expected to be accurately reproduced, particularly with regard to the differences between the cups. However, even though the discrepancies are on average 0.04-0.07%, with the tight clearances required for the analysis a more accurate measurement technique would be advantageous, such as a stylus or non-contact system.

The roundness and surface roughness of the cups were checked using a Talyrond. The stylus traced concentric circles on each cup, from the lip to the pole, and the output was analysed. A typical trace is shown in figure 6.5. The out of roundness was $15\mu\text{m}$ and surface roughness was estimated at less than $1\mu\text{m}$ (R_a). These are similar to values for commercial prostheses.

6.2.4 Experimental Contact Area Studies

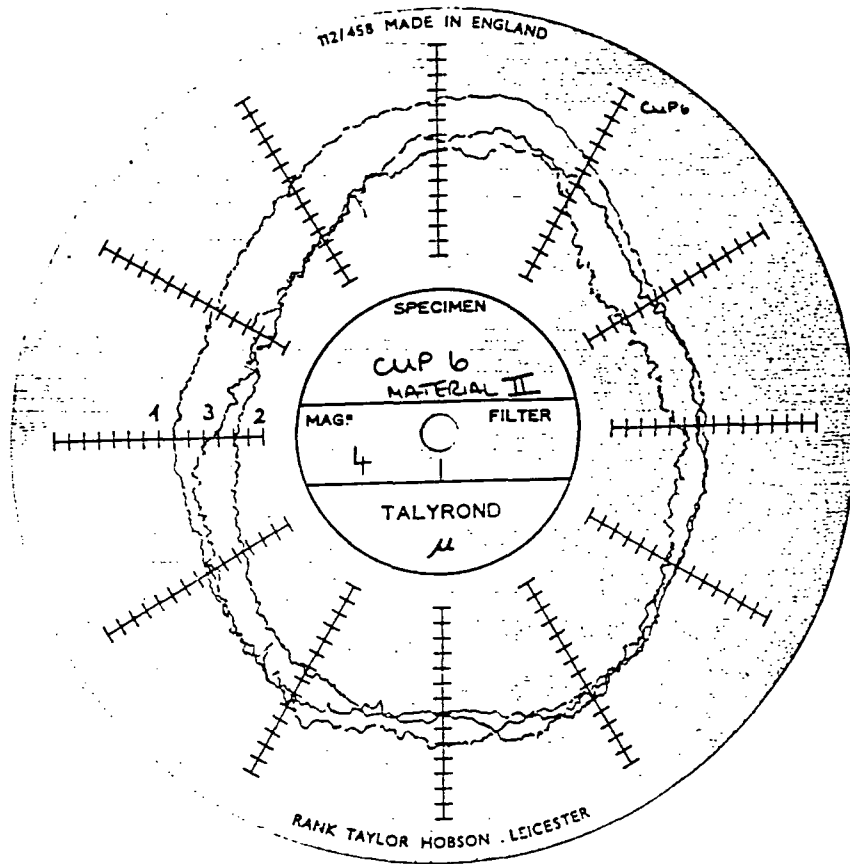
6.2.4.1 Direct Contact Measurement

The transfer of dye between articulating surfaces of human and animal joints has allowed measurement of the load bearing areas (Black *et al*, 1981). Yao and Seedhom (1991) obtained contact areas for flat polyurethane and silicone sheets indented with a stainless steel ball using a carbon black suspension in silicone fluid. This method was attempted without success. However, contacts were visible when engineering blue was used as the dye. The computer controlled Hounsfield testing machine was used to apply loads of 2000N through a 31.76mm diameter stainless steel ball (which acted as the femoral head). A thin layer of blue was applied to the ball and it was loaded at 0.02mm/s into the surface of the acetabular cup. The size of the stained region was measured with vernier callipers. The test was repeated three times with each cup, the dye being removed between tests with acetone.

6.2.4.2 Mouldings and Castings

Casting techniques have been used to measure the load bearing area of the human knee (Walker and Hajek, 1972) and animal joints (Simon, 1970). Unfortunately, in these measurements of contact areas the time under load is important, especially with visco-elastic surfaces such as cartilage. Inaccuracies can be foreseen

Figure 6.5 : Rotary Talysurf Trace for a Polyethylene Cup produced on the CNC Lathe



because this technique requires loaded times at least three orders of magnitude greater than the time under load during the action of walking.

It was decided to undertake a short study to look at the accuracy of the technique for both UHMWPE and polyurethane joints. Loading of the prosthetic assembly with the curing silicone placed between the ball and the cup would produce an annulus of silicone if the load was maintained to the completion of curing. The hole in the centre represents the contact region and the radial clearance of the assembly can be measured from the thickness of the silicone moulding. Dow Corning silicone rubber was mixed with 1% (w/w) of curing agent to facilitate fast curing. The curing time was measured at approximately two hours. The resin was placed in the base of the elastomeric layered cup, following coating of the prosthesis with mould release agent. The ball was then positioned in the cup and the assembly placed between the compression platens of the Lloyd 6000R tensile testing machine. A loading rate of 0.02mm/s was used with the maximum load of 2000N maintained for six hours to allow full curing of the silicone. The silicone moulding was then removed and the central hole measured using vernier callipers.

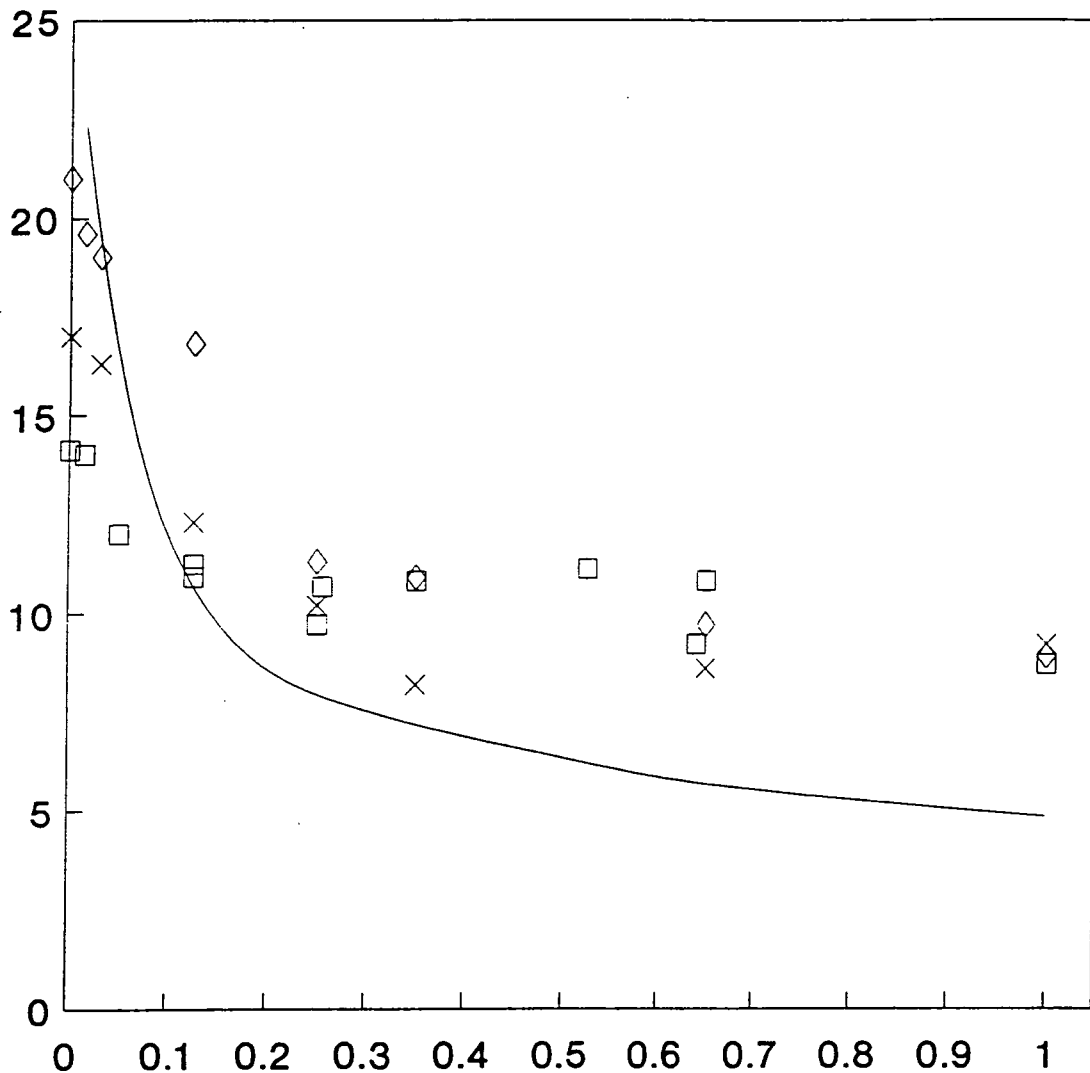
6.2.5 Results

The UHMWPE cups were used to confirm the accuracy of the dye and moulding techniques. Theoretical calculations based on Hertzian theory were made for these cups and the results from the contact radius measured from the silicone mouldings and the dye transfer were compared with these.

The results were displayed in figure 6.6. At higher clearances, above 0.35mm (radial), the values of contact radius measured from the mouldings and dye transfer techniques were greater than the theoretical predictions. However, at closer clearances (below 0.20mm) good correlations were noted. Typical dye impressions

Figure 6.6 : The Effect of Clearance on Contact Radius for UHMWPE Joints incl. experimental results from Dye Transfer and Silicone Mouldings

Contact Radius (mm)



— Cont. Rad. (Theory) □ Dye Transfer
 × Silicone Mouldings ◇ Dye Transfer

and silicone mouldings from UHMWPE cups of varying clearances are shown in figures 6.7 and 6.8. The thicknesses of the mouldings were monitored to indicate the extent of layer deformation under the applied stresses, but deformation of the moulding under measurement precluded any conclusions being drawn.

6.2.6 Discussion

Silicone changes from a medium viscosity liquid to an elastomeric solid during curing. This liquid is much more viscous than the lubricants used in tests on the simulator, which had viscosities typically of 0.010Pa s, and therefore the outflow of silicone from the contact occurred more slowly. This necessitated a longer time under load to mimic *in-vivo* squeeze conditions as well as allowing the silicone rubber to set in situ. This introduced a potential problem with the creep of the polyurethanes under load (in particular the harder grades of Tecoflex) increasing the measured contact area.

The results provided a high degree of compatibility with theoretical values from Hertzian theory in the case of polyethylene cups. The results from both techniques were very similar indicating that the two possible inaccuracies with the moulding technique (detailed above) were relatively insignificant. At large clearances the results from both dye transfer and mouldings were 30-70% higher than the theoretical analysis. This may have been due to the UHMWPE yielding under the high stresses (table 6.3) and forming a larger contact. At small clearances (less than 0.07mm) the experimental results gave lower values for the contact radius than theory, with 15% being typical.

These methods of measurement of the contact radius for artificial hip joints seemed to indicate sensible values. The close correlation between calculated and measured values indicated the application of these techniques to materials which cannot be explained by simple Hertzian theory, allowing soft layer joints to be investigated.

Figure 6.7 : Typical Dyed Regions from Loaded Prosthetic Devices



Figure 6.8 : Typical Silicone Rubber Mouldings from Loaded Prosthetic Devices



6.3 Contact Analysis of Soft Layer Prostheses

6.3.1 Introduction

From the theory introduced earlier in this Chapter the effective elastic modulus of a joint system and its contact radius may be calculated if a Hertzian contact is present. Unsworth *et al* (1987) discovered that grabbing of the soft layer onto the ball occurred at radial clearances of 0.125mm under a maximum load of 2000N but not with clearances of 0.250mm. These values give an equivalent radius, R_x , of 1024mm. This larger clearance has been adopted as that most commonly used in the experimental prostheses. Although the elastic modulus of the bio-compatible polyurethanes in the laboratory is circa. 10MPa, *in-vitro* this dropped to circa. 5MPa (Chapter 3). The effective modulus of the joint assuming a Hertzian contact (E') can be calculated as 15MPa from equation 6.3, which forms a contact radius of 51.2mm (equation 6.2), which is clearly too large. Measurements of hardness from strip and cup samples of identical polyurethanes indicated significant increases in the elastic modulus of the 2mm layer on a rigid backing, up to 20MPa (from Waters', 1965), and a further increase to 26MPa when bonded (sections 2.6 and 2.7). The effective modulus, E' , increases to 50-80MPa, which results in a contact radius of 29.5-34.5mm. These values are larger than the quarter circumference of the femoral head (25mm), which represents the maximum possible size of the contact radius. Therefore, the radius predicted by the ball-on-plate model and Hertzian/layered theory cannot be accurate and other methods must be used.

6.3.2 Materials and Methods

The experimental methods which provided accurate correlation with theory for UHMWPE cups were investigated for the soft layers to determine the contact region of the joints. All of the tests were conducted in the same way, although the loading rates

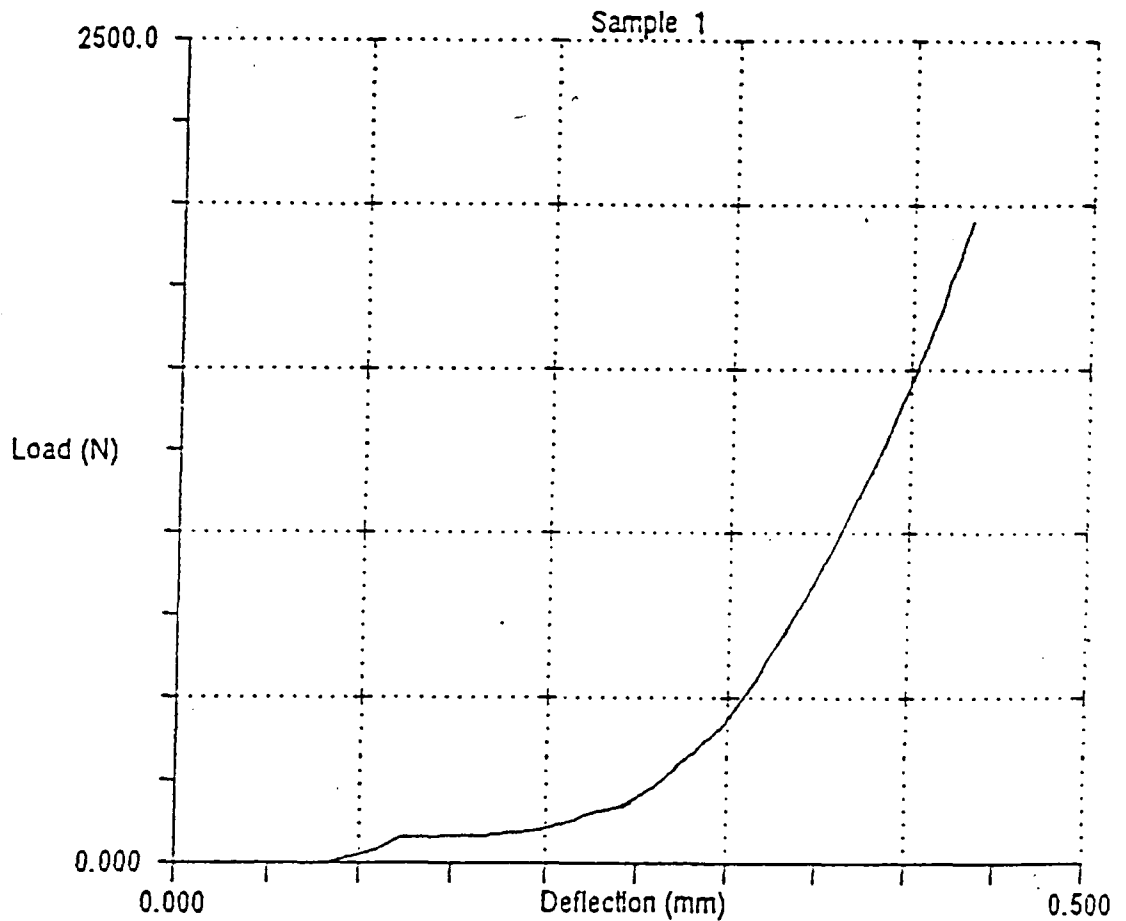
were increased to 0.08mm/s throughout to take account of the increased indenter penetration.

The Lloyd 6000R tensile testing machine was used to load a 31.76 mm ball into the metal backed polyurethane cups. These cups had been previously tested for hardness (H20/30 DIN 53456) and tribological properties in the hip function simulator and had shown excellent properties. Three samples each of Tecoflex 85^oA, Tecoflex 93^oA and Pellethane 80^oA were investigated. The internal diameter of the cups was nominally 32.26 +/- 0.010mm giving a radial clearance of 0.250 +/- 0.05mm. The cups were soaked for 24 hours in Mammalian Ringers' solution prior to testing and the temperature controlled cabinet was used during testing, maintained at 37°C throughout.

6.3.3 Results

A typical load/penetration curve is shown in figure 6.9a. This was for a 2mm thick layer of Tecoflex 85^oA. Values of penetration for the Pellethane, Estane and Tecoflex 85 and 93^oA polyurethane layers ranged from 0.250-0.350mm. This was determined from the increase in displacement from a holding load of 200N up to the maximum of 2000N. These values compare with penetrations of 0.22-0.30mm during the DIN 53456 hardness test (H20/30). Contact radii and maximum generated pressures are shown graphically against penetration (figure 6.9b). It can be seen that over this range of penetrations, contact areas increase from 16 to 18mm, with maximum pressures of 3.0MPa under a load of 2000N, which corresponds to physiological values. Values of contact radii obtained from the dye transfer and silicone mouldings are also shown. Both techniques agree well with the penetration studies, although radii are about 10% below those from the theoretical analysis. Penetrations for the 100^oA grade of Tecoflex were also measured, but were much lower (0.11mm), with contact radii of 10.7mm. This corresponds to contact pressures

Figure 6.9a : A typical load/penetration curve for a 2mm thick layer of Tecoflex EG85°A bonded to a steel cup



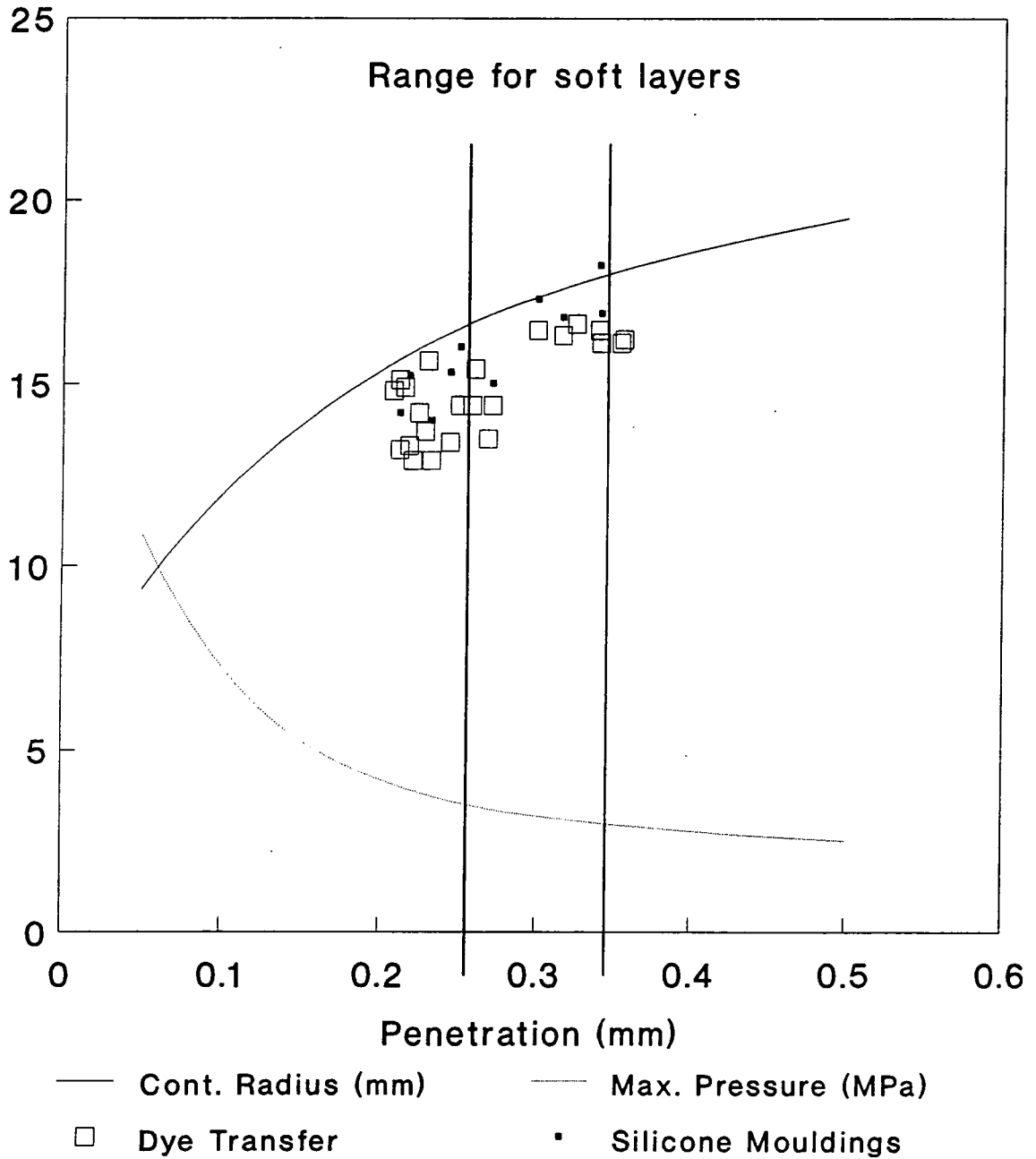
COMPRESSIVE TESTING OF PU CUPS

Operator : J.M.Blamey
 Description : 31.76mm Ball
 Temperature : 20.00 C
 Date : Wed 24 Apr 1991

	Extn 20N (mm)	Extn 100N (mm)	Max Load (N)	Extn 200N (mm)	Extn 300N (mm)	Extn 2000N (mm)
Sample 1	0.097	0.136	2010.0	0.249	0.274	0.436

Figure 6.9b : Geometric Calculations of Contact Area and Pressure for Soft Layers from Penetration Studies, with the results of Dye Transfer and Silicone Mouldings included

Pressure (MPa)/Contact Radius (mm)



at the centre of about 8.0MPa. This seems to be the limit of pressure which can be maintained by the lubrication mechanisms under the dynamic loading applied during walking (section 6.5). However, this information is useful as it can help to determine the film thickness required for film separation and an indication of the micro-EHL (asperity flattening) effect.

6.3.4 Discussion

Penetration of an indenter into the surface should give an accurate indication of the contact region. One slight discrepancy may have been due to bulging at the edge of the contact. This is caused by the loading profile and geometry.

The transfer of dye produced excellent correlation with the penetration studies, and the regions were easier to measure on the polyurethane cups compared with the UHMW polyethylene acetabular components.

The thickness of the dye layer on the ball surface could not be measured. The layer of dye would tend to make this technique under-estimate the actual contact area. Good reproducibility with this technique, even though the quantity of dye applied to the ball could not be standardised, indicated the effect of the dye layer to be small.

The silicone moulding also showed good correlation with the other two techniques, although there were a number of initial reservations. Polyurethanes show a degree of visco-elastic behaviour which can result in creep and material flow away from the contact region. With the loading applied for up to six hours to allow full curing of the silicone, compared with approximately 0.5 seconds under maximum load in the simulator, creep could lead to increases in the area of contact.

If clearances of these joints are to be optimised for the best tribological properties then the deformed shape of the layers must be accurately known. This may indicate that smaller clearances (circa. 0.150mm) may be successfully used without incurring grabbing. Sectioning of the silicone mouldings was performed, but accurate measurements of the deformation of the layer outside the contact were not possible due to the compliant nature of the silicone.

6.4 Tribological Studies of UHMWPE/Stainless Steel Joints

6.4.1 The Effect of Clearance and Material on Friction Factor

6.4.1.1 Materials and Methods

The joints which had been used in the study on the effects of clearance on contact area were again used. The cups were tested in the hip function simulator using loading cycle I (figure 5.25a). The range of lubricant viscosities was 0.011-0.250Pa s with the CMC water based fluids, and 0.100-30.00Pa s with the silicone lubricants (measured at 3000s⁻¹). Tests were also performed dry. A typical value for arthritic synovial fluid is 0.011Pa s (section 4.2.7), which is at the lower end of the range investigated.

6.4.1.2 Results

Stribeck plots were constructed and the results of the experimental prostheses compared. Figures 6.10 and 6.11 show the results of all of the joints with each point plotted. As the clearance of the joint was reduced the friction factor also decreased. At very small clearances the friction factor rose slightly. Testing with silicone fluids gave much lower frictional torques than with CMC fluids. The values with the silicone fluids seemed artificially low, with friction factors of 0.005-0.008 with the 0.010Pa s silicone fluid. A similar viscosity CMC fluid (at a shear rate of 3000s⁻¹) resulted in friction factors of 0.025-0.050. This suggested the transference of a

Figure 6.10 : Stribeck Plots for UHMWPE Joints (Material I)
of different Clearances

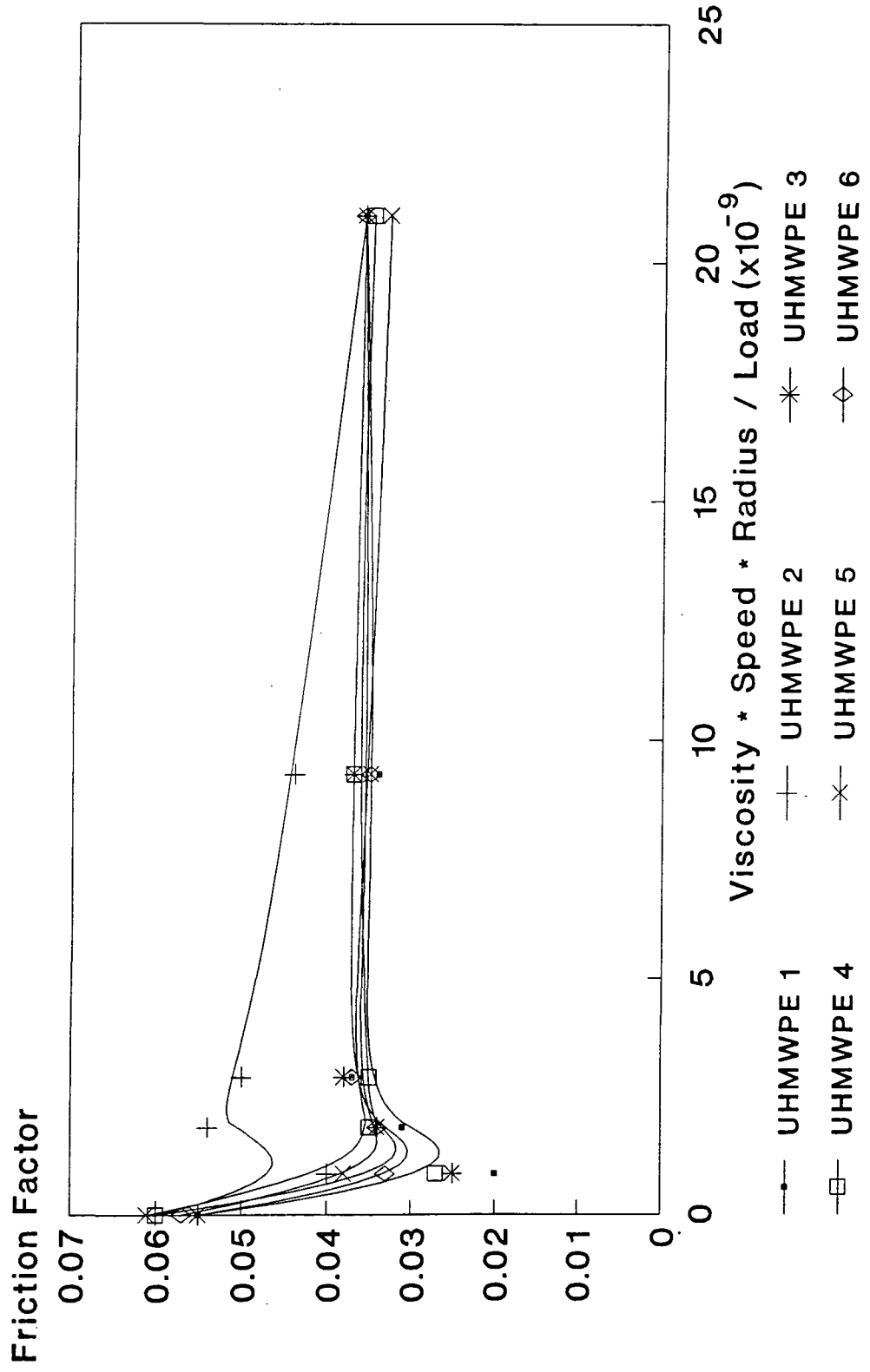
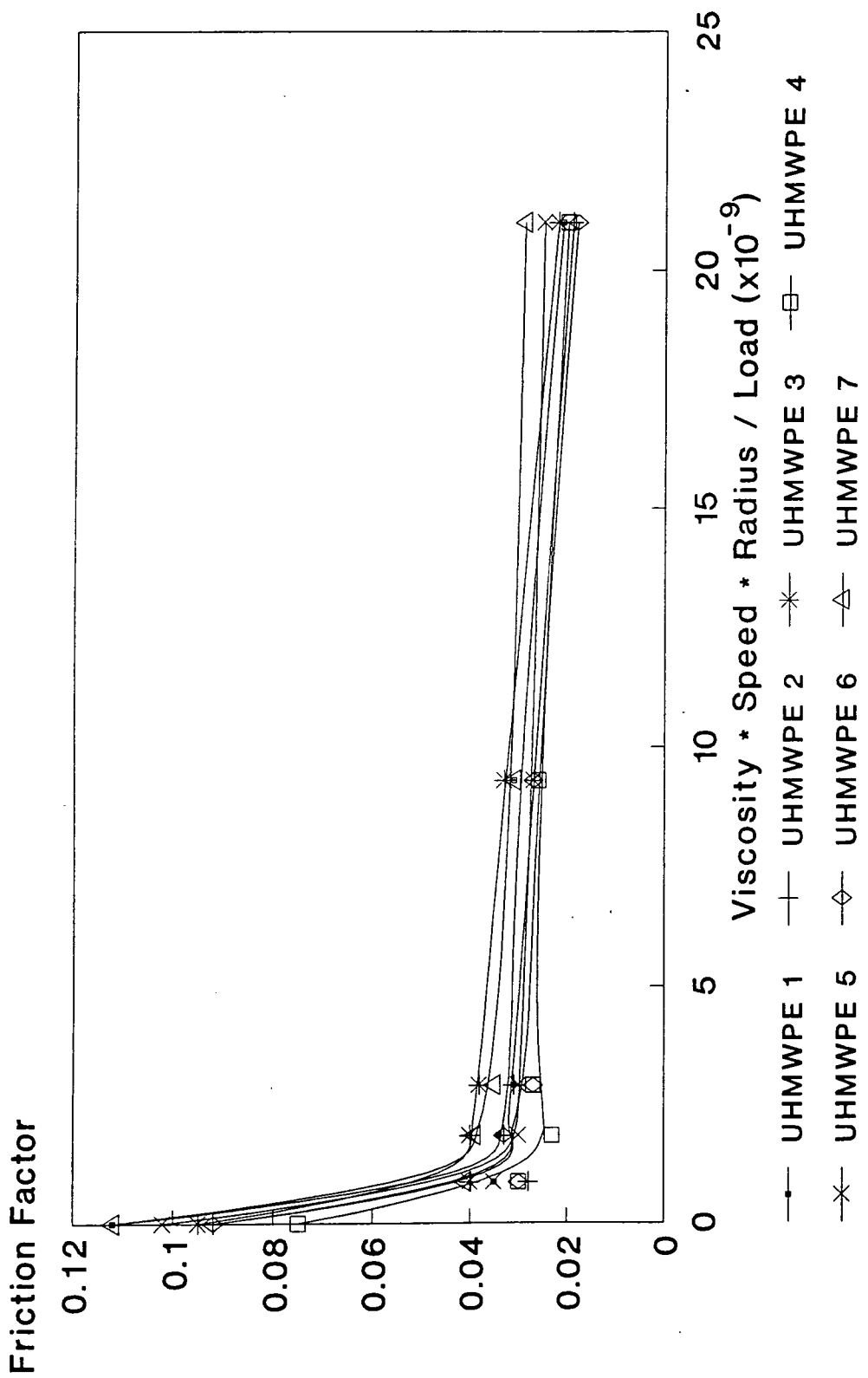


Figure 6.11: Stribeck Plots for UHMWPE Joints (Material II)
of different Clearances



silicone based boundary lubricant to the polyethylene cup. This meant that CMC and silicone fluids could not be used together in the construction of a representative Stribeck plot. Although there was a small decrease in friction with decreasing clearances, this was much smaller than had been measured in earlier studies, the results of which are shown in Appendix IV.

6.4.1.3 Discussion

Charnley suggested that the use of a small diameter joint would reduce the frictional torque developed in the prosthesis due to the shorter lever arm. He neglected the fact that the use of a smaller joint would result in a smaller contact radius to carry the load (if the radial clearance were constant) and thus increase the pressures over this region. This should make little difference to dry rubbing, where Coulomb theory suggests that the coefficient of friction is independent of the apparent contact area as the real contact at the asperity peaks will remain the same. However, lubricated contacts are different. In particular fluid film lubrication is encouraged by lower contact pressures (Chapter 4) which can be obtained by the promotion of a large area of contact.

The study showed no conclusive proof of this, although initial pilot studies had suggested a decrease in friction for low clearance joints. It is possible that with tight clearances the improvement in the lubrication mechanisms is counteracted by deformation of the UHMWPE grabbing the femoral head (in a similar way to 0.125mm radial clearance polyurethane joints) resulting in increased pressures and breakdown of the fluid film. All of the joints showed falling friction factors as the value of the Z term (viscosity x speed x radius / load) increased, representative of mixed lubrication. This indicated that large contact areas (low contact pressures) do not guarantee low friction. Joints of Tecoflex 100^oA, which had contact radii of

10.8mm (slightly larger than a standard Charnley prosthesis), developed fluid film lubrication in many cases with low viscosity lubricants (0.005Pa s). The UHMWPE joints were not able to perform so successfully, even when contact radii were increased to 20mm. This encourages the view that micro-EHL is an important mechanism and the deformation of the surface asperities (likely in polyurethane joints but not with UHMWPE) seems paramount to successful operation.

6.4.2 Investigation of New and Explanted Charnley Prostheses

6.4.2.1 Introduction

A preliminary study of the frictional and hardness properties of Charnley arthroplasties was carried out to evaluate the variation in these properties with time of implantation in the body. Measurements of the dimensions of the articulating surfaces of the femoral and acetabular components were also made to check for possible component mismatches. Visible surface defects were investigated to see if they were responsible for the behaviour of the joints.

The Hip Function Simulator was used to test two explanted joints. Both prostheses had been implanted in patients in their late sixties (one male and one female) and both were removed because of component loosening. The results from these joints were compared with those obtained from a new Charnley prosthesis and one which had been used in the laboratory only.

6.4.2.2 Materials and Methods

The acetabular components of the Charnley prostheses were of ultra high molecular weight polyethylene (UHMWPE) and of nominal internal diameter 22.25mm. The femoral components consisted of a one piece stainless steel stem and

ball with the articulating surface having a diameter of 22mm, giving a radial clearance of 0.125mm.

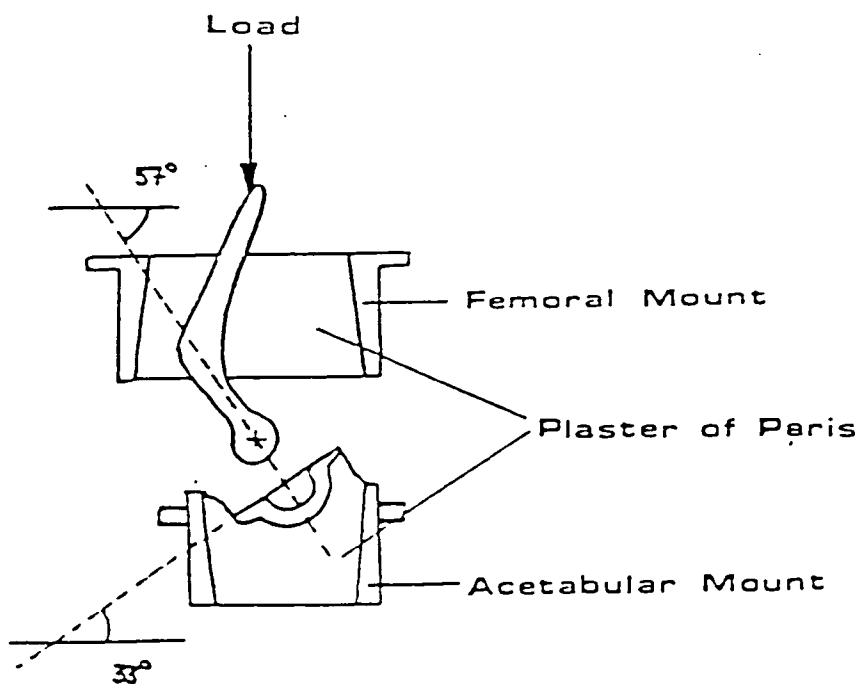
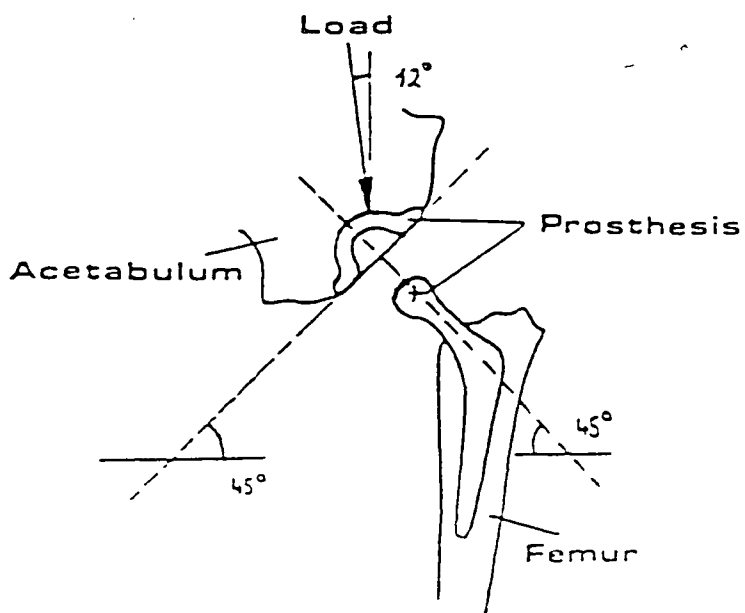
The joints were soaked in a 10% Gigasept solution for 12 hours prior to testing to reduce the risk of infection. As the effects of the disinfectant on the properties of the joints were unknown, all of the joints underwent this treatment.

The components were mounted in plaster of Paris so that their relative positions were the same as when cemented in the body (figure 6.12). They were then placed in the hip function simulator. Peak loads were set to a value of 2000N (approximately 3 times body weight) and a minor load of 20N was used. The data was then used to produce Stribeck plots.

Each of the prostheses was tested with a range of lubricant viscosities, from 0.0033 to 0.065Pa s in addition to a test under dry conditions. This range of viscosities covered the physiological and pathological ranges. The frictional results from each prosthesis were taken on the 21st cycle when the machine and joint had settled down to steady state operation.

Hardness measurements were also made on the two explanted acetabular cups and the unused cup. These tests were performed on the Charnley acetabular components to investigate whether the UHMWPE had degraded or been mechanically damaged during implantation. A ball diameter of 5mm was used with a holding load of 10N and a maximum load of 142.5N. The loads were held for 5 and 30 seconds respectively and the values of hardness for the cups were calculated from DIN 53456. For each of the cups an average was taken of at least six readings.

Figure 6.12 : The angular relationship of the components of the Charnley Arthroplasty in the body and the simulator



The sizes of the femoral heads and acetabular cups were also measured using vernier callipers. This was to check for grabbing of the ball by the cup which can result in drastically increased friction of the joint.

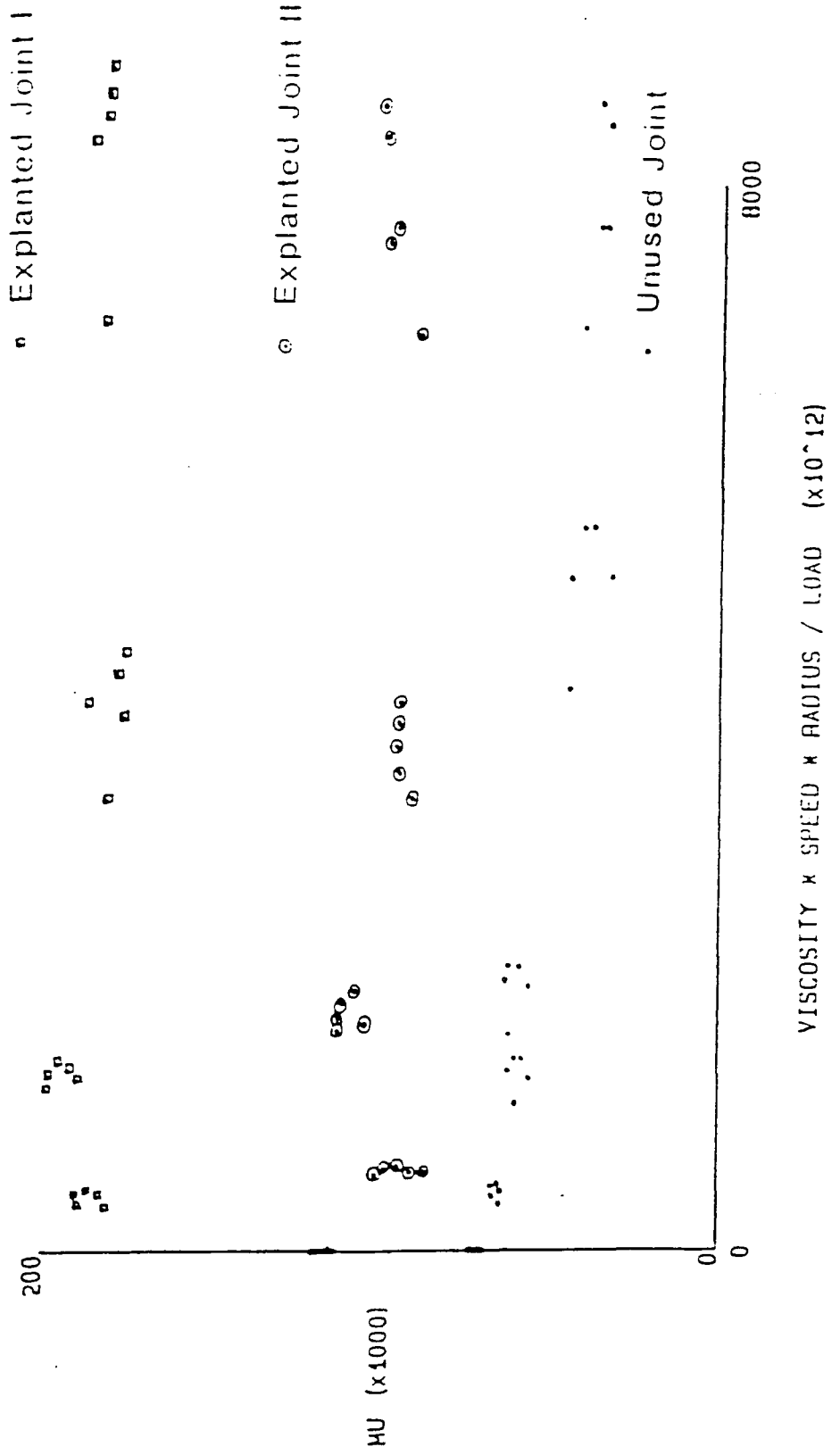
6.4.2.3 Results

The first explanted joint (I) showed a very high frictional torque leading to an average friction factor of 0.32 when dry. This value decreased whilst lubricated to 0.20 and was almost independent of the fluid viscosity used (figure 6.13). The second explanted joint (II) revealed a friction factor of 0.067 when dry and similar values were obtained over the range of lubricating fluid viscosities used. The unused Charnley prosthesis (III) showed a friction factor of 0.050 when dry which decreased as fluids of higher viscosities were used to lubricate the joint. A friction factor of 0.040 was obtained with a viscosity of 0.065Pa s.

Following the very high values of friction in the first explanted cup, an investigation was made to ascertain whether the high friction was due to the femoral or acetabular component of the prosthesis or whether it was a combination of the two. Tests on a fairly new femoral head articulating in the first explanted cup showed a friction factor of 0.21 when dry and 0.19 when lubricated over the range of lubricants used. These values were almost as high as those obtained with the complete explanted prosthesis suggesting that the acetabular component was responsible for the high frictional forces developed.

However, when the same femoral head was used against a brand new cup supplied by Thackrays, the results showed friction which was half the previous value during dry running in the simulator; (coefficient of 0.11) and much lower values when lubricated, with coefficients between 0.050 and 0.040.

Figure 6.13 : Stribeck Plot of Explanted and Unused Charnley Prostheses



Measurements of the sizes of the femoral heads and acetabular cup's internal diameter were made to check the clearance between the components and any out of roundness of the UHMWPE component (table 6.4). As expected the diameters of the femoral heads were similar indicating that very little wear of the metal had occurred. However, the acetabular component of explanted joint I (which showed high friction) seemed to be smaller than the unused cup. This may have led to grabbing between the ball and cup during loaded articulation and hence the high friction. The acetabular component of explanted joint II was measured to be much larger than the unused devices. Estimations regarding the depth of the cup showed that wear debris resulting in penetration to a depth of about 1.0mm had been produced during *in-vivo* operation. This resulted in the centre of rotation of the joint moving medially and towards the superior surface. Hardness measurements were also made for the three UHMWPE cups. The results are shown in table 6.5.

Table 6.4

Joint	Femoral Head (mm)	Acetabular Cup A/P (mm)	Acetabular Cup M/L (mm)
Exp. I	22.07	22.23	22.34
Exp. 2	22.09	23.12	24.15
Unused	22.10	22.33	22.45

Table 6.5

Joint	Hardness (N/mm²)
Explanted Joint I	55.0
Explanted Joint II	75.4
Unused Joint	55.9

These values indicate that work hardening may have occurred in Joint II due to the excessive wear and socket migration which was visible on inspection. However, the measurements did not reveal why explanted joint I showed such high friction.

6.4.3 Conclusions

Improving the tribological properties of the currently implanted prostheses, which rely on mixed lubrication when in the body, appears to be possible by increasing the area of contact of the articulating surfaces. A reduced pressure at this interface improves the performance of Squeeze and EHL, which lowers friction by relying less on boundary lubrication and dry rubbing. As the contact area is increased there does appear to be a movement towards fluid film lubrication, which would significantly reduce surface wear. The reduction in wear debris and frictional torque as a result of this, should improve the life of the articulating surfaces of the prosthesis as well as reducing instances of giant cell formation and resorption of bone. These phenomena can lead to loosening and subsequent failure of the joint and hence the need for revision. This is a costly, traumatic and complicated operation and accounted for 20% of hip surgery as early as 1981 (Stinson and Scheller, 1983).

The first explanted joint clearly had considerably increased friction over the new joint. This seemed to be predominantly caused by changes in the UHMWPE component with only a small detriment due to the femoral component. The measurements of hardness showed little change *in-vivo*, but the size of the articulating surface of the cup indicated the possibility of grabbing. It seems that the clearance between the two components is very important for low friction operation. The results from the second explanted joint revealed that good frictional results may be obtained from a visibly worn and damaged acetabular component and also showed that the hardness of the UHMWPE may change through *in-vivo* loading and wear. However,

accurate data on the hardness of the manufactured joint surface prior to implantation would be required to substantiate the theory of work hardening *in-vivo*.

6.5 Tribological Studies of Soft Layer Prostheses

6.5.1 Introduction

In order to obtain an accurate view of the behaviour of the elastomeric joints, comparisons were made between the currently available prostheses and the soft layer devices. Theoretical studies of film thickness were made in conjunction with experimental studies in the hip function simulator, measuring frictional torque in order to determine the operating mode of lubrication.

6.5.2 Materials and Methods

Four bio-compatible polyurethanes were used for the tribological assessments, Estane 57 and 58, Tecoflex EG (80-100°A) and Pellethane 80°A. Previous work by Unsworth *et al* (1987,1988) had concentrated on non-implantable cast systems, to allow a range of hardness values of one base material to be investigated. Conclusions of this work were that hardness values of 4-8N/mm² (H20/30) produced the best tribological performance. Elastomers with estimated hardness values in this range were used.

Detailed assessment of the chemical structure of the polyurethanes appears in Chapter 3. The samples were prepared by vacuum moulding at temperatures up to 185°C from granules of the polymer. A stainless steel backing was used with bonding obtained through mechanical interlock, with the polymer extruding into holes in the backing during moulding. Traces of the mould release agent were removed by washing to eliminate the hydrophobic surface which interfered with lubrication. Following cleaning, the layers were tested for hardness as is detailed in Chapter 3. They were then placed in a holder which was positioned in the friction carriage of the simulator. A maximum load of 2000N was applied, with a minimum load of 20N. Data was

recorded on the 1st, 21st & 41st cycles to show start-up conditions and the frictional torque once steady state conditions had been reached.

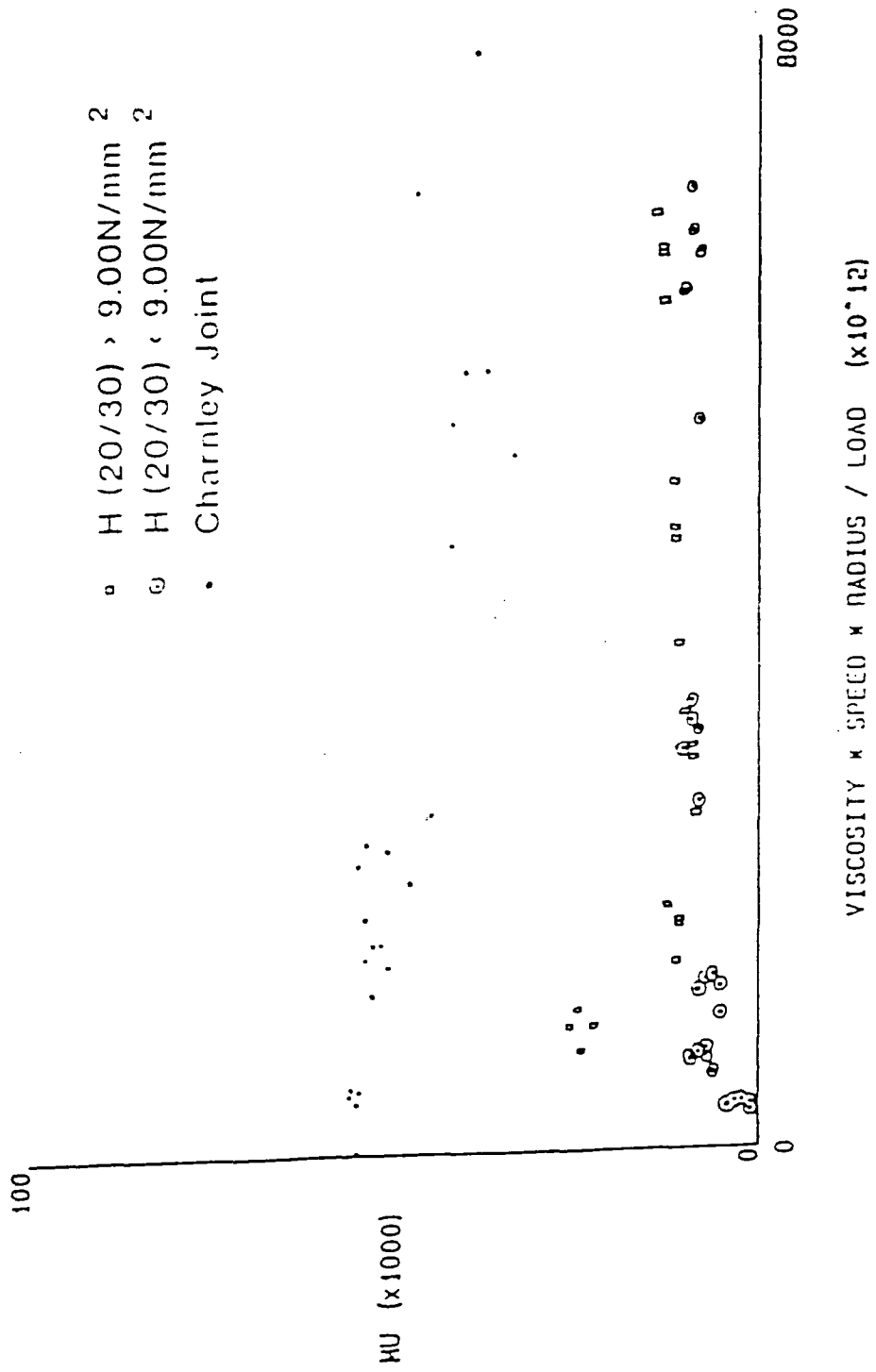
UHMWPE cups of identical internal dimensions were prepared in the CNC lathe to allow for direct comparisons with the soft layers. Lubricants of viscosities between 0.005 and 0.065Pa s were used for the studies. This was to allow Stribeck plots to be obtained, which help to determine the mode of lubrication operating. Conditions in the body, especially when rheumatoid or osteo-arthritic conditions prevail are likely to be at the left hand side of the plot (Chapter 4).

6.5.3 Results

Hardness measurements of all of the polyurethane layers were encouraging. Estane '57' typically gave values of 4.8N/mm², with slightly higher values of 5.2N/mm² for Estane '58'. Pellethane which was designated 80°A on the shore hardness scale typically produced layers of 5.2N/mm² on the DIN scale. The tecoflex polymers were softer when measured using the DIN scale than their designated shore hardness values indicated. Tecoflex 85°A gave layers of 3.8N/mm², with the 93°A grade producing layers of about 6.0N/mm² and the 100°A material at 9-10N/mm².

Stribeck plots for each of the polyurethanes were produced and for simplification the upper and lower ranges only were plotted (figure 6.14). Aside from layers of Tecoflex 100°A, they all showed very low coefficients of friction with a rising tendency as the lubricant viscosity was increased. This suggests that fluid film lubrication was present throughout the range of lubricants for each of the bio-compatible polymers. Tecoflex 100°A, which produced the hardest layers showed a Stribeck plot which decreased to a minimum and the rose as the lubricant viscosity was increased.

Figure 6.14 : Stribeck plots for a soft layer joint of hardness $< 9.0\text{N/mm}^2$
 a soft layer joint of hardness $> 9.0\text{N/mm}^2$ and a Charnley Joint



This shows that mixed lubrication was occurring at low viscosities, which became fluid film as more viscous lubricants were used.

The comparative graph for the model of the Charnley prosthesis, which used an UHMWPE cup, showed much higher friction (figure 6.14) and a falling tendency on the Stribeck curve as viscosity was increased. This suggested that a mixed regime was operating (comprising boundary and fluid film lubrication). Fluid film lubrication is likely at very high viscosities, but frictional torque will not be as low as that obtained with the soft layers because of the greater resistance to shear of the lubricant. In addition the fluids present in the body, especially in diseased joints, are not sufficiently viscous to allow this to happen.

Over the course of the study many tests on the soft layers were done in the simulator and so all the tests for each polymer were collated. In this way it was expected that the effect of hardness on frictional torque and the differences in the tribological properties of the polyurethanes could be investigated.

6.5.4 Discussion

The results from the theoretical analysis for the soft layered joints indicated fluid film lubrication over the range of fluid viscosities. This was also indicated from the Stribeck curves produced from experimental studies in the simulator. The presence of a film of lubricant thick enough to separate the articulating surfaces completely, could almost eliminate wear of the prosthesis. In the past, attempts have been made to measure fluid film thicknesses by direct means. Methods involving electrical resistance and interference caused by the film (Olgar and Tarallaey, 1987), have proved how difficult it is to measure this quantity and results have been inconsistent (section 4.2.6)

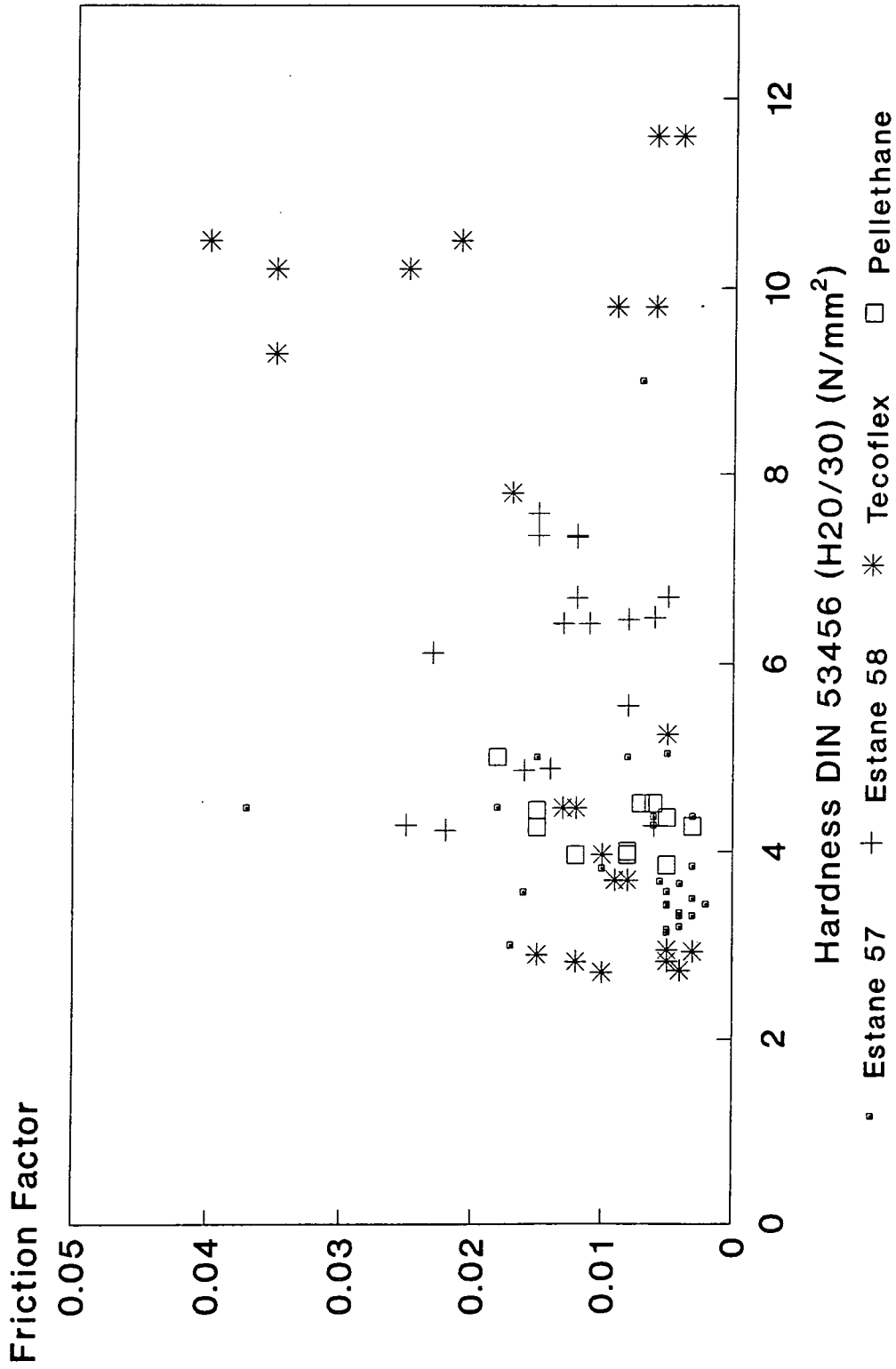
and only qualitative results have been attained (section 6.7). However, this would be the ultimate conclusion to soft layer work.

Collation of the large number of results which have been produced over the course of the study indicated that hardnesses as low as 3.5N/mm^2 and as high as 11.2N/mm^2 could produce low values of friction factor (less than 0.010) with $0.010\text{Pa}\cdot\text{s}$ lubricant (viscosity measured at a shear rate of 3000s^{-1}) (figure 6.15). These results do not seem to be dependent on the polyurethane used, with results from Estane '57', '58', Pellethane and Tecoflex displayed.

However, the preparation of a layer with a hardness value within these extremes does not guarantee very low frictional torques. Other variables encountered during the production of the layers are also important. All of the polymers investigated were successful in producing layers with low friction factors. Processing difficulties and the presence of bubbles in a large number of the Estane '57' and '58' layers indicated that these polymers may not be a wise choice. However, incorrect processing temperatures could be a cause of this even though care was taken to use the lowest possible temperatures to reduce the thermal history of the samples. The Estane polymers may be more susceptible to this form of degradation.

Contact angles of the aqueous lubricants on the surface of the layers were not measured accurately, but visibly little difference between the polymers could be noticed. If a layer of mould release was allowed to remain on the articulating surface of the polyurethane, the hydrophobicity of the layer increased. This was seen as the inability of the lubricant to wet out the surface. Higher values of friction factor (increasing by about 0.010) were noted for two or three cycles until the mould release had been removed by the articulation of the head.

Figure 6.15 : The Friction Factor for Soft Layer Joints with 10cP Lubricant



Grabbing of the layers was originally thought to be a potential problem due to the large deformations expected in the layers. This was only noted when small clearances were used, less than about 0.250mm radially, but the increase in friction could be many orders of magnitude. During production of the layers a large amount of shrinkage was noted with all of the urethanes formed from granules, necessitating a mould former diameter of 32.76mm to produce cups with internal diameters of 32.25 +/- 0.10mm. Measurements of clearances as small as 0.250mm was not easy due the compliant nature of one of the surfaces, unless some sort of secondary mould was used (sections 6.2 and 6.3). Therefore a smaller femoral head was made to reduce grabbing if it were discovered to be a problem. Frictional results did vary when using this head. A lowering of the friction factor indicated some instances of grabbing had been occurring, whilst an increase showed that a radial clearance close to the target value of 0.250mm had been obtained.

The polyethylene cups, although showing higher coefficients of friction of 0.04 and 0.05 were more consistent tribologically, with differences of less than 10% for similarly made joints. However, changes in the properties of these joints whilst in the body were noted (section 6.4.2).

6.5.5 Conclusions

All of the polyurethanes produced fluid film lubrication in a number of samples. The difference in the consistency of results between polyurethanes is likely to be due to the preparation of the samples. Certainly the Tecoflex and Pellethane polymers seemed easier to process without bubbles. However, on tribological properties alone, all of the elastomers showed promise. Degradation and fatigue response will be instrumental in the final choice.

6.6 Theoretical Calculations of Lubrication Film Thickness

6.6.1 Introduction

The use of theoretical analysis in the hip joint is a complicated process owing to the dynamic loads and varying accelerations applied to the surfaces. Simplifications were made and in this analysis Squeeze Film effects only were investigated. The model has some capability for the incorporation of EHL, but for simplicity this was ignored. This was due to the difficulty in assessing the EHL effect because of a reduction in the velocity gradient, because of the thicker films present due to squeeze action. Theoretical analysis of EHL (Hamrock and Dowson, 1977; Dowson and Yao, 1991) was based on the assumption that loading and motion is constant. The change in the loading, which introduces squeeze film effects, will alter the film thickness value calculated from the EHL analysis because of the reduction in the velocity gradient ($\delta u/\delta h$) across the film thickness. The velocity gradient which appears in Reynolds' equation determines the load carrying capacity of the system and so cyclic loading would require a complicated iterative process to determine the film thickness accurately.

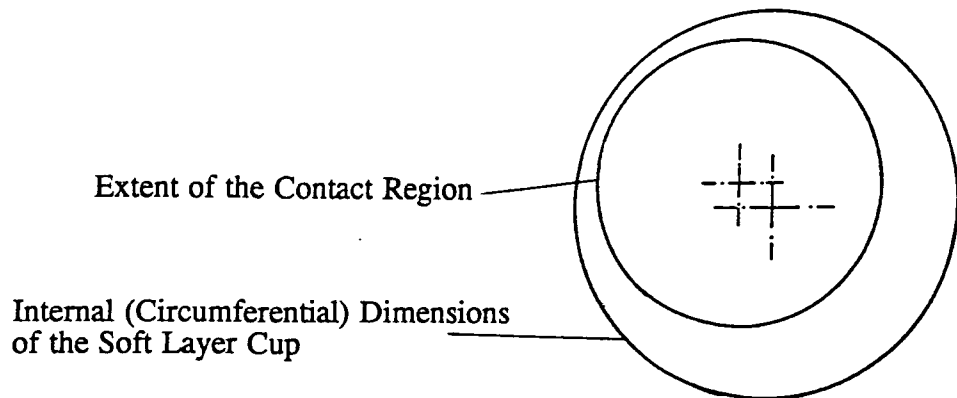
Studies by Medley *et al* (1984) on the ankle joint indicated that the fluctuations in the fluid film thickness during the loading cycle were small after a number of cycles. The assumptions of small film thickness variations would make it a simple process to incorporate some EHL effects. However, incorporation of recent theoretical work done at Leeds (Jin, 1992) may enable the Squeeze and EHL Mechanisms to be combined in this problem.

Micro-EHL effects were not incorporated into the analysis. These effects were seen to be important following experimental measurements of frictional torque with polyurethane and UHMW polyethylene joints of similar contact pressures.

A deformed sphere-on-plate analysis was conducted. The elastic modulus for the soft layers was calculated from the contact region (see section 6.3) using equation 6.2. A value of 350MPa was obtained. This indicated the importance of the backing material and the high Poisson's ratio coupled with the high conformity of the joint, as this value is closer to the bulk modulus (circa. 1500MPa) (Strozzi, 1992) than the elastic modulus (circa. 5-15MPa). For the UHMWPE joints an elastic modulus of 2000MPa was used.

Equation 4.9 was used as the basis for the analysis, with film thickness values calculated at 128 points in each loading cycle. Two loading cycles were considered (figures 5.25a and 5.26b respectively). Loading cycle I was a simplified cycle used for much of the experimental work in the hip function simulator, with maxima/minima of 2000/20. The other loading cycle was derived from Paul (1967) and applied the resultant of the forces during walking. One important consideration was to confirm the shape of the contact as being circular. With soft layer prostheses the contact region is larger than the commercial UHMW polyethylene joints and there was a possibility that the region would extend to the rim of the cup. Figure 5.26c shows the angle of the resultant force, and hence the centre of the contact from the pole. The maximum extremity of the contact will occur at the second peak of the cycle under loads of circa. 2700N. The contact radius increased with load from 15.6-18.0mm at 2000N to 16.8-19.1mm at 3000N (section 6.3). The largest value was used to plot the extent of the contact and its proximity to the edge of the cup can be clearly seen (figure 6.16). This may introduce changes to the shape of the contact in heavier patients, but for this analysis the contact was treated as circular. However, the proximity of the edge of the contact, the region of maximum shear stress, to the edge of the cup may lead to crack propagation. Further stress analysis of the cup would be advantageous.

Figure 6.16 : Proximity of the Contact Region of Soft Layer Prostheses to the edge of the Acetabular Cup



The results were displayed in graphical form through a number of cycles for standard polyurethane and polyethylene joints. The effect of changing the clearance of polyethylene joints and the hardness of the polyurethane layers was measured. Initial conditions assumed a film thickness of $15\mu\text{m}$. Adjusting this value made little difference to the film thickness after 5 cycles.

6.6.2 Results

The squeeze film analysis showed that loading profile I and the cycle predicted by Paul (1967) gave similar fluid film depletion times (figures 6.17a and 6.18). This was found to be the case during experimental work by the author and suggested by Unsworth *et al* (1987).

Theoretical analysis of the harder grades of soft layers constructed from Tecoflex 100^oA (figure 6.17b) indicated a large reduction in contact area and hence a reduction in the minimum film thickness developed after 5 cycles. This analysis indicated the maximum film thickness required for the soft layer joints to operate in the fluid film regime as $0.05\text{-}0.200\mu\text{m}$. The Tecoflex 100^oA layers certainly represent the upper limits of hardness, due to the smaller contact area and the reduced micro-EHL effect. With this material the deformation of the asperities would seem to result in

Figure 6.17a: The Film Thickness variation for a Soft Layer
Prosthesis under Normal Walking Loads

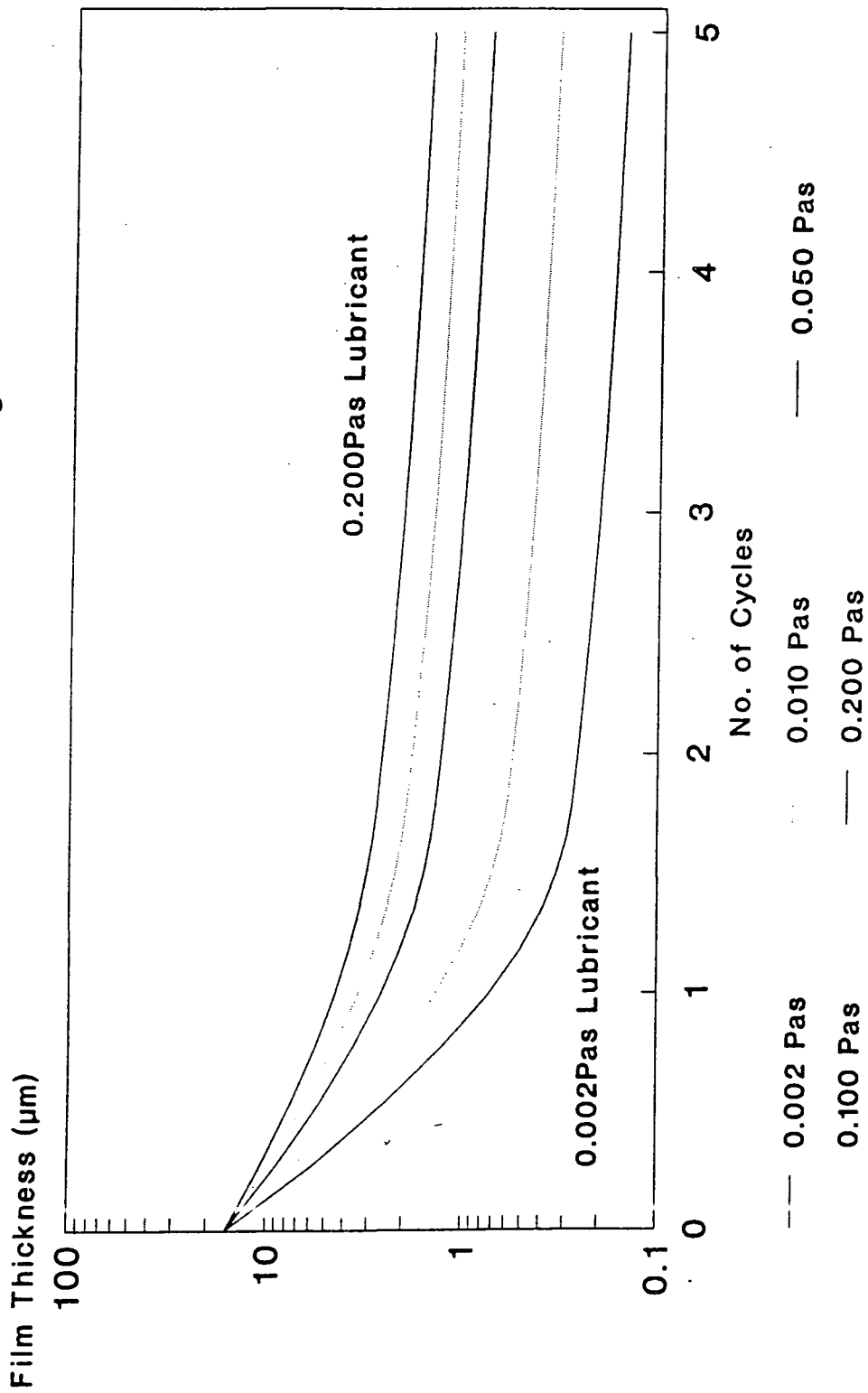


Figure 6.17b: The Film Thickness variation for a Tecoflex 100A Prosthesis under Normal Walking Loads

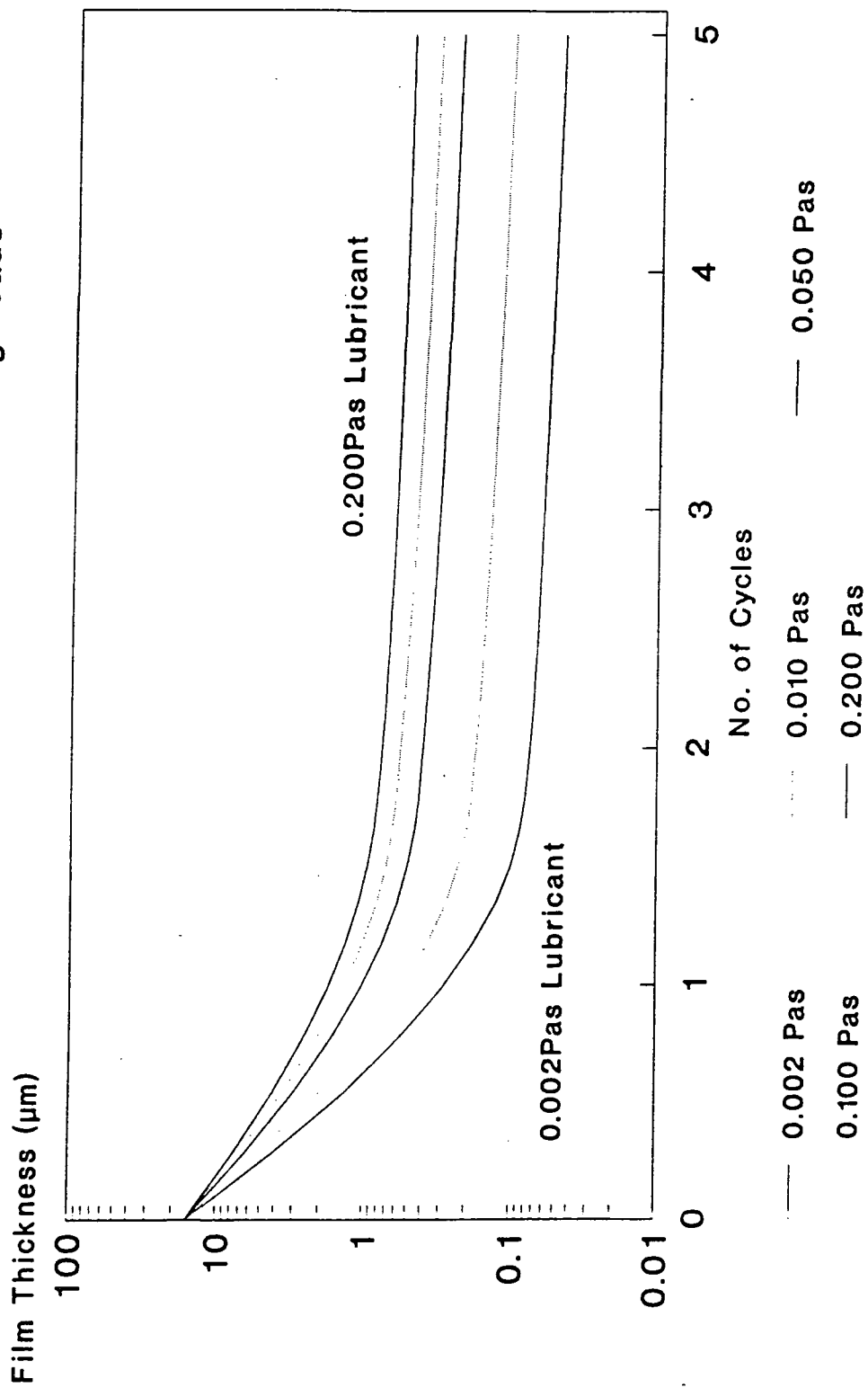
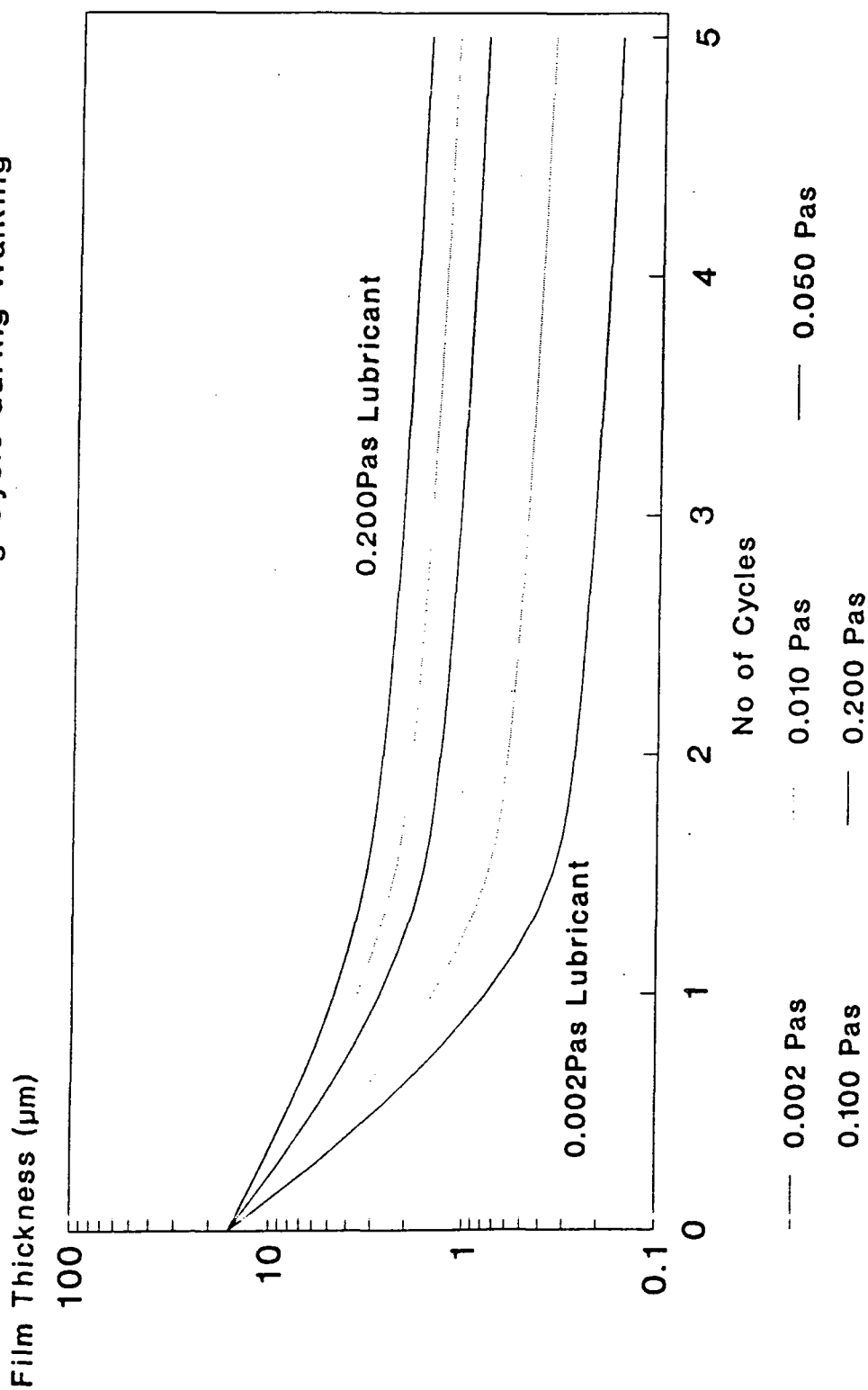


Figure 6.18 : The Film Thickness variation for a Soft Layer
Prosthesis under Paul's Loading Cycle during Walking



surface roughness values of 0.025-0.175 μm , a deformation of 70-95%. The deformation of the softer layers will tend to be greater, resulting in lower roughness.

The UHMWPE joints of the same clearance as the soft layer prostheses showed much lower film thicknesses over the entire lubricant range, with values of circa. 0.9 μm after 5 cycles with 0.200Pa s lubricant (figures 6.19-6.22). This value of film thickness would support a film in a soft layer joint, but due to the reduced micro-EHL deformation of the UHMW polyethylene surface, mixed lubrication is still likely at such film thicknesses. Reduction of the clearance of the joints increased the generated film to 0.8-2.5 μm (0.010-0.200Pa s), which indicated that fluid film lubrication should be attainable with high viscosity fluids. This was found to be the case in Section 6.4.

6.6.3 Discussion with Experimental Results

The theoretical calculations of film thickness indicated a number of important factors in the performance of the soft and hard (UHMWPE) prostheses. The first conclusion was that the squeeze film effect does seem dominant and the contact area is critical due to being raised to a power of 4.0. In these calculations it is important to use the contact areas which actually pertain during dynamic operation of the joint. The most accurate results would be achieved by measurements of the contact over the entire range of loads and inputting these results into the equations. For simplicity, the effective elastic modulus of the layer was calculated from contact area measurements using a load of 2000N, which will tend to over-estimate the value of elastic modulus at low loads (eg. during the recovery phase of the cycle). This will tend to underestimate the film thickness for the soft layer joints due to a reduction in the EHL lift.

The effect of Micro-EHL was not included in this analysis, although the effects on performance are indicated in section 6.10. The deformation of the surface asperities reduces the thickness of the minimum film for complete separation, and film

Figure 6.19 : The Film Thickness variation for an UHMWPE Metal Prosthesis under Walking with 0.010Pas Lubricant

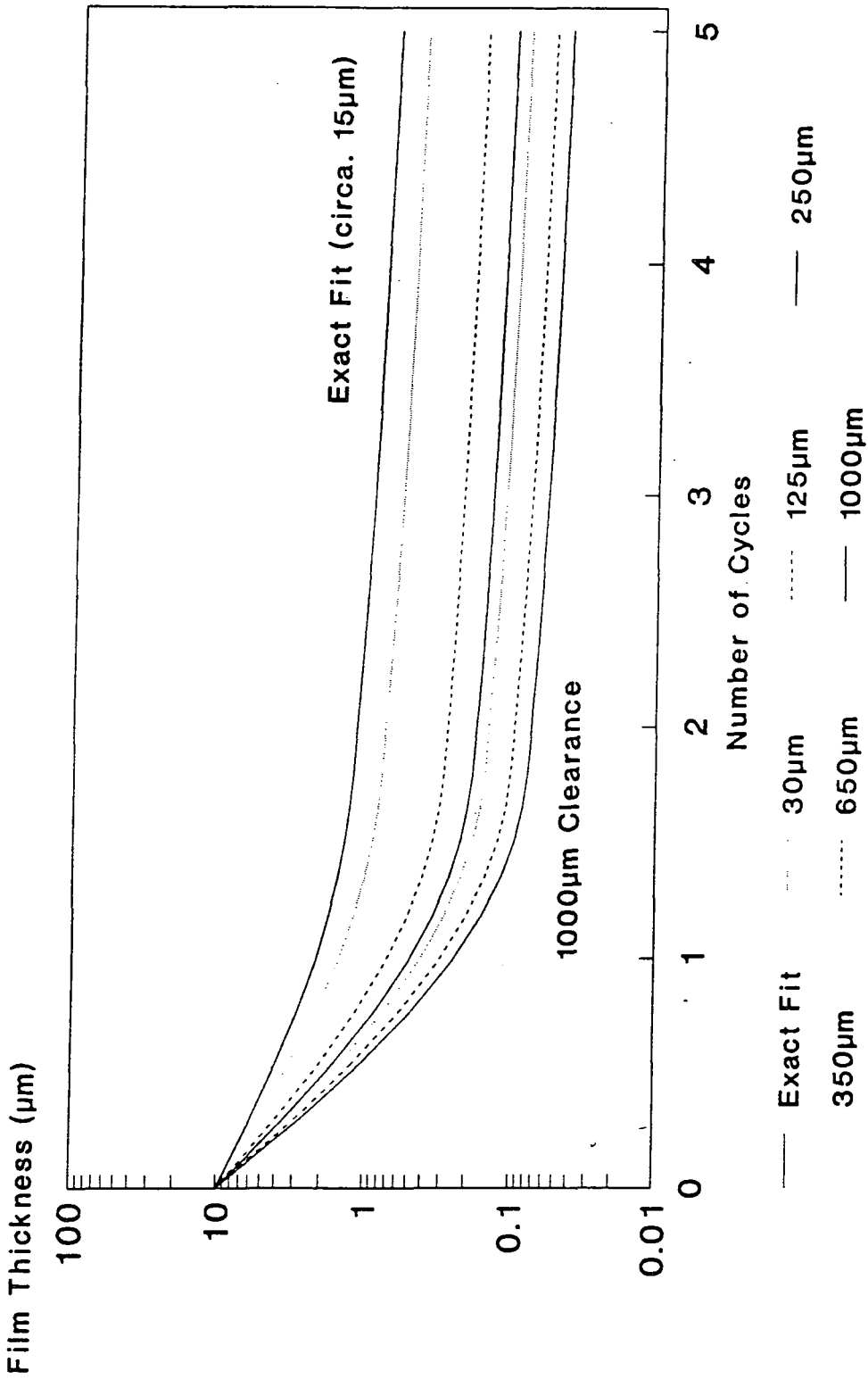


Figure 6.20 : The Film Thickness variation for an UHMWPE Metal Prosthesis under Walking with 0.050Pas Lubricant

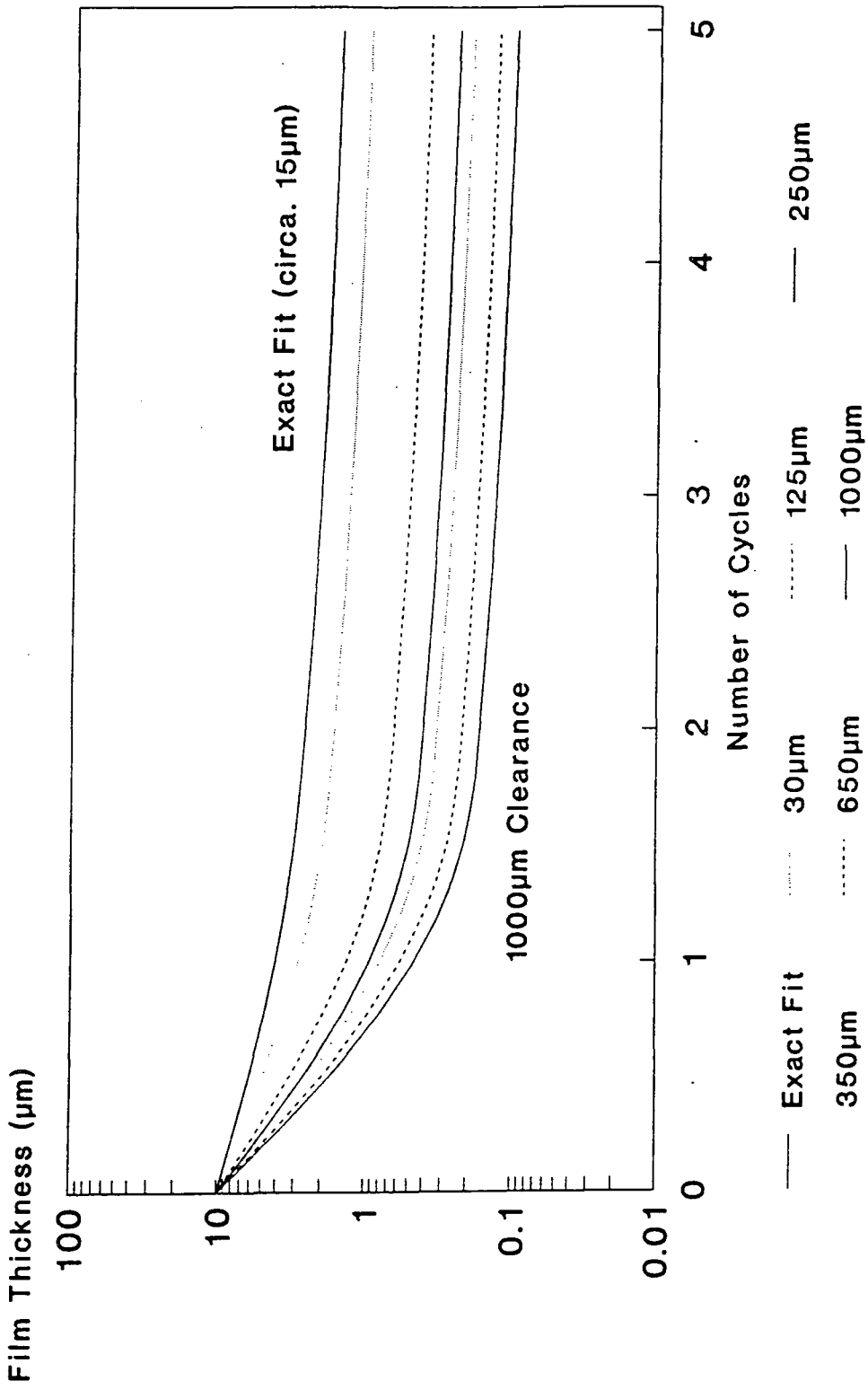


Figure 6.21 : The Film Thickness variation for an UHMWPE Metal Prosthesis under Walking with 0.100Pas Lubricant

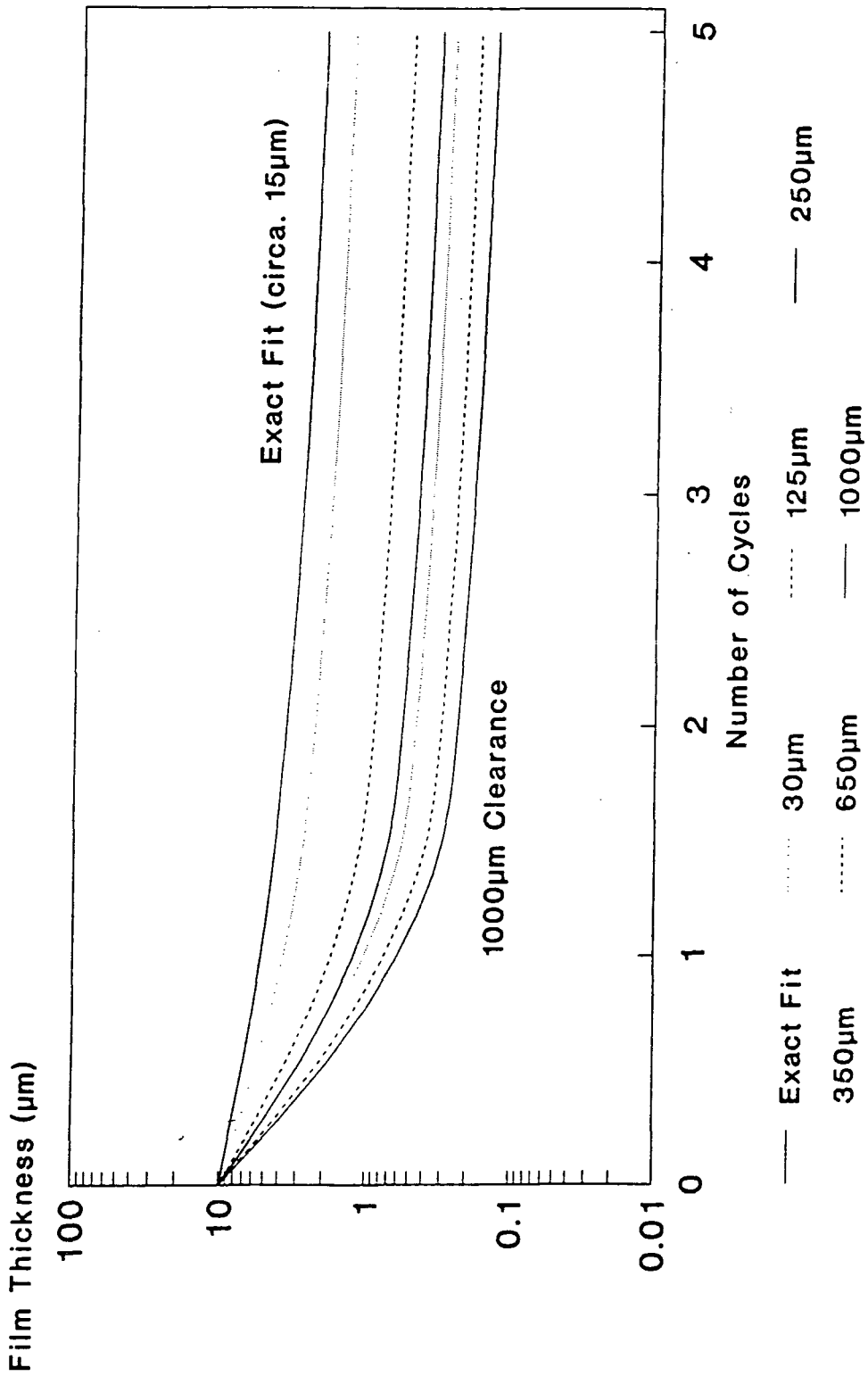
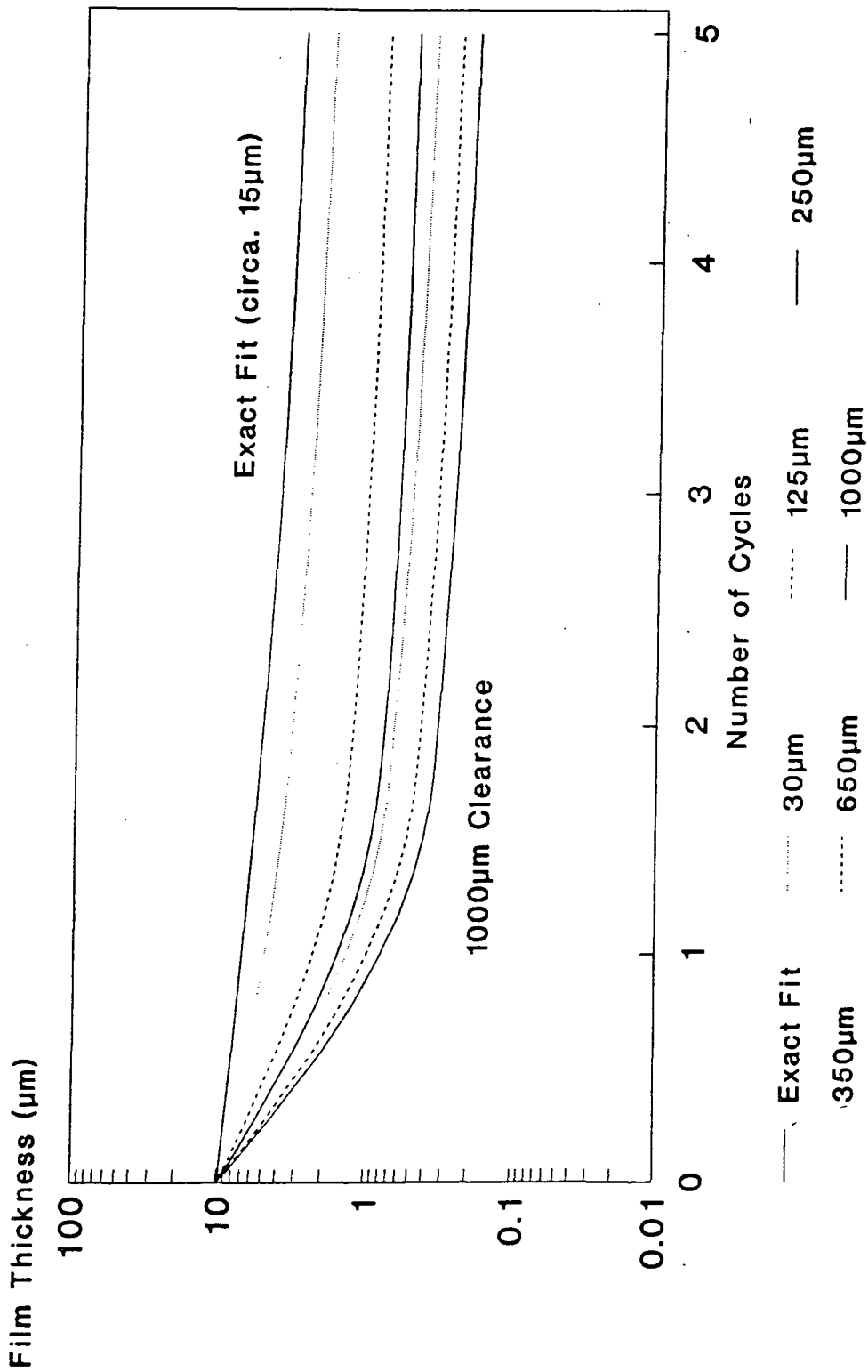


Figure 6.22 : The Film Thickness variation for an UHMWPE Metal Prosthesis under Walking with 0.200Pas Lubricant



thicknesses of circa. $0.20\mu\text{m}$ are postulated as sufficient for soft layers, where $1.0\mu\text{m}$ may be required for an UHMWPE surface. This can be seen from the results of tests with high conformity UHMWPE joints, where although the contact area is similar to a polyurethane joint, the frictional torque is higher, although much improved compared with commercial prostheses (section 6.4).

The loading cycle which has been in use over the course of the project, which simplifies the loading during the stance phase, provided very similar theoretical results (with slightly more demanding conditions) to the cycle suggested by Paul (1967). This confirms the experimental measurements of friction using both loading cycles.

6.7 Experimental Determinations of Lubricant Films

Methods of direct measurement of the thickness of a lubricant film were introduced in section 4.2.6. Experimental work was performed using the resistance technique to measure the film of lubricant between the components of the hip prosthesis. Quantitative measurements were expected, but due to unknown changes to the fluid at the interfaces only qualitative measurements could be made.

6.7.1 Materials and Methods

Hip prosthesis were made with the metal femoral head articulating on an UHMWPE and polyurethane cup. The two soft layers were castomer bonded to the lugged stainless steel cups and exhibited hardness values of 4.2 and $5.0\text{N}/\text{mm}^2$ (H20/30). The UHMWPE components were machined from solid. The acetabular components were coated with gold through vapour deposition to a depth of about 5nm. This had the effect of reducing the clearance of the joint by less than 0.004%. Two femoral heads were employed. In initial studies a standard ball was used and insulated from the simulator. Large fluctuations in the resistance measurements and lack of

information about the shape of the lubricating film led to the manufacture of a second ball, with the current passing through a 3mm^2 cross section insulated wire (figure 6.23). The wire was held in place by araldite two-part adhesive which has an elastic modulus of 3.5GPa , over twice as high as UHMWPE. A simple DC circuit was used and the resistance across the joint measured on an X-Y recorder. A standard loading profile was applied by the simulator and the frictional torque recorded.

6.7.2 Results

The resistance of the joint varied cyclically and showed a similar profile to the loading applied to the prosthesis (figure 6.24). The soft layer joints had a resistance of typically 400Ω which could be calculated from the resistivity measurements as $0.2\text{--}3.0\mu\text{m}$ film thickness, depending on the film used. The UHMWPE joints showed much lower resistances of 30Ω average, dropping to 10Ω during the stance phase (which was the resistance of the circuit when ball and cup were in contact). Friction measurements showed that the soft layer joints gave a low friction factor (circa. 0.005) representative of fluid film lubrication, whilst the friction of the UHMWPE joint was much higher ($0.060\text{--}0.045$), representative of mixed lubrication.

6.7.3 Discussion

Measurements of the resistivity of the water based CMC fluids were performed between platinum electrodes with an area of 100mm^2 on a sample of fluid 10mm thick. This was deemed not to be representative of the joint conditions and only qualitative conclusions were drawn. From the resistance plots the film can be seen to be substantially thicker with the soft layer joints, and indicates no direct solid contact between the surfaces. This confirms the low friction obtained by simulator tests and the improvement which could be obtained by the use of such joints *in-vivo*. Although this method seems successful in predicting the presence of a film it would be beneficial

Figure 6.23 : The Femoral Head and Electrical Circuit used for Film Thickness Analysis

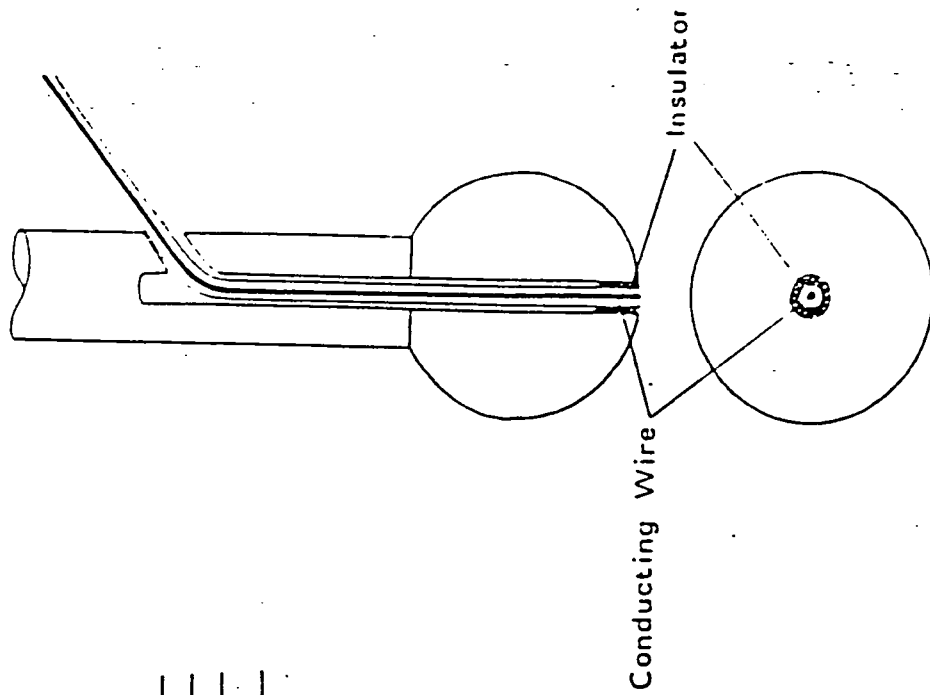
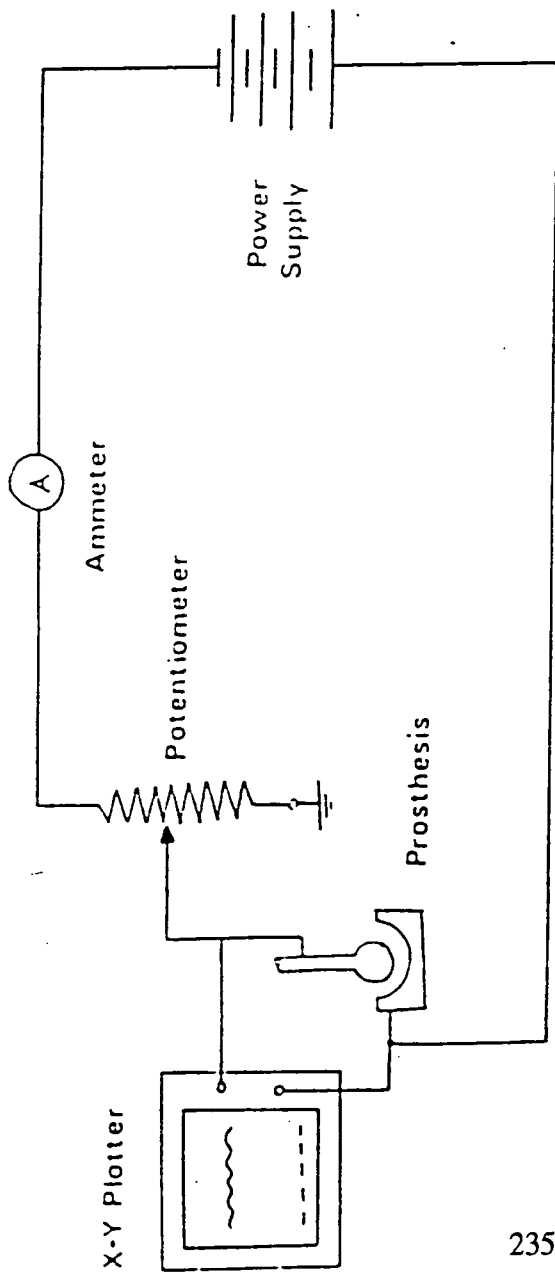
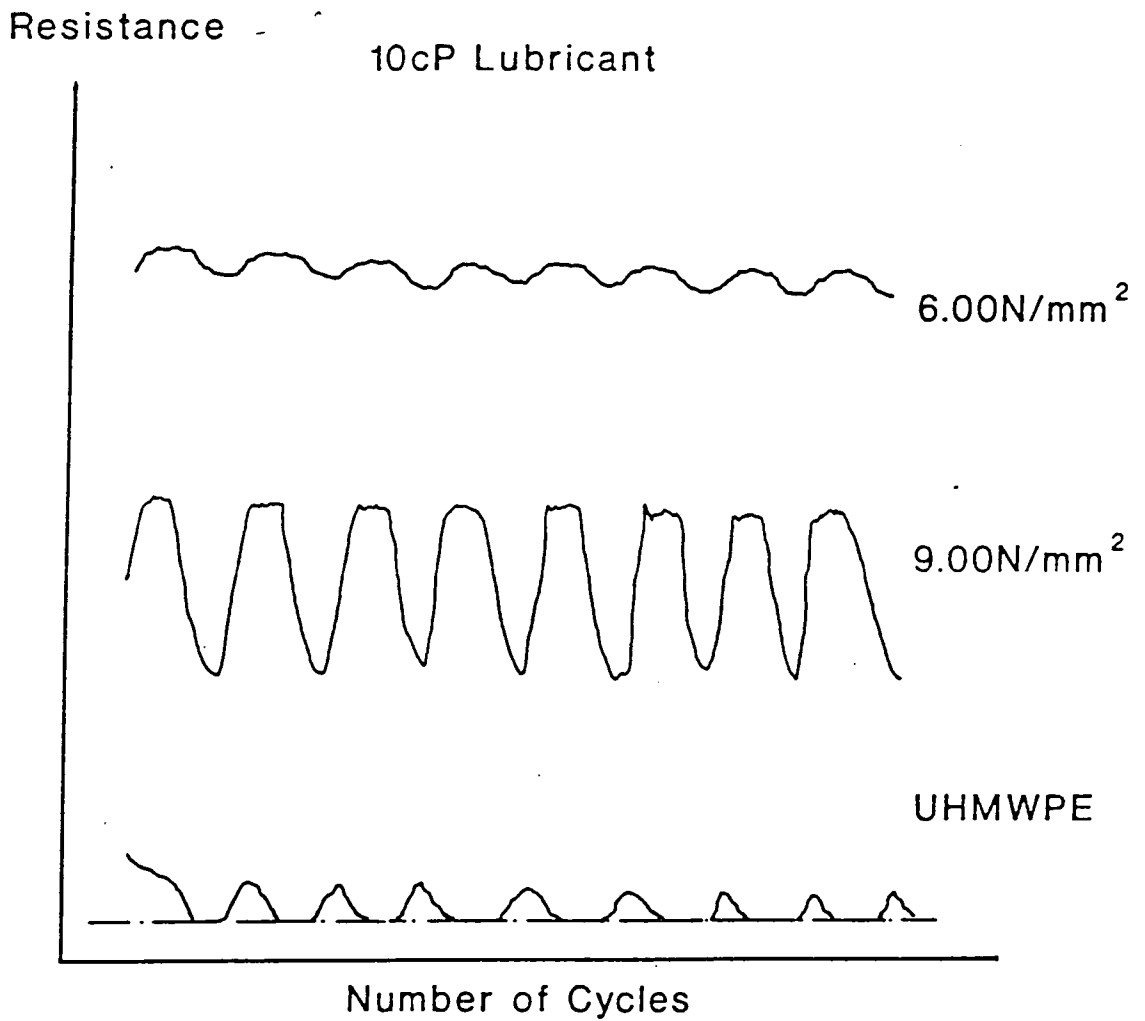


Figure 6.24 : Resistance Measurements for Soft Layer and UHMWPE Hip Prostheses



to test soft layer joints at the upper and lower limits of the hardness values which give low friction. This may show that high friction and surface contact does indeed result in low (circa. 10 Ω) resistance measurements, confirming the thick film results.

6.8 Extended Testing of Polyurethane Prostheses

The experimental Durham prosthesis was tested for extended periods under lubricated conditions. The friction was measured at 10,000 cycle intervals up to a total of 120,000 cycles. A metal backed cup with a 2mm thick vacuum moulded Estane 5714F1 layer was used for the tests.

There was no significant change in the friction over the duration of the test and no noticeable wear on the cup. Two further cups of Estane '57' were tested with similar results. Although this period of testing corresponds to only a matter of weeks of activity it has shown that the polyurethane joints are not limited to short periods of activity. In addition this indicates that where squeeze film during the loaded phase of the cycle and EHL lift during the recovery phase become equal and the film thickness reaches its lowest value, the value of film thickness is greater than the loaded roughness of the layer. This was indicated in theoretical calculations (section 6.6) and experimental measurement from short term testing (section 6.7).

6.9 Inducing Effects of Third Body Wear

The effects of particles of bone and cement on the performance of the polyurethane joints were investigated. Following surgery particles have been shown to cause damage to the acetabular and femoral components of UHMW polyethylene/metal prostheses (Issac *et al*, 1992). The particles were placed in the cup prior to addition of the 0.010Pa s lubricant and loading and motion in the hip function simulator. Typically 0.3g of bone or PMMA (bone cement) particles were added with 3ml of

lubricant. The particles were estimated at $250\mu\text{m}$ in diameter and were obtained from cutting.

On the first cycle the friction factor was very high (circa. 0.5) but this reduced quickly as the foreign particles were seen to be rolled out of the base of the cup. Friction factor on the fifth and seventh cycles approached the fluid film values of 0.005 and at this stage the particles could be seen around the periphery of the cup. The joints were dismantled to reveal an absence of particles in the contact region and little marking of the components. UHMWPE prostheses showed slightly lower initial friction factors (circa 0.3), but this was maintained up to 60 cycles. On completion of the tests particles were still visible on the contact and scratching was visible on the metallic component.

Soft layer joints, due to their high compliance, seem to resist the potentially damaging effects of hard foreign bodies by their speedy removal from the contact zone. Although friction is initially high, this reduces to values representative of fluid film lubrication within a few cycles, minimising damage.

6.10 Conclusions

The work has brought the potential of soft layers in bearings into the hip joint and succeeded in developing a bio-compatible prosthesis using currently available polyurethane systems. Four bio-compatible polyurethane materials were investigated and low friction joints obtained from each. Grades of Tecoflex EG from 80°A to 100°A (Shore) were seen to be capable of low friction joints, however, at each end of this range of hardness values many of the joints did not display the low friction. This allowed the preparation of a friction envelope graph (figure 6.15), which showed that hardness values less than 2.5 and

greater than 9.0N/mm^2 were unlikely to produce the desired effects due to changes in the contact area.

UHMWPE joints of different clearances were investigated, which indicated that similar contact areas could be obtained, and although friction was much lower with the smaller clearances, performance was not as good as the soft layered joints. This indicated the importance of micro-EHL and the deformation of the surface asperities on the performance of the lubricated prosthesis.

Theoretical analysis of the tribological properties of soft and hard (UHMWPE) joints was performed. The reasons for the reduction in the friction of soft layer joints when compared with commercial prostheses was clearly explained by the increase in the minimum film thickness, typically from 0.10 to $0.25\mu\text{m}$ for the 0.010Pa s lubricant. In addition the increased deformation of the asperities on soft surfaces will tend to increase the difference between the tribological performance of the two joints.

Resistance techniques were investigated to explain this experimentally. Results could only be analysed qualitatively due to the unknown effects of solid interfaces and high loads on the electrical properties of the CMC based fluids. Results showed contact in the UHMW polyethylene joints and full separation in the soft layer joints.

Chapter 7 : Surface Modifications

7.1 Introduction

To improve the properties of the soft layer joints under static loading it was decided to investigate the addition of porosity to the polymer surface. The biomedical polyurethanes under investigation tend to have much lower porosities than cartilage with a maximum fluid uptake of 2%. The surface layer accounts for much of this as permeability is low and has a potential fluid reservoir of 10-15%. The addition of discrete pores on the articulating surface should provide little effect during normal operation of the joint, with a dynamic loading cycle, as they will contain fluid. However, under conditions of prolonged loading and little motion the polymer will tend to deform and pressurise the fluid in the pores. The fluid would be forced laterally from the pores and transported into the "contact" area between the cartilage surfaces. This might prevent direct contact and consequent layer damage.

A further advantage of using an elastomer containing discrete pores is that its mechanical properties will be altered. The effects of a high Poisson's ratio have previously been encountered and large radial clearances (of the order of 0.250mm) are required to eliminate grabbing of the femoral ball within the acetabular component under loaded conditions. Poisson's ratios approaching 0.5, which is a common value for polyurethanes (Strozzi, 1992), mean that under the action of external stress the volume change of the material is minimal. However, if discrete pores were present, the incompressibility of the layer would be reduced, leading to a lower incidence of grabbing under application of load. Smaller clearances could then be specified to improve the tribological properties of the joint by increasing the contact area and reducing the peak pressures (Chapter 6). Unfortunately, increased porosity will tend to reduce the fatigue life of the polyurethanes, especially as the stress concentrators are particularly damaging, being on the surface.

7.2 Methods of Producing Discrete Surface Pores

The preparation of discrete pores can be accomplished by a number of methods. The use of waterjets (Lichtarowicz, 1990) and laser ablation (King, 1990) have both been used with considerable success for the cutting of body tissues. The biological results with these methods acting as a scalpel is complemented by industrial applications, which also include the preparation of holes (e.g. Spinneret holes and cooling holes in turbine blades). In addition mechanical means were considered. The use of needles to produce surface pores was investigated at UMIST (Dawber and Healey, 1991) but only a very slight impression was evident due to the polyurethane tending to close back around the pore. Casting techniques to produce surface pores during the moulding process were not considered in detail owing to problems with producing normal mouldings. Surface and sub-surface pore formation was evident in regions where moulding pressures were reduced. This meant that flat sheets were much easier to process without pores. With this in mind, the likelihood of bubbles forming close to cast pores was high. This would cause larger pores to be formed, roughening the surface and reducing the effectiveness of the mechanisms generating the fluid film.

Modifications to the surfaces by plasma erosion were also investigated at UMIST as part of the joint research project. This method increases the roughness of the surface to form a fluid reservoir, rather like the surface of articular cartilage (Gardner and Woodward, 1969). However, the results were disappointing, with regular asperities difficult to obtain. In addition, the effect of heating, which can be as much as 200°C (Pons *et al*, 1991), on the mechanical properties of the polymer have not been assessed, but detrimental effects are expected. In particular an increase in hardness, and reduction in elasticity and embrittlement of the surface layer are likely due to the heat history applied.

Blowing agents had also been tried previously to produce porosity in the polyurethane (Dawber and Healey, 1991). Although these produced an effective lubricating surface, the polyurethanes were too mechanically weak to remain intact under the demanding conditions in the hip function simulator. In addition, the use of hydrogels instead of polyurethanes may be applicable. This would require complete redesigning of the acetabular component due to the lower mechanical strength of such materials. These materials were initially dismissed due to low mechanical strength and although this has been improved it is still a potential problem, especially in such a demanding, weight bearing application.

7.3 Laser Theory

The application of lasers to problems involving cutting of material has only proved successful in the last few years. However, many metal and plastic parts are now cut using this method. When cutting through materials, damage often occurs in the zone adjacent to that which has been vaporised. Certain lasers tend to be easier to focus and therefore produce a smaller zone of damage. Work done on Erbium-YAG lasers at UMIST has revealed that when cutting both soft and hard body tissues, this zone was only 20 μ m wide which compares with values of over 200 μ m for Holmium-YAG lasers and even higher values for CO₂ gas lasers (King, 1990). Excimer laser have recently become important in the ablation of damaged cartilage and polymers (Guo and Lou, 1991) and very low zones of damage have been observed. The heating effects of this laser also seem to be small in comparison with CO₂ gas lasers, with temperatures of only 40°C 1mm from the centre of the spot (Dressel *et al*, 1992) The heating effects are reduced by the use of pulsed lasers compared with continuous wave devices (CW) due to lower general heating effects. In addition multiple pulses reduce the taper of the hole (Wilson and Hawkes, 1987). For large aspect ratios (depth/diameter) a slowly converging laser beam is favoured (Wilson & Hawkes,

1987). This may be implemented by the use of a long focal length collating lens. One problem with holes of large aspect ratios is that material vaporised from the base of the pore may re-deposit further up, reducing the entry aperture of the hole. This would be particularly detrimental to the tribological performance of a device. However, polymers lend themselves to high aspect ratio pores due to their relatively low reflectibility and low conductivity which reduces heat dissipation and general heating.

Absorption of the laser energy is dependent on the water content of the material, especially the long wavelength (infra-red) CO₂ lasers. Higher absorption levels lead to smaller amounts of thermal damage due to the short exposure times required to perform the cutting task. Cutting is achieved by vaporisation of the solid media and at the present time little work has been done on the region adjacent to the hole and the effect on hardness in this region. The pulse energy, pulse duration, repetition rate and spot size will all have an effect on the ablated region and these have been investigated to some extent. Kopchok *et al* (1992) indicated that for Holmium-YAG lasers reducing the pulse energy density from 1070-700mJ/mm² halved the size of the thermal damage zone on an inter vertebral disc. A similar effect was found when ablating in saline.

Transport of the lasing beam to the surface of the material is required to reduce the effects of beam divergence and can be facilitated by the use of optical fibres or lenses. Many of the currently used lasers can now be sent down optical fibres (Er-YAG and excimer lasers have recently been included) and transmission is good. Although used in surgical lasers, focusing can be a problem with optical fibres, and as the cups were ablated in the laboratory under controlled conditions, a lens was used.

Modifications of the layers commenced by making a theoretical analysis of the volume of fluid which would be required to fill the holes and provide an advantageous

effect. Theoretical analysis of elastohydrodynamic contacts (Jin, 1988) (section 6.6) have indicated film thicknesses ranging from 0.5 to 3 μm for fluids of similar viscosities to synovial fluid. Over a typical loaded contact area of the Durham experimental prosthesis (radius of contact = 18mm), the separation of the two surfaces will be almost constant due to the compliant nature of the polyurethane. Therefore, considering the contact region to be covered with equally spaced holes the fluid required from each hole would be:

$$\text{Hole spacing} = 2000 \mu\text{m}$$

$$\text{Volume of Fluid} = \pi \times 1000^2 \times 3 = 9.42 \times 10^6 \mu\text{m}^3$$

$$\text{Volume of Pore} = \pi \times 125 \times 125 \times \text{Depth}$$

Considering 40% fluid outflow,

$$\text{Pore Depth} = 480 \mu\text{m}$$

Preliminary tests on Erbium-YAG solid state lasers using a collating lens of 37.5mm focal length and pulse energies of 80mJ/pulse indicated that hole diameters for the elastomers under investigation were 335 μm for Tecoflex 93 $^{\circ}$ A and 395 μm for Tecoflex 85 $^{\circ}$ A and hole depths of 200 μm /pulse for 85 $^{\circ}$ A material and 240 μm /pulse for the harder grade of material were obtained with little hole widening for multiple pulses. Lasing of Pellethane 2363-80 $^{\circ}$ A resulted in similar hole diameters as the harder of the Tecoflex grades, at 300 μm . This was expected as ablation seemed to be related to material hardness.

7.4 Apparatus for Laser Modification

The solid state laser made use of a single Xenon flash lamp, powered by a 50J source. It consisted of an Erbium-YAG rod with 50% substitution and size 4mm diameter and 76mm length. This laser is currently under investigation for surgical application with the cutting of soft tissues and further details can be found in a number of publications from the Manchester University Laser Physics Group (Charlton *et al*,

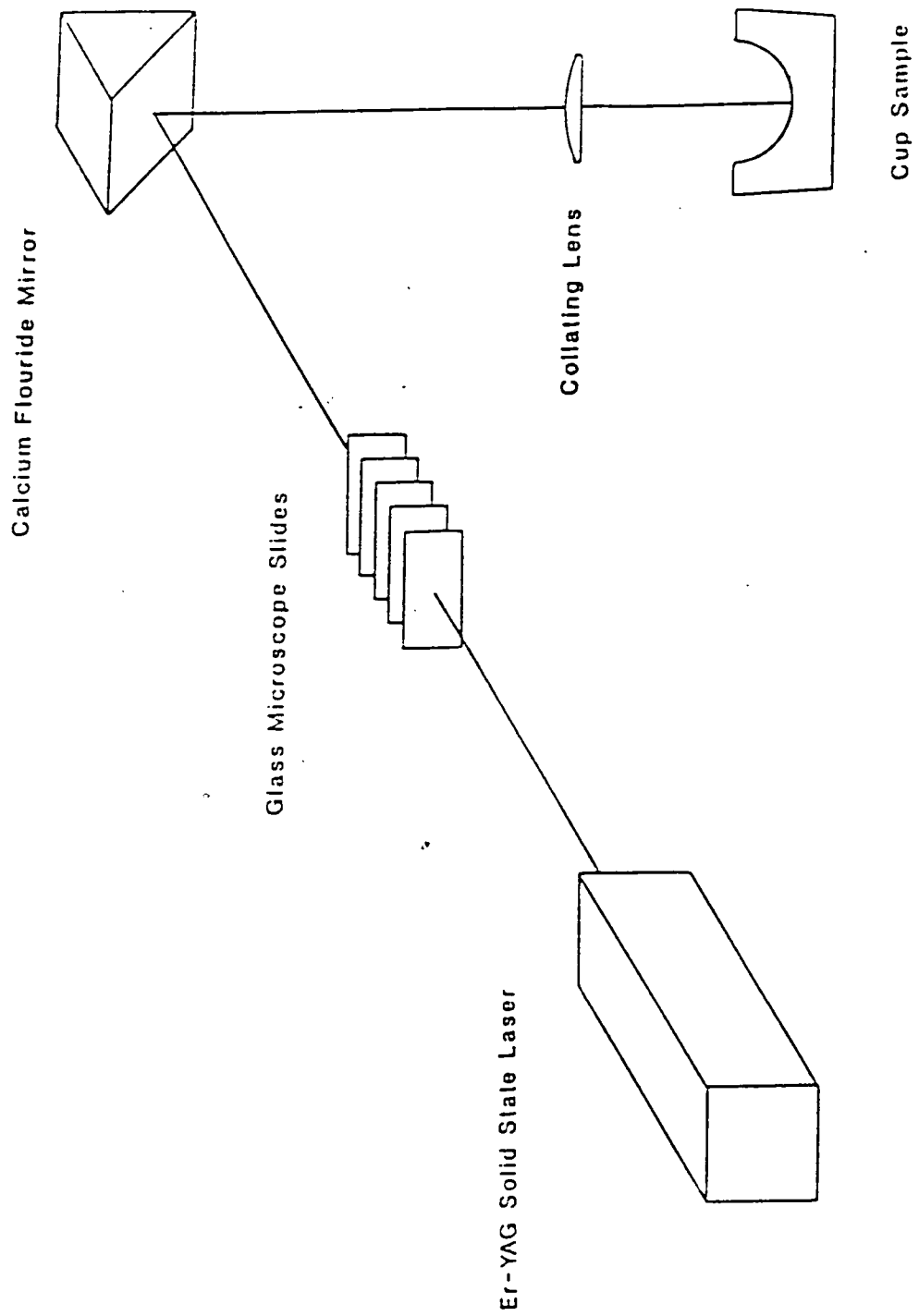
1989). The output coupler was on a ZnSe substrate and had a reflectivity of 95%. The lasing output had a wavelength of $2.94\mu\text{m}$ and was varied between pulse energies of 60 and 200mJ and repetition rates of 1-10Hz were investigated. Pulse duration was fixed at 200ms for the initial experiments, but lower values of 200ns were used for higher repetition rates. When lasing at 80mJ the beam divergence was 5mrad, but this increased as pulse energy rose. The pulse energy was measured with a pyroelectric detector. The collating lens was Calcium Fluoride (CaF_2), focused to a spot size of $350\mu\text{m}$. Glass microscope slides were used to reduce the laser energy (62% transmission) and in this way pulse energies as low as 3.5mJ could be attained with multiple slides. The configuration is shown in figure 7.1. This arrangement allowed pulse energy densities from 830-36mJ/mm² to be investigated.

7.5 Materials and Methods

Tecoflex 85°A, 93°A and Pellethane 80°A were investigated fully, with preliminary studies with Tecoflex 80 and 100°A grades. These materials had the most favourable tribological properties, responded best to *in vitro* conditions (Chapter 3) and have proved reliable in the biological environment (Blamey *et al*, 1991).

Initial studies used injection and compression moulded sheets. Both manufacturing techniques were used to eliminate the possibility of different pore formation with processing techniques. Platen and Injection temperatures were similar for all of the polymers at 170°C, which is a little higher than recommended by the manufacturers. Tribological assessment was investigated using Stainless Steel backed samples formed using compression moulding in a vacuum at a processing temperature of 175-180°C.

Figure 7.1 : The Configuration of the Optical System for the Laser



The flat sheets were placed at the focal length of the collating lens to ensure the holes were of 350 μ m nominal diameter. Calculations for the positioning of equi-distance holes on the cup samples were made but it was decided to use concentric circles for simplicity and accuracy of hole placement. A jig was built (figure 7.2) which allowed the laser to be focused and held sheet and cup samples to allow multiple pulse ablation to form the pores. It enabled the stainless steel backed cups to be manipulated to produce the pores on concentric circles from the pole of the cup.

7.5.1 Stage I

Initially flat polymer samples received varying pulses from the Erbium-YAG laser to assess spot sizes and the depth of cut per pulse with these materials. This laser produced 200mJ/pulse maximum power, and the pulses were initiated manually. The maximum repetition rate was 1Hz. Tecoflex 85 and 93 $^{\circ}$ A grades were investigated. Later this group was extended to include Tecoflex 80 $^{\circ}$ A and 100 $^{\circ}$ A, Estane '57' and '58' and Pellethane. Pulse energies of 100, 150 and 200mJ were used and 1,2,3 and 4 pulses used to prepare each pore. The diameters of the pores and the vertical and horizontal extents of the damage were measured/assessed. Each combination of material, pulse energy and number of pulses was given a score based on damage.

Preliminary studies with Tecoflex 85 $^{\circ}$ A cups involved using two pulses to create each pore at 6 $^{\circ}$, 12 $^{\circ}$ or 18 $^{\circ}$ from the central point together with a central hole. The holes were checked for accuracy of spacing, size and depth using optical microscopy and the samples were then tested in the Durham Hip Function Simulator.

Six cups were then produced under identical conditions. Two laser pulses were used for each pore to obtain the required depth. These were placed on concentric circles at angles of 0 $^{\circ}$, 8 $^{\circ}$, 16 $^{\circ}$ and 24 $^{\circ}$ (figure 7.3) in the first set of

Figure 7.2 : The Jig used to hold samples undergoing Laser modification

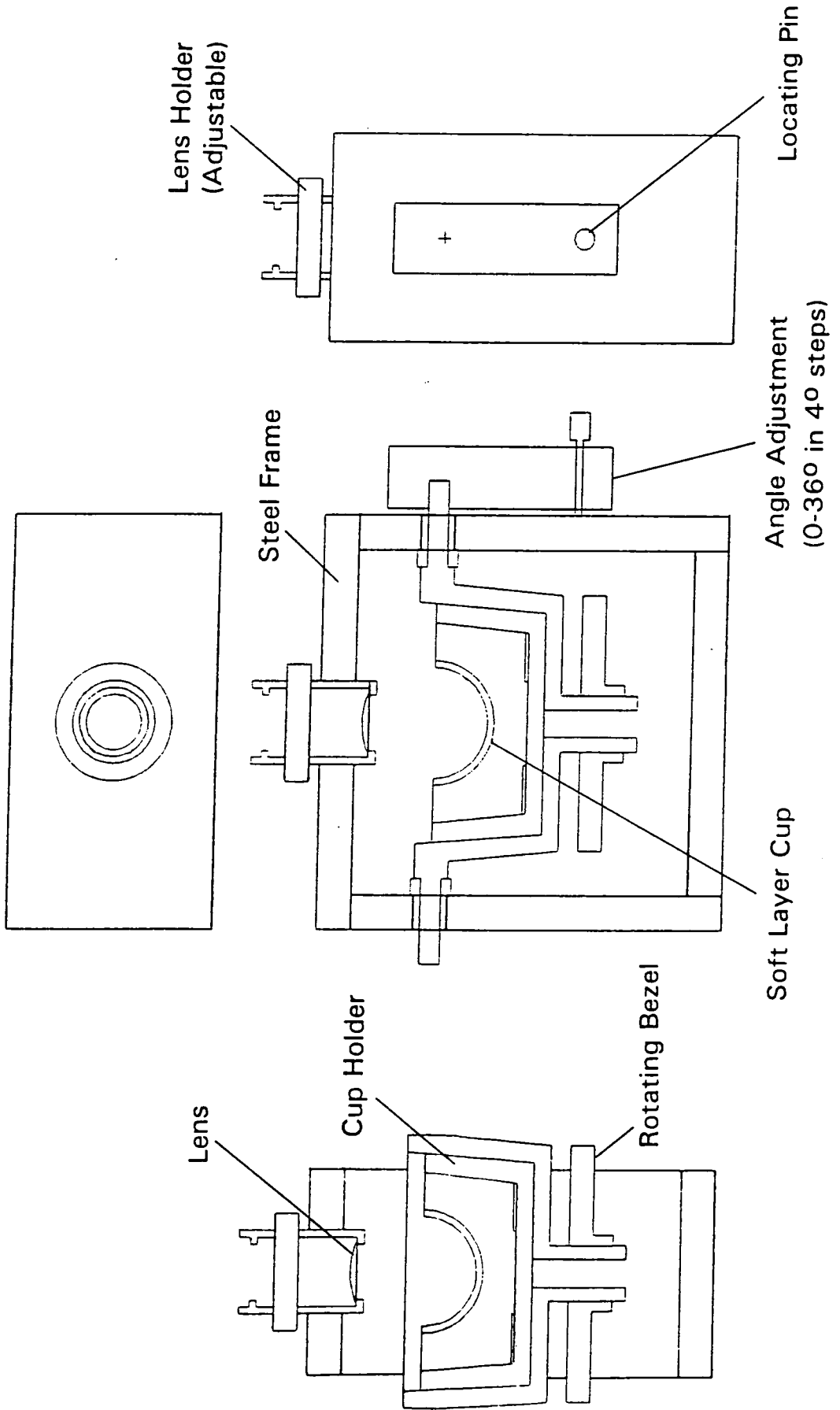
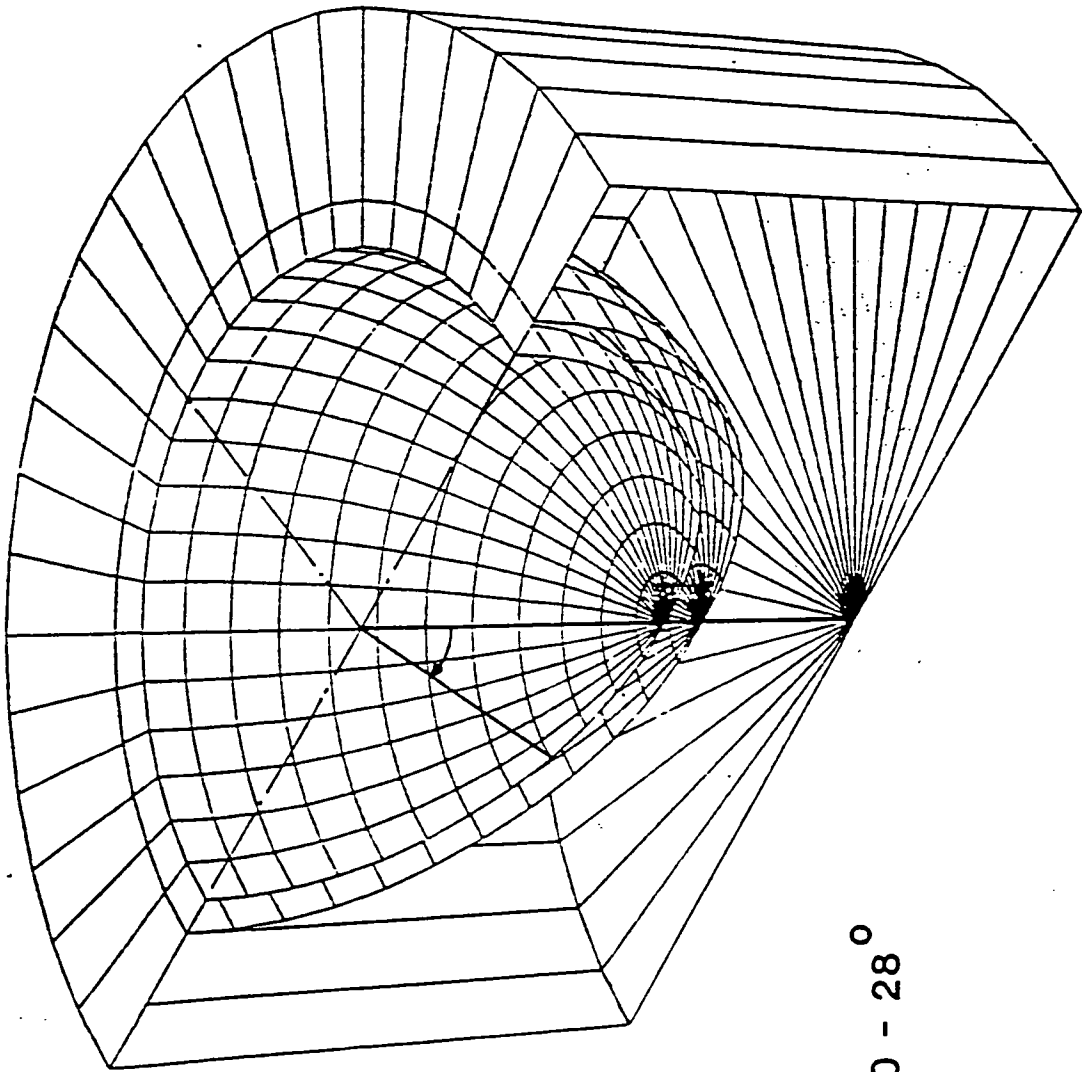


Figure 7.3 : The positioning of the Laser produced Pores



Alpha = 0 - 28°

experiments. Following testing of these hole densities, pores were placed at angles of 4°, 12°, 20°, and 28° to double the density of pores. This would allow the effects of hole density to be studied.

Three loading cycles were designed to show the effects of the pore network. These included the normal loading cycle which is representative of loading on the hip joint during walking (figure 5.25a). It had a peak load of 2000N (approximately 3 x body weight) and 20N during the swing phase. Loading cycle II applied a constant load of 1000N (figure 5.25b). This was to show the lubrication performance of a joint with no possibility of squeeze film or hydrodynamic replenishment. Loading cycle III had an upper load of 2000N and a minimum load of 1000N (figure 5.25c). This was to study the effects of only partial unloading of the joint to see if the joint fluid could be replenished without resorting to very low loads. In addition the effect of an initial low film thickness would be assessed. Comparisons between the frictional results obtained from loading cycles I and III should indicate the effects of the EHL action during the swing phase. Comparisons of the tribological performance of standard and modified layers using loading cycles II and III were designed to show the advantage of using discrete pores to trap fluid near to the loaded region under periods of high loading and low motion (e.g. reduced elasto-hydrodynamic effect).

7.5.2 Stage II

The second study, following poor tribological results from the six Tecoflex 85°A cups, began with a more detailed analysis of the ablation process using flat sheets before using identical conditions on cup samples. Tecoflex 93°A and Pellethane were used. This was because fatigue testing of samples, which had been running in parallel with this research (section 3.5), had suggested advantages in the use of harder materials. Pulse energy, duration and repetition rate were investigated as was the

effects of focusing of the laser. A lower energy (60mJ/pulse maximum) but higher repetition rate (up to 10Hz) Erbium-YAG laser was used. In addition, glass slides were positioned in the optical system (figure 7.1) to allow a wide range of pulse energies to be attained. Seven acetabular cups of Pellethane were then made by vacuum moulding and tested in the simulator prior to surface modification on concentric circles at 8, 16 and 24° from the pole (figure 7.3).

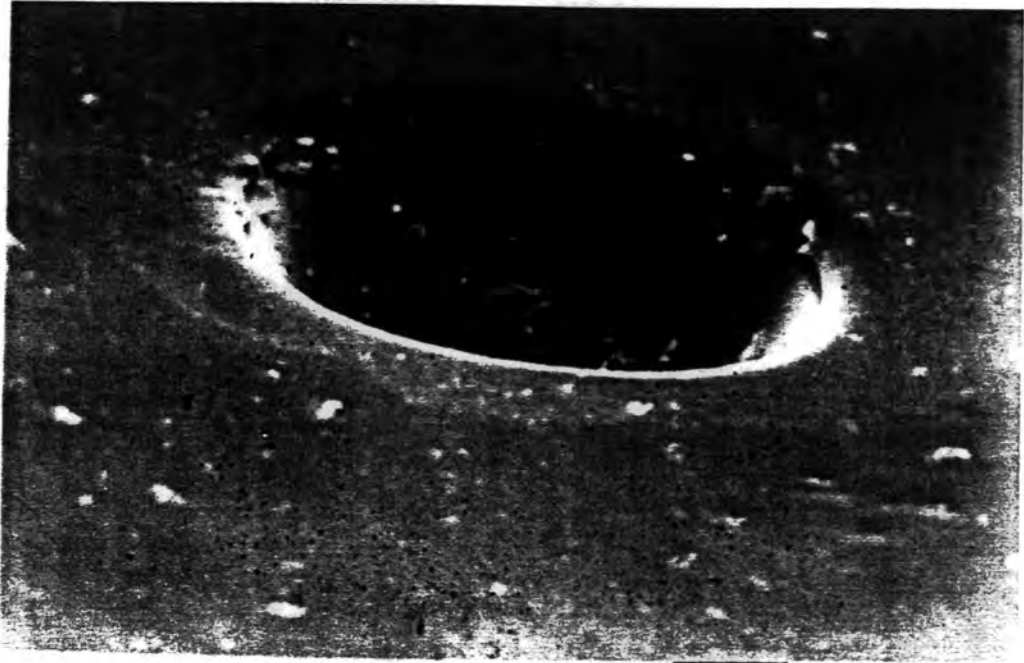
7.6 Scanning Electron Microscopy of the Pores

7.6.1 Stage I

Surface micrographs indicated that pores of 300-400 μ m diameter were formed by the ablation process. Ablation of softer materials resulted in wider, but shallower pores (395 μ m diameter, 200 μ m depth/pulse) than the harder grades (340 μ m diameter, 240 μ m depth/pulse). A rough surface (0.8 μ m R_a) led to a wider but shallower hole/pore, but with a similar quantity of material ablated. The heat affected zone in many cases appeared quite small, 25-40 μ m in width (figure 7.4). The initial group of cup samples also seemed to have little damage at the surface periphery. However, the sample group of six Tecoflex cups showed extensive damage at the periphery of the pores (figure 7.5). This was measured after the poor tribological results in the simulator.

To investigate the ablation of different hardness grades and materials, flat samples of the Tecoflex and Pellethane polyurethanes were ablated using 100, 150 and 200mJ pulse energies and up to 4 pulses (tables 7.1 and 7.2). Tecoflex 80°A showed little surface damage, but this increased with repetitive pulses. The size of the pores increased from 280 μ m average with 100 and 150mJ pulses to 330 μ m with 200mJ. Tecoflex 85°A promoted a larger region of damage, and the height of the damaged zone increased with increasing ablation energy and the number of pulses. Pore

Figure 7.4 : A Typical Surface Micrograph of a Laser Ablated Pore under Favourable Conditions



100μ

Figure 7.5 : A Typical Surface Micrograph of a Laser Ablated Pore under Unfavourable Conditions



Table 7.1 : The Damage Formation around Pores produced by the High Energy 100-200mJ/pulse Erbium-YAG Laser on flat samples of Tecoflex Polyurethanes

Material	Energy (mJ)/ No. of Pulses	Pore Diameter (μm)	Damage (vert.) (μm) (Estimate)	Damage (Horiz.) (μm)	
Tecoflex 80A	100/4	280	10	20	
	150/1	290	5	15	
	150/2	300	10	40	
	150/3	300	10	30	
	150/4	285	5-10	25	
	200/1	290	10	50	
	200/2	300	10	60	
	200/3	315	10	50	
Tecoflex 85A	200/4	345	10	100	
	100/1	310	5	10	
	100/2	310	10	25	
	100/3	310	5	10	
	100/4	330	-	-	
	150/1	330	10	50	
	150/2	320	15	100	
	150/3	310	15	100	
	150/4	320	20	150	
	200/1	380	15	80	
	200/2	340	25	120	
	200/3	330	30	200	
	200/4	320	25	100	
	Tecoflex 100A	100/1	300	20	110
		100/2	300	15	80
		100/3	300	15	80
100/4		300	25	120	
150/1		320	25	80	
150/2		310	25	80	
150/3		310	15	100	
150/4		310	20	100	
200/1		345	25	110	
200/2		335	25	110	
200/3		335	25	125	
200/4		345	25	125	

Table 7.2 : The Damage Formation around the Pores produced by the High Energy 100-200mJ/pulse Erbium-YAG Laser

Energy (mJ)/ Pulses	Tecoflex 80A	Tecoflex 85A	Tecoflex 93A	Tecoflex 100A	Pelletthane 80A	Estane 5714F1	Estane 58271
100/1	-	2	1	4	1	2	2
100/2	-	3	5	3	2	1	3
100/3	-	1	5	3	1	2	2
100/4	0	1	5	5	2	1	3
150/1	1	2	4	6	1	0	1
150/2	1	3	6	6	1	1	2
150/3	1	3	6	5	1	1	1
150/4	0	4	6	6	2	1	2
200/1	1	4	6	6	0	2	2
200/2	1	3	6	6	0	2	2
200/3	1	5	6	6	0	2	2
200/4	1	3	6	6	1	2	2
Average Score	1	3	5	5	1	1	2

diameters were 310 μm for 100mJ, 325 μm for 150mJ and 340 μm for 200mJ pulses. The 93 $^{\circ}\text{A}$ and 100 $^{\circ}\text{A}$ grades of Tecoflex indicated increased damage, with regions 20-25 μm high and 150 μm wide around the pores. This damage seemed unaffected by reductions in pulse energy or the number of pulses. Pellethane 80 $^{\circ}\text{A}$ was also investigated. The damage was minimal with all pulse energies, with a maximum width of only 10-15 μm and 1-2 μm height with 200mJ pulse energies, and this was reduced with 150 and 100mJ pulse energies. These studies indicated that the harder grades of Tecoflex seemed to be more susceptible to damage and higher energies exacerbated this. Lasing of Pellethane seemed to produce little damage and the material seemed much less affected by the pulse energies than Tecoflex. Estane '57' and '58' both responded in a similar way to Pellethane with small amounts of damage.

7.6.2 Stage II (Table 7.3)

Use of the lower energy (60mJ) laser yielded the following. Compression moulded Tecoflex 93 $^{\circ}\text{A}$ showed that the optimum conditions for the formation of pores with little periphery damage was with a pulse energy of 9mJ and a repetition rate of 10Hz (figure 7.6a). Compression moulded Pellethane 80 $^{\circ}\text{A}$ showed a much greater tolerance for lasing parameters and pulse energies from 9-37mJ produced minimal damage at a repetition rate of 10Hz. Injection moulded samples of both polyurethanes proved less easy to ablate successfully, with damaged regions extending for 75-125 μm and being largely unaffected by changes in pulse energy at 10Hz. It was noted that at very low pulse energies (< 5mJ) little ablation took place and only a slight depression was evident on the polymer surface (figure 7.6b). Hole diameters were seen to increase with increasing pulse energy, to a maximum size of 600 μm for both Tecoflex and Pellethane. Focusing of the laser reduced the damaged zone. Initially it was thought that by de-focussing the laser the damaged region would be ablated. However, this was shown not to be the case. The use of a short focal length (20mm) lens

Figure 7.6a : Pore ablation at 9mJ in Tecoflex 93⁰A



Figure 7.6b : Pore ablation at 4mJ in Tecoflex 93⁰A showing poor hole formation



Table 7.3 : The Damage Formation around Pores in Injection and Compression Moulded Samples of Pellethane 80A and Tecoflex 93A, with variations in Pulse Energy and Repetition Rate

Material	Energy (mJ)	No. of Pulses at 2Hz	Pore Diameter (μm)	Damage (Horiz) (μm)	Duration of Pulses at 10Hz	Pore Diameter (μm)	Damage (Horiz) (μm)
T 93A (Comp.)	60	4	300	100	1	550	125
T 93A (Comp.)	37	8	225	250	2	600	100
T 93A (Comp.)	23	12	200	200	3	550	70
T 93A (Comp.)	14	18	180	175	4	500	150
T 93A (Comp.)	9	28	175	50	5	400	10
T 93A (Comp.)	5.6	-	-	-	10	350	10
T 93A (Comp.)	3.5	-	-	-	20	300*	-
T 93A (Inj.)	60	4	300	80	-	-	-
T 93A (Inj.)	37	8	300	100	-	-	-
T 93A (Inj.)	23	12	250	150	-	-	-
T 93A (Inj.)	14	18	175	300	-	-	-
T 93A (Inj.)	9	28	175	300	-	-	-
T 93A (Inj.)	5.6	-	-	-	-	-	-
T 93A (Inj.)	3.5	-	-	-	-	-	-
P 80A (Comp.)	60	4	300	50	1	550	100
P 80A (Comp.)	37	8	300	55	2	600	125
P 80A (Comp.)	23	12	275	50	3	600	150
P 80A (Comp.)	14	18	250	60	4	500	75
P 80A (Comp.)	9	28	200	50	5	430	10
P 80A (Comp.)	5.6	-	-	-	10	350	10
P 80A (Comp.)	3.5	60	150	40	20	-	-
P 80A (Inj.)	60	4	300	100	-	-	-
P 80A (Inj.)	37	8	300	100	-	-	-
P 80A (Inj.)	23	12	275	50	-	-	-
P 80A (Inj.)	14	18	225	50	-	-	-
P 80A (Inj.)	9	28	225	50	-	-	-
P 80A (Inj.)	5.6	60	160	50	-	-	-
P 80A (Inj.)	3.5	-	-	-	-	-	-

compared with the standard (37.5mm) lens resulted in increased ablation damage. Repetition rates of 2Hz were investigated, but the damage at the pore periphery was increased, even when the number of pulses was reduced.

7.7 Tribological Results

7.7.1 Stage I

Cups of Tecoflex 85^oA were tested in the simulator using two of the loading cycles. The layers were modified with an open pattern of holes. Three rings of holes were introduced and the layers tested in the hip function simulator. The results were encouraging with a small increase in frictional values with the 2000/20 loading cycle (figure 7.7a), coefficients of friction of 0.010 being typical. A decrease in friction of approximately 50% under loading cycle II was observed when the porous specimens were used with values of 0.080 being typical (figure 7.7b).

The 6 identical Tecoflex 85^oA cups were tested over the three loading cycles, and revealed a consistent increase in the friction factor for all of the cycles with the addition of pores (figures 7.8a,b,c). This contrasted with the earlier results and indicated that the modification was having a substantial deleterious effect, in particular with loading cycle I. More holes were introduced on concentric circles at angles of 4^o, 12^o, 20^o and 28^o from the central point. Friction again rose with coefficients of 0.35 measured under a constant loading of 1000N. These compared with initial values of less than 0.100 for the unmodified cups.

7.7.2 Stage II

Seven acetabular cups of Pellethane 80^oA were moulded and tested in the simulator. Coefficients of friction for the standard 2000/20N loading cycle were 0.005-0.020 for six of the cups with a range of lubricants from 0.036-0.141Pa s. The

Figure 7.7a: A Stribeck Plot for a Tecoflex 85A Cup before and after Laser modification, tested with Loading Cycle I

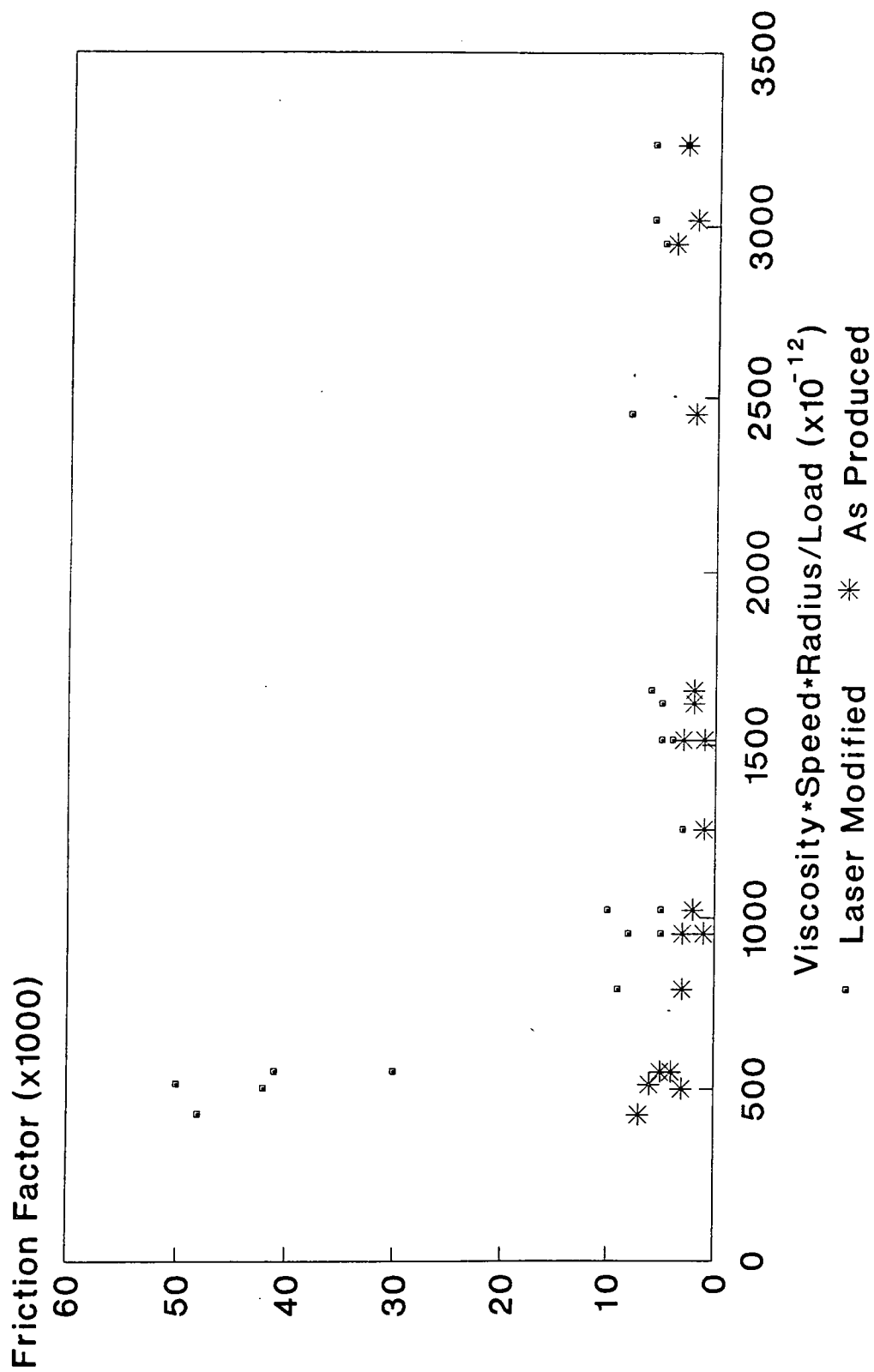


Figure 7.7b: A Stribeck Plot for a Tecoflex 85A Cup before and after laser modification, tested with Loading Cycle II

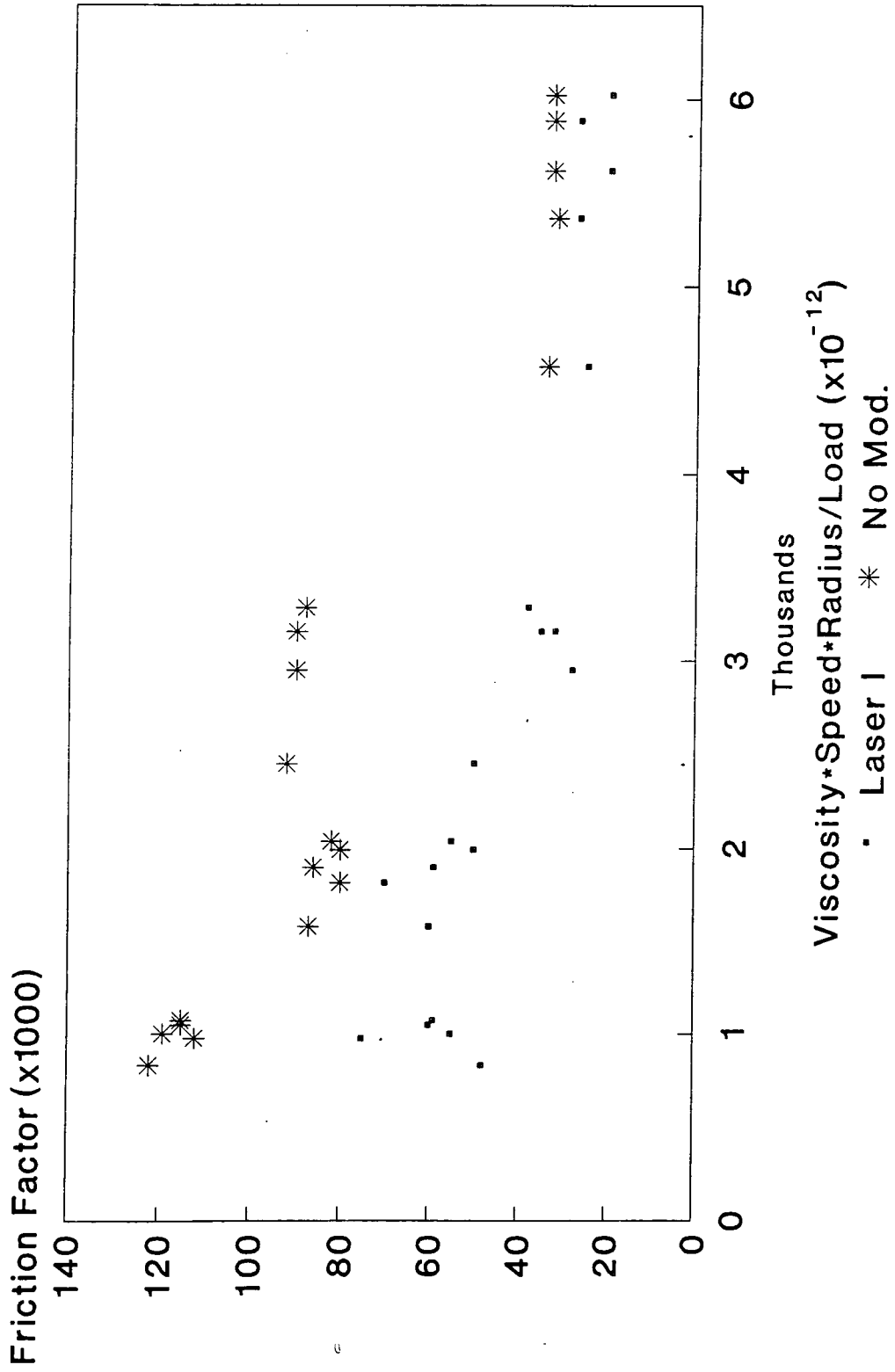


Figure 7.8a: A Stribeck Plot for a Tecoflex 85A Cup before and after Laser modification, tested with Loading Cycle I

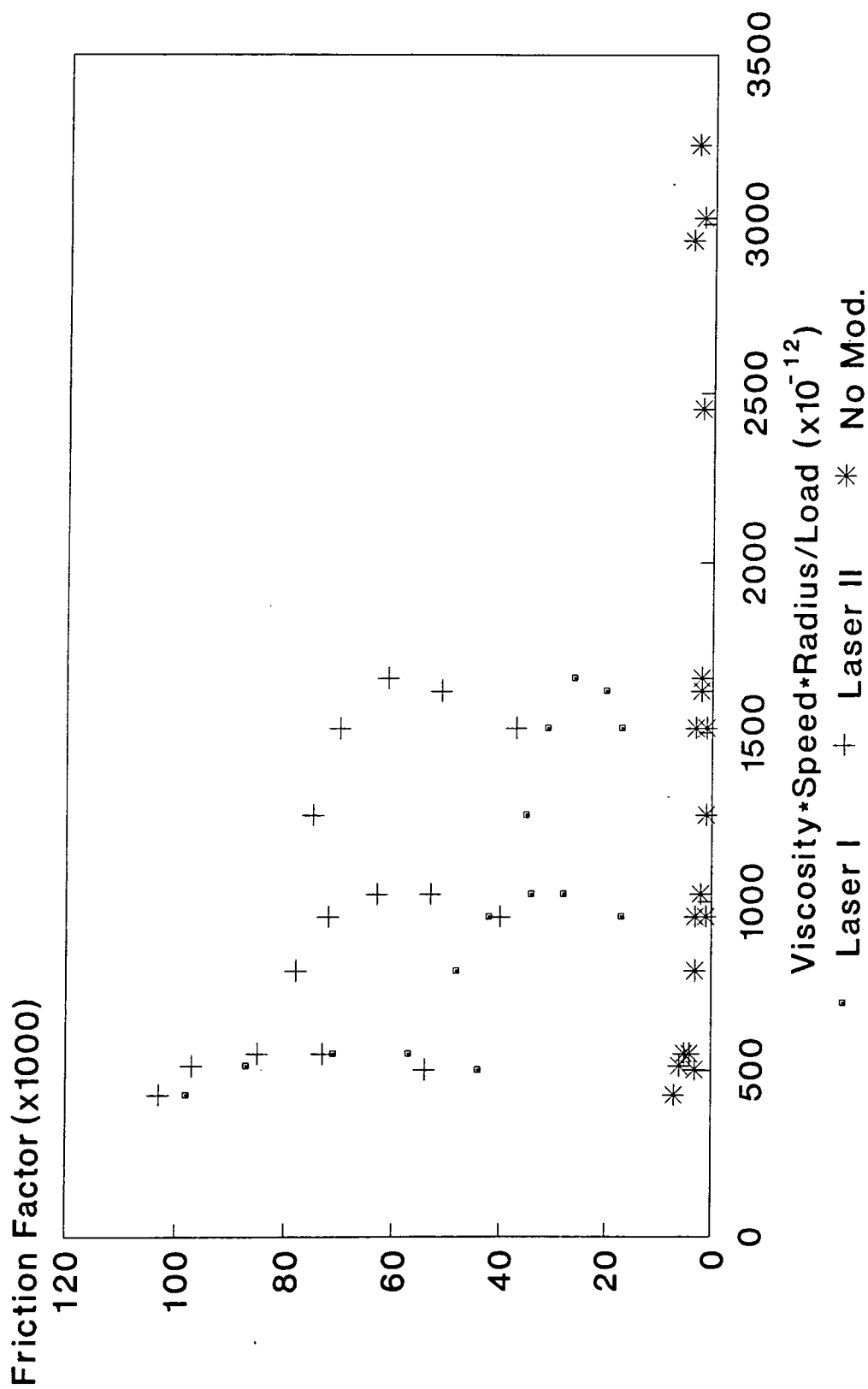


Figure 7.8b:A Stribeck Plot for a Tecoflex 85A Cup before and after laser modification, tested with Loading Cycle II

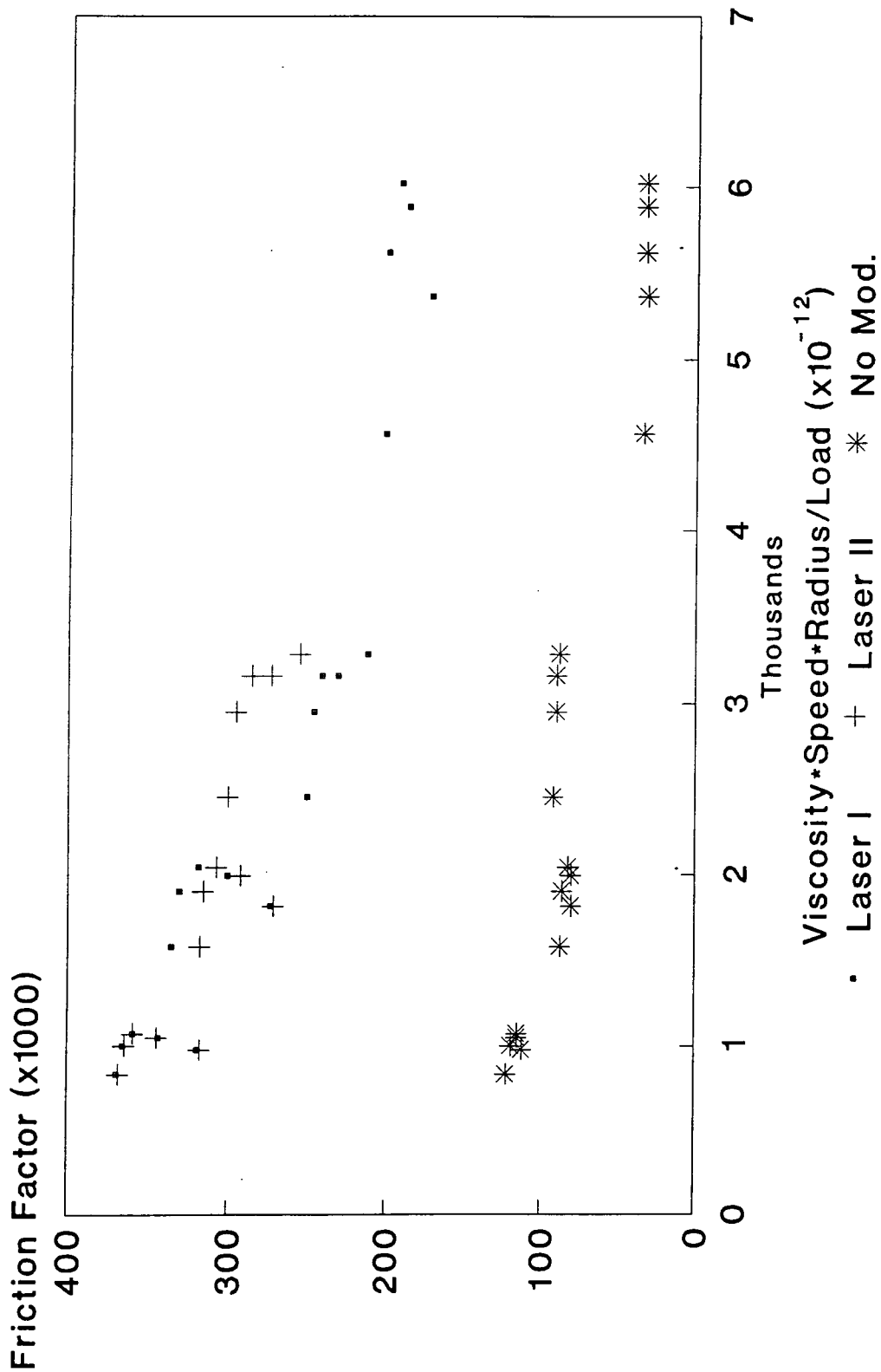
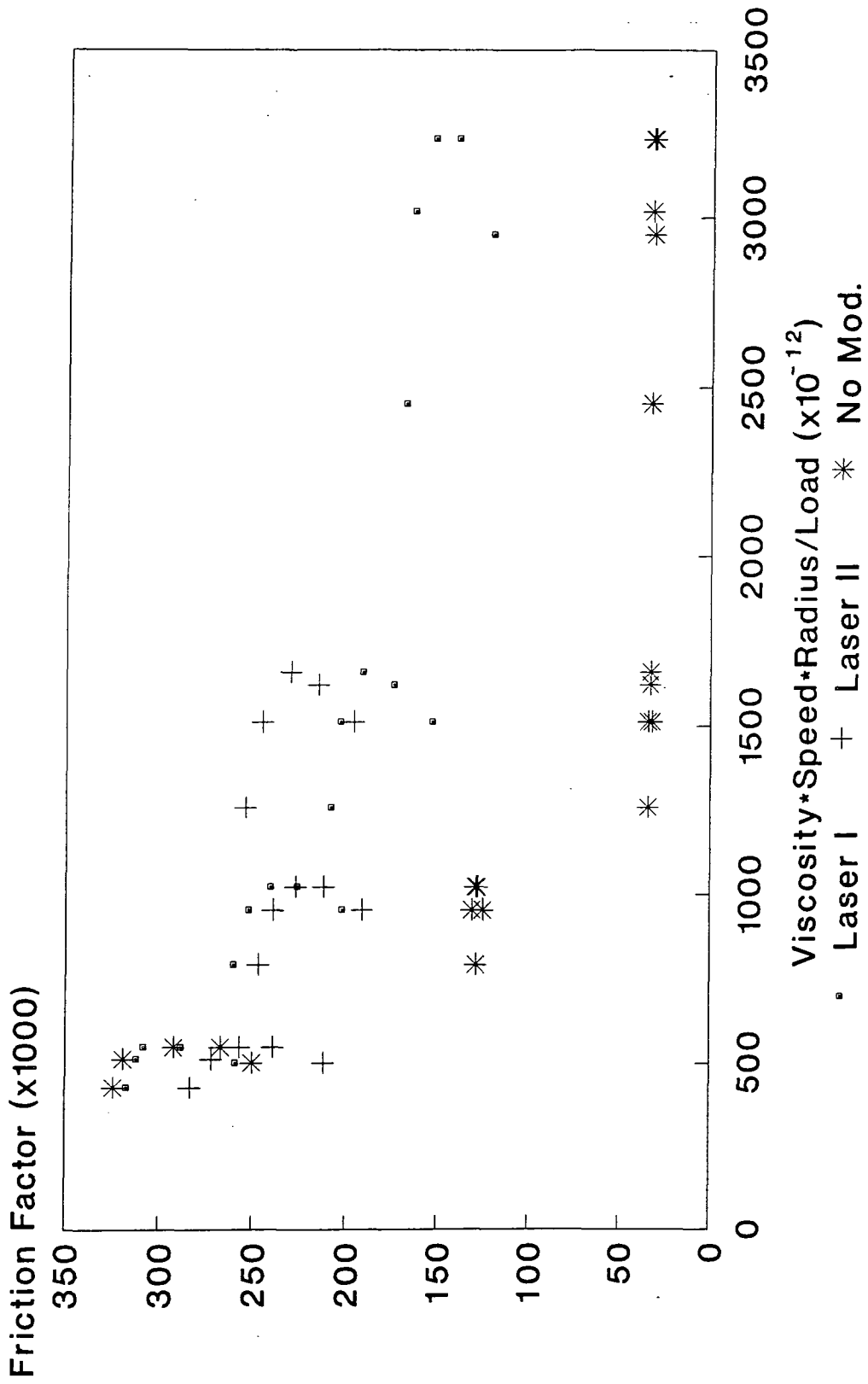


Figure 7.8c: A Stribeck Plot for a Tecoflex 85A Cup before and after laser modification, tested with Loading Cycle III



seventh cup was discounted as it did not exhibit low friction representative of fluid film lubrication. Under loading profiles II and III coefficients of friction increased with successive cycles, but after 21 cycles with profile II the friction was typically 70-140N depending on the lubricant viscosity. After 4 cycles on loading profile III the frictional force ranged from 70-300N over the range of lubricant viscosities. Following laser ablation all of the cups exhibited low friction with loading profile I (circa. 30N) (figure 7.9). Under loading cycle II the friction varied markedly with the lubricant viscosity used and the cup (friction 7.10). Variations were 220-450N using 0.141 and 0.003Pa s lubricants respectively for the highest friction cup. The cup which displayed the lowest friction showed changes of 50-100N over the same viscosity range. Loading profile III gave frictional results of 80-190N for the 0.003Pa s fluid and 30-70N for the 0.141Pa s lubricant (figure 7.11).

7.8 Discussion

The introduction of discrete pores into the surface of the polyurethane layers caused a large change in their tribological properties. Initially little change was noted for the 2000/20N loading cycle, representative of walking. However, a reduction in friction was noted when a constant load was applied. However, when six cups of Tecoflex 85°A were tested in the simulator a detrimental effect for all of the loading cycles was noted. Increases in friction with loading cycle I suggest that fluid film lubrication has been affected and a mixed regime is operating. This is confirmed by Stribeck plots. A falling tendency was noted following laser modification (figures 7.8a), representative of mixed lubrication. The results for the same layer prior to modification are also presented and the lower frictional values and the stable or slightly rising tendency can clearly be seen indicating that fluid film lubrication was taking place. The loss of the full fluid film would result in wear of the polyurethane surface

Figure 7.9 : A Stribeck Plot for the Pellethane samples before and after Laser ablation, tested with Loading Cycle I

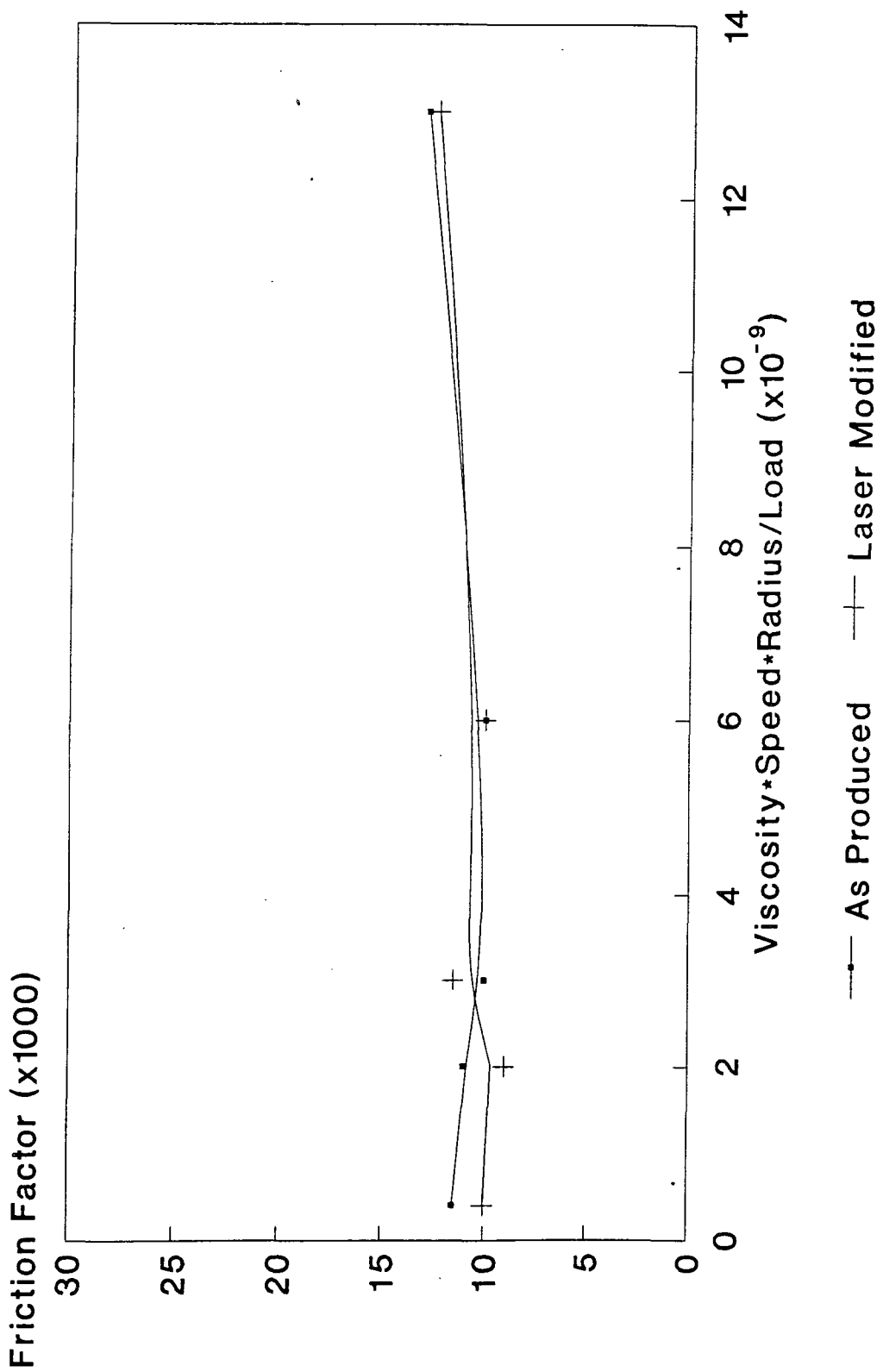


Figure 7.10 : A Stribeck Plot for the Pellethane samples before and after Laser ablation, tested with Loading Cycle II

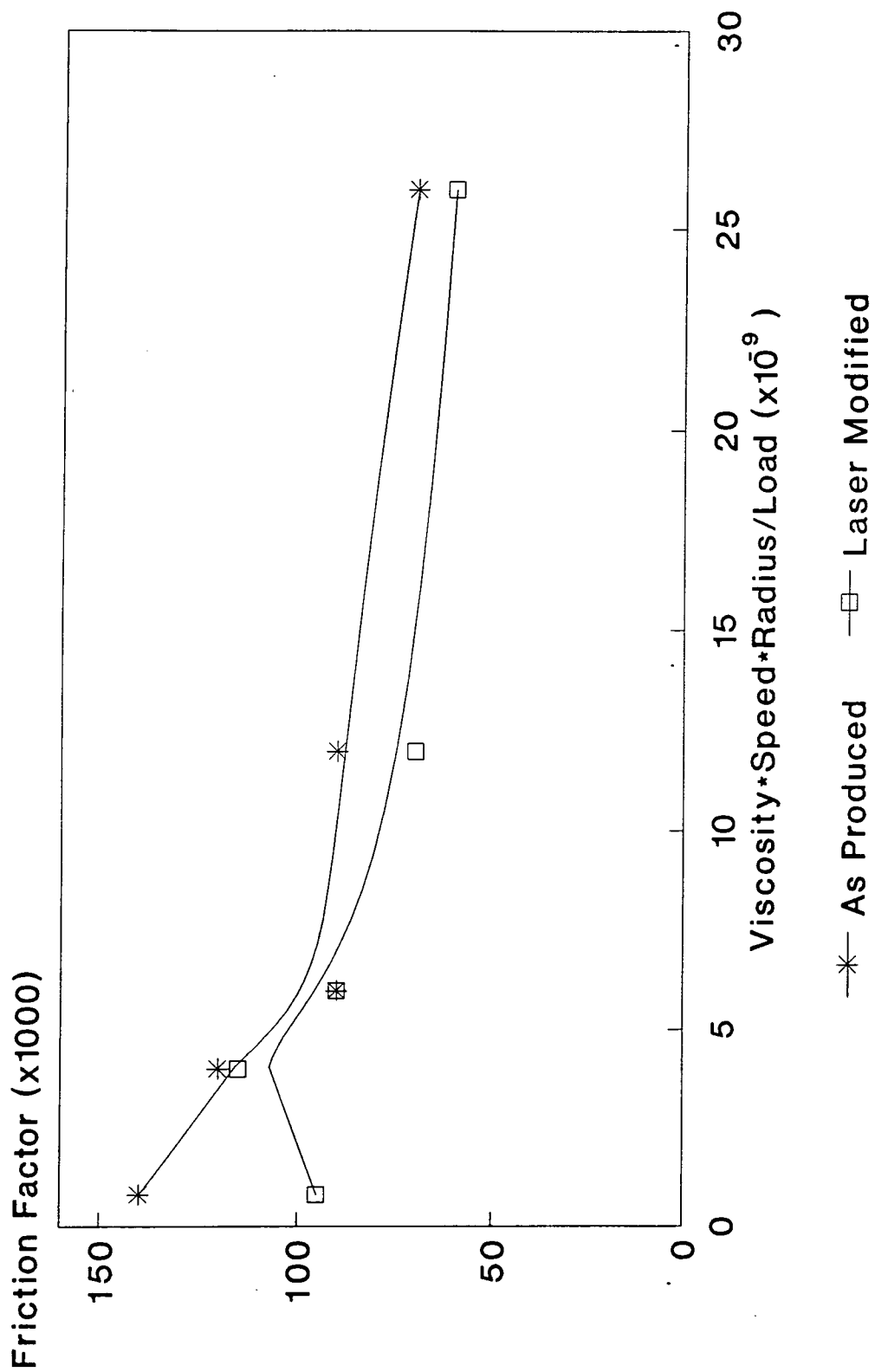
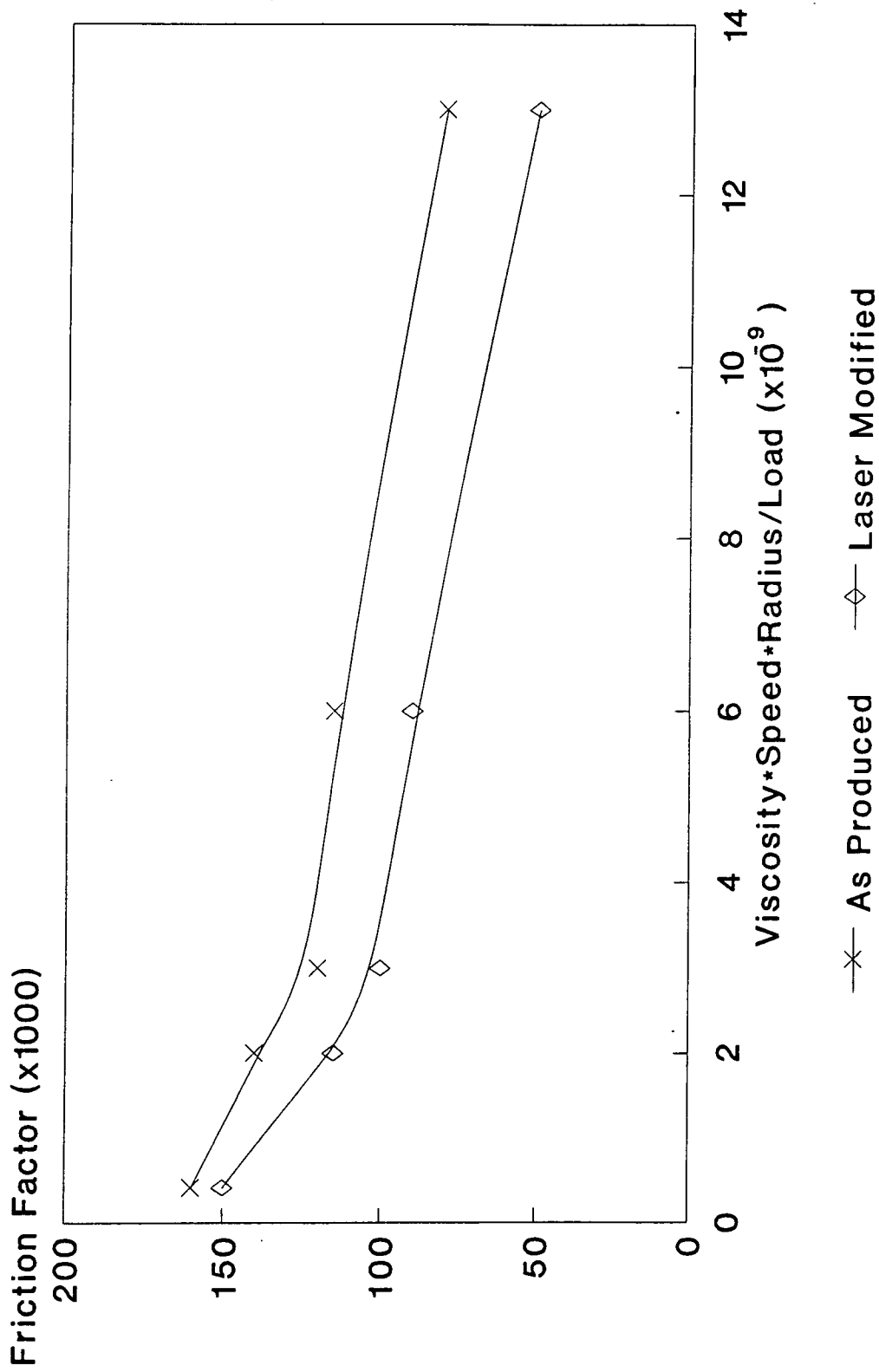


Figure 7.11 : A Stribeck Plot for the Pellethane samples before and after Laser ablation, tested with Loading Cycle III



and higher frictional torques than the currently available devices, which would preclude the use of this material in joint replacement applications.

Loading cycles II and III indicated the response of the prosthesis to EHL only and EHL with reduced Squeeze mechanism respectively. Friction factors reached 0.35, which is not much less than friction for dry rubbing. Use of these loading cycles does show that elastohydrodynamic effects appear to provide some lubrication, as friction values for the unmodified layers were only about 20% of that obtained for dry rubbing of elastomeric layers on steel. In addition, this suggests the importance of both the squeeze and EHL mechanisms for a successful prosthesis. The laser modification, introduced to provide a weeping mechanism to improve lubrication, was largely unsuccessful. Modified layers seemed to move the mode of lubrication towards dry rubbing with friction values 80% of dry values.

The Erbium-YAG laser was chosen because of the relatively small zone of damage around the pores. Its use in bone and soft tissues confirms this. However, the vaporisation of polymer in the formation of the pore is likely to lead to a change in hardness around the hole, which may not be confined to the visibly damaged region (figure 7.5). Unfortunately the change of hardness cannot be measured on such a small scale, no change being detectable using the DIN 53456 hardness test with a 2.5mm radius indenter. The laser modified cups of Stage I contained material raised $20\mu\text{m}$ above the surface prior to modification in the heat affected zone. This material looks to be a product of incomplete vaporization.

Although some deformation of this region will occur during loading the fluid film will tend to be destroyed around the holes increasing the friction substantially. The friction factor of a dry polyurethane/steel contact is very large, approaching 1.0

and so with a lubricated joint showing a friction factor of 0.003 it can be seen that only a small amount of direct contact is needed to increase friction substantially. This was confirmed by the results following testing using the 2000/20N loading cycle. The friction factor doubled as the number of holes and the hole density was also increased by a factor of two.

The other loading cycles indicated that fluid film lubrication was not present throughout the cycle. There was little change in friction as the hole density was doubled. This can be explained by considering the elastic deformation of the raised regions around the holes. In the first case the deformation will tend to be large with a big area of contact for each "hole". When the numbers of holes are doubled then the deformation will be smaller but the actual area of dry contact will be little changed. The friction factor is highly dependent on the area of dry contact and if this is little changed then friction should remain approximately constant.

A further possibility for the poor tribological results is that fluid is not entering the holes. This would seem unlikely considering the pressures developed in the contact area are up to 3MPa and the viscosity of the lubricating fluid are from 0.002 - 0.0165Pa s. The holes were checked using microscopy and this indicated that the entrance to the holes was defect free (figures 7.4 and 7.5). However, if this were the case, the hole would act to provide a pressure relief to the lubricating fluid reducing the load carrying capacity of the fluid film ultimately leading to contact and a mixed lubrication regime. This may lead to the fluid film developed under loading and motion not being sufficiently large to provide full separation of the surfaces, hence leading to mixed lubrication and higher friction.

Study II indicated how important the lasing parameters are as well as the material to be cut. Pellethane was found to be much more suitable as a large range of energies could be used. Vapourisation of Tecoflex 93^oA required lasing parameters within a small range, with both pulse energy and repetition rate important.

Although the results of Study I were discouraging the initial pilot studies proved that good results could be obtained. Further assessment of the need for this sort of surface modification is required as there will be a penalty in the fatigue strength of the urethane layer with the introduction of pores. These will act as stress concentrators and may form sites for crack propagation. Micrographs of the sides and bases of the holes (figures 7.12 and 7.13) indicated the introduction of cracks up to 150 μ m in length.

Stage II of the study using Pellethane layers showed little change in tribological performance with the addition of the pores. Using these results it can be deduced that the pores are either not containing fluid or the effect of weeping lubrication is very small in this application. Either way no significant advantage can be gained by the addition of pores, and the reduced fatigue resistance due to the surface and subsurface cracking cannot be justified in a commercial joint at this stage.

7.9 Conclusions

Soft layers of polyurethane have provided good frictional results when incorporated into artificial joints. However, under static loading the lubrication mechanisms break down and friction increases by many orders of magnitude.

Laser modification provided slightly improved lubrication in a limited number of cases, but there is a requirement for minimal debris at the pore periphery in order to facilitate fluid film lubrication. It was found that variations in the pulse energy and

Figure 7.12 : The surface of the polyurethane at the base of the laser ablated pore

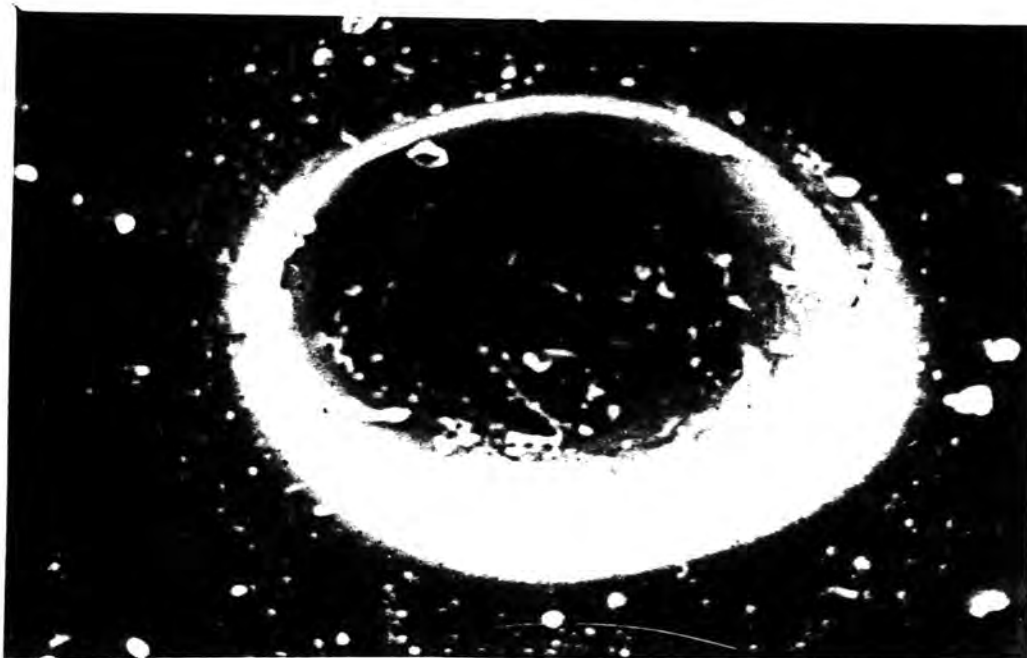
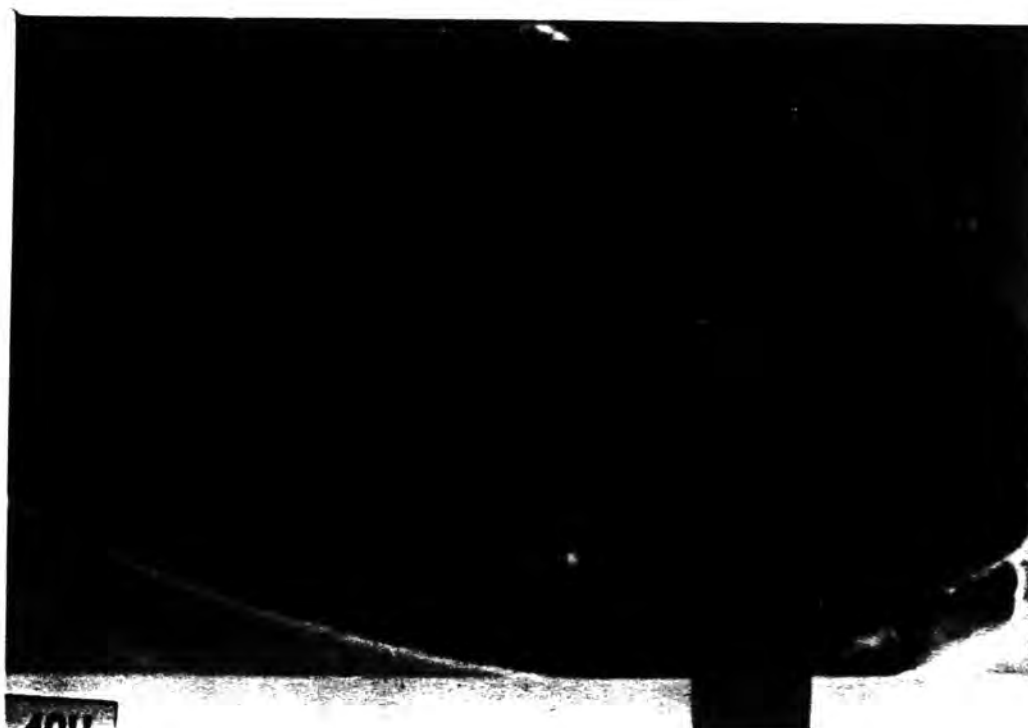


Figure 7.13 : The surface of the polyurethane at the side of the laser ablated pore



repetition rate of the Erbium-YAG laser and the polyurethane material used were very important. Scanning electron microscopy of laser modified strip samples showed that high repetition rates and low pulse energies were required to minimise damage around the pores. Both Tecoflex 93°A and Pellethane responded best to pulse energies of 7mJ, frequencies of 10Hz and between 50 and 100 pulses to produce each pore. Pellethane was much more tolerant of lasing parameters than Tecoflex in the preparation of debris free pores.

Chapter 8 : Conclusions

8.1 Mechanical Properties of Bio-compatible Polyurethanes

Although polyurethanes only hydrate to 1.5-2.0% by mass, the effect of soaking in Mammalian Ringer's solution at a temperature of 37°C was very noticeable. The Tecoflex polyurethanes showed decreases in elastic modulus of 64% for the 93°A grade, and 45% for the 85°A grade, whilst the other bio-compatible polyurethanes showed decreases of 47% for Pellethane and 32% for Estane '57'. The harder materials showed a larger drop in elastic modulus and hardness, which was particularly evident with the 100°A grade of Tecoflex which showed a drop in modulus of 65% when hydrated. Measurements of the hardness of the materials showed a similar pattern, but the reduction in the property with a hydrated material was much less, with a maximum of 35% for Tecoflex 100°A. A large difference between the response of the 100/93°A and the 85°A grades of Tecoflex to the hydration and elevated temperatures was apparent. This may be due to the PTMO (1000) used in the harder grades and the reduction in the quantity of 1,4 Butanediol used in the manufacture of the harder grades (figure 3.3b).

8.2 Degradation and Fatigue Testing of Polyurethanes

Studies of degradation in Mammalian Ringer's solution at 37°C indicated that the smallest changes were noticed with Tecoflex and Pellethane materials, with Estane polyurethanes showing some degree of cracking or crazing (figure 3.7c) and a reduction in elastic modulus. Increases in friction, indicated the breakdown of fluid film lubrication. Fatigue studies of tensile samples in Mammalian Ringer's solution with Tecoflex 93°A and Pellethane 2363-80°A revealed little visual damage or change in elastic modulus after 9 million cycles. The failure strength of fatigued samples was

higher than the controls and similar to the passive samples. Elastic modulus of the fatigued samples showed little difference to the controls up to 400% extension.

8.3 Fabrication of the Prostheses

The fixation of the elastomeric layers to the backing material, which is important in maintaining stability of the joint, has been investigated over the course of the study. A bond formed by moulding the polyurethane pellets into a powdered polyethylene backing at a temperature of 180°C and under a load of 5 tonnes has produced good cup samples. The peel strength of the bond has proved to be good at 10-15N/mm when dry and about 7N/mm when hydrated. Blister tests have concluded that the energy required to cause failure is high, although the scatter of results with this form of testing has also been high.

8.4 Contact Area Measurements and Influence on Performance

Contact area is important in determining tribological performance. Modification of polyethylene joints to yield contact areas of similar dimensions to polyurethane joints resulted in some instances of lower friction but results were not as good as soft layer joints, indicating that micro-EHL (asperity flattening) is an important mechanism.

Silicone rubber, dye transfer and indenter penetration techniques have been used to assess the contact area, with a great deal of success. These techniques were compared with theoretical calculations for UHMWPE joints, and then applied to soft layer joints, for which contact calculations are much more difficult. To allow theoretical calculations of tribological performance, the effective elastic modulus of the layers was determined. This was done using data obtained from simple hardness tests on bonded and lubricated samples of a range of thicknesses.

8.5 Lubrication of Polyurethane and Polyethylene Joints

Theoretical assessment of the lubrication mechanisms indicated fluid film lubrication for the soft layers which was confirmed by experimental studies using the dynamic loading cycle. The polyethylene prostheses showed mixed lubrication which was due to the larger pressures generated at the contact under applied loading and the smaller asperity deflection under the action of micro-EHL.

All of the five polyurethanes used to produce layered prostheses exhibited low friction factors of 0.005 and a rising tendency on the Stribeck curve (coefficient of friction against viscosity * speed * radius / load) indicating fluid film lubrication.

Explanted Charnley arthroplasties showed increased frictional torque when compared with new and unused joints. This could be as a result of cement or bone particle damage and roughening or wear. When the components were tested in isolation it was found that the acetabular cup was responsible for the majority of the increase. However, increases in friction can lead to loosening of the prosthesis because of the increased torque on the joint. This often results in failure of the procedure and the need for revision surgery, making this increase in friction an important consideration.

Inclusion of surface pores into the polyurethane layers was investigated, in order to provide a reservoir of fluid which would drain during periods of high load and low surface velocities (i.e. start up conditions). However, results were inconsistent, possibly due to damage caused by incomplete vaporisation of the elastomer during modification, increasing the friction factor. Further work is required using the laser to determine the parameters required for optimum pore preparation.

8.6 Recommendations for Future Research

Much of the research work which must be done in order to bring this prosthetic device to clinical application will need to concentrate on the manufacturing process used to produce the joint. Although the bond to the backing material has achieved some success and seems to be resistant to the ingress of fluids, the interlock seems mainly mechanical. This is due to the polar UHMWPE surface and modifications to this are currently underway. However, development of an injection mouldable system may remove many of the problems by developing a polymer blend at the interface, graduating hardness and reducing the stresses at the interface. This may require HDPE or some other rigid polymer to be employed. Application of the soft layer theory to the knee may result in a simpler production process.

Accurate measurement of the film thickness between the components of the soft layer hip prosthesis would improve the support for such a prosthetic device. In addition, the technique would have an application in many tribological systems where non-conductive materials were in use. The use of interferometry and fluorescence techniques would be simplified in a knee prosthesis, and this may be the model which should be considered initially.

Accurate analysis of the stresses within a layered acetabular cup is required to optimise the preparation of the acetabular cup. The advantages in strength from the use of a rough surface, or an elastic modulus which varies from 10MPa at the articulating surface to 2000MPa at the back should be calculated. Finite element methods have been used for simplified analysis by the group at Leeds and others, however, the use of this technique is limited and a move to boundary element analysis would be required in order to model the polyurethanes (with their high values of Poisson's ratio) accurately.

References

- Albertson, T. (1992) "The Choice of Implant Materials" SIROT 2nd Inter-Meeting, Bruxelles, July.
- Andrews, E.H., and Stevenson, A. (1978) "Fracture Energy of Epoxy Resin under Plane Strain Conditions" *J. Mat. Sci.* **13**, 1680-1688.
- Armstrong, C.G., Lai, W.M. and Mow, V.C. (1984) "An analysis of the unconfined compression of articular cartilage" *J. Biomech. Engng.* **106** 165-173.
- Armstrong, C.G., (1986) "Analysis of the stresses in a thin layer of articular cartilage in a synovial joint" *Engng. in Med.* **Vol.15 No.2**, 55-62.
- Arnold, J.C. and Hutchings, I.M. (1992) "A model for the corrosive wear of rubber at oblique impact angles" *J. Phys. D: Appl. Phys.* **25**, A222-A229.
- Bannister, G.C. & Miles, A.W. (1988) "The influence of cementing procedure on cementing technique and blood on the strength of the bone-cement interface" *Engng. in Med.* **Vol.17 No.1** 131-35.
- Bennett, A. and Higginson, G.R. (1970) "Hydrodynamic Lubrication of Soft Solids", *J. Mech. Eng. Sci.*, **12 (3)**, 218-222.
- Bernstein, E.F., Cosentino, L.C., Reich, S., Stasz, P., Levine, I.D., Scott, D.R., Dorman, F.D. and Blackshear, P.L. (1974) "A compact, low hemolysis, non-thrombogenic system for non-thoracotomy prolonged left ventricular bypass" *Trans. Am. Soc. Artif. Intern. Organs*, **20**, 643.
- Binnington, P. (1991) "The measurement of Rotary Shaft Seal Film Thickness" PhD. Thesis, University of Durham.
- Black, J.D., Matejczyk, M. and Greenwald, A.S. (1981) "Reversible cartilage staining technique for defining articular weight bearing surfaces" *Clin. Orthop. Rel. Res.*, **159**, 265-267.

- Black, J., Sherk, H., Bonini, J., Rostoker, W.R., Schajowica, F. and Galante, J.O. (1990) "Metallosis associated with a stable Titanium-Alloy femoral component in total hip replacement : A case study", *J. Bone Jt. Surg.*, **72A**, 126-130.
- Blamey, J.M., Rajan, S., Unsworth, A. and Dawber, W.R.K. (1991) "Soft layered prostheses for arthritic hip joints: a study of materials degradation", *J. Biomed. Eng.*, **Vol.13, May**, 180-184.
- Boretos, J.W. and Detmer, D.E. (1970) "In-Vivo stability of segmented polyurethanes" *Proc. 23rd Annual Conf. Eng. Med. Biol.* **12** pp148.
- Boretos, J.W., Detmer, D.E. and Donachy, J.H. (1971) "Segmented polyurethanes: A polyether polymer II. Two years experience" *J. Biomed. Mater. Sci.* **5** 373.
- Brown, D.L. (1988) "Custom made aliphatic polyurethanes for medical use" presented at "Medical Plastics '88 Conference", Oxford, U.K., Sept 8th.
- Buchholz, H.W. Elson, R.A. and Engelbracht, E. (1981) "Management of Deep Infection of Total Hip Replacement" *J. Bone & Jt. Surg.* **63B** 342-353.
- Calnan, J.S. (1963) "The use of inert plastic materials in reconstructive surgery" *Br. J. Plast. Surg.* **16** pp1.
- Charlton, A., Dickenson, M.R. and King, T.A. (1989) "High repetition rate, high average power Er:YAG laser at 2.94 μ m" *Journal of Modern Optics*, **Vol.36 No.10**, 1393-1400.
- Charnley, J. (1970) "Acrylic Cement in Orthopaedic Surgery" E & S Livingston, Edinburgh & London.
- Charnley, J. (1979) "Low Friction Arthroplasty of the Hip" Springer - Verlag, Berlin.
- Chow, L.S.H. and Cheng, H.S. (1976) "The effect of surface roughness on the average film thickness between lubricated rollers" *J. Lub. Technology (ASME)*, **98(1)** 117-124.
- Christensen, H. (1962), "The oil film in a closing gap", *Proceedings Royal Society, London, Ser. A*, **266**, 312.

- Clarke, I.C. (1981) "Wear of Artificial Joint Materials IV : Hip Joint Simulator Studies" *Eng. in Med.*, **Vol.10 No.4** 189-197.
- Cooke, A.F., Dowson, D. and Wright, V. (1978) "The rheology of synovial fluid and some potential synthetic lubricants for degenerate synovial joints" *Engng. in Med.* **7**, 66-72.
- Dasse, K.A. (1984) "Infection of percutaneous devices; prevention, monitoring and treatment" *J. Biomed. Mater. Res.* **18** 403-411.
- Dasse, K.A., Poirier, V.L. and Szycher, M. (1988) "In-vivo Evaluation of Tecoflex Polyurethane" Report obtained directly from Thermedics, USA.
- Davidson, J. (1992) Presentation at Durham University Biomedical Engineering Series, June.
- Davies, D.V. and Palfrey, A.J. (1968) "Some of the physical properties of normal and pathological synovial fluids" *J. Biomechanics*, **1** 79-84.
- Davy, D.T., Kotzar, G.M., Brown, R.H., Heiple, K.G., Goldberg, V.M., Heiple, K.G.Jr., Berilla, J. and Burnstein, A.H. (1988) "Telemetric force measurements across the hip after total arthroplasty" *J. Bone & Jt. Surg.*, **70A(Jan)** 45-50.
- Dawber, W.R.K. and Healey, G. (1991), Materials Science Centre, UMIST, Private Communication.
- Dintenfass, L. (1963) "A theoretical approach to the problem of joint movements and joint lubrication" *J. Bone & Joint Surg.*, **45A**, 1241.
- Dowson, D. (1969) "Transition to Boundary Lubrication from Elasto-hydrodynamic lubrication" Chapter 11 (pp229-240) in *Boundary Lubrication - An appraisal of the World Literature*. Eds. F.F.Ling, E.E.Klaus & R.S.Fein., ASME Publications.
- Dowson, D, Unsworth, A and Wright, V. (1970) "Analysis of 'Boosted Lubrication' in Human Joints", *J. Mech. Eng. Sci.*, **12(5)**, 364-369
- Dowson, D. and Jin, Z-M. (1986) "Micro-Elastohydrodynamic Lubrication of Synovial Joints", *Engng. in Med.*, **Vol.15 No.2** 63-66.

- Dowson, D., Fisher, J., Jin, Z.M., Auger, D.D. and Jobbins, B. (1991) "Design Considerations for Cushion Form Bearings in Artificial Hip Joints" *Proc. Instn. Mech. Engrs., Part H : Journal of Engineering in Medicine*, Vol. 205 (H2), 59-68.
- Dowson, D. and Yao, J.Q. (1992) "A study of the deformation and lubrication of synovial joints" *Proc. Instn. Mech. Engrs., Part H : Journal of Engineering in Medicine*, Awaiting Publication.
- Dressel, M., Jahn, R., Neu, W. and Jungbluth, K-H. (1992) "Studies in Fiber Guided Excimer Laser Surgery for Cutting and Drilling Bone" *Lasers in Surgery and Medicine*, Vol.11 No.6, 569-579.
- Eberhardt, A.W., Keer, L.M., Lewis, J.L. and Vithoontien, V. (1990) "An Analytical Model of Joint Contact" *ASME J. Biomech. Eng.*, Vol.112 Nov., 407-413.
- Engh, C.A., Green, W.L. and Marx, C.L. (1990) "Cementless Acetabular Components" *J. Bone & Jt. Surg.* 72B No.1 53-59.
- English, T.A. and Kilvington, M. (1979) "In-Vivo records of hip loads using a femoral implant with telemetric output", *Biomed. Eng.*, 1, 111-115.
- Farquar, T., Damwson, P.R. and Torzilli, P.A. (1990) "A Microstructural model for the anisotropic drained stiffness of articular cartilage" *ASME J. Biomechanical Engineering* Vol.112 (Nov), 414-425.
- Fein, R.S. (1967) "Are synovial joints squeeze film lubricated?" *Proc. Instn. Mech. Engrs.* 181(3J), 125-128.
- Ford, R.A.J. and Foord, C.A. (1978) "Laser-based fluorescence techniques for measuring thin liquid films" *Wear*, 51, 289-297.
- Fote, A.A., Slade, R.A. and Feuerstein, S. (1978) "The behavior of thin oil films in the presence of porous lubricant reservoirs", *Wear*, 46, 377-385.
- Freeman, M.A.R. (1979) "Adult Articular Cartilage", Pitman Medical, London.
- Gaman, I.D.C., Higginson, G.R. & Norman, R. (1974) "Fluid entrapment by a soft surface layer", *Wear*, 28, 345-352.

- Gardner, D.L. and Woodward, D. (1969) "Scanning Electron Microscopy and replica studies of articular surfaces of guinea pig's synovial fluid" *Ann. Rheum. Dis.*, **28**, 379.
- Gardner, D.L. (1972) "The influence of microscopic technology on knowledge of cartilage surface structure" *Ann. Rheum. Dis.* **31(4)** 235-258.
- Gibbons, D.F. (1978) "Polymeric Biomedical Materials" *The British Polymer Journal*, **Vol.10**, Dec. 232-237.
- Gibbs, D.A., Merrill, E.W., Smith, K.A. and Balazs, E.A. (1968) "Rheology of Hyaluronic Acid" *Biopolymers*, **6**, 777.
- Gore, D.M., Higginson, G.R. and Minns, R.J. (1983) "Compliance of articular cartilage and its variation through the thickness" *Phys. Med. Biol.*, **Vol. 28 No. 3**, 233-247.
- Gore, T.A., Higginson, G.R. and Kornberg, R.E. (1981) "Some evidence of Squeeze Film Lubrication in Hip Prostheses" *Engng. Med.*, **10 (2)**, 89-95.
- Graham, J.D. and Walker, T.W. (1973) "Motion of the Hip: The relationship of split line patterns to surface velocities" in "Perspectives in Biomedical Engineering" pp161-165 ed Kenedi, R.M., Macmillan Press, London.
- Gruebel-Lee, D.M. (1983) "Disorders of the Hip" Chapter 14 "Replacement Arthroplasty - Long Term Prosthetic Failure" pp241, J.B.Linnincott, Philadelphia.
- Guo, H. and Lou, Q. (1991) "Cumulative effect near ablation threshold of polymer by 308nm excimer laser pulse" *J. Appl. Phys.* **70 (4)**, 2333-2336.
- Gupta, J.L. and Patel, K.P. (1975) "Effect of axial pinch on the porous walled squeeze film with velocity slip", *Wear*, **31**, 381-389.
- Hall, R.W. (1990) "Pressure Spikes in Elastohydrodynamics - Some elastic considerations" *Wear*, **23 (3)**, pp129-135.
- Hamrock, B.J. and Dowson, D. (1977) "Isothermal Elastohydrodynamic Lubrication of Point Contacts III: Fully Flooded Conditions" *J. Lubrication Technology* **99**, 264-276.

- Hastings, G.W. (1978) "Load Bearing Polymers used in Orthopaedic Surgery" *The British Polymer Journal*, Vol.10, Dec., 251-255.
- Hepburn, C., (1982) "Polyurethane Elastomers", Applied Science, London, pp350.
- Hennig, E. and Bucherl, E.S. (1984) "Mineralization of circulatory devices made of polymers" in "Polurethanes in Biomedical Engineering" pp109-134.
- Herrebrugh, K. "Elastohydrodynamic squeeze films between two cylinders in normal approach", *J. Lub. Tech.*, Series F No.2, 292-302.
- Higginson, G.R. and Norman, R. (1974) "The lubrication of porous elastic solids with reference to the functioning of human joints", *J. Mech. Eng. Sci.*, 16, 250-257.
- Higginson, G.R. (1977) "Elastohydrodynamic lubrication in human joints" *Proc. Instn. Mech. Engrs.* 191, 217-223.
- Higginson, G.R. (1978) "Squeeze Films between Compliant Solids" *Wear*, 46, 387-395.
- Higginson, G.R. and Snaith, J.E. (1979) "The Mechanical Stiffness of Articular Cartilage in confined oscillating compression", *J. Engng. Med.*, 8 (1), 11-14.
- Homsey, C.A., Stanley, R.F. and King, J.W. (1973) "Pseudo-synovial fluids based on sodium carboxymethylcellulose" in *Rheology of Biological Systems*, pp278-298 Eds. Gabelnich, H.L. and Litt, M. Springfield, Illinois.
- Hooke, C.J., Brighton, D.K. and O'Donoghue, J.P. (1967) "The effect of elastic distortions on the performance of thin shell bearings", *Proc. Instn. Mech. Engrs.*, 181, Part 3B 63-69.
- Isaac, G.H., Wroblewski, B.M., Atkinson, J.R. and Dowson, D. (1992) "A tribological Study of Retrieved Hip Prostheses" in *Clinical Orthopaedics and related research*, Eds. E.A.Salvati and A.H.Burstein, No. 276, March, 115-125.
- Jackson, A. and Cameron, A. (1976) "An Interferometric Study of the EHL of Rough Surfaces", *Trans. ASLE*, 19(1), 50-60.

- Jaffar, M.J. (1989) "Asymptotic behavior of thin elastic layers bonded and unbonded to a rigid foundation" *Int. J. Mech. Sci.*, **31 (3)**, 229-235.
- Jin, Z-M. (1988) "Micro-Elastohydrodynamic Lubrication of Human Joints" PhD. Thesis, University of Leeds.
- Jin, Z-M., Dowson, D. and Fisher, J. (1991) "Stress Analysis of Cushion Form Bearings" *Proc. Instn. Mech. Engrs. Part H : Journal of Engineering in Medicine*, **Vol.205 (H4)**, 219-226.
- Jin, Z-M. (1992), Private Communication.
- Johnson, G.R., Dowson, D. and Wright, V. (1977) "The elastic behavior of articular cartilage under sinusoidally varying compressive stress" *Int. J. Mech. Sci.* **19**, 301-308.
- Johnson, R.L. (1969) discussion to "Separation of Principal Stresses" by A. Kuske, *Experimental Mechanics*, **Sept.**, 432.
- Judet, J. and Judet, R. (1950) "The use of an artificial femoral head for arthroplasty of the hip joint", *J. Bone Jt. Surg.*, **32B**, 166.
- Jurvelin, J., Saamanen, A-M., Arokoski, J., Helminen, H.J., Kiviranta, I. and Tammi, M. (1988) "Biomechanical properties of Canine knee articular Cartilage as related to Matrix Proteo-Glycans and Collagen" *Engng. in Med.* **Vol.17 No.4** 157-162.
- Kilvington, M. and Goodman, R.M.F. (1981) "*In-vivo* hip joint forces recorded on a strain gauged "English" Prosthesis using an implanted transmitter", *Engng. in Med.*, **10**, 175-187.
- King, T. "New developments in lasers for cutting hard and soft tissues", Keynote Lecture in session "Novel methods of cutting hard and soft tissues" 30th annual meeting of Biological Engineering Society, Durham, Sept 19-20, 1990.
- Kodnir, D.D. and Zhilnikov, E.P. (1976) "An investigation into the field of elastohydrodynamics", *J. Lub. Technology (ASME)*, **98(4)** 491-499.

- Kopchok, G., Gottlob, C., Tabbara, M. and White, R. (1992) "Ho-YAG laser ablation of human inter-vertebral disks - preliminary investigation" *Lasers in Surgery and Medicine*, Vol.11 No.3 Suppl.1, 216-225.
- Kuske, A. (1968). "Separation of Principal Stresses in the Freezing Method." *Experimental Mechanics*, Aug., 384.
- Laberge, M., Kirkley, S. and Drovin, G. (1992) "In-Vitro and In-Vivo contact mechanics of hemiarthroplasty surfaces" Presented at the SIROT 2nd Inter-Meeting, July, Brussels.
- Lelah, M.D. and Cooper, S.L. (1986) " Polyurethanes in Medicine" pp206 CRC Press, Florida.
- Lemm, W. (1984) "Bio-degradation of Polyurethanes" in *Polyurethanes in Biomedical Engineering* pp103-108.
- Lemm, W. and Buckerl, E.S. (1984) "Preparation and quality control of polyurethane solutions" in *Polyurethanes in Biomedical Engineering* Eds. Plank, H., Egbers, G. and Syre, I. pp201-208.
- Li, J. and Hutchings, I.M. (1990) "Resistance of Cast Polyurethane Elastomers to Solid Particle Erosion", *Wear*, 135, 293-303.
- Lichtarowicz, A. (1990) "Use of water jets for cutting in medicine" Presented at the 30th Annual Meeting of BES, University of Durham, Sept.
- McCutchen, C.W. (1962) "The frictional properties of animal joints" *Wear*, 5, 1-17.
- Mak, A.F. (1986) "The apparent Viscoelastic Behavior of Articular Cartilage - The contributions from the intrinsic matrix viscoelasticity and interstitial fluid flows" *ASME J. Biomechanical Engineering* Vol.108 123-130.
- Mansour, J.M. and Mow, V.C. (1977) "On the Natural Lubrication of Synovial Joints: Normal and Degenerate" *J. Lubrication Technology* (April) 163-172.
- Maroudas, A. (1967) "Hyaluronic Acid Films", *Proc. Instn. Mech. Engrs.* 181, 122-124.

- Mathieson, E.B., Lindgren, J.U., Reinholt, F.P. and Sudmann, E. (1987) "Tissue reactions to wear products from polyacetal (Delrin) and UHMW Polyethylene in Total Hip Replacement" *J. Biomed. Mater. Res.* Vol.21 459-466.
- Mathys, R. and Burri, P. (1983) "The Isoelastic Principle" in *Disorders of the Hip* Chapter 15, Gruebel-Lee, D.M.
- Meachim, G. and Stockwell, R.A. (1979) "The Matrix" in *Adult Articular Cartilage* pp1-66 Ed. Freeman, M.A.R. Pitman Medical, London.
- Medley, J.B., Dowson, D. and Wright, V. (1984) "Transient elasto-hydrodynamic lubrication models for the human ankle joint", *Engng. Med.*, **13**, 137-151.
- Moore, D.F. (1978) "Scale effects in Elastohydrodynamic Lubrication for Rubberlike materials", in *Surface Roughness Effects in Lubrication, Proceedings of the 4th Leeds-Lyon Symposium on Tribology*, Eds. D. Dowson, C.M. Taylor, M. Godet and D. Berthe. Mechanical Engineering Publications, Bury St. Edmonds, 315-320.
- Murray, M.P., Drought, A.B. and Kay, R.C. (1964) "Walking Patterns of Normal Men" *J. Bone & Jt. Surg.* **64A**, 335-360.
- Nyilas, E. (1972) "Development of blood compatible elastomers II : Performance of Avcothane blood contact surfaces in experimental animal implantations" *J. Biomed. Mater. Res. Symp.*, **3** 97-127.
- Olgar, A.C. and Tavallaey, S.S. (1987) "Elastohydrodynamisk Smorjning, Experimentella undersokningar for att visa inverkan av ytojamnheter pa oljefilmsupbyggnaden, Chalmers, tekniska hogskola, Sweden. (From Binnington, P. 1991)
- Oonishi, H., Yamamoto, M., Ishimaru, H., Tsuji, E., Kushitani, S., Aono, H. and Ukon, Y. (1989) "The effect of Hydroxyapatite coatings on bone growth into porous Titanium Alloy Implants" *J. Bone Jt. Surg. (Br)* Vol.71B No.2, 213-216.
- Parins, D.J., McCoy, K.D., Harvath, N.J. and Olson, R.J. (1985) "In-Vivo degradation of a polyurethane", *Preclinical Studies, Corrosion and Degradation of*

- Implant Materials: Second Symposium, ASTM STP 859*, (Eds) Fraker, A.C. & Griffin, C.D., ASTM, Philadelphia, 1985, pp322-339.
- Paul, J.P. (1967) "Force transmitted by joints in the human body" in *Lubrication and wear in living and artificial human joints, Proc. Instn. Mech. Engrs. Vol.181 Pt.3J*, 8-15.
- Paul, J.P. (1976) "Force Actions Transmitted by Joints in the Human Body" *Proc. R. Soc. London., Ser. B*, 163-172.
- Pons, M., Joubert, O., Paniez, P. and Pelletier, J. (1991) "Plasma etching of polymers: A reinvestigation of temperature effects" *J. Appl. Phys.* **70** (4), 2376-2379.
- Pinkus, O. and Sternlicht, B. (1961) "Theory of Hydrodynamic Lubrication", pp 233-234, McGraw-Hill.
- Redler, I., (1962) "Polymer Osteosynthesis" *J. Bone Jt. Surg.*, **44**[A], 1621.
- Reynolds, O. (1886) "On the theory of lubrication and its appliacion to Mr. Beauchamp Tower's experiments including an experimental determination of olive oil" *Phil. Trans. Royal Soc.*, **177 Part 1**, 157-234.
- Roberts, A.D. (1971) "Squeeze Films between Rubber and Glass", *J. Phys. D*, **4**, 423.
- Rydell, N.W. (1966) "Forces acting on the femoral head prosthesis" *Acta. Orthop. Scand. Suppl.* **88**.
- Sayles, R.S., Thomas, T.R., Sanderson, J., Haslock, I. and Unsworth, A. (1979) "Measurements of the surface geometry of articular cartilage" *J. Biomechanics* **12**(3) 257-267.
- Schollenberger, C.S. and Stewart, F.D. (1971), "Thermoplastic Polyurethane Hydrolysis Stability", *J.Elastoplast.*, **3**, 28.
- Semlitsch, M., Lehmann, M., Weber, H., Doerre, E. and Willert, H.G. (1977) "New prospects for a prolonged functional life span of artificial joints using the material combination Polyethylene / Aluminium Oxide Ceramic metal" *J. Biomech. Mater. Res.*, **11**, 294-303.

- Shukla, J.B. (1978) "A new theory of lubrication for rough surfaces", *Wear*, **49**, 33-42.
- de Silva, G.M.S. and Sayles, R.S. (1986) "The influence of surface topography on the lubricant film thickness in an Elastohydrodynamic Point Contact" in *Mechanisms and Surface Distress, Proceedings of the 12th Leeds-Lyon Symposium on Tribology*, Eds. D.Dowson, C.M.Taylor, M. Godet and D. Berthe, Butterworths, 258-272.
- Simon, W.H. (1970) "Scale Effects in Animal Joints 1. Articular Cartilage thickness and compression stress" *Arth. Rheum.*, **13**, 244-254.
- Smeathers, J.E. and Wright, V. (1990) "New Engineering Concepts and Alternative Materials for Prostheses" *Proc. Instn. Mech. Engrs. Part H : Journal of Engineering in Medicine*, **Vol.204**, 259-261.
- Smith-Peterson, M.N. (1948) "Evaluation of the mould arthroplasty of the hip joint", *J. Bone Jt. Surg.*, **30B**, 59.
- Spowart, A.R. (1978) "Real Time Determination of Oil Film Thickness by Neutron Imaging and Scattering" *Wear*, **49**, 195-196.
- Stinson, J.T. and Scheller, Jr., A.D. (1983) "Clinical Evaluation of the Symptomatic Total Hip Replacements" Chapter 1 in *Revision Total Hip Arthroplasty* Turner, R.H. and Scheller, A.D., Grune and Stratton, New York and London.
- Stokes, K. (1984) "Environmental stress cracking in implanted polyether polyurethanes" in *Polyurethanes in Biomedical Engineering* pp243-256.
- Strozzi, A. (1992) "Contact Stresses in Hip Replacements" PhD. Thesis, University of Durham.
- Swann, A.C. and Seedham, B.B. (1989) "Improved techniques for measuring the indentation and thickness of articular cartilage" *Proc. Instn. Mech. Engrs. Part H : Journal of Engineering in Medicine* **Vol.203** 143-150.
- Szeri, A.Z. (1980) *Tribology : Friction, Lubrication and Wear*. McGraw-Hill, New York.

- Szycher, M., Poirier, V. and Keiser, J. (1977) "Selection of materials for ventricular assist pump development and fabrication" *Trans. Am. Soc. Artif. Organs*, **23**, 116.
- Taylor, D., Moalic, J.M., Clarke, F.M., McCormack, B. and Sheehan, J. (1988) "Fibre Reinforcement of Bone Cement" *Engng. in Med.*, **Vol.17 No.1**, 31-35.
- Taylor, D.J. and Kragh, A.M. (1970) "Determination of the rigidity modulus of thin soft coatings by indentation methods" *J. Physics D: Appl. Phys.*, **3**, 29-32.
- Thompson, and Sezgin, (1962)
- Ting, L.L. (1972) "Engagement behavior of lubricated porous annular discs", *Wear*, **34**, 159-188.
- Ulrich, H. and Bonk, H.W. (1984) "Emerging biomedical applications of polyurethane elastomers" in *Polyurethanes in Biomedical Engineering*, pp165-180.
- Unsworth, A., Dowson, D. and Wright, V. (1975) "Some new evidence on Human Joint Lubrication" *Ann. Rheum. Dis.*, **Vol.34**, 277-285.
- Unsworth, A. (1978) "The effects of Lubrication in Hip Joint Prostheses" *Phys. Med. Biol.*, **23** 253-268.
- Unsworth, A., Roberts, B.J. and Thompson, J.C. (1981) "The Application of Soft Layer Lubrication to Hip Prostheses" *J. Bone & Jt. Surg.*, **63B** 297.
- Unsworth, A., Percy, M.J., White, E.F.T. and White, G. (1987) "Soft Layer Lubrication of Artificial Hip Joints" *Proc. Instn. Mech. Engrs. Tribology Volume*, 715-724.
- Unsworth, A., Percy, M.J., White, E.F.T. and White, G. (1988) "Frictional Properties of Artificial Hip Joints" *Engng. in Med.*, **Vol.17 No.3**, 101-104.
- Villacin, A.B. and Bullough, P.G. (1977) "The response of the tissue to the implanted joint endoprosthesis" in *Human Joints and their artificial replacements*, pp409-422, C.C. Thomas Publishing, Springfield, Illinois.

- Walker, P.S., Unsworth, A., Dowson, D., Sikorski, J. and Wright, V. (1970) "Mode of aggregation of hyaluronic acid protein complex on the surface of articular cartilage" *Ann. Rheum. Dis.* **Vol.29 No.6**, 591-602.
- Walker, P.S. and Hajek, J.V. (1972) "The load bearing area in the knee joint" *J. Biomech.*, **5**, 581-589.
- Waters, N.E. (1965) "The indentation of thin rubber sheets by spherical indentors" *Brit. J. Appl. Phys.* **Vol.16**, 557-563.
- Williams, D.F. (1982) "Review: Biodegradation of Surgical Polymers" *J. Mat. Sci.* **17** 1233-1246.
- Willert, H. and Semlitsch, M. (1976) "Tissue reactions to plastic and metallic wear products of joint endoprotheses" in *Total Hip Protheses*, pp205-238, Williams and Wilkins, Baltimore.
- Wilson, J. and Hawkes, J.F.B. (1987) "Lasers : Principles and Applications", pp195-196, Prentice Hall, London.
- Wu, H. (1971) "The squeeze film between rotating porous annular disks", *Wear*, **18**, 461-470.
- Wu, H. (1978) "A review of porous squeeze films", *Wear*, **47**, 371-375.
- Yao, J.Q. and Seedhom, B.B. (1991) "A new technique for measuring contact areas in human joints-the '3S technique'" *Proc. Instn. Mech. Engrs. Part H : Journal of Engineering in Medicine*, **Vol. 205(H2)**, 69-72.
- Zhang, Y.T. (1987) "Linear Deformation of a Journal Bearing and its relationship to hydrostatic pressure" *Wear*, **115**, 41-52.

Bibliography

- Cameron, A. and Ettles, C.M.Mc. "Basic Lubrication Theory - 3rd Edition", Ellis Horwood, John Wiley, New York.
- Dowson, D. and Higginson, G.R. "Elastohydrodynamic Lubrication" (1977), Pergamon Press, Oxford and New York.
- Dowson, D. and Jobbins, B. (1988) "Design and Development of a versatile hip joint simulator and a preliminary assessment of wear and creep in Charnley total replacement hip joints", *Eng. in Med.*, Vol.17 No.3 111-117.
- Dugdale, D.S. & Ruiz, C., "Elasticity for Engineers" (1971), McGraw-Hill, Maidenhead.
- Freeman, M.A.R (Ed) "Adult Articular Cartilage" (1979), Pitman Medical, London.
- Higginson, G.R. and Unsworth, A. (1981) "The lubrication of natural joints" Chapter III in *Tribology of natural and artificial joints* Ed. Dumbleton, J.H. Elsevier 47-73.
- Lees, W.A. "Adhesives in Engineering Design" (1984), The Design Council, Springer-Verlag, Berlin and New York.
- Lelah, M.D. and Cooper, S.L. "Polyurethanes in Medicine", (1986), CRC Press, Florida.
- Moore, D.F. "The Friction and Lubrication of Elastomers" (1972), Pergamon Press, Oxford and New York.
- Moore, D.F. "The Principles and Applications of Tribology" (1975), Pergamon Press, Oxford and New York.
- Manley, R.S, "Adhesion in Biological Systems" (1970), Academic Press, New York & London.
- Parker, R.S.R. and Taylor, P. "Adhesion and Adhesives" (1966), Pergamon Press, Oxford and New York.
- Thomas, T.R. "Rough Surfaces" (1982), Longman Group, New York.

Planck, H., Egbers, G. and Syre, I. (Eds)(1984) "Polyurethanes in Biomedical Engineering", Elsevier, Amsterdam and New York.

Timoshenko, S.P. and Goodier, J.N. "Theory of Elasticity, Edition 3" (1970), McGraw-Hill

Turner, R.H. and Scheller, A.D. (Eds) "Revision Total Hip Arthroplasty", Grune and Stratton, New York and London.

Williams, D. (Ed) (1976) "Bio-compatibility of Implant Materials", Pitman Medical, Bath.

Engineering Standards

BS 903 Part A26 (1969) "Methods of Testing Vulcanised Rubber : Determination of Hardness.

BS 903 Parts A49-A51 (1984) "Methods of Testing Vulcanised Rubber".

BS 3518 Parts 1 & 3 (1963) "Methods of Fatigue Testing : General Principles and Direct Stress Fatigue Tests"

BS 5350 Parts C9-C14 on Peel Testing Methods.

BS 7251/1 - 1990 "Part I : Specifications of General Requirements"

BS 7251/8 - 1990 "Part VIII : Orthopaedic Joint Prostheses"

BS 7252 - 1990 "Metallic Materials for Surgical Implants"

BS 7253/2 - 1990 "Part II : Specification for Ceramic Materials based on Alumina"

BS 7253/5 - 1990 "Part V : Non-Metallic Materials for Surgical Implants"

DIN 53456 (January 1973) "Testing of Plastics : Indentation Hardness Test".

Appendix I - Mamalian Ringer's Solution

The Mamalian Ringer's solution contained the following chemicals in 1 litre of distilled water. Ten litre batches were made throughout the degradation and fatigue studies.

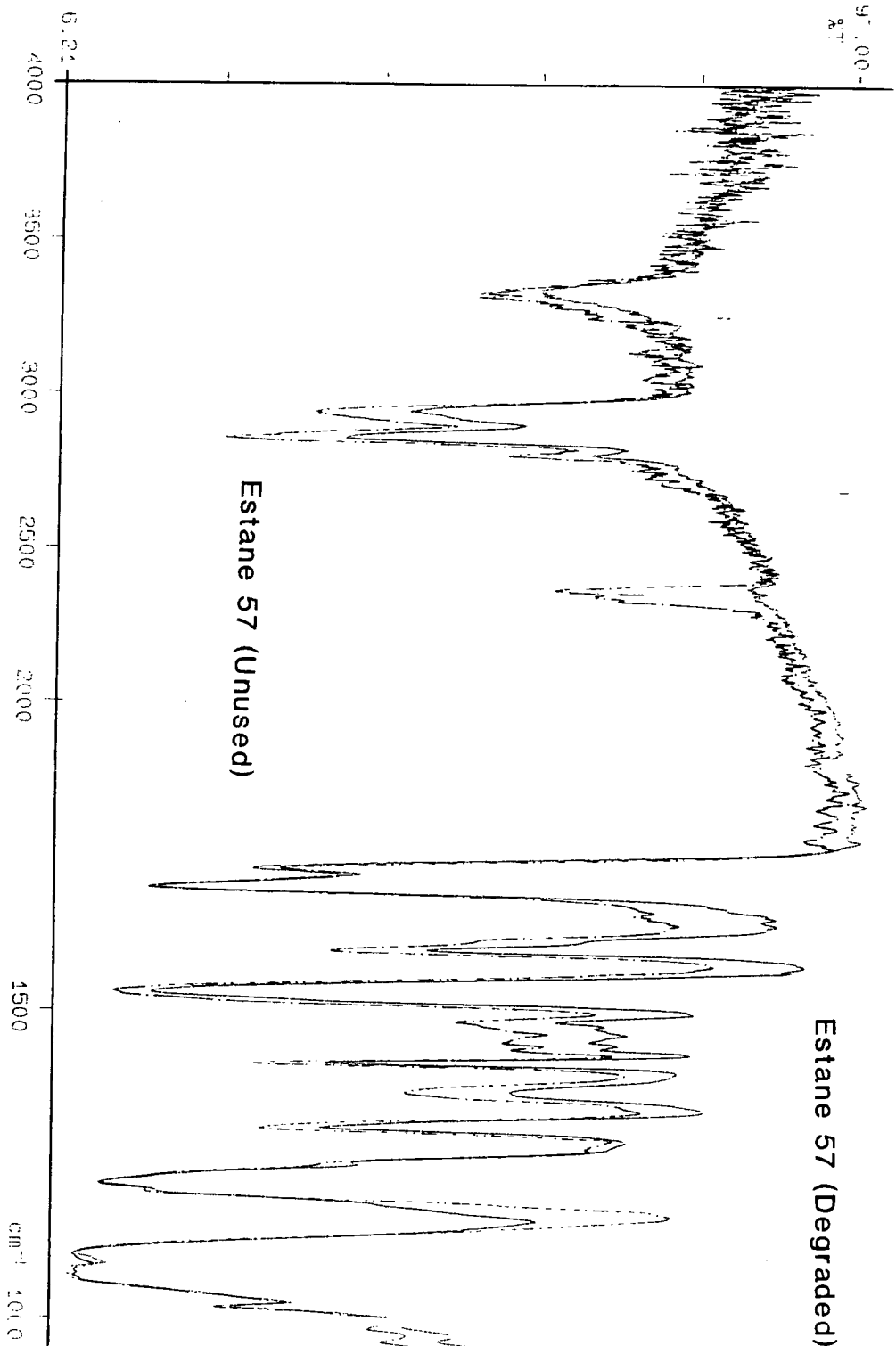
Glucose	$C_6H_{12}O_6$	1.0g
Magnesium Chloride	$MgCl_2$	0.3g
Potassium Chloride	KCl	0.2g
Sodium Chloride	NaCl	8.0g
Sodium Bicarbonate	$NaHCO_3$	1.0g

Appendix II - Degradation of Polyurethanes

The degradation tests monitored the change in the mechanical properties, mass and tribological properties of the samples. At the completion of the study samples of each polyurethane were removed from the solution, washed and subjected to chemical analysis. Attenuated Total Reflected Infra-Red Analysis was performed to characterise the bonds and groups within the (i) as produced and (ii) degraded samples. Plots of the materials are shown with the degraded samples in black and set at a lower scale than the as produced samples. No Major differences were noted in the region of expected change (circa. $1700-1710\text{cm}^{-1}$).

PERKIN ELMER

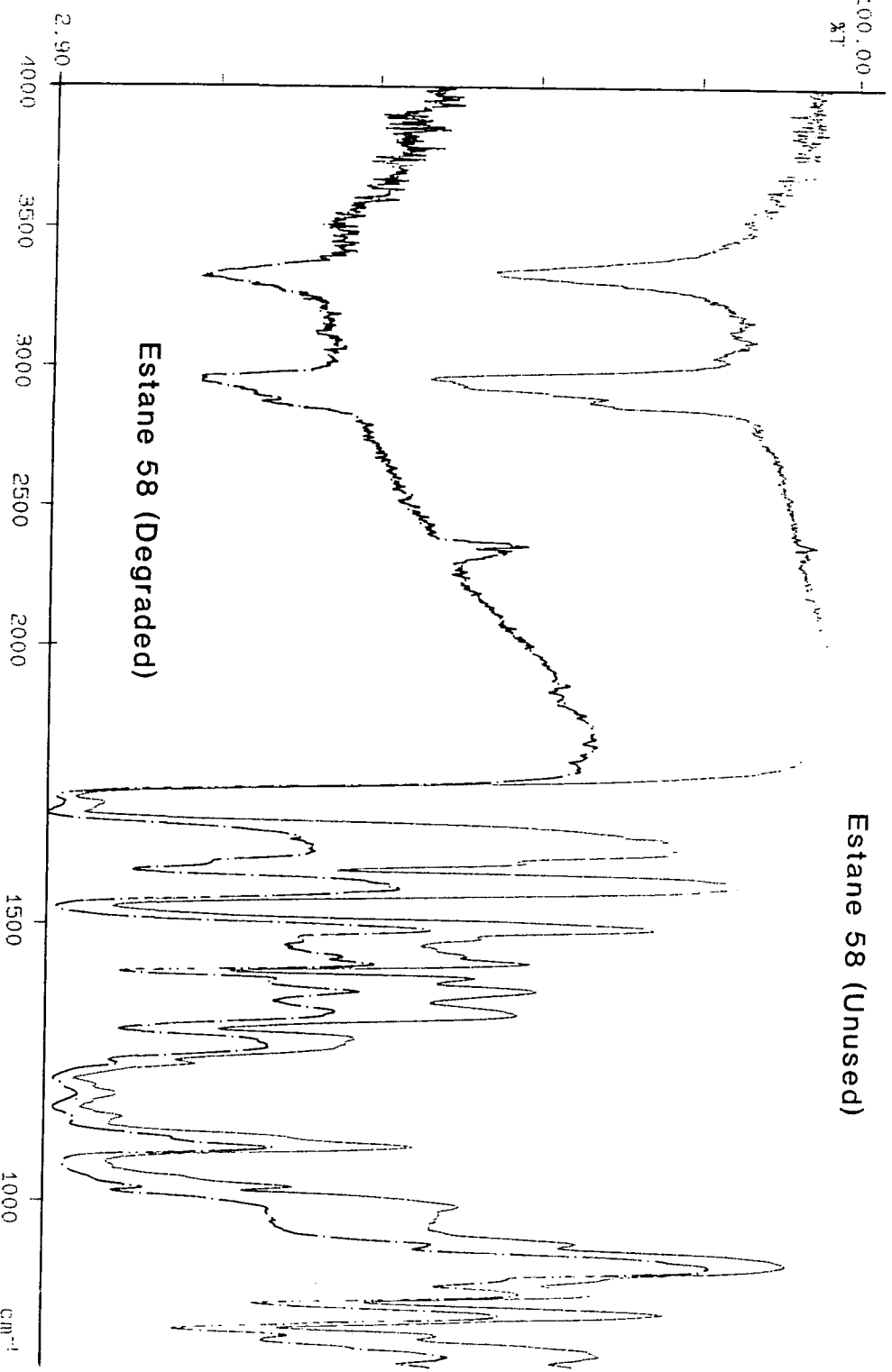
97.00 -
27



X: 91 scans, .0cm-1 flat, abex
Y: 47 scans, .1.0cm-1 flat, abex

1 1/94
507 703

100.00 -
%T

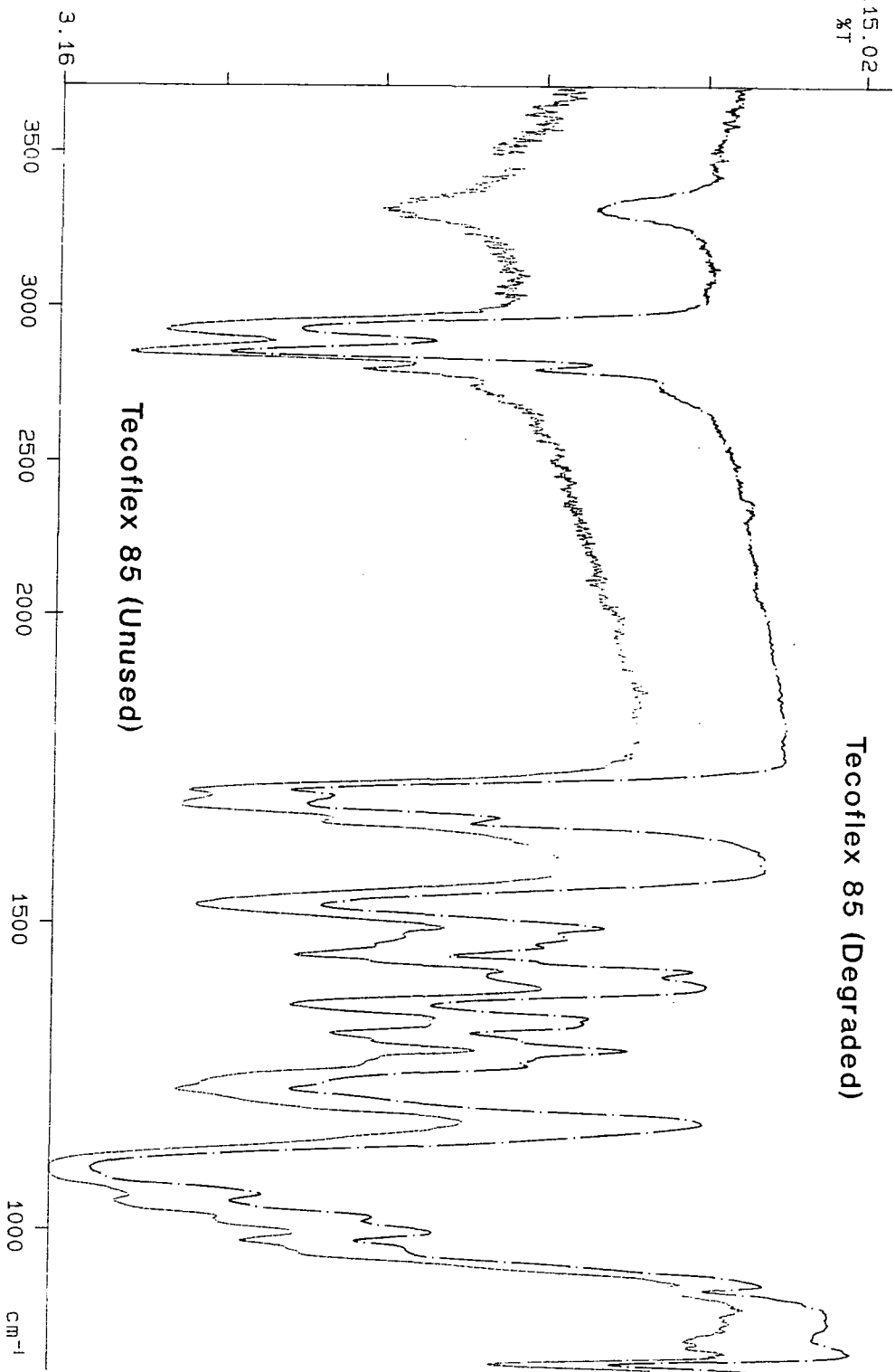


X: 60 scans, 4.0cm-1, flat, abex
Y: 101 scans, 4.0cm-1, flat, abex

11/11/03
92/11/03

115.02
%T

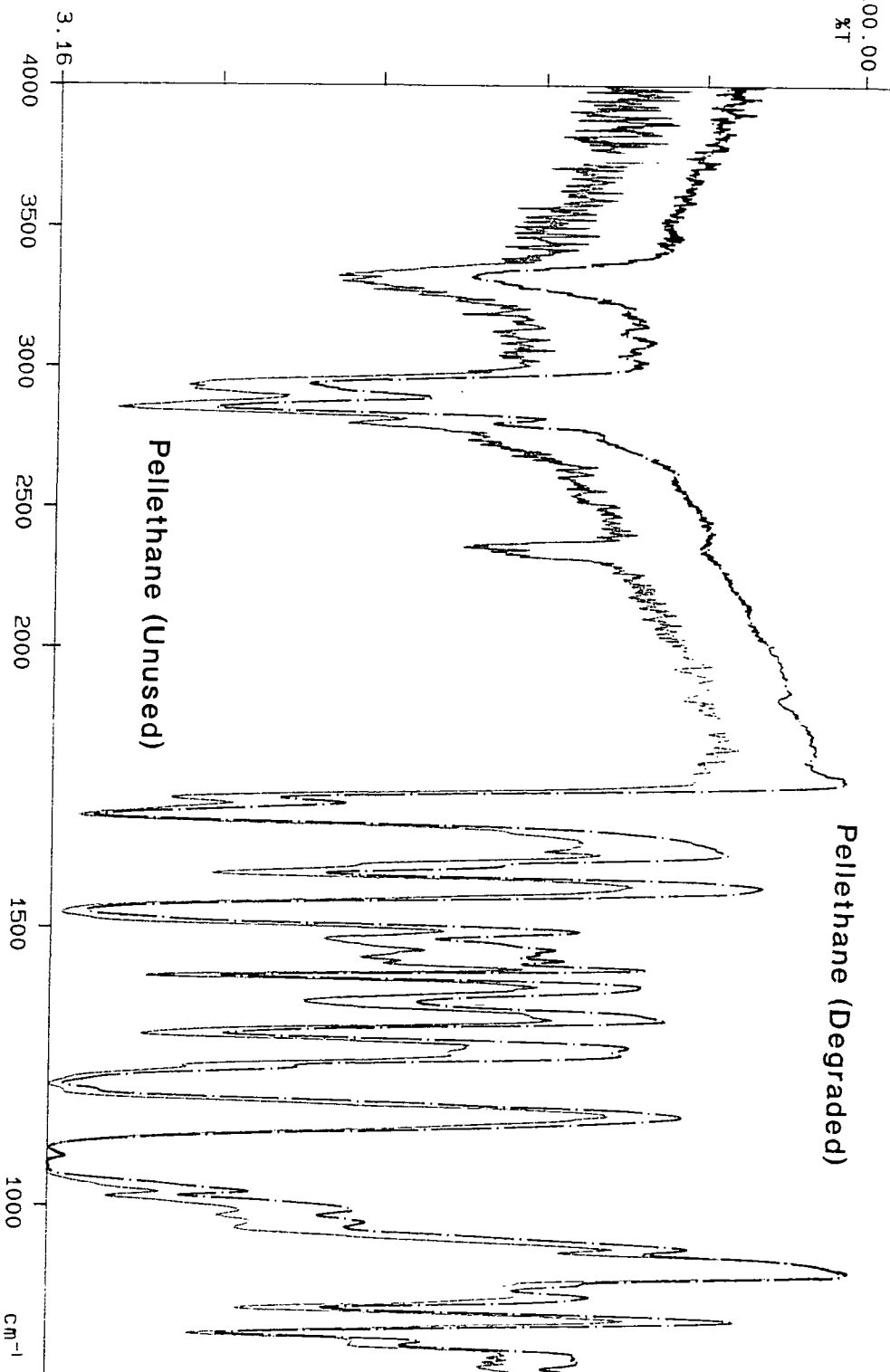
Tecoflex 85 (Degraded)



Y: 156 scan 19, 4.0cm-1, flat, abex
Z: 120 scans, 4.0cm-1, flat

11/11/06
92/11/06

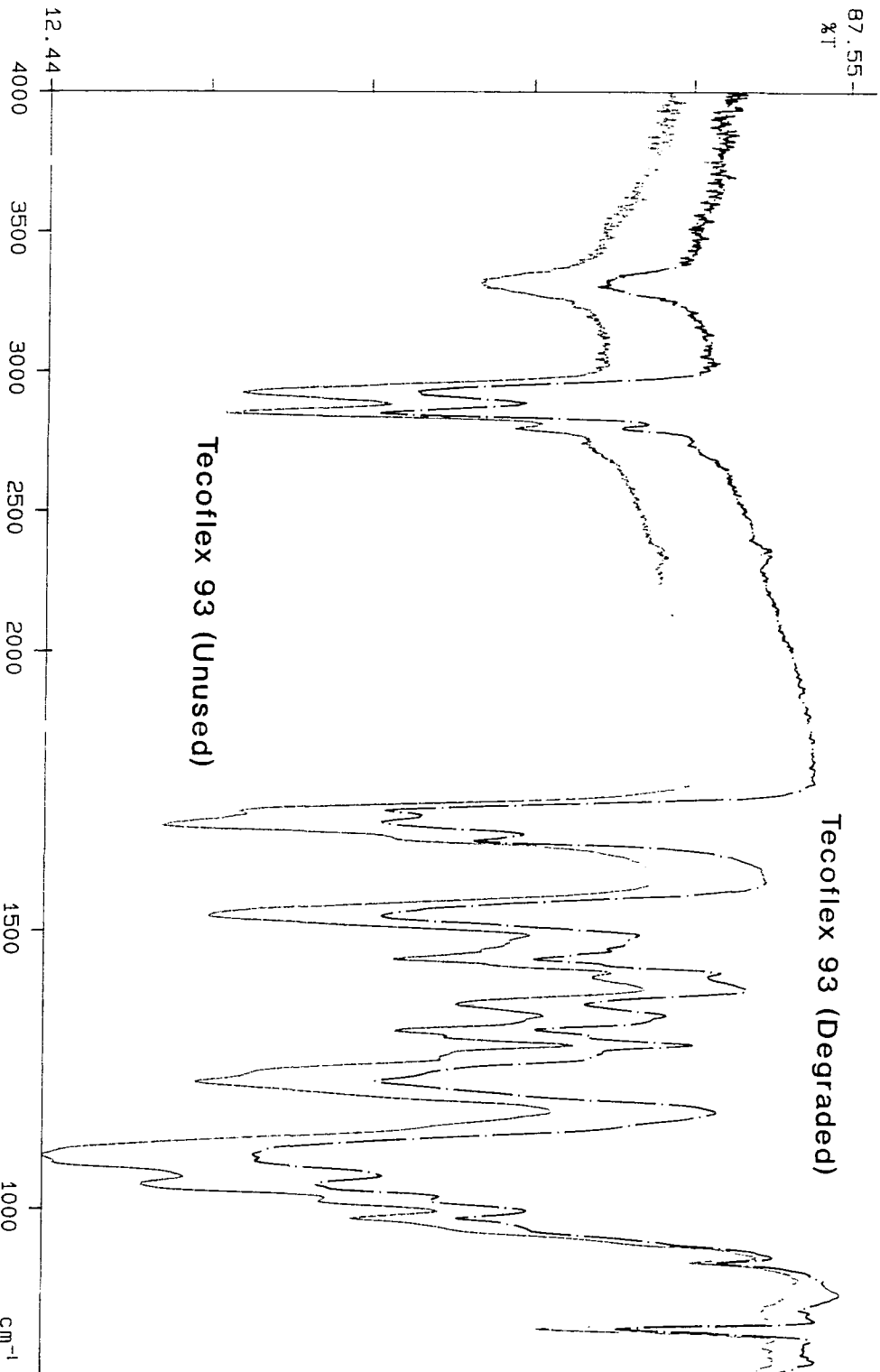
100.00
%T



X: 89 scans, 4.0cm-1, flat, abex
Y: 74 scans, 4.0cm-1, flat, abex

92/11/08
92/11/08

87.55-
%T



X: 256 scans, 4.0cm-1, flat
Y: 100 scans, 4.0cm-1, flat

2/11/06
92/11/06

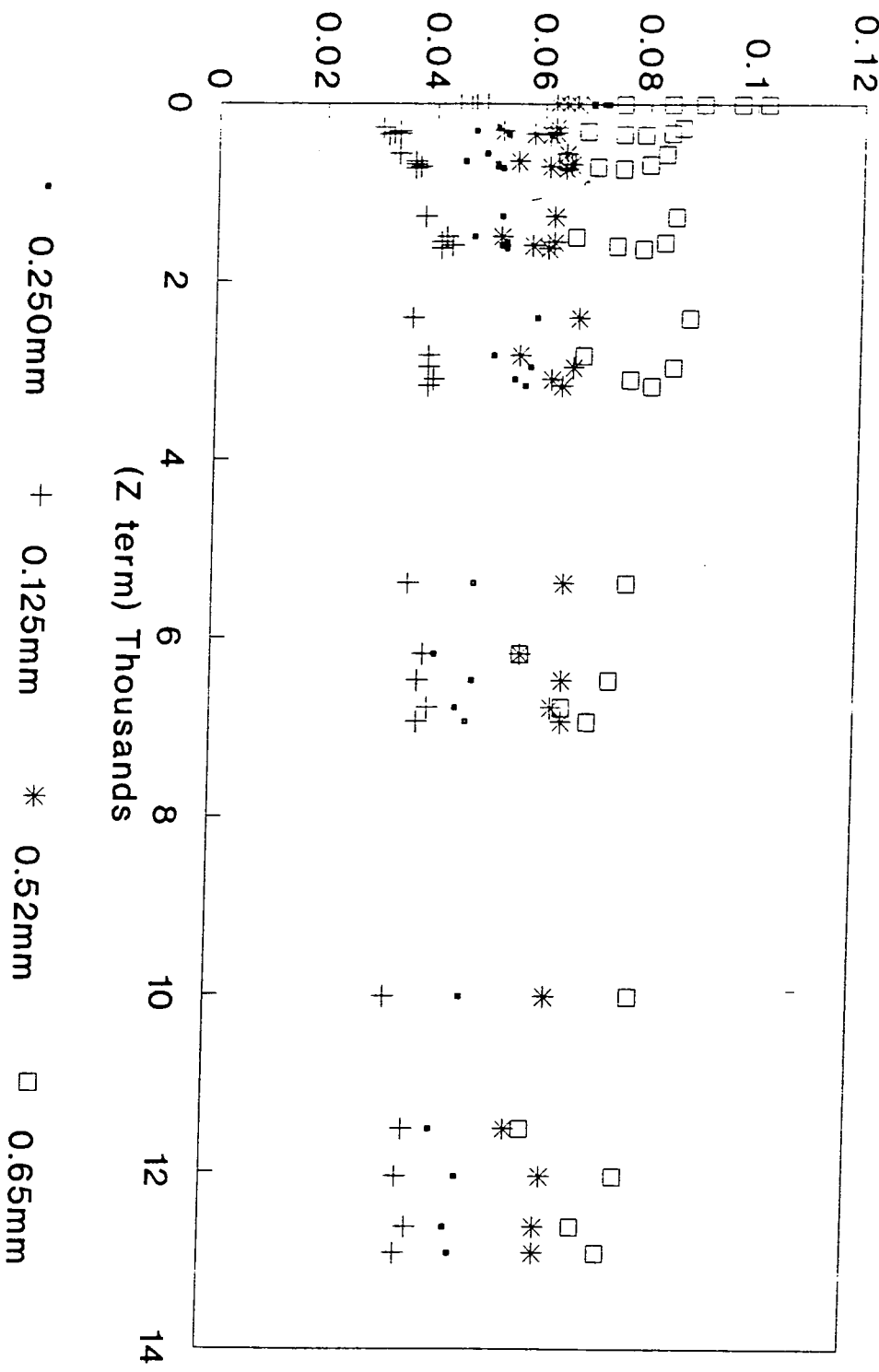
Appendix III - Crystallinity of UHMWPE Samples

Differential Scanning Calorimetry was used to investigate the crystallinity in samples of UHMWPE used in for tribological analysis and degradation studies of bonded samples.

Three distinct tribological bands could be seen after testing in the simulator under dry conditions using loading cycle I. Material I gave friction factors of typically 0.05 and material II gave values of 0.09. A third material, formed by compression moulding of the powder gave friction factors which were much higher (circa. 0.150-0.200). The sizes of the components and the surface roughness were all similar, material III had the lowest roughness (circa. $0.3\mu\text{m } R_a$). Therefore, the degree of crystallinity of the materials was checked. Material I had the highest (62%), material II (54.5%) and material III the lowest (47.3%). This is certainly significant and a further study may reveal why there is variation in the properties of new and explanted prostheses.

The crystallinity of samples placed in Mamalian Ringer's solution for 900 days (as the backing material for polyurethane cups) was also measured. These samples had been compression moulded in a single heat cycle from UHMWPE powder. Crystallinity was 47.3% average (47-48%), which is very close to values for 'as produced' samples, indicating that the hydrated environment and elevated temperatures (37°C) had little effect on crystallinity.

Appendix IV : A Plot of Coeff. of Friction against the Z Parameter
 (viscosity*radius*speed/load) for Polyethylene Prostheses
 Coefficient of Friction



PUBLISHED PAPERS

Biocompatible Materials for a Soft Layer Hip Prosthesis

J.M.Blamey, W.R.K.Dawber & A. Unsworth

Presented at SIROT Inter-meeting, 1992, Bruxelles

Soft layers, when incorporated into an experimental hip prosthesis, have proved effective in reducing friction. This is through improved mechanisms of lubrication. However, prior to clinical trials tribological properties require evaluating and the material optimised.

A number of bio-compatible polyurethanes were investigated during the course of the study, with the emphasis placed on tribological performance and degradation studies. All the joints gave exceptional tribological properties, coefficients of friction being about 1/10 of a Charnley or Muller Prosthesis. Elastic Modulus for all of the polyurethanes reduced following immersion, but little degradation was noticed for Tecoflex or Pellethane urethanes under long term soaking in Mamalian Ringer's at 37°C. These two polyurethanes were also more successful during *in-vivo* studies in rats. This consisted of sub-cutaneous implantation of specimens. Elastic modulus and ultimate tensile strength were measured before and after 7 months of implantation.

Tecoflex EG 93⁰A has also shown good fatigue properties, with tensile samples having completed 7 million cycles from zero to 15% extension with little change in modulus.

Surface modification of the joints has also been conducted in order to provide a porous surface to aid lubrication under conditions of high load and little motion (eg. extended periods standing).

Summary for Clinical Digest Series, May 1991.

A great deal of interest is being shown in compliant bearing surfaces for artificial joints. Under loading representative of walking these can produce very low friction. This is because the synovial fluid is able to form a fluid film between the surfaces during motion, thus separating them and avoiding solid-to-solid contact. This has the effect of both reducing frictional torque on the joint surfaces as well as reducing wear.

There are a number of biocompatible polyurethanes that have been in use in the body for a number of years, in such devices as Heart Valves and Catheter Tubes. However, these applications are not dependant on the change in elastic modulus or tribological (lubrication) properties of the material in the body.

In-vitro studies were conducted on four polyurethane materials. These were kept in Mamalian Ringer's solution at 37°C to investigate changes in Hardness and elastic modulus and the mode of lubrication operating with time of immersion. The materials included a polyether-urethane (Estane 57), a polyester-urethane (Estane 58), an aromatic polyester-urethane (Pellethane) and two grades of an aliphatic polyether-urethane (Tecoflex EG 85 and EG 93).

Samples of Estane 57 showed a decrease in hardness and elastic modulus of 21% and 28% respectively. This was much better than Estane 58 which indicated decreases in the above of 32% and 42%. This polymer has since disintegrated (after 400 days in solution). Better results were

obtained with the Tecoflex grades with changes of less than 5% and Pellethane which showed decreases in hardness of 14% and elastic modulus of 17%.

When tested in a Hip Function Simulator, both grades of Tecoflex showed little change in coefficient of friction from initial values of 0.005. This value is about 1/10 of the value for a Charnley or Muller Arthroplasty. Pellethane showed an increase in coefficient of friction of about 50% (up to 0.012), whilst Estane 57 and 58 both doubled in friction.

The best candidates for a compliant surface in hip replacement are Tecoflex EG 93 and Pellethane, as their mechanical properties do not change substantially and fluid film lubrication seems to be maintained throughout.

Editorial

The ancient and beautiful city of Durham was the venue for the 30th Annual Scientific Meeting of the Biological Engineering Society which this year successfully combined 'Health Care in the 90's' with 'Blood Flow '90'. The aim of the amalgamated meeting was to face the next decade with determination, meeting the challenges that present themselves and identifying positive future trends.

It is not surprising therefore, that the meeting included such topics as novel ways of cutting tissues, both hard and soft, and this really meant applications of lasers and high speed water jets, nanotechnology, data handling, robots and unusual and promising new materials. The level of activity was such that parallel sessions had to be arranged, so alongside the topics already mentioned were vibration induced white finger, laser Doppler measurements of flow, vascular aspects of ulcers in diabetes and many more related topics.

The fact that parallel sessions had to operate meant that members who attended the combined meeting inevitably missed some of the presentations and I know that I found myself wishing to divide at least two ways. This makes the Special Conference Issue of the *Journal of Biomedical Engineering* even more worthwhile since not only can those who couldn't attend the meeting obtain a flavour of the scientific presentations, but those who did attend can catch upon the papers in parallel sessions.

The Round Table discussion on 'Bioengineering - Safe in Our Hands?' generated much lively debate and together with a superb Woolmer Lecture by the Bishop of Durham who discussed medical ethics, as only he knows how, gave us all much to think about in the wider context. We heard some excellent presentations on the future of Biomedical Engineering, but in the end the judges were persuaded by the work of RJ Baker and JB Colvin from the Dundee Limb Fitting Centre, who won the 1990 IBES Lecture Prize.

It all amounted to a splendid meeting, the flavour of which can be sampled by reading this volume. My thanks to all the contributors who produced papers at incredibly short notice and a particular thanks to the array of referees who must remain anonymous, but who laboured swiftly to maintain the technical standard of this Special Issue of the *Journal of Biomedical Engineering*.

Anthony Unsworth
Guest Editor

Soft layered prostheses for arthritic hip joints: a study of materials degradation

J. Blamey*, S. Rajan*, A. Unsworth* and R. Dawber†

*Centre for Biomedical Engineering, School of Engineering and Applied Science, University of Durham, DH1 3LE, and †Materials Science Centre UMIST, Manchester, UK

ABSTRACT

A great deal of interest is being shown in compliant bearing surfaces for artificial joints. These produce very low friction because of the fluid-film lubrication that they exhibit, and therefore should produce lower wear than current prosthetic materials as the two surfaces of the joint are completely separated by a film of synovial fluid. However, one problem with soft elastic materials *in vivo* is that the elastomers may degrade with time. Specimens of four polyurethanes were kept in Ringer's solution at 37°C for about 4 months to investigate changes in mechanical properties and the mode of lubrication with time of immersion. The materials tested were a polyether-urethane (E57), a polyester-urethane (E58), an aromatic polyether-urethane (P1) and an aliphatic polyether-urethane (A1). Samples of E57 showed a decrease in hardness and elastic modulus of 21% and 28% respectively. This was much better than E58 which showed decreases of 32% and 42% respectively. Better results were achieved with A1 (hardness change 2%) and P1 (decrease in hardness of 14% and modulus 17%). When tested in a hip-function simulator, A1 showed virtually no change in its very low coefficient of friction (0.004), P1 showed an increase of 60%, while E57 and E58 both showed a doubling in friction over the course of the study. The modes of *in vitro* degradation were considered and surface effects determined to be most damaging. Currently the best candidate for a compliant material in hip replacement is the aliphatic polyether-urethane which maintains fluid-film lubrication.

Keywords: Polyurethanes, hip prostheses, *in vitro* degradation, fluid-film lubrication

INTRODUCTION

Total joint replacement is now widespread in the treatment of severe osteoarthritis; current estimates of the numbers of such operations each year are 400 000 hips and 15 000 knees worldwide. Over half of the joints used are of the metal on plastic type (Charnley, Muller, etc.).

However, it was shown by Unsworth¹ that the operation of such contacts under realistic conditions of loading and motion rely on the inherent low friction and low wear properties of the plastic used (ultra-high molecular weight polyethylene (UHMWPE)), rather than on fluid-film lubrication, which completely separates the solid surfaces and hence reduces friction and wear.

Extensive studies of human joint lubrication have shown that in normal healthy hip joints, which are lubricated with synovial fluid, the cartilage surfaces are completely separated by a thin film of fluid capable of withstanding loads imposed by the actions of walking, running and jumping²⁻⁵. This is achieved by several factors. First, dynamic loads help promote fluid-film lubrication by allowing the replenishment of fluid between the surfaces of cartilage during low load periods, such as 'swing through' in walking. Second, heavy loads are only applied for very short periods (circa 0.15 s) and hence squeeze-film mechanisms prevail during these periods. Third, cartilage

layers are soft and elastic, which leads to lower maximum pressures in the human joints.

Artificial joints are also subject to dynamic loading during walking and so benefit could be derived from potential fluid-film lubrication. However, in practice current joint designs do not achieve this¹. Unsworth *et al.*⁶ suggested that this was because the surfaces of the artificial joints are too hard to generate the film of fluid by elastohydrodynamic action and to confirm this they made a range of artificial joints with soft elastomeric surfaces, which produced fluid-film lubrication in a laboratory hip-function simulator. As a result, the new design of artificial joint could produce a coefficient of friction that was 10% of that of currently available artificial joints and of a similar value to normal healthy human joints. These artificial joints were made mainly by moulding polyurethane layers of about 1–3 mm thick onto the surface of metal cups and then testing these against standard femoral head components.

Following testing in a simulator, the coefficient of friction was plotted against the parameter $\eta uR/P$ where η is the fluid viscosity, u the surface velocity, R the femoral head radius and P the load on the joint. A theoretical curve for this is shown in *Figure 1*. At high values of $\eta uR/P$, the high values of viscosity and velocity result in a large film thickness, but as η and u reduce (either because of arthritis or changes in fluid properties and speed of walking), the film thickness decreases since, theoretically, the joint surfaces are smooth. This reduction in film thickness

Correspondence to: Professor A. Unsworth

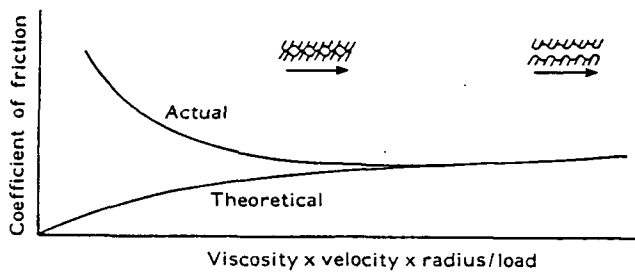


Figure 1 Coefficient of friction against viscosity \times velocity \times radius/load for a perfectly smooth surface (theoretical) and a rough surface (real), showing transition from fluid film to 'mixed' lubrication

does not result in solid contact of the surfaces. However, since both η and u have reduced and the friction is related to both of these, a reduction in coefficient of friction occurs. In real joints, however, surfaces are not perfectly smooth and asperities penetrate the thin film of fluid when η and u are small, giving rise to solid-solid contact in addition to the fluid shearing, thus leading to a rise in total friction. This produces a curve as seen in *Figure 1*. Thus by plotting the results in this way the mode of lubrication may be identified.

Figure 2 shows coefficient of friction results for a Muller joint and a compliant polyurethane layered joint plotted on the same axes. Clearly, the latter operates in the fluid-film region at a much lower value of $\eta u R/P$ than the Muller joint. In osteoarthritic joints, the region of operation is confined to the portion of the curve (*Figure 2*) to the left of the vertical line and so, in clinical practice, the soft surfaced joints would perform much better than the Muller or Charnley joints. In addition, because the surfaces are completely separated, the wear rate ought to be minimal.

Having shown that soft layers improve the performance of artificial joints and that, since wear rates should be much lower, joint life should be increased, it is necessary to evaluate the material properties in the long term after implantation since this may be a limiting factor. This study therefore reports the results of immersion of several types of biocompatible polyurethanes in Ringer's solution at 37°C for 4 months. The physical characteristics that were evaluated include hardness, elastic modulus, fluid uptake and the coefficient of friction as tested in the hip function simulator under normal walking conditions.

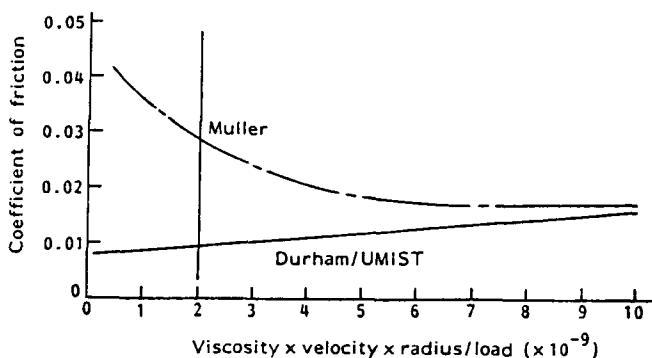


Figure 2 Comparison between a Muller prosthesis and a prosthesis with a soft compliant surface layer

APPARATUS

Hardness testing

Two types of specimens were used to evaluate changes in hardness with time in Ringer's solution: the acetabular cups, which were also evaluated for friction; and tensile test specimens used to evaluate elastic modulus. The method contained in the standard DIN 53456 was used, which loads a 5 mm ball into the surface to be investigated; 5 N is used as a holding load which is maintained for 5 s and then the load is ramped up to 25 N and held for 30 s. Deflections were measured at the holding and maximum loads and these formed the basis of the hardness calculations. A Hounsfield tensile test machine was used for the measurements, which were made on at least three regions over each polyurethane surface.

Elastic modulus

The same Hounsfield materials testing machine was used to perform standard tensile tests on polyurethane specimens in the shape of dumb-bells. The region over which loading was applied was 100 mm in length with a cross-section of 10 mm width and 4 mm thickness. The ends of the specimens were 25 mm in width to withstand the contact stresses applied by the spring-loaded grips used for tensile testing. A rate of extension of 2.5 mm s⁻¹ was used and the maximum load to which each sample was subjected was 100 N. This represented a stress level of 2.5 MPa, which was calculated to be similar to the stresses developed in an elastic layer bonded to a rigid backing experiencing loads similar to those of a walking cycle. The samples were tested over five cycles to account for any initial slippage and elastic modulus was calculated from the final cycle.

Hip function simulator

Measurements of coefficient of friction of the joints were made in the Durham Hip-Function Simulator. It consisted of a fixed main frame with a loading frame that oscillated with simple harmonic motion about a central point with a maximum amplitude of 20°.

The joint was inverted in the simulator with the femoral component held in the upper moving frame and the acetabular component placed in the low friction carriage, which was mounted on thick-film hydrostatic bearings to the static frame. These externally pressured bearings displayed a coefficient of friction at least two orders of magnitude lower than those of the test prostheses.

Under motion and loading the friction generated tried to rotate the cradle, but was resisted by the piezoelectric transducers, which allowed measurements of frictional loads to be made.

The loading was applied by a servo-controlled hydraulic ram and measurements were taken from strain gauges on the fixed frame, which formed the feedback circuit for the ram.

The control of the simulator was through a single-board computer (SBC) based on a 68000 microprocessor. This allowed dynamic loads to be applied through the servo-command as well as measurements

of load, friction, the joint flexion and the absolute position of the drive shaft. A personal computer acted as the input for the SBC and allowed data analysis to be made as well as storage on disk or in graphical form.

MATERIALS AND METHODS

Four types of polyurethane were tested: E57 — polyether-urethane; E58 — polyester-urethane; P1 — aromatic polyether-urethane; A1 — aliphatic polyether-urethane. All of these materials produced fluid-film lubrication when tested in the hip-function simulator, although their physical properties were slightly different to begin with.

Acetabular cups were made by compression moulding of the polyurethane into stainless steel cups of 36.26 mm diameter. This gave a layer thickness of 2 mm and a radial clearance between the layer and the femoral component of 0.25 mm when a ball diameter of 31.76 mm was used. Later in the tests, swelling of some of the polyurethanes caused this clearance to be eliminated and a second ball of 31.00 mm was then used as the femoral component where conditions warranted.

The tensile test specimens were injection moulded using a Negri Bossi NB60 machine. These were 4 mm thick and the working section for the elastic modulus tests was 10 mm wide. To avoid end effects in the testing machine grips, the specimens had a wider cross-section at the ends.

Methods of testing

All the specimens were immersed in Ringer's solution at 37°C. Before testing the specimens were removed from the fluid, dried, weighed and then left for 60 min to equilibrate to laboratory conditions before the hardness, elastic modulus and friction were tested.

Frictional tests

To characterize friction an aqueous solution of

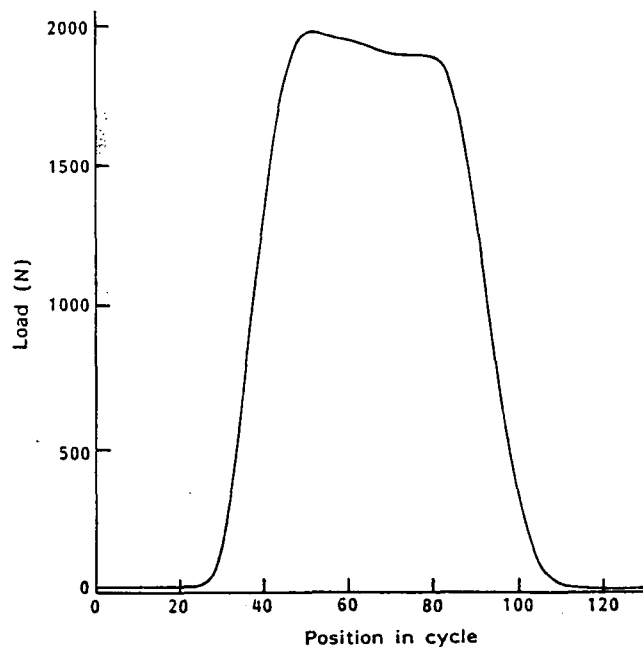


Figure 3 Loading profile applied by the simulator

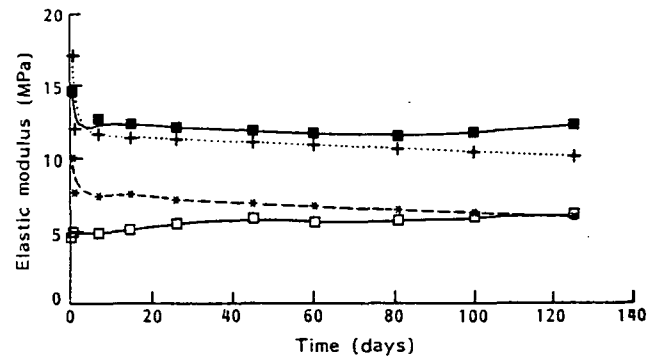


Figure 4 Variation of the elastic modulus of strip samples of elastomers immersed in saline solution at 37°C. ■ = P1; + = E58; * = E57; □ = A1

carboxy-methyl cellulose (CMC) was used as the lubricating fluid in the simulator. This has similar rheological properties to those of synovial fluid⁷ and does not carry a health risk to the research staff. Viscosities from 0.002–0.071 Pa s were used to cover the range normally associated with arthritic fluid (circa 0.008 Pa s).

The loading cycle used is shown in Figure 3. The maximum load applied was 2000 N and the minimum one 20 N. A frequency of 0.8 Hz was used and the amplitude of motion was 21°.

RESULTS

Strip samples

Elastic modulus. The changes in elastic modulus with time are shown in Figure 4. P1, E57 and E58 all show an initial decrease as water is taken up by the polymer, but A1 shows little initial change. As the study progressed gradual decreases in elastic modulus were apparent in E57 and E58 with little subsequent change for P1 and a slight increase for A1.

Hardness. Similar results were obtained from hardness measurements on the samples (Figure 5), with initial decreases after the first 2 days and a slight decrease thereafter for E57 and E58 and stable properties for P1 and A1. It was noted that the initial values of hardness did show a large variation between polymers. A1, which company literature suggested to be the hardest material, provided the lowest initial values of elastic modulus and hardness. However towards the end of the study the material properties were much more evenly matched.

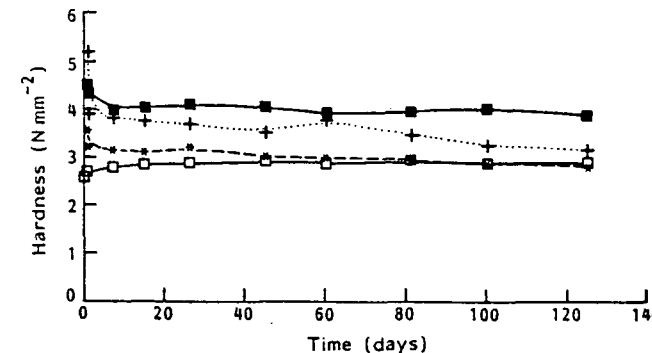


Figure 5 Variation of the hardness of strip samples of elastomers immersed in saline solution at 37°C. ■ = P1; + = E58; * = E57; □ = A1

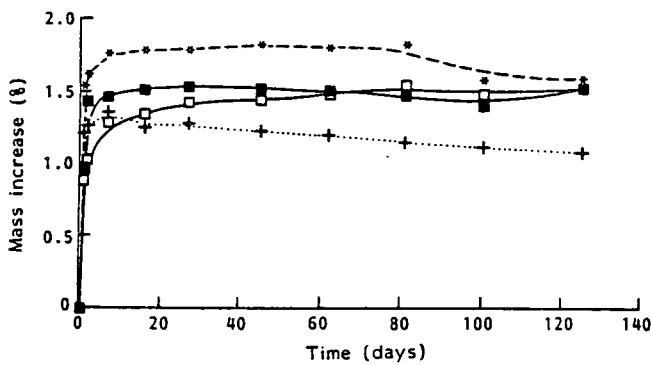


Figure 6 Variation in the mass of strip samples of elastomers immersed in saline solution at 37°C. ■ = P1; + = E58; * = E57; □ = A1

Mass increase. The increase in the mass of the specimens was monitored and a fluid uptake equal to approximately 1.5% by mass of the polymer was noted (Figure 6). Whilst A1, P1 and E57 tended to retain the mass of water taken up throughout the study, E58 showed a reduction in mass, which may correspond to the polymer being attacked by the saline solution.

Cup samples

Hardness. The cup samples showed a wide variation of hardness values (Figure 7). The values obtained were higher than the results from the strips owing to the nature of the backing material. However, the changes that occurred were similar to the strip samples with an initial sharp decrease for samples E57 and E58, followed by a continued decrease in the property over the course of the degradation study that amounted to a total reduction of 25%. A1 and P1 both showed little change in hardness over the entire course of the study.

Frictional measurements. The coefficients of friction measured for each polyurethane layer lubricated with fluids of differing viscosities are shown in Figures 8 and 9. All of the materials showed low values of friction at the beginning of the study with a rising tendency as the value of the viscosity of the fluid (and hence the $\eta uR/P$ /load term) increased in magnitude. The values of coefficient of friction were also very low, being 0.005 or less for all of the materials tested for the range of values of $\eta uR/P$ representative of *in vivo* conditions.

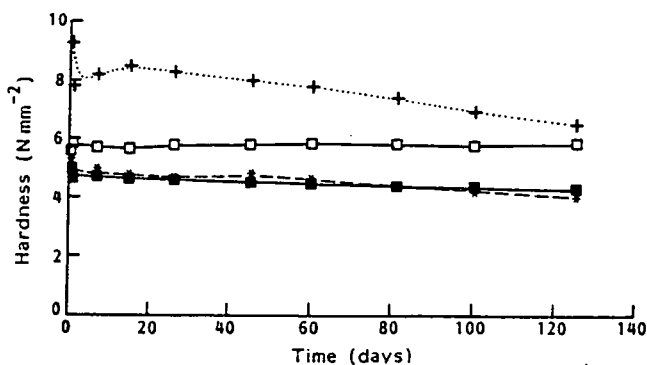


Figure 7 Variation of the indentation hardness of cup samples of elastomers immersed in saline solution at 37°C. ■ = P1; + = E58; * = E57; □ = A1

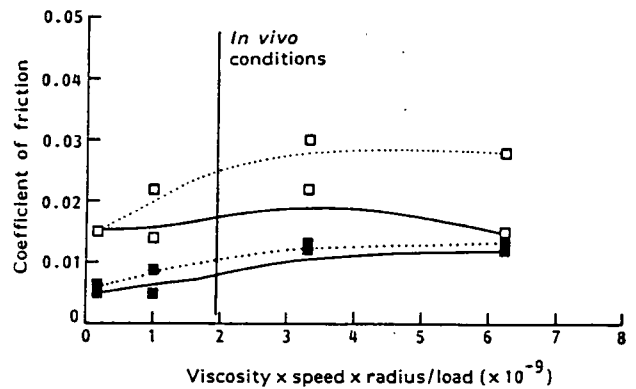


Figure 8 Changes in the coefficient of friction with immersion in saline solution at 37°C displayed by lubricated elastomeric layers of E57 and E58 with a function comprising viscosity \times speed \times radius/load. ■—■, E57 0 days; □—□, E57 120 days; ■·····■, E58 0 days; □·····□, E58 120 days

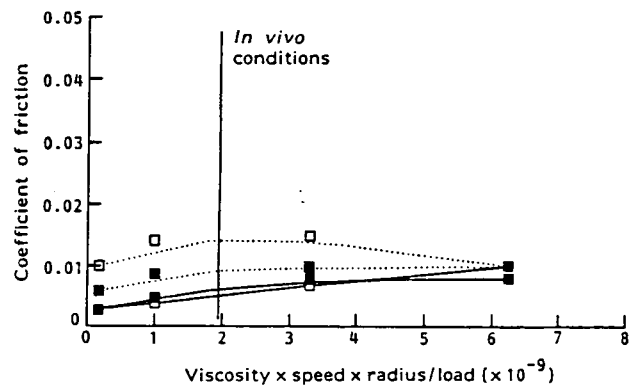


Figure 9 Changes in the coefficient of friction with immersion in saline solution at 37°C displayed by lubricated elastomeric layers of P1 and A1 with a function comprising viscosity \times speed \times radius/load. ■—■, A1 0 days; □—□, A1 120 days; ■·····■, P1 0 days; □·····□, P1 120 days

Following immersion in saline at 37°C, E57 and E58 both showed increased values of friction at all values of $\eta uR/P$, with rises of 150% in the physiological range expected from osteoarthritic synovial fluid. P1 also showed a slight increase in friction, amounting to 40% for conditions *in vivo*, but still showed a rising tendency of friction with $\eta uR/P$, indicating that fluid-film lubrication was still taking place. A1 showed a virtually unchanged coefficient of friction from its initial very low value with the rising tendency clearly evident.

DISCUSSION

Five modes of degradation have been identified in polyurethanes⁸.

- **Random chain scission** occurs because of bond breakage leading to decreases in chain lengths, a slow gradual decrease in strength and a measurable decrease in a polymer's resistance to wear.
- **Depolymerization** can also occur and results in the polymeric material being transformed into monomeric units owing to the breakage of weak C—C bonds normally in the presence of strong C=C bonds.
- **Bond changes** often linked with depolymerization can lead to the formation of C=C bonds from the

single bond, leading to by-products and tending to weaken the other bonds in the chain of material.

- *Cross linking* is a phenomenon that is sometimes induced to increase the wear resistance of polymers and involves linking chains together along their length. However, it often causes hardening and embrittlement of the polymer, which is important for urethanes under conditions of large deformations, leading to premature mechanical failure. In addition, hardness changes can lead to changes in the lubrication mode that is operating.
- *Side chains* may also be attacked (e.g. acid and alcohol groups), leading to a total change in the chemical properties of a molecule and hence the mechanical properties of the material.

The polyurethanes investigated displayed a number of differing material structures. E58 was a polyester urethane. The ester grouping responds to an aqueous environment by hydrolysing and causing breakage of the chains. This was evident from the large decreases in hardness and elastic modulus and the gradual decrease in mass of the specimens. However, the amount of water absorbed by the ester seemed to be less than for a corresponding ether, E57, and so hydrolysis may have been limited to a fairly small region at the material surface. Hydrolysis involves a form of depolymerization and it is likely that the ensuing surface damage causes breakdown of the fluid film and thus increases friction.

E57, a polyether-urethane, showed stable specimen mass, but also indicated gradual decreases in hardness and elastic modulus. The ether linkage is not so easily broken by the action of hydrolysis. However, chain scission may be occurring at other points, leading to a lower proportion of long chain molecules, thus increasing the number of soft segments and reducing the material hardness and elastic modulus. It is likely that this may also be a surface phenomenon leading to the changes in tribological properties of the layer.

P1 and A1 showed little change in any of the measured quantities and following initial fluid uptake there was no change in fluid content over the course of the study. Tribological properties were consistent at very low values of coefficient of friction (0.005), indicating little change in the material surface and in addition little swelling was noted for these layers.

These low values and the shapes of the coefficient of friction against $\eta uR/P$ curves indicate fluid-film lubrication. When this regime is operating the surfaces are completely separated and so wear should be extremely low. Fatigue of the polymers thus becomes the major factor, which is currently being investigated. Initial results have been very favourable as the resilience of these materials seems very good.

CONCLUSIONS

The generation of a fluid film between two articulating surfaces is compromised by degradation of the polymeric surface. E57 and E58, which showed the largest decreases in both hardness and elastic modulus, also showed higher coefficients of friction measured in the hip-function simulator following immersion in mammalian Ringer's solution for 4 months. These results indicate a change in the mode of lubrication away from fluid film towards a 'mixed' mode, with part of the load being carried by direct solid contact.

P1 and A1 both showed consistent hardness and elastic modulus values, as well as frictional results that changed little over the course of the study. Frictional values were at least an order of magnitude less than the best currently available prostheses, showing a coefficient of friction of 0.005 for fluid viscosities representative of osteoarthritic synovial fluid.

The range of hardness values that can promote fluid-film lubrication was extended to include the range from 3.0 to 9.5 N mm⁻². Clearly, to date P1 and A1 provide the best chance of success in the long-term use of polyurethanes in this application.

ACKNOWLEDGEMENTS

The authors acknowledge Mrs Susan Carter for typing the manuscript, and Mr George Turnbull and Mr Gerard Healey for technical assistance. The Wolfson Foundation and SERC are funding this work and the authors wish to record their appreciation.

REFERENCES

1. Unsworth A. The effects of lubrication in hip joint prostheses. *Phys Med Biol* 1978; 23: 253-68.
2. Unsworth A, Dowson D, Wright V. Some new evidence on human joint lubrication. *Ann Rheum Dis* 1975; 34: 277-85.
3. O'Kelly J, Unsworth A, Dowson D, Hall DA, Wright V. A study of the role of synovial fluid and its constituents in the friction and lubrication of human hip joints. *Eng Med* 1978; 7: 73-81.
4. Roberts BJ, Unsworth A, Mian N. Modes of lubrication in human hip joints. *Ann Rheum Dis* 1982; 41: 217-24.
5. Higginson GR, Unsworth A. The lubrication of natural joints. In Dumbleton JH, ed. *Tribology of Natural and Artificial Joints*. Oxford: Elsevier, 1981, pp. 47-73.
6. Unsworth A, Pearcy, MJ, White EFT, White G. Frictional properties of artificial joints. *J Eng Med* 1989; 17: 101-4.
7. Cooke AF, Dowson D, Wright V. The rheology of synovial fluid and some potential synthetic lubricants for degenerate synovial joints. *J Eng Med* 1978; 7: 66-72.
8. Lelah MD, Cooper SL. *Polyurethanes in Medicine*. Florida: CRC Press, 1986.

Presented at 'The 19th Leeds-Lyon Symposium on Tribology, "Thin Films in Tribology"', 8-11th September 1992, held at Leeds University, U.K. To be published in the Conference Proceedings, 1993, Elsevier Science Publications B.V.

Measurements of Elastic Modulus and Hardness of Biocompatible Polyurethanes and the effects on Contact Area within the Hip Prosthesis

J.M.Blamey

Centre for Biomedical Engineering, School of Engineering and Computer Science
University of Durham, Durham DH1 3LE, U.K.

SYNOPSIS

The use of soft layers on the bearing surfaces of artificial hip joints has shown large advantages over current devices. However, the Hardness and Elastic Modulus of the layers are critical for good tribological properties. Thus, these properties must be monitored during optimisation of materials for this application. This paper reveals the interaction between the two mechanical properties and indicates how Elastic Modulus can be calculated from a simple Hardness test. The advantage of the Hardness test is that it may be performed on any size or thickness of sample. This removes processing differences between components and test pieces. The results from Hardness measurements were found to be highly dependent on the backing material and the extent of bonding to it as well as the thickness of the material. In addition, it was noted that the 93 and 100A grades from the Tecoflex range of biocompatible polyurethanes exhibited substantial visco-elastic properties. The work on Hardness / Elastic Modulus interactions has allowed the effective modulus of an acetabular component to be estimated, which can then be applied to the lubrication equations. These theoretical studies support current experimental findings.

1. INTRODUCTION

Artificial hip joints formed from metal cups lined with soft layers have provided excellent tribological properties when lubricated with fluids of similar viscosities to synovial fluid. However, the tribological properties of elastomeric layers are highly dependent on their elastic properties. Unsworth *et al* [1] [2] and more recent work by the author has concluded that hardness values of 3.5 - 9.0 N/mm² (H20/30 DIN 53456) are required for the best tribological results. The reason for this is that lubrication is highly dependent on the contact area. If the layer is made harder the area of the contact decreases and contact pressures rise. This can cause breakdown of the fluid film between the articulating surfaces and increase friction substantially. Moving to a softer material can increase the contact area but dimensional changes under load will tend

to be greater, requiring larger clearances to eliminate grabbing. In addition, the fatigue strength of the softer polymers tends to be lower. This means that for a commercial hip prosthesis a compromise must be reached with mechanical strength and tribological properties.

Hardness is a measurement of the ability of an indenter to penetrate a surface (DIN 53456, Brinell or Vickers) or the loss of energy of a ball dropped onto the surface (Shore). It can be used to estimate the elastic modulus of a material [3], [4]. However, hardness is dependent on the thickness of the layer as well as its surface properties. In addition, the interface between indenter and layer and the layer and the rigid substrate are important [5]. Changing the applied load can lead to changes in the measured hardness values. As such it is only possible to use hardness

measurements as a comparison with other materials tested under identical conditions. In addition materials exhibiting visco-elastic properties will tend to show different values if the speed of loading and time at maximum load are altered.

The aim of this study was to assess the effect of changing layer parameters on the hardness values obtained from tests based on DIN 53456 with a holding load of 5N and a maximum load of 25N. A comparison was also made between hardness and the elastic modulus measurements made on strip samples in order to make comparisons between the experimental and theoretical results. This enabled a calibration to be made from the results for strip samples which could be applied to metal or polyethylene backed cups.

2. THEORY

2.1. Theory of Hardness Measurements

The hardness test detailed in DIN 53456 seemed the most appropriate to use for an elastic material since the penetration is monitored during the test. This is unlike the Brinell test, which relies on measurements of the size of the indentation in the surface following removal of the load (irreversible plastic deformation).

The DIN 53456 hardness test relies on a loaded steel ball (Vicker's Hardness > 800) penetrating the surface of a layer and defines

$$\text{Hardness} = \frac{\text{Major Load}}{\text{Area of Indentation}} \quad (1)$$

which can be rewritten as

$$H (20/30) = \left[\frac{0.21}{0.21 - e_r + e} \right] \left[\frac{F}{\pi d e_r} \right] \quad (2)$$

A minor load is applied to the specimen to allow accurate determination of the starting penetration. A plot of load

against penetration for Estane 57, one of the biocompatible polyurethanes, is shown in figure 1. It can be seen that at low loads (below 3-4N) the initial contact is still being formed and results would be inaccurate if a load below this were used as the minor load.

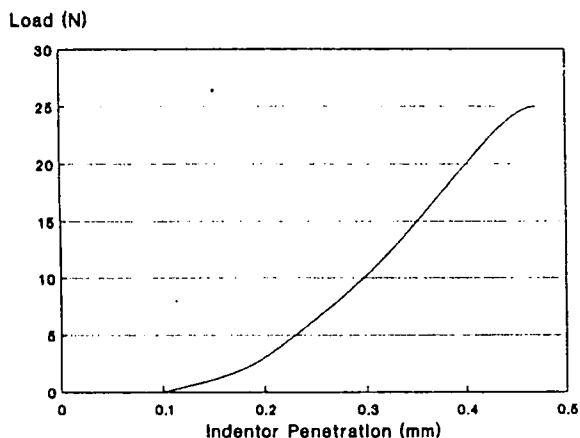


Figure 1. A Plot of Load / Penetration for the Hardness Test

Tests were done whereby the minimum load was altered and the change in final hardness values could be seen.

Table 1
Hardness when Minimum Load is Altered

Minor Load (N)	Major Load (N)	Hardness (N/mm ²)
2.5	22.5	2.99
5.0	25.0	3.28
10.0	25.0	3.32

The minor load was held for 5 seconds and then quickly ramped to the major load. The major load could be chosen to give a penetration between 0.150 and 0.350mm after thirty seconds at that value, as detailed in DIN 53456.

A major load of 20N was chosen to give a range of Hardness values of 9.5 - 3.4 N/mm², corresponding to the acceptable range of penetrations (figure 2).

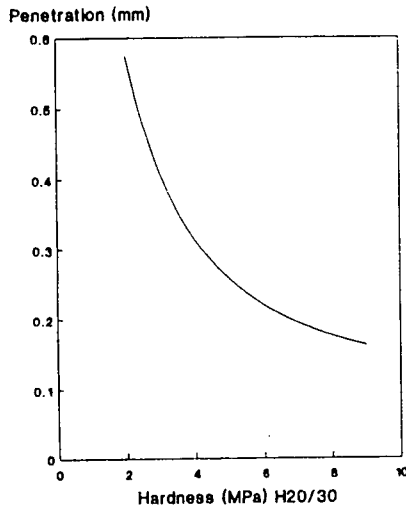


Figure 2. A Plot of Indentor Penetration Versus Hardness for the DIN 53456 Hardness Test

At low penetrations or with harder samples the results from equation 2 tended to drift away from the load/indentation area plot (figure 3), indicating the problem of using too small an indentation. At low values of hardness the curves are very similar, thus it is likely that penetrations greater than 0.350 mm are acceptable (providing the samples are thick enough), increasing the range of hardness values that can be accurately measured down to 2.0 N/mm².

The DIN test specified a minimum material thickness of 4 mm to eliminate the effects of the backing material. Unsworth *et al* [1], [2] have specified that layer thicknesses of 2 mm gave good tribological results and by using a thin layer the shear

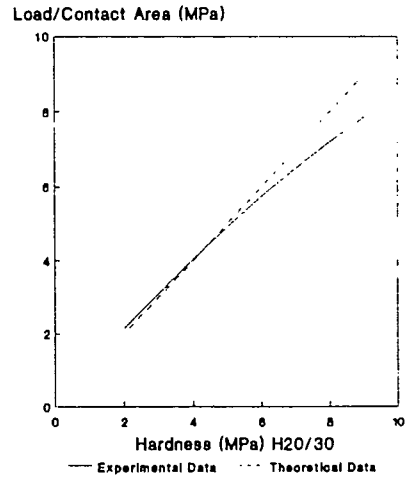


Figure 3. A Plot of the Calibration of the DIN 53456 Hardness Test

stresses at the interface between this layer and its backing material will be reduced [6].

2.2. Theory of Hardness and Elastic Modulus Interactions

The load / extension curves of a polymer shows many different regions which represent activities within the matrix. Urethanes consist of many chains containing both hard and soft segments, and variations in the quantity of each alters the mechanical properties of the polymers.

A typical load / deflection curve is shown in figure 4. It can be seen that at low loads the curve is quite steep, representing a stiff sample. This corresponds to untangling of the coils of the chains which make up the polymer and a re-orientation of these chains. This part of the curve can be explained theoretically with a good degree of accuracy. The second part of the curve, which shows a constant gradient, involves stretching of the coils of polymer to produce straight chains of material. The upturn in the modulus of the material prior to failure represents the

behaviour of the chains which have been stretched near to their maximum lengths. The gradient and extent of the final region can indicate crystallization induced by molecular orientation.

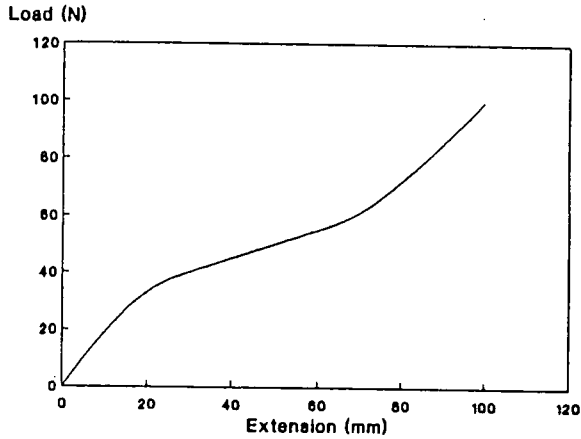


Figure 4. A Load / Extension Plot for a Tensile Polyurethane Specimen

Therefore, the value of elastic modulus measured is highly dependent on the part of the curve used. In use as a compliant layer in an artificial prosthesis it has previously been calculated that the maximum value of compressive stresses caused by the pressures generated is 3.5 MPa [6]. This value of stress corresponds to a point on the first region of the load / extension curve, so the modulus during this region is most important.

Hertzian Theory predicts that elastic modulus may be calculated directly from parameters obtained from indentation of a ball into the surface of the solid. This is the same arrangement as the hardness test used in this study.

$$E = \left(\frac{9}{16} \right) \left(\frac{F d}{2 a^3} \right) \quad (3)$$

a, the contact radius is calculated from the penetration of the ball between the minimum load of 5N and the maximum load of 25N used for the hardness test.

$$a = (d e - e^2)^{1/2} \quad (4)$$

This analysis does not take into account the effects of sample thickness and as such relies on an infinite solid. From the previous hardness tests it can be seen that for thickness values greater than 4mm the effect of further changes in thickness is minimal. Therefore, this analysis should be limited to thickness at or above 4mm.

Waters [4] used results obtained by Timoshenko and Goodier [7] to obtain expressions for elastic modulus from indentations on thin sheets, where interaction with the backing material was apparent. He used a number of ball sizes from 3 to 10 mm in diameter pressed into thin rubber sheet which were from 1.5 to 18.5 mm in thickness. They were supported on a rigid metal block. His experimental results allowed the following equation to be formed:

$$E = \left(\frac{9}{16} \right) \left(\frac{2 F}{d} \right) \left(\frac{1 - (\exp)^{-At/a}}{e} \right)^{3/2} \quad (5)$$

where A = 0.67 for a lubricated lower boundary and 0.41 for a non-lubricated lower boundary

In all of the tests done at Durham a PTFE spray was used to ensure lubricated conditions when the polyurethane sheets were tested. Thus, a value of 0.67 was used for A in the theoretical analysis.

3. MATERIALS AND METHODS

A number of commercially available elastomers were used covering a range of specified hardness values, measured on the Shore scale.

The thermosetting Castomer system was produced in three grades, 75, 80 and 85A, as a three part system and was cast onto flat plates to form the samples. The upper surface was not constrained by a plate as a better surface finish could be obtained by leaving it to cure in the air. The biologically compatible urethanes were formed using two methods. The thicker samples (4mm) were produced by injection moulding while the thinner samples were made by compression moulding between flat plates. In this way thickness could be specified by shims placed between the plates. Tecoflex EG80, 85, 93 & 100A materials (Aliphatic Polyether Urethane) were all investigated as was Pellethane 2363-80A (Aromatic Polyether Urethane) and Estane '5714F1' (Polyether Urethane) and '58271' (Polyester Urethane). The Tecoflex polyurethanes seemed softer than the other materials of the same Shore hardness, which is why so many grades of material were investigated.

DIN 53456 specifies that samples should be smooth, flat and the faces parallel, but does not quantify this. Samples were checked for flatness and parallelism by taking measurements of thickness over the surface. Surface roughness was measured on a number of samples using an Alpha-Step as 0.6-1.1 μ m (R_a). The samples were placed on a lubricated flat steel plate of 12 mm thickness. A five millimeter hardened steel ball was used as the indenter, with a Hounsfield testing machine providing the loading. A further investigation was made by bonding samples of Tecoflex to a polyethylene backing with cyanoacrylate cement.

4. RESULTS

As expected, the hardness values for all of the elastomers increased as the sample thickness was reduced. Figure 5 shows the results for the castomer samples and figure 6 shows a similar plot for the biocompatible urethanes.

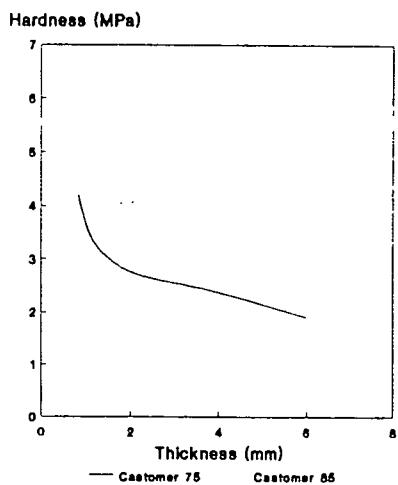


Figure 5. The Effect of Sample thickness on Hardness Values (DIN 53456)

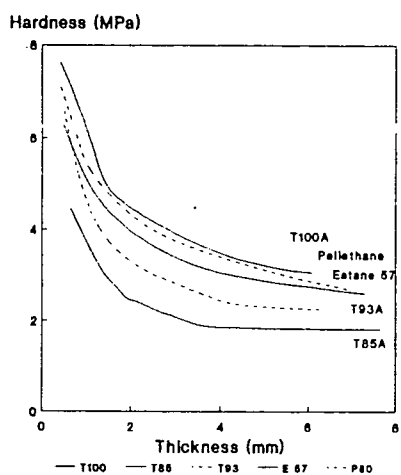


Figure 6. The Effect of Sample thickness on Hardness Values (DIN 53456)

The general shape of the curves is the same with a lower limit of hardness at thicknesses greater than about 4.0mm. This represents the stage at which the stressed region under the ball is not affected by the lower surface of the material. At very low

thickness values it would be expected that the curves for all of the materials would coincide as the effect of the steel support becomes dominant. This is suggested by the shape of the curves in figures 5 and 6. During the period at maximum loading it was noted that the Tecoflex elastomers, in particular the 93 and 100A grades, consistently showed extensive 'creep' with the penetration increasing by as much as 0.15 mm. This is much greater than the other biocompatible elastomers where increases were only about 0.03 mm. This was investigated by measuring the penetration of the indenter (and hence calculating hardness) immediately on reaching the major load and comparing values. Figure 7 shows that this accounted for 25 and 40% of the total penetration for Tecoflex 93 and 100A respectively and 5-10% for the other biocompatible urethanes.

The bonded samples of Tecoflex showed a similar shape of curve (figure 8) to figures 5 and 6, but with higher hardness values, especially with the thinner samples. Typical increases were in the region of 30%. At higher thickness values the curves for the 85 and 93A grades coincided with those for the unbonded samples.

Results from the hardness / elastic modulus interactions were collated on three graphs. Figures 9a and 9b show the accuracy of the basic Hertzian theory for sheets of 4 mm thickness. It can be seen that the slope of the experimental data, which comprises a number of different urethanes, fits well with the theoretical line. Differences in the magnitude of the hardness values from experiment and theory for measured elastic moduli are also small. Figures 5 & 6 showed that the variation of hardness with thickness was similar for all of the elastomers.

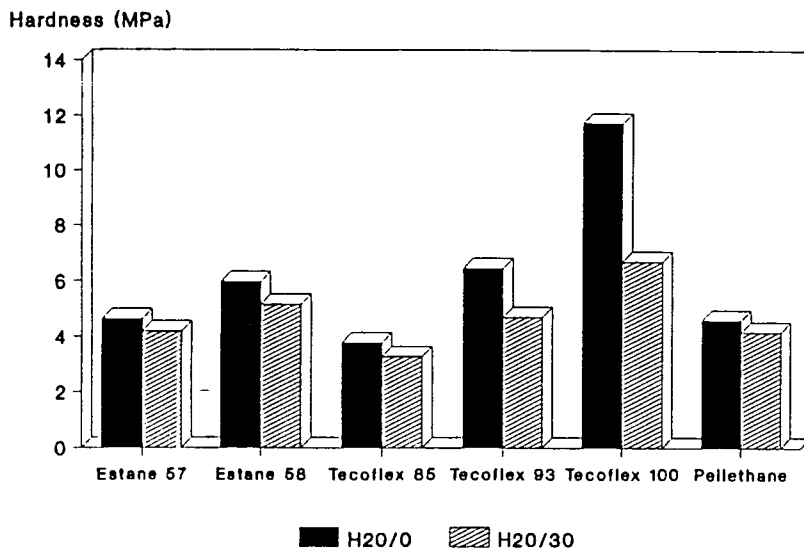


Figure 7. The Visco-elasticity of thin samples of Biocompatible Polyurethanes undergoing Hardness Testing

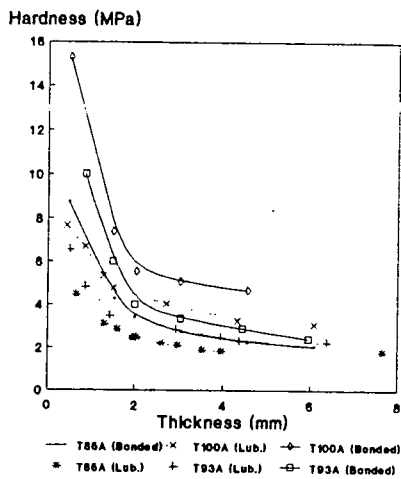


Figure 8. The effect of sample thickness and bond with backing material on hardness for Tecoflex urethanes

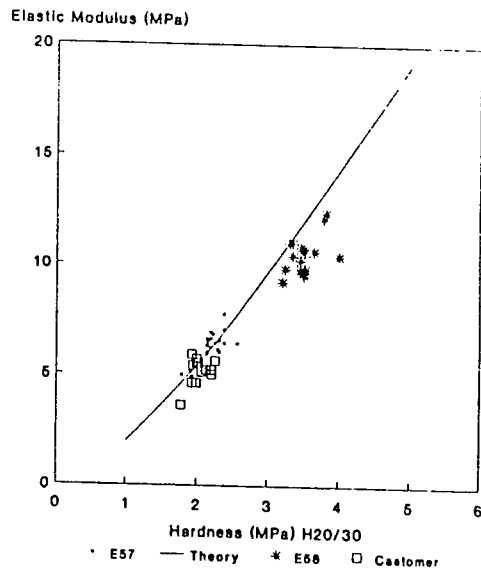


Figure 9b. A Plot of Elastic Modulus against results from the DIN 53456 Hardness Test, showing Hertzian Theory

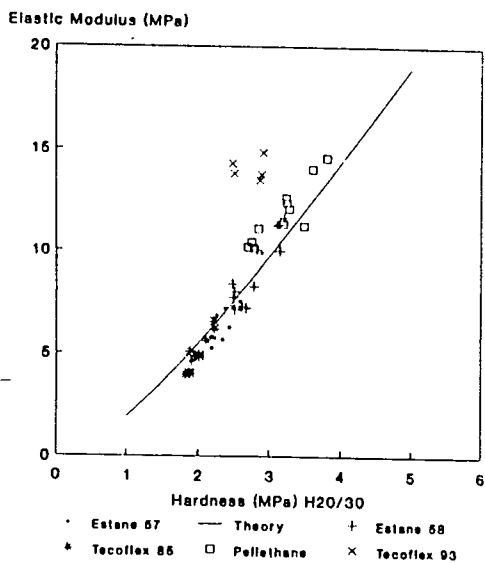


Figure 9a. A Plot of Elastic Modulus against results from the DIN 53456 Hardness Test, showing Hertzian Theory

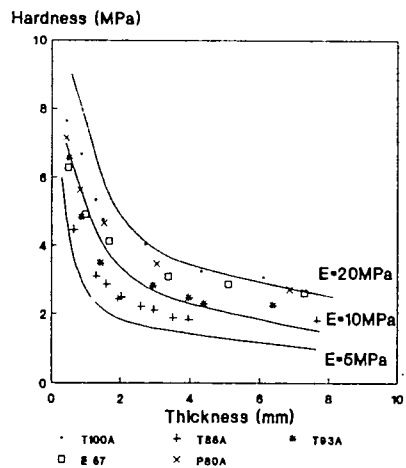


Figure 10. Waters' Theoretical Results and the comparisons with practical data from the range of biocompatible polymers

Therefore for simplicity only the biocompatible polyurethanes were used to investigate Waters' theoretical results. His data was expressed as lines of constant elastic modulus on figure 10. It can be seen that there is good agreement between the theoretical curve and the measured data.

5. DISCUSSION

The DIN 53456 hardness test specifies that "the maximum penetration of the ball into the samples should not exceed 10% of the sample thickness". To investigate the changes that occur at large relative penetrations, the data from figures 5 and 6 was modified to produce figures 11 & 12 where hardness is plotted against the percentage penetration of the indenter.

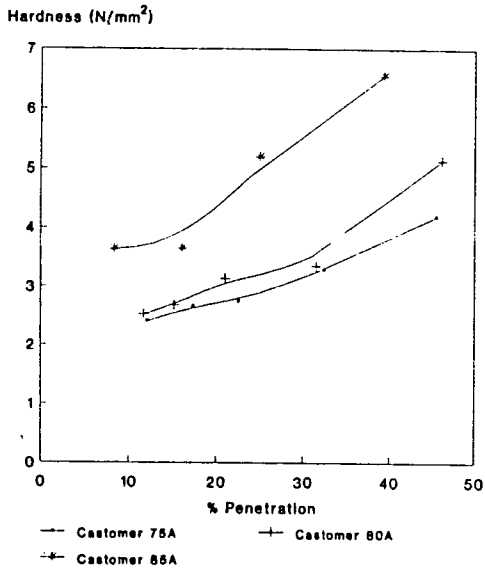


Figure 11. The Change in Hardness with Penetration of the Indenter as a percentage of the sample thickness

This showed that hardness was approximately constant at penetrations of up to 20% of the sample thickness. Therefore, if this test is being performed on samples

where the material properties are important, penetration values must be kept below this proportion of the sample thickness. However, with samples destined for tribological testing, a bond is formed between the urethane and the backing material.

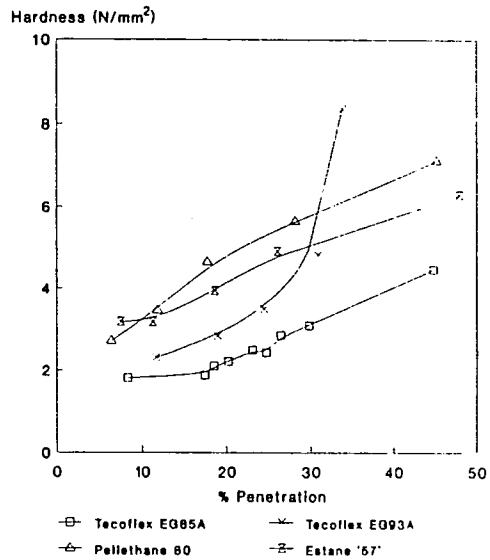


Figure 12. The Change in Hardness with Penetration of the Indenter as a percentage of the sample thickness

The effect of this bond on the hardness value was also assessed. A 13.3% reduction in hardness was obtained when the bond to the metal backing was destroyed. This was with a 2 mm layer, which is the optimum thickness for the cup, and indicates the effect of the backing material even though the penetration of the indenter was less than 20%. It is thought that this is due to the reduction in the flow of the elastomer with a 100% bond (figure 13). From figures 6 & 8 it can be seen that a bond with the backing material seems to reduce the effective layer thickness by about 15%.

Therefore this must be taken into account when estimating the hardness of the bonded layers.

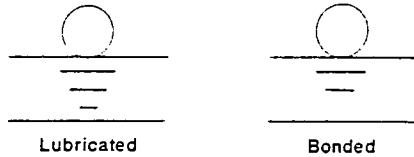


Figure 13. The effect of the bond with the backing material on the Indenter Penetration

Measurement of the elastic modulus of a material is not easy to accomplish. It relies on testing samples which can rarely be produced from the actual manufactured component. Tensile samples (dumbbells) have to be produced, leading to possible inaccuracies if processing has been accomplished differently. The tensile specimens have to be cut and checked for stress concentrations and then accurately measured dimensionally. The testing machine must have grips which provide good transference of stress with minimal slippage and the forces developed can be quite high necessitating a stiff loading frame on the testing machine.

Figures 9a & b and 10 have shown that the elastic modulus can be determined easily and simply from hardness tests on any thickness of sample. Account can even be made for the backing material, such as in the case of cup samples used for tribological assessment. Using figure 10 the effective elastic modulus of a 2mm bonded layer can be estimated at $> 20\text{MPa}$.

6. CONCLUSIONS

The effects of backing materials and bonding of the lower face of polyurethane layers have been quantified. Information has been presented which will allow the elastic modulus of elastomeric materials to be obtained from the results of a simple hardness test on any sample thickness. In

addition the effective elastic modulus of acetabular cups has been estimated. This will allow greater accuracy in the tribological assessment of soft layer prostheses. The test is both simple and quick to perform and the spread of results from samples of the same material is normally small. The use of this method will certainly speed up research in this area and will help *in-vivo* testing as smaller samples could be implanted. Work on other polymers of different moduli would allow this technique to be expanded.

Acknowledgements

The author wishes to thank Professor A. Unsworth and Dr. T.V. Parry for their comments. The Wolfson Foundation funded this work and Action Research are now funding its application. Thanks are due to them

REFERENCES

1. Unsworth, A., Pearcy, M.J., White, E.F.T. and White, G. (1987) "Soft Layer Lubrication of Artificial Hip Joints" *Proc. Instn. Mech. Engrs. Tribology Vol.*, 715-724.
2. Unsworth, A., Pearcy, M.J., White, E.F.T. and White, G. (1988) "Frictional Properties of artificial hip joints" *Engng. in Med.* 17(3), 101-104.
3. Taylor, D.J. and Kragh, A.M. (1970) "Determination of the rigidity modulus of thin soft coatings by indentation methods" *J. Physics D: Applied Physics*, 3 29-32.
4. Waters, N.E. (1965) "The indentation of thin rubber sheets by spherical indentors" *Brit. J. Appl. Phys.* Vol. 16, 557-563.
5. Jarrar, M.J. (1989) "Asymptotic behavior of thin elastic layers bonded and unbonded to a rigid foundation" *Int. J. Mech. Sci.*, 31(3), 229-235.
6. Armstrong, C.G., Lai, W.M. and Mow, V.C. (1984) "An analysis of the unconfined compression of articular cartilage" *J. Biomech. Engng.* 106 165-173.
7. Timoshenko, S.P. and Goodier, J.N. "Theory of Elasticity, Edition 3" (1970), McGraw-Hill

NOMENCLATURE

a	contact radius	e_r	reduced penetration
A	Waters' constant	E	elastic modulus of polyurethane
d	diameter of indenter	F	load applied during hardness test
e	penetration	t	thickness of polyurethane layer

Presented at 'The 19th Leeds-Lyon Symposium on Tribology, "Thin Films in Tribology"', 8-11th September 1992, held at Leeds University, U.K. To be published in the Conference Proceedings, 1993, Elsevier Science Publications B.V.

BONDING OF SOFT LAYERS TO RIGID BACKINGS

J.M.Blamey, P.J.Mullin, J.Seaton, A.Unsworth & T.V.Parry
Centre for Biomedical Engineering
School of Engineering and Computer Science,
University of Durham, Durham City, DH1 3LE, U.K.

SYNOPSIS

Successful bonding of polyurethane layers to polyethylene backings has been achieved using a combination of mechanical and chemical mechanisms. These joints have been analysed using peel and blister testing as well as microscopy. Strength was found to be high, but largely as a result of the mechanical interlock between the two materials rather than chemical bonding and this is currently being addressed to improve strength still further. Bonded samples have been soaking in Mamalian Ringers solution at 37°C for 750 days with no visible signs of delamination. Long term fatigue studies of the bond in Mamalian Ringers have recently started, using loaded femoral heads to introduce representative stresses in the bond.

1. INTRODUCTION

The use of soft elastomeric layers in hip prostheses poses problems with fixation. In the same way as cartilage they must be supported by a rigid backing to maintain dimensional stability under high loading. This backing material should be bonded to the elastomer to eliminate problems with grabbing owing to the high poisson's ratio of the material. When no bond is present the layer tends to be pushed from the surface of the backing onto the ball leading to increased friction (figure 1).

When correctly bonded, the rigid backing will reduce the effective Poisson's ratio of the elastomeric layer from its initial value of 0.48-0.50 allowing closer clearances, without the risk of grabbing. The tribological properties are improved because the larger contact area reduces pressures on the articulating surfaces and promotes fluid film lubrication [1].

Use of adhesives in this application poses problems with biocompatibility, biostability, hydrolysis, fatigue and creep response. In addition it requires a relatively flexible adhesive due to the low elastic modulus of the adherands.

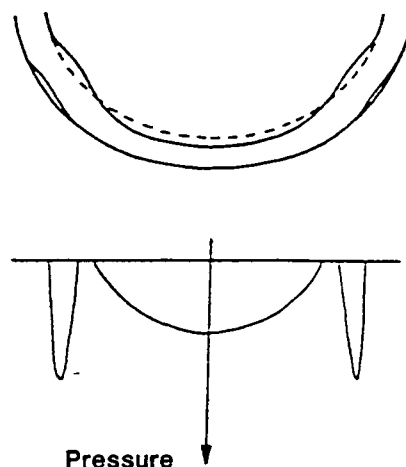


Figure 1. Grabbing of the Femoral Head onto the Acetabular Cup

2. THEORY

2.1. Theory of Joint Design

Joints should be specifically designed to facilitate several bonding criteria:

1. Allow adhesive application
2. Allow adhesive to cure
3. Put the adhesive under acceptable loading

Bonding of the elastomeric layer to the rigid backing would take place in a controlled environment (i.e. not *in-vivo*) and so the first two criteria are easily achieved. However ensuring that the loading is not too high for the adhesive requires thorough stress analysis and possible redesigning of the interface. Forces must be transmitted between the substrates through the adhesive bond which consists of many minute adhesion sites. If enough of these sites are sharing the load, a successful joint can be formed. A number of loading types may be applied to joints:

2.1.1. Tensile/Compressive Loading

In their idealised form these joints have the highest strength with stress being distributed over the entire bond area (figure 2a). However deflection of the joint components can lead to non-uniform loading and give rise to cleavage stresses (Figure 2b) reducing the load carrying capacity of the joint with stresses concentrated over a small cross-section of adhesive.

Figure 2a. Tensile/Compressive Loading of Adhesive Joints

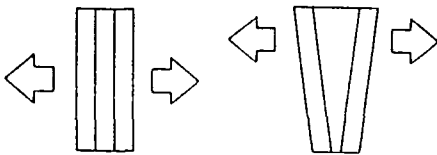


Figure 2b. Cleavage in Adhesives

2.1.2. Shear Loading

Joints which include shear loading of the adhesive apply stress over the entire bond area, but higher stresses are concentrated at the ends of the bond in this simple model (figure 3). The strength of a joint under shear loading is typically 10% of that of a compressively (with no cleavage) loaded bond. In-service conditions are normally limited to situations where shear stresses are less than 20% of the ultimate shear stress of the adhesive [2].

2.1.3. Peel Loading

The peel strength is usually the weakest property of a joint, with only toughened adhesives capable of maintaining reasonable peel strengths. This property is normally assessed with a similar arrangement to that shown with a peel angle of 90 to 180° (figure 4). Bond strengths of only 0.1% of those obtained under compressive loading and 1% of the strengths obtained in shear loading are typically measured under peel loading.

Figure 3. Shear Loading of Adhesives

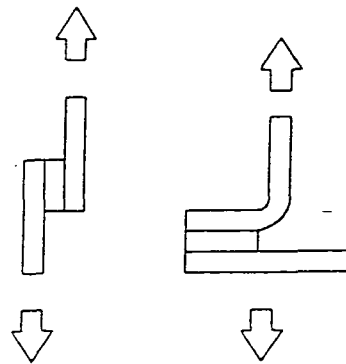


Figure 4. Peel of Adhesive Joints

2.2. Materials

Initially, metal backed cups were used in the assessment of soft layers with the layer bonded directly to the backing under compression moulding. The bond was found to be extremely weak and holes had to be drilled in the stainless steel backing to provide a mechanical interlock and allow the layers to be tribologically tested [3] (figure 5).



Figure 5. Stainless Steel backed Acetabular Cups

This would be unsuitable for an *in-vivo* model and does not maximise the potential of the layers, requiring large clearances to limit grabbing during operation. Also if there were problems with the elastomeric layer during operation and failure of the lugs occurred (as has been noted during long term *in-vitro* studies) the resulting metal on metal contact would tend to require immediate revision surgery.

Polyethylene in its ultra high molecular weight (UHMW) form has been widely used in knee and hip prostheses since Charnley optimised his hip prosthesis to make use of it. Since this time its biological properties have been well documented, with little tissue response as well as minimal polymer degradation [4], [5]. Therefore it would seem to be a good material to act as a backing for

the elastomers. Failure of the elastomeric layer would lead to a large clearance UHMWPE/metal contact which could maintain hip mobility for a reasonable time, reducing the need for emergency revision surgery.

A further reason for using UHMWPE can be understood by considering the fixing arrangements for many currently available prostheses. Porous and hydroxyapatite coatings on metallic surfaces have become popular for improving bone fixation with the polyethylene acetabular component a "snap-fit" into a metallic ring. The Durham prosthesis could easily be incorporated into many of the currently available systems. This would allow a direct comparison to be made between the performance of soft layers and UHMWPE in clinical prostheses.

2.3. Adhesive Theory

The performance of an adhesive is highly dependent on the adherands. Surface cleanliness is often important with degreasing often mandatory prior to application of the cement. However, some adherands are generally considered to produce poor bonds and polyethylene is amongst these. This is because of its waxy hydrocarbon surface which does not allow the polar molecules of the adhesive to bond well [6]. This material requires oxidation of the surface, replacing the hydrogen (H^+) ions with oxygen ions (O^{2-}) to exhibit a polar surface for improved adhesion. Even with such modification there are only a few adhesives which are suitable.

2.3.1. Hot-melt Adhesives

Thermoplastic polymers are used in a liquid form at an elevated temperature to cover the surfaces prior to pressure and cooling to complete the bond. Problems can occur because full wetting of the surface may be poor due to the low surface energy of polyethylene. In addition elevated (in-service) temperatures will tend to lead to weakening of the bond through adhesive softening. This may be a problem in the body ($37^{\circ}C$) if a low

temperature adhesive were to be used. Biocompatibility should be good, assuming a compatible thermoplastic was used. Bond strength is highly dependent on suitable adherands and a polar surface which may also be roughened.

2.3.2. Polyurethane Adhesives

Base materials of isocyanate and an amine or glycol are mixed and form a liquid material with quite a high viscosity which is cast onto the surfaces to effect a bond. The castomer resin (non-biocompatible) which was used during the early phases of soft layer work [7] was moulded in-situ through this reaction. The bonds produced can be of good strength especially in peel and impact loading but they are often the result of cross-linking of the urethane which can render it non-biocompatible. Also problems can occur in hot wet environments due to hydrolysis. This was observed with the castomer material following studies at 80°C in saline, with cracks appearing on the surface (figure 6)

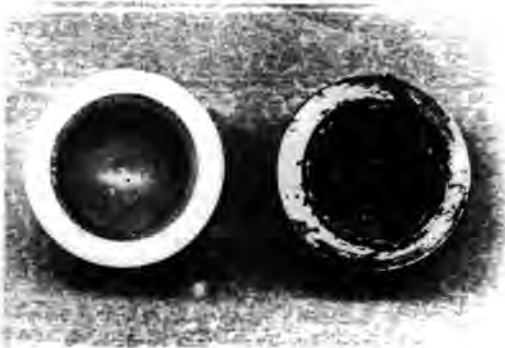


Figure 6. Hydrolysis Damage to a Castomer (Polyurethane) Cup

2.3.3. Solvent Cast Systems

These range from low viscosity liquids to pastes and represent a thermoplastic polymer (or urethane) carried by a suitable solvent. These can be highly biocompatible, for example Tecoflex resins in Tetrahydrofuran have been successfully used in the body [8]. Cross linked materials tend to give the greatest strength with only light loading possible with non-cross linked adhesives. Precise placement is mandatory as there is an instantaneous "grab" with curing often required to remove all of the solvent. The adhesive layers can be quite thick and so surface roughening can be used. Because of their thickness, adhesives are suitable for fatigue applications.

2.3.4. Alternative Systems

Other possible adhesives include Nitrile and Silicone rubbers. Although both are highly resistant to biodegradation and they are obtainable in a variety of hardnesses, the strength of bonds obtained with the two adherands will be questionable. Toughened acrylics, a family which includes bone cement, show good biocompatibility, but are often of high elastic modulus and as such are not suitable for bonding such a flexible material as polyurethane.

2.3.5. Contributing Considerations

Biocompatibility and minimal degradation in a hostile liquid environment at an elevated temperature are necessary for all biological adhesives. However, to improve the adhesive process the adherands should have elastic modulli close to or straddling that of the adhesive. Thus the adhesive acts as a form of stress reliever at the interface. Also if a large amount of motion is required, high values of ultimate elongation for the adhesive are essential.

Roughening of a surface is a good method of improving a bond and many successful bonds rely on mechanical interlock. In this application this would be an important

avenue to explore as many of the biocompatible adhesives are only capable of withstanding nominal loads with all but the polyurethane systems incapable of supporting shear stresses above 3.5MPa for prolonged periods.

2.4. Bond Analysis

Tests by Unsworth *et al* [3], [7] indicated that layer thicknesses of 2 mm or larger were required for optimum tribological properties. Armstrong [9] studied the interface between cartilage and bone and obtained the following simplified expression for shear stress:

$$\tau_{\max} = \left(\frac{\delta P}{\delta x} \right) \gamma \quad (1)$$

This analysis assumed an incompressible layer i.e. $\nu = 0.500$ and a flexible layer on a rigid backing material. The maximum shear stress of the bond can be seen to occur at the interface between the two layers beneath the point of maximum pressure gradient. Reductions in shear stress thus require a thinner layer and lower value of the pressure gradient.

Eberhardt *et al* [10] expanded on this work and obtained similar expressions with normal stresses (representing compressive loads) reaching $1.92 P/\pi a^2$ at the interface between soft and hard layers. For the soft elastomeric joints this represents 3.5-6.3MPa. Shear stresses reach a maximum at a distance of 14mm from the central point, measured along the bond line. Previously layer thicknesses of 2mm had exhibited good tribological properties, however mechanical interlock has been suggested as being paramount to a successful bond. This would require an average layer thickness of 3-4mm to allow at least 2mm of uncontaminated (with UHMWPE) elastomeric layer. This corresponds to ν_t values of 6.1-4.6. Shear stresses of 0.68-0.90MPa can be calculated from Armstrong [9].

Lees [2] stated that for fatigue applications the proof stress of the adhesive in the mode of expected stress should be five times that expected under the loading to give a good bond life. This means that strength of the bond must be above 18MPa in compression and 4.5MPa in shear. Although this value of compressive stress should not cause a problem to many adhesives, because of the non-uniform loading cleavage stresses will be introduced, which will probably be a maximum at the edge of the contact area.

In any bond regions of low strength or pores within the adhesive layer will be present. The ability of an adhesive to limit crack growth from regions of high stress concentration such as pores is an inexact science which can depend on many inherent properties. However, most joints fail because they cannot meet peel and cleavage overloads with shear overloads being rare. The measurement of this property which may be related to peel strength is also a problem with many potential tests. Peel tests have been previously introduced and a range of specimen geometries exist as no peel test can fulfil the requirements of all cases (BS 5350 Parts C9-14, 1978). However, blister tests can also be used. The interface is expanded using a pressurised fluid over an area where the bonding has been interrupted (figure 7).

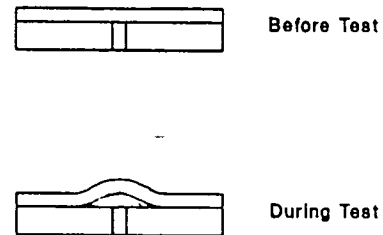


Figure 7. The Blister Test Arrangement

This test indicates the resistance of an adhesive to crack growth in a cleavage

configuration and the fluid used (which should be relatively incompressible) can mimic a degrading in-service environment.

Fracture mechanics for the blister test arrangement can be simplified by a number of assumptions [11]:

Opening Loading: Tensile loads are applied perpendicular to the plane of the crack, leading to opening. This is Mode I loading as there are no shear stress components parallel to the crack.

Plane Strain: conditions also apply, as the crack is internal

For adhesive cases, the following equation was derived [12]:

$$\theta = \frac{P_c^2 b}{E (1-\nu^2)} \left[\frac{3}{32} \left(\left(\frac{b}{t} \right)^3 + \left(\frac{c}{t} \right) \frac{4}{(1-\nu)} \right) + \frac{2}{\pi} \right]^{-1} \quad (2)$$

A full finite element analysis of the cup is planned to confirm the loading applied to the bond during in-service conditions. This is likely to reveal some degree of peel, cleavage, compressive and tensile forces on the bond. Problems arise because of the high Poissons' ratio of the elastomer and it has been noticed from early fatigue testing that there are cleavage forces operating around the upper edge of the cup under loading, leading to fracture of the bond in this region. This confirms that it is not only the contact area which has to be rigidly bonded and indicates the need for a full analysis.

3. Materials and Methods

3.1. Preparation Methods

Much of the research concentrated on the preparation of hot melt processed components. These consisted of test pieces formed in dies which were compressed between the heated plattens of a compression moulding machine. Temperature control allowed the plattens to be adjusted independently and pressures of up to 45 tonnes could be applied. Three moulds were

used for the majority of specimens and they are shown schematically in figure 8.

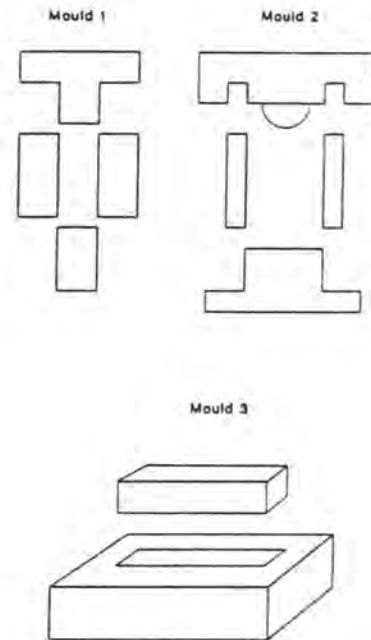


Figure 8. The Moulds used for the Bonded Specimens



Figure 9. The Specimens Produced

Mould 1 prepared disc specimens of 31mm diameter and thickness of 8mm (figure 9). These could be easily prepared because of the simplicity of the mould, with trapped air not causing a problem. Blister test specimens could be constructed by incorporating a disc of PTFE (to stop bonding) over the central portion of the PE/PU interface. The discs could also be sliced to yield peel test specimens although these had a relatively short bond length which could lead to inaccuracies (BS 5350 Parts C9-14, 1978).

Mould 2 addressed this problem and yielded specimens of 70mm in length and 20mm wide. PTFE could be used in the moulding process to yield an unbonded region but it was found that slicing along the bond line was adequate to start the "crack". Mould 3 allowed prototype acetabular cups to be constructed. These required a layer thickness of at least 2mm to give the required cup hardness for acceptable tribological properties. The internal radius of the component and the bone line could be adjusted by the use of a range of acetabular moulds.

Extensive experimental results concluded that the best components were formed when the component was made on one heat cycle. UHMWPE which was in powdered form was compacted with a load varying between 10 and 30 tonnes depending on the mould. Polyurethane granules (circa 3mm in diameter) were then added and compressed into the polyethylene surface and the mould was heated. Thermal degradation can be a problem with urethanes so it is preferable to spend as little time at the higher temperatures as possible. A higher pressure tends to allow better conduction between mould and sample but can adversely affect the removal of trapped air from the sample. [The acetabular cup specimens proved to be the most difficult samples to produce without bubbles]. A compromise pressure was found by experimentation, and this was used at the

higher temperatures during the moulding process. A graph of platten and mould temperatures and pressures for a bubble free acetabular cup is shown in figure 10. The temperature measured in the centre of the mould can be seen to lag behind the platten temperature due to the length and large thermal mass of the die. The temperature of the centre of the component will also lag behind that of the mould because of the low thermal conductivities of the polymers. Although the melting temperature of the polyethylene (130°C) was lower than the urethanes no degradation was noticed, possibly due to the reduced conduction of the polyethylene powder compared with the urethane pellets.

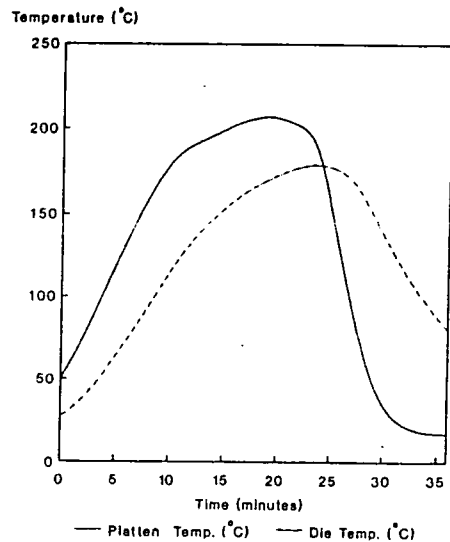


Figure 10. The Temperatures of Plattens and Mould 2 during moulding

3.2. Materials

Three biocompatible polyurethanes were investigated. All had been previously assessed for degradation resistance [13] and all are currently being used in medical

applications. The processing temperatures of the materials were in the range 155-170°C, although lower temperatures could be employed if high compaction pressures were used. The use of very high temperatures led to bubble formation, whilst lower temperatures meant incomplete melting and inter-granular pores. Estane 5714F1 (77°A), Pellethane 2363 (80°A) and Tecoflex EG (85 & 93°A) were used, all polyetherurethanes. The materials were in the form of pellets of typically 3-4mm diameter. Pellethane was of regular angular particles and tecoflex of regular spheroids. Estane was in the form of irregular chips. The reliance of the bond on the mechanical interlock meant that the shape of the urethane particles was likely to have a substantial effect on the mechanical strength of the bond.

3.3. Testing Methods

3.3.1. Peel tests

A floating roller arrangement was used as it produced more constant numerical data than other methods (BS 5350) with a bond formed mainly on mechanical interlock. [The chemical bond was found to be relatively weak as specimens with little or no interlock could easily be pulled apart by hand] it was likely that a large spread of results would be apparent and so the test had to produce as consistent results as possible. The geometry of the arrangement (figure 11) was as BS 5350 Part C9 (1978).

A computer controlled Houndsfield tensile testing machine was used to apply the loading at a constant strain rate of 0.4 mm/second.

The effect of soaking in saline at 37°C for 48 hours prior to testing was investigated. The urethane would be fully hydrated at this stage [13].

Specimens were prepared in widths of 10 and 20 mm and a cut was prepared along the bond line using a 0.5mm width saw blade. At least 15mm of the bond line was

failed and a graph of load/time obtained which allowed the bond strength to be calculated as load/unit width of bond line.

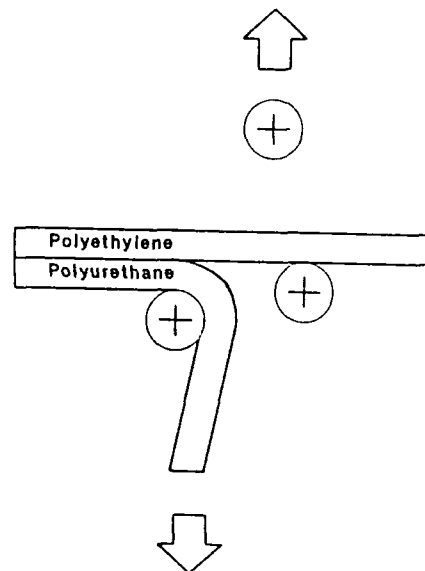


Figure 11. The Floating Roller Peel Test Arrangement

The specimens prepared with mould 3 were also assessed for shear strength through tensile testing of the polyurethane component and assessing failure if there was delamination along the bond line.

3.3.2. Blister Tests

Tecoflex 85°A/polyethylene specimens were prepared in mould 1 with a PTFE disc incorporated into the interface. In fact the disc was often above the interface because of the rough nature of the bond with granules up to 5mm in diameter forming the interface. This moves the geometry to one which favours cohesive rather than adhesive failure [12].

A PTFE disc of 11 mm and a nominal layer thickness of 4 mm were used. The disc

was cut from a sheet using a simple punch. Although this method can produce imperfect cracks, with sharper edges than specified [12] in this case this was thought to be unimportant because of the irregular nature of the bond. A countersunk hole was drilled in the specimens to transfer the pressurised oil to the crack thus forming the blister. The sample was mounted in a brass fitting which contained a perspex window so that failure could be seen as the crack extended. A dye was added to the oil to allow easier identification of the crack front.

4. Results

4.1. Peel Tests

The results of peel testing are displayed in Table 1.

Table 1
Peel Strengths of PE/PU Bond

Polymer	Hardness (MPa)	Bond Strength (N/mm)	Sample Width (mm)
Estane 57	2.85	9.75	10
Estane 57 (saline)	2.42	7.25	10
Pell 2363	3.21	13.9	10
Teco 85	2.15	15.0	10
Teco 93	3.35	12.2	19
Teco 93 (vacuum)	3.26	6.8	19

These strength values compare favourably with results for adhesives. For example the peel strength of a toughened epoxy is 5.2N/mm. However, this is a pure chemical bond however with no mechanical interlock. The reduction in strength of 25% when the samples have been hydrated in

saline is acceptable and will be due to the softening of urethanes when hydrated [13] and the increased deformation and hence failure at the mechanical interlock.

The improvements in strength with Pellethane and Tecoflex may be due to the higher elastic modulus or more regular granules which form the interlock. However, a larger sample group is required before conclusions may be drawn, as these results were drawn from testing 6-8 samples of each material.

It can be seen that vacuum formed tecoflex layers (which are then compression moulded to the polyethylene backing in a two stage process) are much less strong. This is because of the inferior mechanical interlock.

4.2. Blister Tests

The movement of the crack front was monitored and the failure energy was calculated with a range of values of 2.9-8.5kJ/m². These values compared favourably with results obtained from epoxy/brass bonds of 0.4kJ/m². Failure was adhesive at the Polyurethane/ Polyethylene bond in the vast majority of cases.

For the blister test the thickness of the elastomeric layer and the initial crack size both govern the failure pressures. At low values of t_a the elastomeric material will undergo plate like deflection. This causes larger destructive forces than for a high value of t_a which acts as an infinite medium with deflection within the material giving a "near field" only analysis. This can be seen from calculations of the adhesive fracture energy which increases as t_a increases (figure 12) and the results of Andrews and Stevenson [12] which showed a many fold increase in the failure pressure as the thickness of specimen was increased.

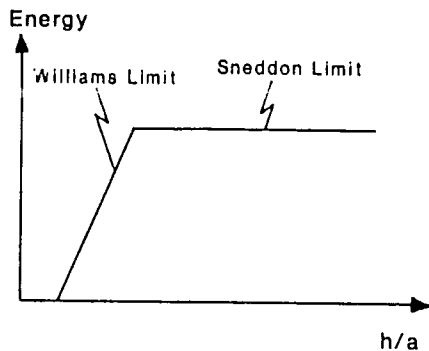


Figure 12. Graph of Adhesive Fracture Energy for the Blister Test

5. Conclusions

The results from the peel tests showed a low scatter, even with such low failure lengths, which was surprising with the irregular nature of the bond. However, much longer specimens should improve the accuracy of the results.

The specimens which had the bond tested in shear by tensile loading of the polyurethane showed very high bond

strengths as failure was always of the polyurethane, and not at the bond. This means that the failure shear stress of the bond is in the region required for the application.

The use of the blister test in this application is still at an early stage and much work is required in this area. Widely scattered results of other researchers have been found to be the result of imperfect PTFE discs leading to very sharp cracks. This should not be so critical in this application owing to the compliant nature of the materials blunting the crack tips and the very irregular bond.

A full analysis of the acetabular cup using finite elements techniques is planned to accurately display the damaging interface forces and this may necessitate the testing of the bonds in shear.

Long term tests on the bond strength have begun on a Dartec Fatigue Testing Machine. The cups are loading in compression to 4000 N in an attempt to fail the bond. This should give an indication of the most likely crack propagation sites so these can be improved if necessary.

REFERENCES

1. O'Carroll, S., Jin, Z.M., Dowson, D., Fisher, J. and Jobbins, B. (1990) "Determination of contact area in 'cushion form' bearings for artificial hip joints" *Proc. Instn. Mech. Engrs.: Part H*, Vol. 204, 217-223.
2. Lees, W.A. "Adhesives in Engineering Design" (1984), The Design Council, Springer-Verlag, Berlin and New York.
3. Unsworth, A., Pearcy, M.J., White, E.F.T. and White, G. (1988) "Frictional Properties of Artificial Joints" *J. Engng. Med.* 17: 101-104.
4. Gibbons, D.F. (1978) "Polymeric Biomedical Materials" *The British Polymer Journal*, Vol.10, December, 232-237.
5. Hastings, G.W. (1978) "Load Bearing Polymers used in Orthopaedic Surgery" *The British Polymer Journal*, Vol.10, Dec. 251-255.
6. Thomas, D.R.K. (1991) Private Communication
7. Unsworth, A., Pearcy, M.J., White, E.F.T. and White, G. "Soft Layer Lubrication of Artificial Hip Joints" (1987) *Proc. Instn. Mech. Engrs. Tribology Volume*, 715-724.

8. Brown, D.L. (1988) "Custom made aliphatic polyurethanes for medical use" presented at "Medical Plastics '88 Conference", Oxford, U.K., Sept 8th.
9. Armstrong, C.G., (1986) "Analysis of the stresses in a thin layer of articular cartilage in a synovial joint" *Engng. in Med.* Vol.15 No.2, 55-62.
10. Eberhardt, A.W., Keer, L.M., Lewis, J.L. and Vithoontien, V. (1990) "An Analytical Model of Joint Contact" *ASME J. Biomechanical Engineering*, Vol.112, 407-411.
11. Timoshenko, S.P. and Goodier, J.N. "Theory of Elasticity, Edition 3" (1970), McGraw-Hill
12. Andrews, E.H., and Stevenson, A. (1978) "Fracture Energy of Epoxy Resin under Plane Strain Conditions" *J. Mater. Sci.* 13, 1680-1688.
13. Blamey, J.M., Rajan, S., Unsworth, A. and Dawber, W.R.K. (1991) "Soft layered prostheses for arthritic hip joints: a study of materials degradation" *J. Biomed. Eng.*, 13(5), 179-184.
- BS 5350 Parts C9-C14 (1978): Peel Testing Methods.

NOMENCLATURE

a	Contact Radius	x	Distance along Contact from Pole
b	Blister Radius	y	Distance through Soft Layer
c	Initial Crack Length for Blister Test	ν_1	Poisson's Ratio of the Femoral Comp.
p	Pressure in the Contact Area	ν_2	Poisson's Ratio of the Acetabular Component
P_c	Critical Pressure in Blister Test	θ	Adhesive Fracture Energy
R_1	Radius of the Femoral Component	τ_{max}	Maximum Shear Stress at the Layer interface
R_2	Radius of the Acetabular Comp.		
t	Thickness of the Urethane Layer		
W	Load Applied in the Prosthesis		

